Effect of plant-parasitic nematodes on rhizosphere interactions in oaks

Dissertation

Zur Erlangung des akademischen Grades

Doctor rerum naturalium

(Dr. rer. nat.)

eingereicht an der

Lebenswissenschaftlichen Fakultät der Humboldt-Universität zu Berlin

von

M.Sc Hazel Ruvimbo Maboreke

Präsident der Humboldt-Universität zu Berlin: Prof. Dr.-Ing. Dr. Sabine Kunst

Dekan der Lebenswissenschaftlichen Fakultät:

Prof. Dr. Bernhard Grimm

Gutachter

1. Prof. Dr. Liliane Rueß
2. Prof. Dr. Johannes Hallmann
3. Prof. Dr. Francois Buscot

Date of thesis defence: 02.05.2017

“Look deep into nature, and then you will understand everything better.”

Albert Einstein

TABLE OF CONTENTS

LIST OF TABLES

LIST OF FIGURES

ABSTRACT

This thesis investigated the response of Pedunculate oak to the plant-parasitic nematode Pratylenchus penetrans, using RNA-sequencing, stable isotope labelling and fatty acid analyses. Insight into rhizosphere interactions was gained by employing beneficial biotic partners (ectomycorrhizal fungi, rhizosphere helper bacteria), fungal grazers (Collembola) and multitrophic environments. Microbial biomass and community structure as well as oak fitness were assessed.

The effects of root-feeding nematodes on oak were largely governed by the endogenous rhythmic growth of the tree. The nematodes triggered a stronger response during shoot flush, e.g. activation of multi-layered defence mechanisms and repression of photosynthesis, as compared to root flush where pathogen-related signalling was repressed. With the presence of the mycorrhizal symbiont plant defence was attenuated and stress tolerance enhanced, indirectly promoting the growth of rhizosphere microorganisms. The helper bacteria fostered the ectomycorrhizal fungus, which in turn stimulated plant growth, counteracting the negative effects of nematodes. Plant-parasitic nematodes and Collembola grazers had independent roles in plant carbon allocation patterns, with nematodes hampering whilst Collembola enhancing the flux of recent photoassimilates to Gram-positive bacteria. Lastly, increasing trophic diversity of the soil fauna in the rhizosphere of oaks was crucial for the maintenances of a microbial community equilibrium that promotes plant growth.

In sum, this study highlights the importance of endogenous resource allocation pattern of plants in determining the outcome of belowground biotic interactions. Therefore such plant traits should be considered as important drivers for rhizosphere processes in future studies. Moreover, taking into account the rhizosphere main players in studies on parasitic nematode-plant interactions will result in a more realistic picture and thus more effective nematode management.

Keywords

Plant-parasitic nematodes, oak, rhizosphere, trophic, interaction

ZUSAMMENFASSUNG

Diese Arbeit untersucht die Reaktion der Stieleiche auf den pflanzenparasitären Nematoden *Pratylenchus penetrans* mittels RNA-Sequenzierung und Analyse von stabilen Isotopen und Fettsäuren. Einblicke in Rhizosphäreninteraktionen wurden über mutualistische Partner (Ektomykorrhizapilze, Rhizosphärenhelferbakterien), fungivore Collembolen und multitrophische Gemeinschaften gewonnen. Die Struktur und Biomasse der Mikroorganismen sowie die Fitness der Eichen wurden erfasst.

Die Effekte wurzelfressender Nematoden auf die Eiche wurden durch das endogene rhythmische Wachstum des Baumes reguliert. Die Nematoden lösten eine stärkere Reaktion während des Sprosswachstumsschubs aus, u.a. Aktivierung von Abwehrmechanismen und Hemmung der Photosynthese, wohingegen beim Wurzelwachstumsschub pathogen bezogene Signale unterdrückt waren. Die Anwesenheit des Pilzsymbionten schwächte die Pflanzenabwehr und verbesserte die Stresstoleranz, was indirekt das Wachstum der Mikroorganismen förderte. Die Helferbakterien begünstigten den Mykorrhizapilz, was wiederum das Pflanzenwachstum stimulierte und dem negativen Effekt der Nematoden entgegenwirkte. Parasitäre Nematoden und fungivore Collembolen beeinflussten die Verteilung des pflanzlichen Kohlenstoffes unabhängig voneinander; Nematoden verringerten und Collembolen verbesserten die Allokation von Photoassimilaten in Gram-postiven Bakterien. Zudem war steigende trophische Diversität der Bodenfauna in der Rhizosphäre entscheidend für die Balance innerhalb der mikrobiellen Gemeinschaft, welche das Pflanzenwachstum fördert.

Diese Arbeit stellt die Bedeutung der endogenen Ressourcenzuteilung von Pflanzen für unterirdische biotische Wechselbeziehungen heraus. Diese Pflanzenstrategie als bedeutender Faktor für Rhizosphärenprozesse sollte in zukünftige Studien Berücksichtigung finden. Die Einbeziehung der Hauptakteure in der Rhizosphäre ermöglicht zudem ein realistischeres Bild von Nematoden-Pflanzen Interaktionen und damit ein effektiveres Management.

Stichworte

Pflanzenparasitäre Nematoden, Stieleiche, Rhizosphäre, trophische Interaktionen

CHAPTER ONE: INTRODUCTION

1.1 Nematodes

Nematodes are roundworms ranging between 40µm - 9m in length (Maggenti and Allan, 1959) with a relatively simple body plan. This simplicity in morphology has led in the establishment of *Caenorhabditis elegans* as a general model for metazoa (Blaxter, 1998). Despite this little morphological variation, nematodes show a vast taxonomic diversity (Blumenthal and Davis, 2004; De Ley, 2006). They form one of the largest Phylum in the animal kingdom with more than 25 000 species described to date (Abad and Williamson, 2010) and are estimated to comprise ≈10 million species (Blaxter, 2011). Nematodes are ubiquitous exploiting almost every possible ecological niche worldwide, ranging from depths of the ocean to mountain peaks, polar to tropics regions, wetlands to deserts, marine and freshwater as well as parasites of plants, insects and vertebrates (Andrássy and Zombori, 1976; Bongers and Ferris, 1999). Moreover, they are considered the most abundant metazoans (Cobb, 1915; Bernard, 1992), e.g. in soils 3.5 - 5 million individuals per square meter are common (Yeates, 2003).

In soil ecosystems, nematode life strategies and food resources are important factors contributing to niche specialization (Perry and Moens, 2011). Nematodes can be either free-living or parasites of plants and animals (Yeates et al., 1993; Bongers and Bongers, 1998). Free-living nematodes display a high trophic diversity and consume bacteria, fungi, protozoa, algae, small rotifers, enchytraeids, as well as other nematodes. They can be found at all trophic levels in the soil micro-food web, i.e. primary, secondary and tertiary consumers, thereby occupying key positions in bottom-up and top-down controlled webs (Ferris, 2010; Yeates, 2010).

Nematodes are involved in many soil processes such as organic matter decomposition (Bardgett and Cook, 1998; Hunt et al., 2001) and nutrient cycling (de Ruiter et al., 1993; Ferris et al., 1997), dispersal of microorganisms (Knox et al., 2003; Gibbs et al., 2005) and diseases suppression by feeding on bacterial and fungal pathogens (Yeates and Wardle, 1996). Most importantly, moderate grazing by bacterial and fungal feeders alters microbial community composition, stimulates microbial growth and maintains the populations in a youthful state, thereby accelerating decomposition rate (Bardgett and Cook, 1998; Savin et al., 2001; Djigal et al., 2004). Moreover, microbial feeding nematodes contribute

significantly towards plant production as they excrete nutrients in excess of their metabolic needs in forms that can be readily taken up by plants such as NH_4^+ and PO_4^- (Irshad et al., 2011; Gebremikael et al., 2016).

Besides these beneficial taxa, plant-parasitic nematodes, a group contributing ≈ 20% of the described nematode species (Helder et al., 2015), present a serious problem to primary production, predominantly in annual crop plants (Table 1). Estimated financial losses are between $ 80 - 118 billion annually, on a global scale (Chitwood, 2003; Nicol et al., 2011). Consequently, due to their economic importance as agricultural pests they have generated a lot of interest among researchers (Neher, 2010).

Table 1 Estimated crop yield and financial losses caused by plant-parasitic nematodes on a global scale

Crop	FAO production estimates (1000 metric tons)	Estimated yield losses due to nematodes (%)	Estimated monetary loss due to nematodes - 2008 (x1000 U.S.$)
Banana	81,263	19.7	14,855,056
Barley	136,209	6.3	2,044,978
Cassava	228,138	8.4	3,353,629
Citrus	105,000	14.2	10,601,170
Cocoa	4,012	10.5	1,134,626
Coffee	7,742	15	2,223,425
Corn	637,444	10.2	11,895,929
Cotton (lint only)	112	10.7	12,463
Field bean	6,371	10.9	833,327
Oat	25,991	4.2	127,327
Peanut	30,670	12	5,410,188
Potato	321,736	12.2	10,362,473
Rice	432	10	26,957
Sorghum	64,589	6.9	262,942
Soybean	56,389	10.6	2,024,967
Sugar beet	247,878	10.9	1,258,234
Sugar cane	1,557,664	15.3	8,462,835
Sweet potato	126,299	10.2	5,242,210
Tea	3,871	8.2	89,637
Tobacco	6,326	14.7	6,137,485
Wheat	676,300	7	11,237,807

Source: http://plpnemweb.ucdavis.edu/nemaplex/Plntpara/damage.htm

1.2 Plant-parasitic nematodes

Often referred to as “the hidden enemy”, plant-parasitic nematodes are one of the most widespread herbivores, posing a great threat in agricultural and arboriculture ecosystems, pastures and forests throughout the world (Ruehle, 1973; Chitwood, 2003; Nicol et al., 2011). Additionally, they are a cause of concern to recreational businesses such as golf courses, turfs and ornamental crops (Rahman-Khan et al., 2005, Crow and Luc, 2014;). Depending on life strategy, plant-parasitic nematodes attack different parts of the plant including stems, leaves, flowers and seeds, though the majority are root pathogens, where they produce extensive damage such as galling and necrosis (Shurtleff and Averre, 2000).

These nematodes are well equipped for parasitism, possessing a sharp protractible, hollow stylet used to: (i) pierce the plant cell wall, (ii) dispense a cocktail of pathogenicity related secretions called effectors, and (iii) take up nutrients from cell contents (Bird et al., 2015; Helder et al., 2015). Some of these effector proteins are cell wall-degrading enzymes such as cellulase, endoglucanases pectate lyase, used to facilitate feeding and migration within the plant tissues (Davis et al., 2011; Haegeman et al., 2012; Rybarczyk-Mydlowska et al., 2012). Additionally, some effectors manipulate plant development and induce physiological and morphological changes resulting in nutrient-rich nursing cells for the nematode (Gheysen and Mitchum, 2011; Jones et al., 2013). The modified host plant cells induce metabolic sinks in the roots, altering the general translocation patterns of photoassimilates (Hofmann et al., 2007; Kaplan et al., 2011).

Plant-parasitic nematodes display high variations in the modes of parasitism as shown in Figure 1 (Baldwin et al., 2004; Perry and Moens, 2006), with the following functional groups: (1) ectoparasites with a short stylet to feed on root epidermal cells and hairs or with a long stylet to feed on root parenchyma, predominantly at root tip; (2) migratory endoparasites, which periodically feed as they migrate, causing extensive destruction of root tissue alongside, and (3) sedentary endoparasites forming very intimate and long-term feeding relationships at specialized feeding sites, while the nematode becomes immobile in a root-knot or gall (Figure 1; Tytgat et al., 2000).

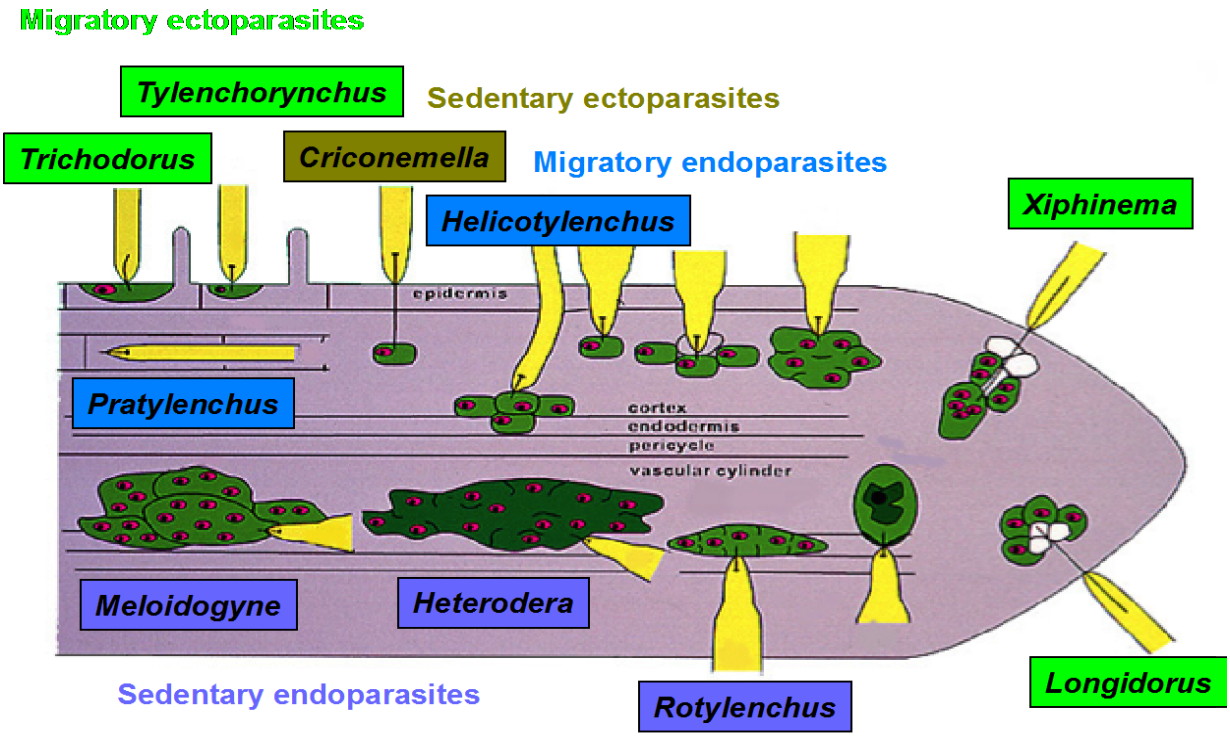

Figure 1 Feeding sites of selected plant-parasitic nematodes with economic importance. Image courtesy: NemaPix

Damage by plant-parasitic nematodes is insidious and often yield loss is underestimated due to unspecific plant symptoms that are less obvious compared to damage caused by plant pathogens and resemble abiotic stresses hence the name "hidden enemy" (Zunke et al., 1997; Escobar et al., 2015). The direct damage to root tissues can range from necrosis to cell death and in severe cases may cause root pruning (Umesh et al., 1988; Zunke, 1990) weakening plant anchorage and resulting in toppling (Gowen et al., 2005). Consequently, this disturbance to the root system reduces the plant's efficiency in uptake of nutrients and water and decreases the rates of evapotranspiration (Ruehle, 1967). The cumulative effects of plant-parasitic nematodes activity results in loss of plant vigour, shoot growth suppression and leaf chlorosis, premature wilting and other symptoms characteristic of nutrient efficiency; eventually leading to overall yield decline of plants over time, seedling mortality and death (Fraedrich and Cram, 2002; Duncan, 2005).

Plant-parasitic nematodes also affect plants indirectly; some studies have reported stimulation of root growth at low-levels of herbivory (Bardgett et al., 1999a; De Deyn et al., 2004). Moreover, enhanced leakage of labile plant metabolites from damaged roots stimulates growth of soil microorganisms; which promotes microbial activity and mineralization of

nutrients (Haase et al., 2007; Poll et al., 2007). Additionally, plant-parasitic nematodes alter the quality of root exudates (Van der Putten, 2003; Hofmann et al., 2010; Kaplan et al., 2011), which in turn regulates the microbial community structure through changes in resource availability. Further, nematode-induced damage of the roots reduces ectomycorrhizal colonization (Francl, 1993) and lessens the positive effects of mycorrhizal fungi, hampering plant growth (Rabatin and Stinner, 1988; Villenave and Duponnois, 2002). Furthermore, the damaged roots serve as entry sites for other pathogens such as bacteria and fungi (Back et al., 2002; Bjösell et al., 2017). Overall, these direct and indirect effects of plant-parasitic nematode make infected plants more susceptible to other unfavourable environmental conditions such as drought injury, winter injury or excessive moisture (Perry and Moens, 2006). Figure 2 summarises the major effects on host plants.

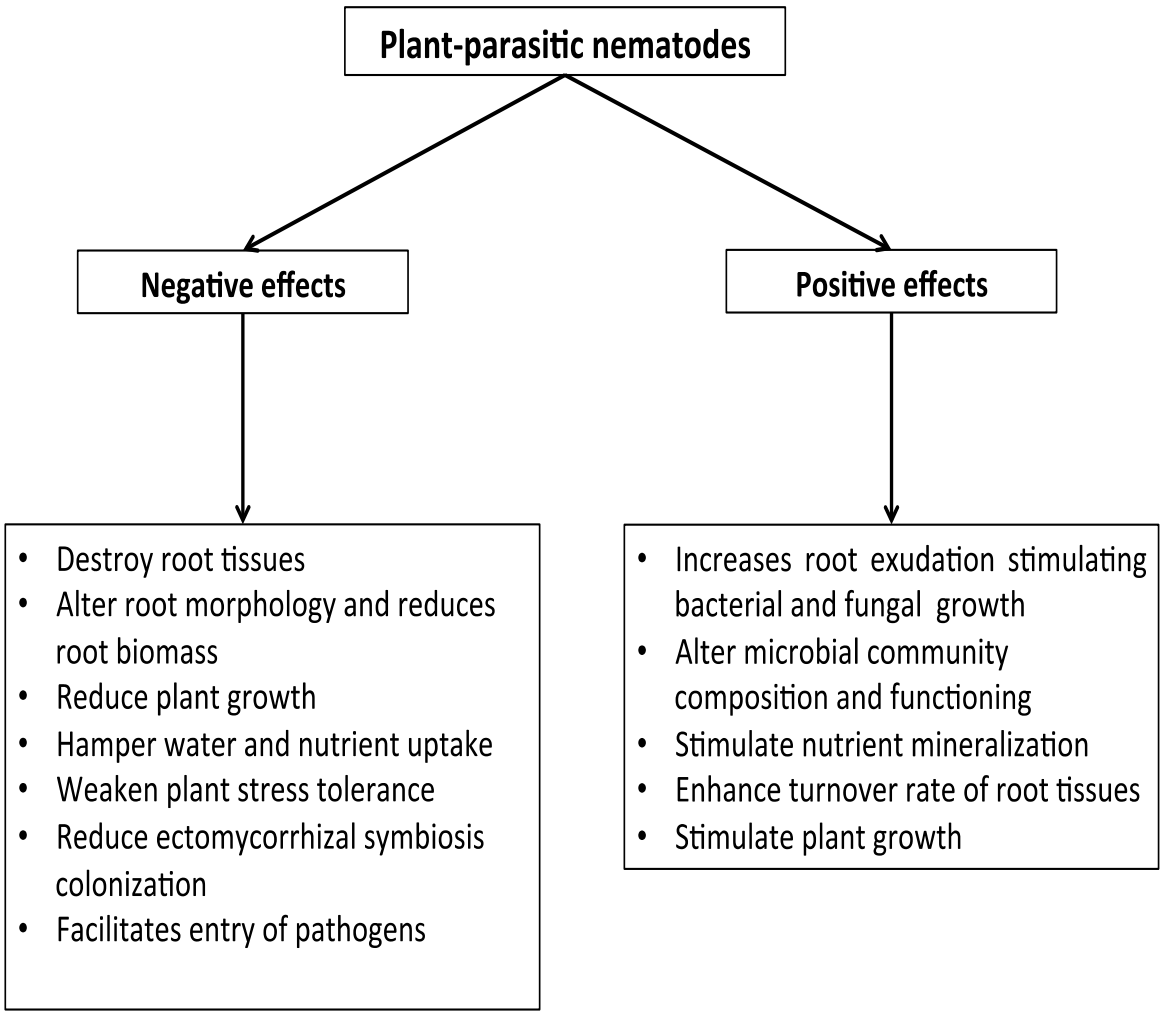

Figure 2 Direct and indirect effects of plant-parasitic nematodes on host plants

1.3 Multitrophic interactions in the rhizosphere of forest trees

Recent years have seen great strides in application of next-generation sequencing, bioinformatics and functional genomic analyses to unravel the interactions between plants and plant-parasitic nematodes (Mitchum et al., 2013; Quentin et al., 2013). Despite these advancements, huge gaps in knowledge on the relationships of forest trees and plant-parasitic nematodes still exist. To date, most knowledge is derived from studies involving agriculture crops, horticultural trees and pasture grasses, deemed as more valuable, overshadowing research on interactions between forest trees and plant-parasitic nematodes (Ruehle, 1973; Sohlenius, 1980; Neher, 2010). Further, studies have often been conducted in over simplified artificial set-ups using one host plant and nematode species (Anwar and Van Gundy, 1989; Poll et al., 2007) and do not encompass the complexity of interactions in natural ecosystems such as forests. Yet present in the rhizosphere of forest trees are a multitude of microorganisms such as bacteria and ectomycorrhizal fungi, microfauna such as nematodes and mesofauna such as Collembola, which interact directly or indirectly with the tree as well as with each other, forming complex interrelationships involving competition, facilitation, antibiosis as well as predation (Wardle, 2006).

Most temperate forest trees form obligatory symbiotic relationships with ectomycorrhizal fungi forming (Smith and Read, 2008). Plant-parasitic nematodes, such as migratory endoparasitic *Pratylenchus* sp., hamper these symbiotic interactions by reducing supply of carbon to the fungi and by limiting habitable sites for fungal colonization due to necrotic damage of roots (Wallace, 1987; Umesh et al., 1988). Grazing by fungal-feeding nematodes and Collembola additionally reduces growth of the fungal symbiont, disrupting its nutrient acquisition and in turn retards plant growth (Ruess et al., 2000; Partsch et al., 2006). Meanwhile, established mycorrhiza can protect roots against nematodes (Schouteden et al., 2015), as does the opportunistic feeding on nematodes by Collembolans (Lee and Widden, 1996; Kaneda and Kaneko, 2008). Consequently, plant-parasitic nematodes influence and are influenced by soil microorganisms and other fauna inhabiting the rhizosphere, and collectively they affect the fitness of the host tree.

1.4 Carbon dynamics in forest trees and their rhizosphere

Forests play a very important role in the global carbon cycle; they act as sinks storing approximately one third of recent anthropogenic emissions of carbon dioxide to the atmosphere (von Lützow et al., 2006; Mackey, 2014). Global elevations in the concentrations of atmospheric carbon could change tree communities, affect carbon sequestration and transfer belowground, with distinct consequences on the functioning of forests in carbon cycling (Percy et al., 2002; Lindroth, 2010). Moreover, global change could alter plant-pathogen interactions in a manner that can profoundly re-shape plant communities (Mitchell and Power, 2006). This global change would undoubtedly have significant ecological as well as economic consequences and calls for improved long-term management of forests.

Trees provide rhizosphere microorganisms and fauna with carbon resources in the form of exudates (Prescott and Grayston, 2013), with as much as 33 - 50% of the photoassimilated carbon allocated to soil via roots (Högberg et al., 2001). Thereby, features such as the endogenous rhythmic growth pattern displayed by most temperate tree species such as oak (Willaume and Pages, 2006, 2011; Herrmann et al., 2015), directly or indirectly regulate biotic interactions in the rhizosphere. Soil fauna including plant-parasitic nematodes can alter these carbon allocation patterns (Kaplan et al., 2011). All these intertwined processes make unravelling of interactions between forest trees and plant-parasitic nematodes as well as other soil inhabitants a challenge. Therefore a thorough understanding of the relationships between trees and rhizosphere biota is essential for improving long-term management of forest trees (Gilbert 2002; Wisz et al., 2013).

This thesis work was performed within the research project "TrophinOak" funded by the German Science Foundation, which investigates the impact of multitrophic interactions on the pedunculate oak (*Quercus robur* L.) (www.trophinoak.de) (Figure 3). This tree is amongst the most economically important temperate forest tree species in Europe, providing high quality and durable timber used for furniture and in construction (Praciak et al., 2013) and is a habitat to a very diverse species-rich assemblage of below- and aboveground organisms (Brandle and Brandl, 2001). It is a long-lived hardwood tree species widely distributed across European temperate forests (Ducousso and Bordacs, 2003). It acts as a pioneer tree, can replace other species and has a high tolerance to drought (Müller, 2000; Savill, 2013) therefore it would be a good candidate to diversify forest ecosystems. Pedunculate oak has co-evolved with most of its interacting species (Plomion and Fievet,

2013) and displays endogenous rhythmic growth (Lavarenne, 1966), enabling investigations of the impact of carbon allocation to above- and belowground compartments of the tree on biotic interactions. This makes it a good platform to investigate multitrophic interactions (Figure 3).

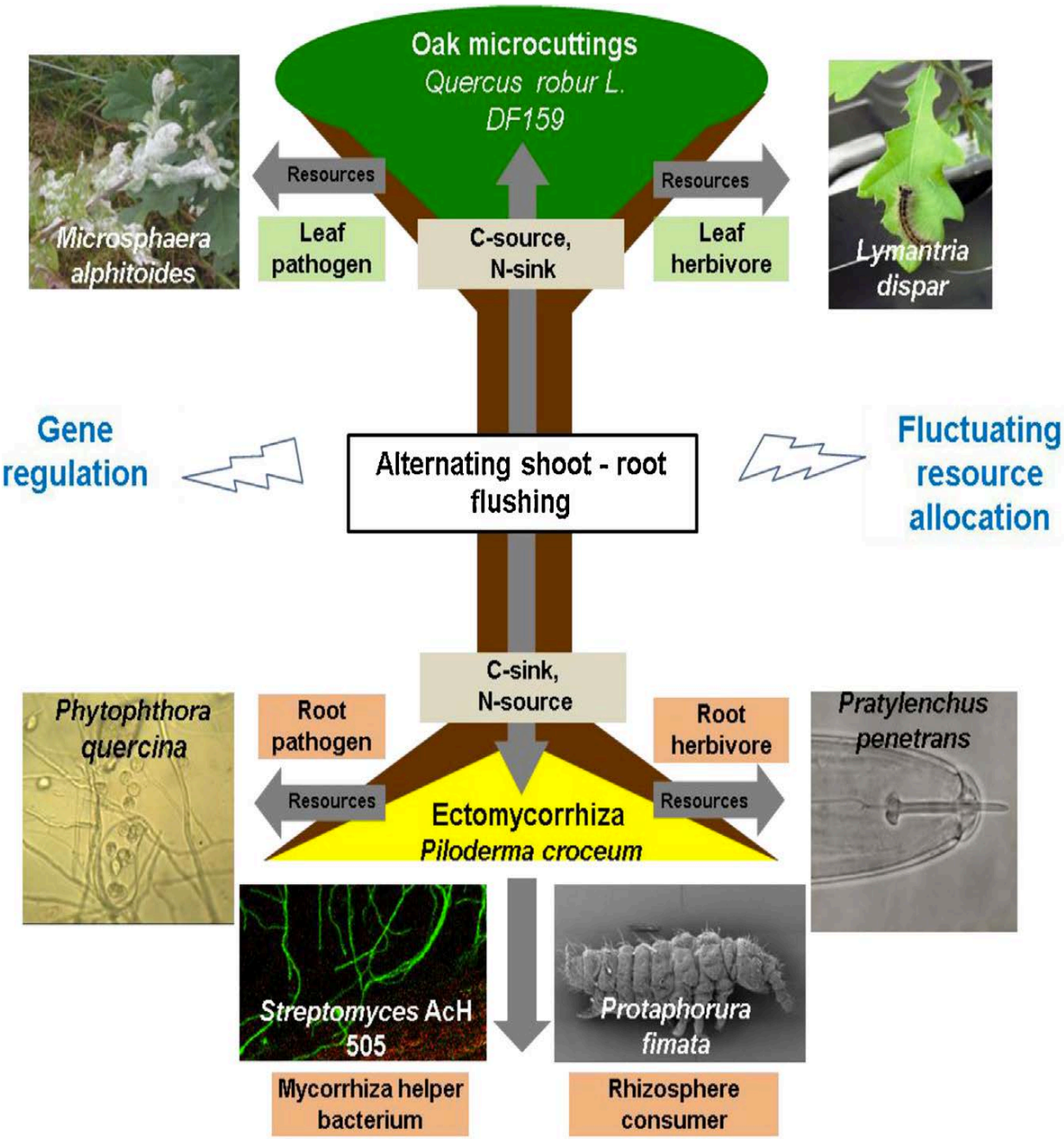

Figure 3 Schematic illustration of the TrophinOak project concept. The trees are considered as a double C and N pump fluctuating during the phases of the endogenous rhythmic growth. In addition above- and belowground biotic interactors demand and influence the resource shifts (Herrmann et al., 2015)

1.5 Objectives of the study

This thesis work tries to disentangle the underlying mechanisms in the interaction of pedunculate oak (*Quercus robur* L.) with the migratory endoparasitic nematode *Pratylenchus penetrans* Cobb. It investigates the molecular and physiological responses of oaks to nematode infection and how the tree, in turn, influences belowground processes by exerting its endogenous control of nutrient allocation. This work attempts to address the complexity of rhizosphere interactions by incorporating soil organisms at different trophic levels, and to determine how they affect each other as well as tree's fitness. The main goals were to assess: (1) genetic, nutrient allocation and growth responses of oak to plant-parasitic nematodes; (2) effects of plant-beneficial organisms such as ectomycorrhizal fungi and mycorrhiza helper bacteria on the oak-nematode interactions; (3) changes in the allocation and flux of plant carbon induced by soil animals, and (4) effects of increasing trophic diversity (root, bacterial and fungal feeding nematodes) on rhizosphere microbial communities and plant performance. These goals were achieved by conducting laboratory and greenhouse experiments using *Q. robur* microcuttings and seedlings.

The major hypotheses were:

1. The plant-parasitic nematode induces genes associated with plant defence. These responses are modulated by the ectomycorrhizal fungus, which primes the tree against pathogen infection as well as oak´s growth stage, with a stronger impact when shoots are the main C-sink.
2. The protecting strength of rhizosphere helper bacteria is weakened by root infection by plant-parasitic nematodes; the reciprocal effects in the rhizosphere create dynamic feedbacks that are not simply additive but antagonistic.
3. The interaction between the two functional groups, root-feeding nematodes and fungal grazing Collembola, increases plant carbon allocation to roots and soil microorganisms, favouring bacteria in particular opportunistic species exploiting rhizodeposits.
4. Increasing trophic diversity in the soil micro-food web counteracts negative effects of plant-parasitic nematodes on plant growth due to fostering of the soil microbial communities that participate in nutrient mineralization.

CHAPTER TWO: MATERIALS AND METHODS

2. Microcutting investigations

An experimental culture system was established using microcuttings of pedunculate oak *Quercus robur* L. propagated and rooted from a long-term established clone DF159 (Herrmann et al., 2004; Herrmann and Buscot, 2008) to ensure genetic homogeneity and synchronized growth of the plants. The oak microcuttings display an endogenous rhythmic growth pattern (Figure 4) characterized by alternating root and shoot flushes under controlled climatic conditions allowing investigations on the impact of the endogenous growth on biotic interactions. In addition, root morphogenesis of the microcuttings is similar to that of miniaturized adult trees; therefore this warrants a comparable carbohydrate allocation in the model system (Harmer, 1990; Alaoui-Sossé et al., 1994).

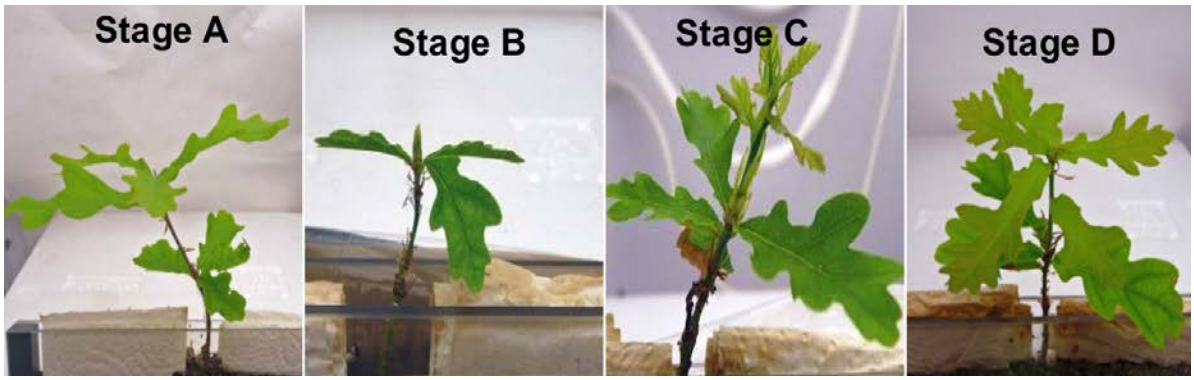

Figure 4 Developmental stages of an apical bud during an endogenous rhythmic growth cycle in microcuttings of *Quercus robur* DF159. Bud rest - stage A, Bud swelling - stage B, shoot elongation - stage C, leaf expansion - stage D. (Herrmann et al., 2015)

Herrmann et al., (1998) defined the endogenous rhythmic growth of the oak microcuttings as four distinct phases: 1) bud rest (stage A), 2) bud swelling (stage B), 3) shoot elongation (stage C), and 4) leaf expansion (stage D) shown above (Figure 4). Stage B correlates to maximal root elongation representing the root flush (RF), while stage D corresponds with maximal leaf expansion represented the shoot flush (SF) (Herrmann et al., 1998).

Tarkka et al. (2013) generated a reference library OakContigDF159.1, made up of more than 60,000 contigs differentially expressed in microcuttings of the oak clone DF159 during series of beneficial and detrimental below- and aboveground biotic interactions, including plant-

parasitic nematodes during all four oak bud developmental stages (www.trophinoak.de). This library provides support for the genetic studies on the localized and systemic responses of oaks to different biotic interactors.

2.1 The genetic, nutrient allocation and growth responses of oaks to plant-parasitic nematodes

This study investigated the interaction between oak and a migratory endoparasitic nematode, and how this plant-nematode interaction is altered by oak's endogenous rhythmic growth in the presence or absence of a mycorrhizal partner. Assessment of the systemic transcriptomic responses, nutrient allocation and growth responses of oak microcuttings were performed at root and shoot flush growth stages of the plant (stage B and stage D, respectively (Figure 4)). In addition, the study investigated the impact of the biotic interactions at the two different plant growth stages on the rhizosphere microbial communities.

2.1.1 Materials

2.1.1.1 Oak microcutting culture system

The soil medium used in the oak microcuttings microcosms was collected from an oak forest stand in Dölauer Heide (51.51016 °N, 11.91291°E) near Halle/Saale, Germany. The soil was taken separately from two layers of the upper soil horizons i.e. A0 (humus layer, 0 - 10 cm depth) and A1 + A2 (mineral soil layer, 10 - 30 cm depth). Subsamples of these two soils were then immediately frozen at -20 °C and later used to prepare a bacterial filtrate inoculum. The bulk of soil was air dried at room temperature and then sieved through 5 mm mesh to remove debris. Equal volumes of the soil taken from the two soil horizons were thoroughly mixed and 500 ml aliquots of the homogenized soil were gamma (γ) sterilized at 50 kGy by BSG Beta-Gamma-Service (Wiehe, Germany), and subsequently store at 8°C. Prior to use, the soil was subjected to sterility tests performed by plating soil aliquots on Lysogeny broth agar (LB).

Axillary and apical nodes of the oak clone DF159 were rooted according to Herrmann et al. (2004) and Herrmann and Buscot (2008). Shortly before the development of a new leaf flush,

microcuttings displaying successful rooting were transplanted into 12 × 12 cm petri dishes filled with gamma-sterilized soil substrate (one plant per microcosm) (Figure 5).

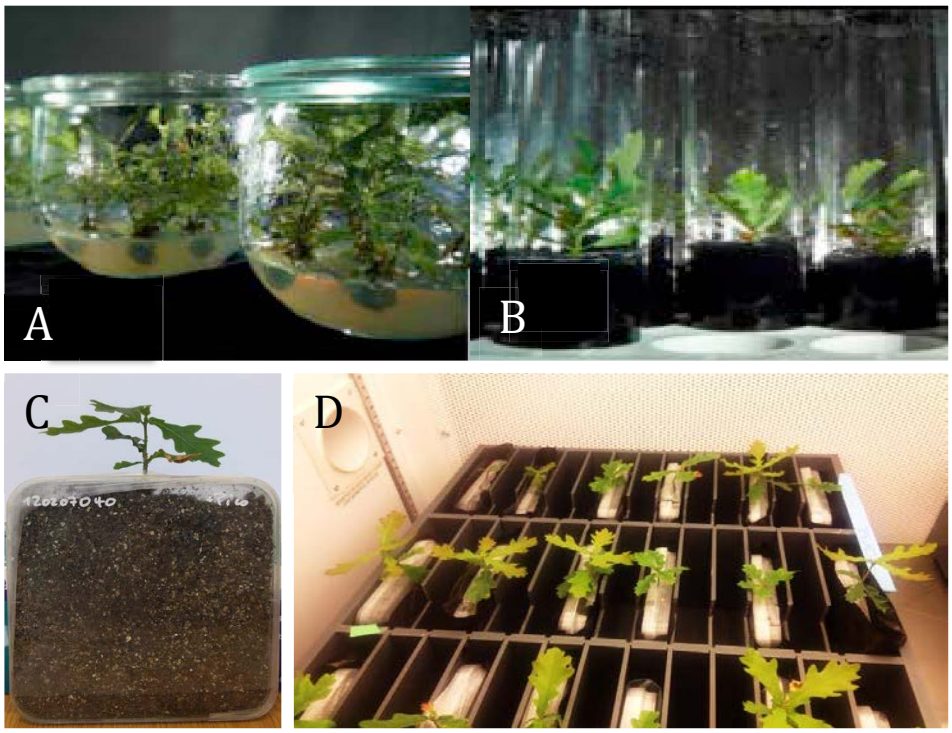

Figure 5 Oak clone DF159 microcuttings production. (Images A and B – courtesy of S. Herrmann).

Microcuttings were then grown in a climate controlled growth chamber with the following conditions: mean day/night temperature of 23°C, 16 h photoperiod with photosynthetic photon flux density of 180 μmol$m^{-2}s^{-1}$ at the leaf level, 400 ppm CO_2 and 80% relative humidity for the duration of the experiment and bud development was characterized bi-weekly. Five weeks after transplant, each oak microcosm irrespective of treatment received 5 ml of a diluted (1/1000) fresh bacterial filtrate, evenly pipetted in the soil, to restore the native bacterial community in the γ-sterilized soil. The bacterial filtrate was prepared following a protocol described by Rosenberg et al. (2009) to eliminate fungi and protozoa.

2.1.1.2 Plant-parasitic nematode

Pratylenchus penetrans Cobb referred to as the lesion nematode was chosen as a model for soil plant-parasitic nematodes (Figure 6). It is an economically important nematode with global distribution, polyphagous > 400 plant host species including *Q. robur* and with destructive parasitic habits (Castillo and Volvas, 2007). *P. penetrans* migrates intracellularly

within the plant root tissues causing extensive physical damage to roots, predominantly necrotic lesions (Zunke, 1990; Perry and Moens, 2006). This nematode remains vermiform throughout its life cycle; it feeds and reproduces within the plant with all stages of the nematode present in roots, i.e. eggs, juveniles and adults.

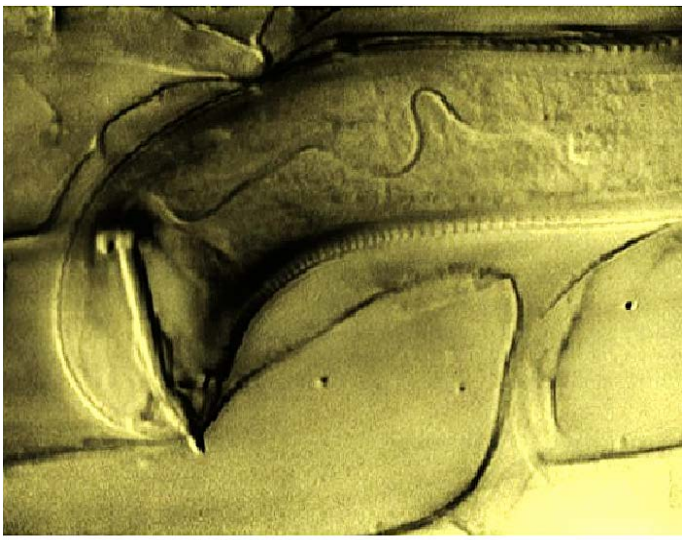

Figure 6 An image of Pratylenchus penetrans anterior region penetrating a plant root cell (Photo courtesy of Ulrich Zunke)

Axenic cultures of *P. penetrans* were established on carrot discs following a protocol described by O'Bannon and Taylor (1968). The nematode cultures were incubated in the dark at room temperature. Prior to use in experiments, nematodes were extracted from the carrot discs using wet funnel method (Baermann, 1917). Afterwards individuals were surface-sterilized by soaking in 0.01% Mercury chloride solution for 10 min and then rinsed in autoclaved Volvic water, with the washing step repeated three times. Using a light microscope, the number of individual nematodes in a known volume of water was determined. The desired nematode inoculum density per ml was achieved by adjusting the volume of water in the nematode suspension.

2.1.1.3 Ectomycorrhizal fungus

The basidiomycetes, *Piloderma croceum* J. Erikss. & Hjorts, belonging to the family of the Atheliaceae, was used as a model for the ectomycorrhizal fungus symbiotic interaction. *P. croceum* is a symbiotic partner of hardwood and conifer tree species and a frequent symbiont of oak root systems in temperate forests. Moreover, its interaction with *Q. robur* has been intensively investigated (Krüger et al., 2004; Herrmann and Buscot, 2007; Tarkka et al.,

2013). It is a late-stage fungus (Dighton and Mason, 1985) with medium distance exploration type (Rúa et al., 2016). This ectomycorrhizal fungus has a high demand for carbohydrates (Gibson and Deacon, 1990) and is a strong sink for assimilates (Herrmann et al., 1998).
The ectomycorrhizal fungus strain F1598 was cultured on modified Melin-Norkrans medium (Marx, 1969) and was incubated at 20°C in the dark as detailed in Herrmann et al. (1998). A solid fungal inoculum substrate, to facilitate even distribution of inoculum, was produced following a protocol described in Tarkka et al. (2013). In summary, the fungal liquid inoculum was added to a substrate mixture of vermiculite and sphagnum peat to produce a solid inoculum (Figure 7) and incubated at 20°C for four weeks in the dark.

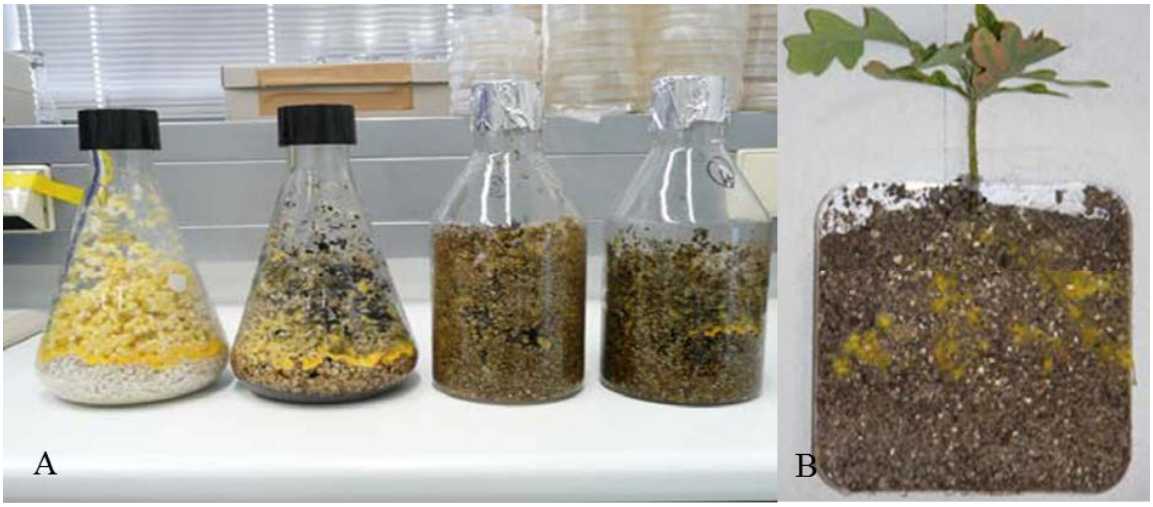

Figure 7 Image shows: A – Ectomycorrhizal fungus Piloderma croceum inoculum production and B - pedunculate oak (Quercus robur) microcutting in petri-dish culture system displaying root colonization by the ectomycorrhizal fungus *P. croceum* (Photos courtesy of S. Herrmann)

2.1.2 Experimental design

At transplant of the microcuttings to the soil-based microcosms, 120 oak microcuttings were randomly assigned to four treatments in a full factorial design: Control – no plant-parasitic nematode or ectomycorrhizal fungus, inoculated with either *P. penetrans* or *P. croceum* and inoculated with both *P. penetrans* and *P. croceum* each with 40 replicates (Figure 8). The microcuttings assigned to the ectomycorrhizal fungus and nematode × ectomycorrhizal fungus treatments were transplanted into microcosms filled with a homogenous substrate containing mixing equal volumes 1:1 (v/v) of the γ-sterilized soil and *P. croceum* inoculum substrate. In contrast, microcuttings assigned to the Control or *P. penetrans* treatments were

transplanted into microcosms filled with only γ-sterilized soil. Eight weeks after transplant, half of the plants inoculated with and without the ectomycorrhiza fungus, were then inoculated with 2 300 ± 20 individuals of *P. penetrans* nematodes per plant, done by inserting a 1ml pipette tip adjacent to microcuttings root system and releasing the nematode suspension aliquots.

Control Soil medium :1:1 (v/v) γ-sterilized soil	**Ectomycorrhizal fungus** Soil medium: 1:1 (v/v) γ-sterilized soil + *Piloderma croceum* inoculum
Nematode Soil medium:1:1 (v/v) γ-sterilized soil *Pratylenchus penetrans*	**Nematode × Ectomycorrhizal fungus** Soil medium: 1:1 (v/v) γ-sterilized soil + *Piloderma croceum* inoculum *Pratylenchus penetrans*

Figure 8 Experimental design layout used to investigate the effects of the plant-parasitic nematode *Pratylenchus penetrans* and ectomycorrhizal fungus *Piloderma croceum* on oak microcuttings

2.1.3 Stable isotope labelling

Stable isotopes of nitrogen (^{15}N) and carbon (^{13}C) were used to investigate the allocation patterns of nutrients in the oak microcuttings. Seven days post nematode inoculation, 5 ml aliquot of 0.02 L^{-1} $^{15}NH_4{}^{15}NO_3$ (98 atm % ^{15}N, Sigma, Germany) was applied to each microcutting root compartment under sterile conditions. Two days after application of the ^{15}N label, at the start of the 8 h night period, the microcuttings were transferred into a labelling chamber (Figure 9) with similar conditions to the climate chamber and allowed to acclimatize. The air of the labelling chamber was circulated through a soda lime scrubber to remove the CO_2. During the following 16 h photoperiod, $^{13}CO_2$ enriched gas containing ^{13}C atm % of 8.4 ± 0.04 (mean ± SD) (Eurisotop, Saabrücken, Germany) was introduced into the labelling chamber and the CO_2 concentration adjusted to 400 ± 2 µl L^{-1} (mean ± SD). To ensure that the atmosphere within the labelling chamber contained enriched $^{13}CO_2$ within

acceptable concentration at all times, quality control checks were performed every 4 hours using an isotope ratio mass spectrometer (Isoprime; Elementar, Hanau, Germany). The $^{13}CO_2$ pulse labelling was followed by another 8 h night period before harvesting of plants.

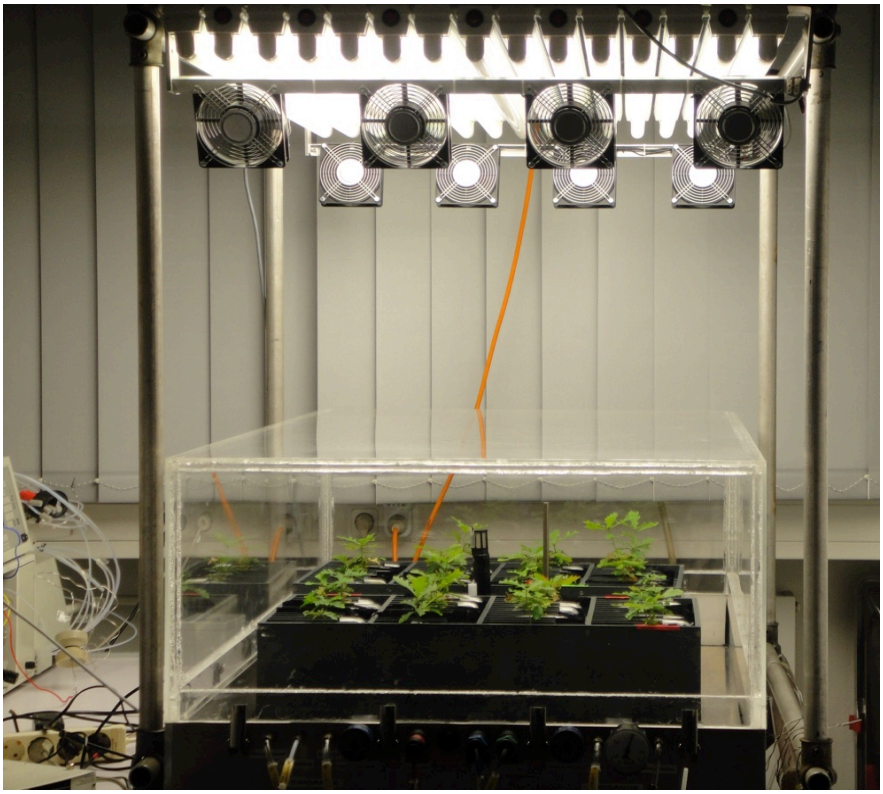

Figure 9 Oak microcuttings inside the $^{13}CO_2$ /$^{12}CO_2$ mobile labelling chamber

2.1.4 Sampling

Ten days after nematode inoculation, microcuttings were sorted according to growth stages and plants displaying bud development in B and D stages were harvested. This corresponds to three days after ^{15}N and one day after ^{13}C labelling of oaks. Destructive sampling was performed, swiftly the plant was gently removed from the soil, divided into five fractions; principal roots (PR), lateral roots (LR), stem, the terminal developed leaves i.e. source (SFt-1 and SFt-2) and sink leaves (SFt) for plants at stage B and D, respectively (Figure 10). For each plant, the leaves and roots were spread out on a white background with a scale and photographed for further analyses.

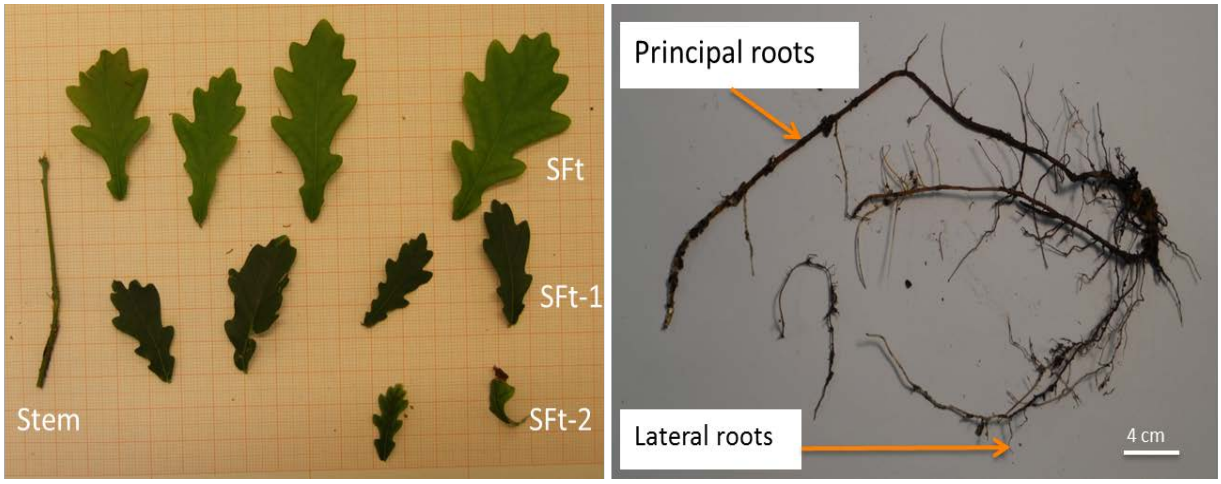

Figure 10 Image shows the different plant organs of oak microcuttings used for the analyses belonging to a plant sampled during the shoot flush stage

The plant fractions were individually weighed; the leaf and root tissues were divided into two portions for transcriptomic and resources allocation patterns analyses. Approximately two thirds of the total fresh weights of terminal leaves and lateral roots for each plant was allocated for transcriptomic analyses, these were immediately individually wrapped in aluminium foil, submerged in liquid nitrogen and subsequently stored at -80 °C. The remaining plant material from each fraction was oven dried at 60 °C for 48 h. From each microcosm, the total soil was weighed and subsampled for phospholipid fatty acid analyses (8 g) and to determine the wet weight: dry weight ratio of the soil (20 g). Soil samples collected for PLFAs analyses were stored at -20 °C, while the samples for the wet weight: dry weight ratio was oven dried at 60 °C for 48 h.

2.2 Interrelationships between plant-parasitic nematodes and beneficial rhizosphere microorganisms

This study investigated the interrelationships between plant-parasitic nematodes and mycorrhizal helper bacteria in the rhizosphere of oak microcuttings and the effect of their interactions on oak microcuttings as well as how these interactions shape the rhizosphere microbial communities structure.

2.2.1. Materials

Q. robur microcuttings and *P. penetrans* were cultured and prepared as described in Chapter **2.1.1.1** and **2.1.1.2**. In this study all the oak microcuttings were inoculated with the ectomycorrhizal fungus *P. croceum* during establishment of the microcosms (see **2.1.1.3**).

2.2.1.1 Mycorrhizal helper bacteria

The mycorrhiza helper bacterium *Streptomyces* sp. AcH 505 (Figure 11), a gram-positive filamentous Actinobacteria, was used as a beneficial organism to trees. Pure cultures of *Streptomyces* sp. AcH 50 isolated from the soil around Norway spruce mycorrhizas in Haigerloch, Germany (Maier et al., 2004), were grown on ISP2 agar medium (Shirling and Gottlieb, 1966). Prior to use the *Streptomyces* AcH 505 culture was centrifuged to pellet the cells and then re-suspended in distilled water to a concentration of 10^8 colony forming units (CFU) ml^{-1}.

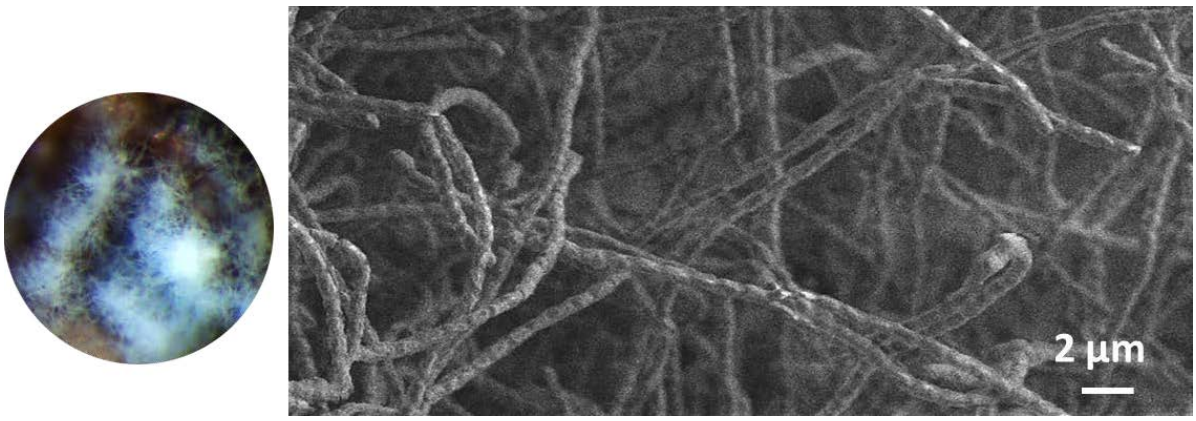

Figure 11 *Streptomyces* sp. AcH 505 on soil particles in the microcosm (Kurth et al. 2013)

2.2.2 Experimental design

Ninety-six microcuttings were randomly assigned to four treatments each with 24 replicates, in a full factorial design: Control – no application of biotic interactors, inoculated with either *P. penetrans* or *Streptomyces* sp. AcH 505 or both (Figure 12). Twenty-four days post establishment of the microcuttings in the microcosms, plants assigned to the mycorrhizal

helper bacteria and nematode × mycorrhizal helper bacteria treatments were inoculated with 2.5×10^7 CFU of the *Streptomyces* sp. AcH 505 bacterial suspension, evenly pipetted into the soil of each plant. Ten days later (five weeks after establishment of microcuttings) 4 200 ± 50 individuals of *P. penetrans* were evenly pipetted into the soil of each plant assigned to the nematode and nematode × mycorrhizal helper bacteria treatments.

Control Soil medium: 1:1 (v/v) γ-sterilized soil + *Piloderma croceum* inoculum	**Nematode** Soil medium: 1:1 (v/v) γ-sterilized soil + *Piloderma croceum* inoculum *Pratylenchus penetrans*
Mycorrhizal helper bacteria Soil medium: 1:1 (v/v) γ-sterilized soil + *Piloderma croceum* inoculum *Streptomyces* sp. AcH 505	**Nematode × Mycorrhizal helper bacteria** Soil medium: 1:1 (v/v) γ-sterilized soil + *Piloderma croceum* inoculum *Pratylenchus penetrans* + *Streptomyces* sp. AcH 505

Figure 12 Experimental design layout used to investigate the effects of the interrelationships between the plant-parasitic nematode *Pratylenchus penetrans* and mycorrhizal helper bacteria *Streptomyces* sp. AcH 505 in the rhizosphere on oak microcuttings

2.2.3 Sampling

Since both the nematode and helper bacteria are root-associated organisms for this study we compared stage A (bud rest), which is correlated with little to no root growth activity, with the active root proliferation stage B (RF). Sampling was performed twice, at seven (first) and nine (second) weeks after the establishment of oak microcosms. This was at 25 and 39 days post inoculation with *Streptomyces* sp. AcH 505 and 14 and 28 days post inoculation with *P. penetrans*. At each sampling, from each treatment six microcuttings in bud rest (stage A) and root flush (stage B) developmental stages were randomly selected and harvested. Soil in each microcosm was weighed and subsamples were collected from each microcosm for quantification of *Streptomyces* sp. AcH 505 (8 g), nematodes (50 g) and phospholipid fatty acid (PLFAs; 8 g). Samples for Streptomyces AcH 505 DNA quantification were immediately submerged in liquid nitrogen and stored at -80 °C until analysis. Soil samples

for PLFA analysis were frozen at -20 °C, and stored until analysis. An additional 20 g of the soil was collected to determine the wet weight: dry weight ratio of the soil. The fresh weights of the microcuttings were recorded after which the plant material and soil samples for the wet weight: dry weight ratios of the soil were oven dried at 60 °C for 48 h and then re-weighed.

2.3 Rhizopshere carbon dynamics modulated by plant-parasitic nematodes and fungivorous Collembola

This study investigated the interrelationships between soil animals belonging to two different functional groups i.e. plant-parasitic nematodes and fungal grazing Collembola and their effect on the growth of oak microcuttings and the carbon allocation patterns in belowground microorganisms.

2.3.1 Materials

Q. robur and *P. penetrans* were cultured and prepared as described in Chapter **2.1.1.1** and 2.1.1.2. In this study all oak microcuttings were inoculated with the ectomycorrhizal fungus *P. croceum* (see **2.1.1.3**).

2.3.1.1 Collembola

Collembola of the species *Protaphorura armata* Tullberg 1869 was used as soil fungivorous animal model. Laboratory cultures were established using specimens collected from field populations close to Darmstadt (Germany). The Collembola were reared for several generations in a glass crib on a mixture of sterilized potting soil and clay pellets (3:1) on a diet of baker´s yeast at room temperature in the dark.

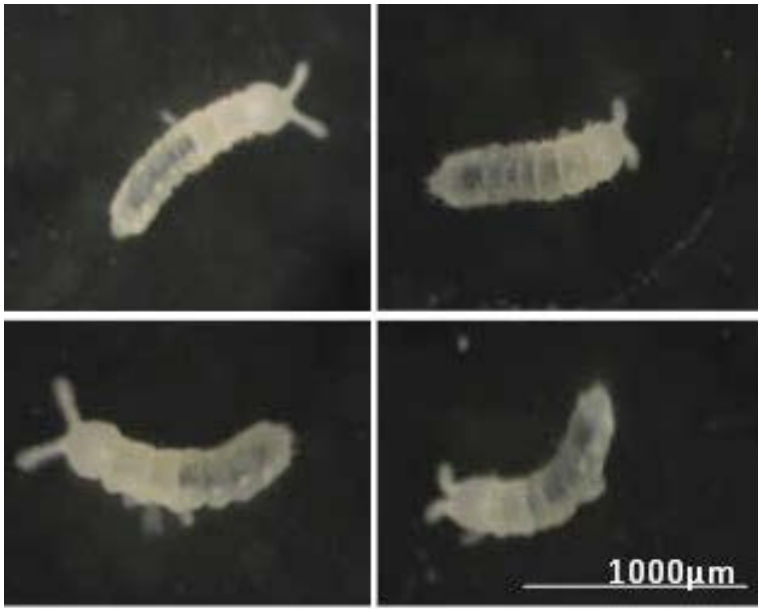

Figure 13 Images of Collembola *Protaphorura armata* (Photos courtesy of Katja Costabel)

2.3.2 Experimental design and labelling

In a complete randomized factorial design, 96 oak microcuttings inoculated with an ectomycorrhizal fungus were assigned to four treatments each with 24 replicates i.e. Control - no application of biotic interactors, inoculated either with *P. penetrans* or *P. armata* or both (Figure 14). Six weeks after establishment of oak microcuttings, depending on the assigned treatment plants were inoculated with 10 000 ± 50 individuals of *P. penetrans*, 90 ± 5 individuals of *P. armata* (equates average density for temperate forest soils) or both. The experiment was carried out in a climate chamber under the same controlled conditions described above (see **2.1.1.1**).

Treatment: Control Soil medium: 1:1 (v/v) γ-sterilized soil + *Piloderma croceum* inoculum	**Treatment: Nematode** Soil medium: 1:1 (v/v) γ-sterilized soil + *Piloderma croceum* inoculum *Pratylenchus penetrans*
Treatment: Collembola Soil medium: 1:1 (v/v) γ-sterilized soil + *Piloderma croceum* inoculum *Protaphorura armata*	**Treatment: Nematode × Collembola** Soil medium: 1:1 (v/v) γ-sterilized soil + *Piloderma croceum* inoculum *Pratylenchus penetrans* + *Protaphorura armata*

Figure 14 Experimental design layout used to investigate the effects of interrelationships between the plant-parasitic nematode *Pratylenchus penetrans* and Collembola *Protaphorura armata* in the rhizosphere on oak microcuttings

2.3.3 Pulse labelling of oaks

Ten days post animal inoculation; ^{13}C isotopic labelling was applied to half the plants from each treatment using the $^{13}CO_2$ pulse labelling procedure described in **2.1.3**. Replaced CO_2 in the labelling chamber contained 8.3 ± 0.2 atm % $^{13}CO_2$ and the microcuttings were exposed to the $^{13}CO_2$-enriched atmosphere for a complete 16 h photoperiod, with the CO_2 concentration adjusted to 400 ± 2 µl L^{-1} (mean ± SD). The ^{13}C labelled microcuttings were then transferred to a separate controlled climate growth room with identical conditions as that of the climate chamber with the non-labelled microcuttings described in Chapter **2.1.1.1** for the remaining duration of the experiment to prevent gaseous exchange between labelled and non-labelled plants.

2.3.4 Sampling

Destructive sampling of the oak microcuttings was performed at 2, 5 and 20 days post $^{13}CO_2$ labelling. Four replicates of non-labelled and labelled plants (mixed growth stages) from each treatment were randomly selected at each sampling time, weighed and separated into shoot and root tissues. The roots were then divided into two portions used for the ^{13}C bulk analyses and to quantify nematode infection of roots. The shoots and root portion for ^{13}C bulk analyses

were oven dried 60°C for 48 h. Collembola were retrieved from the soil by hand sorting using a brush. The specimens were stored in HPLC grade methanol at -20°C until lipid analysis. The soil from each microcosm was weighed and subsamples were collected for PLFA analyses (8 g) soil wet weight/dry weight ratio determination (20 g) and nematode quantification (50 g). Soil samples for PLFAs extraction were frozen immediately at -20°C until analysis.

2.4 Impact of multitrophic interactions on oak growth and rhizosphere microbial community

This study was conducted to investigate interrelationships between soil nematodes belonging to two trophic levels of the soil micro-food web with different functions i.e. plant-parasitic nematodes (primary consumers) and bacterial and fungal feeding nematodes (secondary decomposers) and how they in turn influence the overall fitness of the oaks. This experiment was performed using of oak seedlings grown under semi-natural conditions in a greenhouse.

2.4.1 Materials

2.4.1.1 Soil

Soil [composite sandy soil: sand 94%; silt 5%; clay 2%; pH 5.75] was collected from a biodiversity experimental site in Kreinitz (51°23'10" N, 13°15'43" E), Germany. The soil was air dried at room temperature and then gently sieved through a 1 mm mesh to remove debris and macrofauna, which was followed by defaunation of the soil. A modified freeze-thaw method (Poll et al., 2007) was used to defaunate the soil, here the soil was frozen at -20 °C for 48 h, allowed to thaw and stand at room temperature for 7 days, before repeating the process.

2.4.1.2 Production of oak seedlings

Q. robur acorns collected from the previous fall season purchased from Staatsklenge Nagold (Baden-Würtemberg, Germany) were used. Acorns were surface sterilized in a 1% aqueous

solution of sodium hypochlorite and germinated in trays filled with rinsed autoclaved sand in a climate chamber at 23°C, 65-70 % humidity, 16/8 h light/dark regime, 180µmol $m^{-2}s^{-1}$light intensity and 400 ppm CO_2. Ten-week-old oak seedlings were individually transplanted into 1 L pots filled with 1 kg of non-sterile defaunated soil inoculated with the ectomycorrhiza fungus *P. croceum*. Transplanted oak seedlings were transferred and kept in a greenhouse with 16/8 h light/dark regime and ambient temperature and CO_2 conditions for the duration of the experiment (Figure15). The oaks seedlings were watered regularly and fertilized once a week with NPK-fertilizer (Nitrogen: Phosphate: Potassium as 8:8:6) diluted to 150mg L^{-1}.

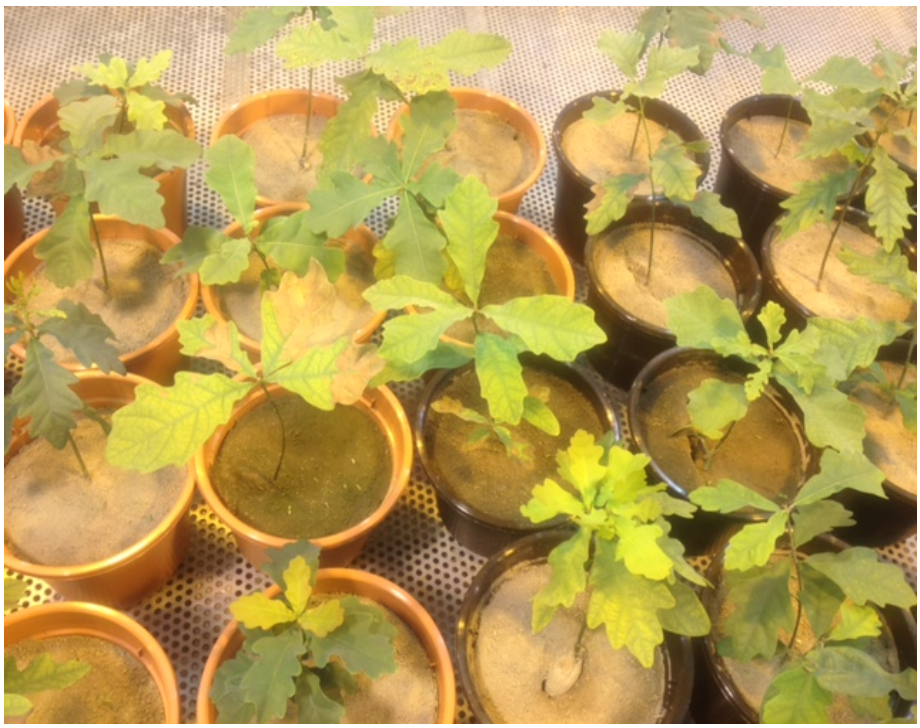

Figure 15 *Quercus robur* seedlings four weeks after transplanting into pots

2.4.1.3 Bacterial feeding nematode

Acrobeloides buetschlii De Man 1884 was used as a model for bacteria grazers in the soil. Stock cultures established from specimens isolated from a Sitka spruce (*Picea sitchensis* (Bongard; Carrière)) stand in northwest England. In the laboratory, cultures of *A. buetschlii* were maintained on PDA (potato dextrose agar, Carl Roth GmbH, Germany) plates with the decomposer fungus *Chaetomium globosum* (Kunze 1817) incubated at 15°C in the dark.

2.4.1.4 Fungal feeding nematode

The nematode *Aphelenchoides saprophilus* Franklin 1957, which feeds on fungi, was used as a model for fungal grazers in the soil. Monoxenic cultures established from specimens originally isolated from an organic layer (O_l + $_f$/O_h) of a *Picea abies* (Linné 1753) stand in east Belgium in the Haute Ardenne region were grown in the laboratory. Monoxenic cultures of the fungal-feeding nematode were reared on fungal mat of the basidiomycetes *Laccaria laccata* (Scopoli 1772; Cooke 1884) cultured on Pachlewska agar plates (Pachlewska 1968) and incubated at 15°C in the dark.

2.4.1.5 Plant-parasitic nematode

Similar to the above studies *P. penetrans* was used as the model for plant-parasitic nematodes infecting forest trees (see **2.2.1.2**).

2.4.2 Experimental design

Four weeks after establishing the oak seedlings in pots, 96 plants were randomly assigned to eight treatments each with 12 replicates in a full factorial design: Control – no nematode inoculated, inoculated with *A. buetschlii* (BF), *A. saprophilus* (FF), *P. penetrans* (PF) and their co-inoculations, i.e. (BF + FF), (BF + PF), (FF + PF) and (BF + FF + PF) (Figure 16). Depending on the treatment assigned, a suspension containing either 600 ± 30 individuals of *A. buetschlii* or 1500 ± 70 individuals of *A. saprophilus* or 1000 ± 50 individuals of *P. penetrans*, or both or all was evenly pipetted into the soil.

Control Soil medium: defaunated forest soil + *Piloderma croceum* inoculum	**BF** Soil medium: defaunated forest soil + *Piloderma croceum* inoculum *Acrobeloides buetschlii*
FF Soil medium: defaunated forest soil + *Piloderma croceum* inoculum *Aphelenchoides saprophilus*	**PF** Soil medium: defaunated forest soil + *Piloderma croceum* inoculum *Pratylenchus penetrans*
BF + FF Soil medium: defaunated forest soil + *Piloderma croceum* inoculum *Acrobeloides buetschlii + Aphelenchoides saprophilus*	**BF + PF** Soil medium: defaunated forest soil + *Piloderma croceum* inoculum *Acrobeloides buetschlii + Pratylenchus penetrans*
FF + PF Soil medium: defaunated forest soil + *Piloderma croceum* inoculum *Aphelenchoides saprophilus +Pratylenchus penetrans*	**BF + FF + PF** Soil medium: defaunated forest soil + *Piloderma croceum* inoculum *Acrobeloides buetschlii + Aphelenchoides saprophilus + Pratylenchus penetrans*

Figure 16 Experimental design layout used to investigate the effects of multitrophic interactions in the soil of oak seedlings. BF – inoculated with *Acrobeloides buetschlii*, FF – inoculated with *Aphelenchoides saprophilus,* PPN – inoculated with *Pratylenchus penetrans*

2.4.3 Sampling

Six replicates from each treatment were destructively sampled at four and eight weeks after nematode application to assess plant biomass, root length, nematode abundance and identification and phospholipid fatty acid analysis. Each seedling was divided into shoot and roots fractions, the roots were then spread out on a white background with a scale and photographed for root length analysis. A subsample of roots (0.5 g) was then collected from each replicate and frozen at -20°C and later checked for successful infection by *P. penetrans.* The remaining plant tissues were oven dried at 60°C for 48 h and the dry weights recorded.

The soil from each pot was weighed and subsamples were then collected for nematode quantification (50 g), soil wet weight/dry weight ratio determination (20 g) and phospholipid fatty acid (PLFA) quantification (8 g). The soil for the PLFA quantification samples was collected close to the root system and immediately stored at -20°C until analysis.

2.5 Analyses

2.5.1 Transcriptomic analyses

2.5.1.1 RNA Assay

Leaf tissue samples derived from 3-4 microcuttings at the same developmental stage per treatment were pooled to provide sufficient material for RNA resulting in 20-pooled RNA samples (RF - 4 treatments x 3 replicates) and (SF - 4 treatments x 2 replicates). RNA was extracted from the leaf tissues (50 mg) using the MasterPure Plant RNA Purification Kit (Epicentre, Hessisch Oldendorf, Germany). Gel ectrophoresis, Nanodrop1000 spectrophotometer (Thermo Scientific, Waltham, MA, USA) and Bioanalyzer 2100 (Agilent) were used to check the quality and quantity of the RNA. RNA sequencing was performed at the Beijing Genomics Institute (Hong Kong, China). 100 bp paired-end Illumina Truseq version 2 libraries were constructed and sequenced using the Illumina HiSeq2000 sequencing platform. The sequence data from this study was deposited into the NCBI Short Read Archive database as fastq files linked to a report specific BioProject termed PRJNA330761.

2.5.1.2 Read processing and analysis of differential expression

The Illumina sequenced data sets were pre-processed according to Tarkka et al. (2013). The processed Illumina reads were aligned against the reference transcriptome OakContigDF159.1 (Tarkka et al., 2013) using BOWTIE an alignment program (Langmead et al., 2009) and quantification of transcript abundances was performed using RSEM (Li and Dewey, 2011). Differences in contig expression during pairwise comparative transcriptomic profiling of leaf tissues of oak microcuttings inoculated with *P. penetrans*, *P. croceum* and co-inoculated with both (*P. penetrans* × *P. croceum*) versus the non-inoculated leaf tissues was determined using the edgeR function (Robinson et al., 2010) implemented in the Bioconductor package (Gentleman et al., 2004) in R (R core group, http://www.r-

project.org/). The fold change (FC) was calculated as the ratio of the average number of reads + 1 (to avoid 0 values) in the different biotic interactions at RF and SF growth stages. Log2-transformed values of FC were used and Benjamini and Hochberg false discovery rate (FDR) correction was performed to adjust the *P*-value. Statistical significance for differential expression of contigs during pairwise comparison was set at an FDR cut-off of 0.01. Statistical significance for GO terms and Pfams enrichment analyses was set at *P*-values of < 0.05.

The description of individual contigs was made using Blast2GO based on up to 20 hits against the NCBI NR - database (E-value 1e-5). Homologues for oak contigs were determined by performing a BLASTX search against *Arabidopsis thaliana* L. TAIR online database (http://arabidopsis.org) and hits with an E-value of at least 1e-5 alone were considered for the assignment.

Transcriptome annotation to provide information related to the function and biological process of the differentially regulated transcripts and proteins they encode using the Gene Ontology (GO) (Harris et al., 2004), Protein families (Pfam) (Punta et al., 2012) and Kyoto Encyclopedia of Genes and Genomes (KEGG) pathway (Kanehisa et al., 2014) enrichment analyses were performed with the Bioconductor package GOseq (Young et al., 2010). GOseq performs a statistical test based on a hypergeometric distribution to determine if in a given list of DE tags (e.g. genes or contigs) tags assigned to a certain category (e.g. GO terms) are significantly enriched, i.e. if they occur more frequently than expected by chance. GO is a hierarchically organized collection of functional gene sets based on a controlled vocabulary that classifies gene products at protein domains by biological process, molecular function and cellular component (Harris et al., 2004). Enriched GO terms were condensed and visualized using REVIGO (Supek et al., 2011).

2.5.2 Carbon and Nitrogen allocation patterns

Oven dried material from each plant fraction of the microcuttings as well as Collembola and soil belonging to the different treatments were weighed to obtain the total dry weight for the respective samples. The plant material was then ground to a powder using a ball mill (Mixer Mill MM 200, Retsch GmbH, Haan, Germany). Subsamples from each plant fraction (2 mg), Collembola (50 - 400 µg), and soil (33 - 35 mg) was weighed into tin capsules (HE 24005300, HEKAtech GmbH, Wegberg, Germany) and stored in a desiccator until analyses.

Plant tissues were analysed for ^{15}N and ^{13}C abundance while Collembola and bulk soil were analysed for ^{13}C.

The excess levels of ^{15}N and ^{13}C i.e. the difference between measured and natural ratios of $^{13}C/^{12}C$ and $^{15}N/^{14}N$ in the samples was analysed using combined system GVI-Isoprime isotope ratio mass spectrometer (Elementar, Hanau, Germany) coupled to an EA3000 element analyser (Euro Vector, Milan, Italy) was used to analyse the plant material. Vienna Pee Dee Belemnite was used as the standard for ^{13}C ($R = 0.0112$) and repeated measurements of a laboratory working standard gave a precision of $\delta^{13}C < 0.1$ ‰ (SD, n = 10). For ^{15}N, atmospheric nitrogen served as the primary standard ($R = 0.0037$). Stable isotope abundance is expressed using the δ-notation calculated according to Peterson and Fry (1987):

$$\delta X\ [‰] = (R_{sample} - R_{standard})/ R_{standard} \times 1000 \quad (1)$$

where X represents the heavier isotope (^{13}C or ^{15}N) and R the ratio between the heavy and light isotopes.

Excess ^{13}C and ^{15}N amount in the plant fractions was calculated as follows:

$$\text{excess } {}^{y}X_X = ((\text{atom \%}_S - \text{atom \%}_C)/ 100) \times DW \times (C\%/100) \quad (2)$$

where "excess ${}^{y}X_X$" represents the total amount of ^{13}C or ^{15}N incorporated by the labelling to the dry weight of measured sample; atom $\%_S$ is the ^{13}C atom percent of the sample; atom $\%_C$ is the ^{13}C atom percent of the unlabelled control; DW is the dry weight of the biomass for the measured sample and C% is the percentage of C in the sample.

2.5.3 Fatty acids analysis

2.5.3.1 Extraction

PLFAs were extracted from the soil following the protocol described by Frostegård et al. (1993). Concisely, using the Bligh and Dyer solvent (chloroform: methanol: citrate buffer ratio of 1:2:0.8, pH 4) lipid material was extracted from 2 g of soil (wet weight) from each replicate. The obtained lipids were then fractionated into neutral lipids, glycolipids and PLFAs on a silica column by elution with chloroform, acetone and methanol, respectively. The PLFAs were subjected to mild alkaline methanolysis and the fatty acid methyl esters (FAMEs) were extracted with hexane-chloroform. The PLFA samples were dissolved in isooctane and stored at -20ºC until analysis.

Total lipid fatty acids (TLFAs) from Collembola were saponified and methylated following the Sherlock Microbial Identification System protocol (MIDI Inc., Newark, Delaware). Lipids were saponified in a solution of sodium hydroxide-methanol at 100°C for 30 min, followed by acid methanolysis in HCl-methanol at 80°C for 10 min. FAMEs were extracted with hexane/methyl tertiary butyl ether and washed with aqueous sodium hydroxide. The lipid containing phase was transferred to sample vials and stored at -20°C until analysis.

2.5.3.2 Identification and quantification

Fatty acids methyl esters (FAMEs) analyses were performed using an Agilent 7890 gas chromatograph (GC) coupled to a flame ionization detector (FID) equipped with an HP Ultra 2 capillary column (25 m x 0.2 mm i.d., film thickness 0.33 mm) and a computer associated software (Sherlock Pattern Recognition Software, MIDI®). The GC was operated in split mode (1:100) with hydrogen as carrier gas. The oven temperature program started with 170°C, then increased by 5 °C min^{-1} to 260 °C, followed by 40 °C min^{-1} to 310 °C (hold time 1.5 min). FAMEs were identified on the basis of their retention times in comparison to a standard mixture; Methylnondecanoate (19:0) was used as internal standard for quantification.

FAMEs identity (chain length and saturation) verification was performed using gas chromatograph coupled to a mass spectrometry (GC-MS), this enables identification of chromatograph retention peaks, coelution and separation of targets from matrix (Rosenfeld, 2002). Representative samples were analysed by the Agilent Series 7890A GC system and a Mass Selective Detector (Agilent 7000 Triplequadrupole) equipped with HP5MS capillary column (30 m x 0.25 mm i.d., film thickness 0.25 mm), operated in splitless mode with helium as carrier gas. Oven temperature program started with 40 °C and then increased by 46 °C min^{-1} to 200 °C, followed by 5 °C min^{-1} to 238 °C and 120 °C min^{-1} to 295 °C and 2 °C min^{-1} to 300 °C, held for 2 min. The transfer line temperature was 280 °C and mass range of 40-400 m/z (mass-to-charge ratio) was monitored twice a second in scan mode.

2.5.3.3 Biomarkers

Microbial communities were assigned using FA biomarkers for major groups. PLFAs i14:0, i15:0, a15:0, i16:0 G, i16:0, 16:1ω5, 16:1ω7, 16:0 10-meth, i17:0, a17:0, cy17:0, 17:0 10-meth, 18:1ω9t, 18:0 10-meth and cy19:0 represent bacteria according to Frostegård et al. (1993) and Zelles (1999). Further, the iso/anteiso methyl-branched fatty acids are considered

as markers for Gram-positive and cyclic forms for gram-negative bacteria, whilst 10-methyl-substituted fatty acids are characteristic for actinobacteria (Frostegård and Bååth, 1996; Stromberger et al., 2012; Bird et al., 2011). PLFAs 18:1ω9 and 18:2ω6,9 generally represent fungi according by Frostegård and Bååth (1996). In support, an analysis of the PLFA pattern of the ectomycorrhizal fungus *P. croceum* from axenic cultures was performed and revealed that 18:1ω9 was the most dominant fatty acid (43% of total PLFAs), followed by 18:2ω6,9 (17% of total PLFAs). The PLFA 20:4ω6c is indicative for animal biomass, i.e. nematodes and Collembola. The response of microorganisms to carbon fluxes was assessed by the fungal/bacterial ratio calculated by dividing the amount of fungal origin PLFAs (sum of PLFAs 18:2 ω6,9 and 18:1ω9) by the estimated sum of all bacterial specific PLFAs.

2.5.3.4 Compound-specific carbon isotopic ratios

Gas-chromatography-combustion-isotope-ratio-monitoring-mass spectrometer system (GC-C-IRM-MS) was used to determine the isotopic ($^{13}C/^{12}C$) composition of individual fatty acids. The system consisted of a gas chromatograph (6890 Series, Agilent Technology, Minnesota, USA) coupled via a Conflow II interface (ThermoFinnigan, Bremen, Germany) to a MAT 252 mass spectrometer (ThermoFinnigan, Bremen, Germany). A polar capillary column (VF-23ms: 30 m, 0.25 mm i.d., film thickness: 0.25 µm) was used for the separation of FAMEs. A volume of 2 µl was injected in splitless mode and helium was used as carrier gas. The temperature program was set as follows: 60 °C, 2 min isotherm, 6 °C min^{-1} to 140 °C; 2 °C min^{-1} to 150 °C, 1 °C min^{-1} to 160 °C, 4 °C min^{-1} to 180 °C, 10 °C min^{-1} to 230 °C and held for 5 min. For the identification of FAs a fatty acid methyl standard (Suppelco 37 Component FAME Mix, Lot 47885-U) was employed. The carbon isotope composition is reported in δ-notation (‰) relative to Vienna Pee Dee Belemnite standard (V-PDB) according to:

$$\delta^{13}C\ [‰] = (({}^{13}C/{}^{12}C)_{sample} / ({}^{13}C/{}^{12}C)_{standard} - 1) \times 1000.$$

The measured isotope ratios of FAMEs were corrected for the carbon isotope ratio of the methyl moiety using the formula of Abraham et al. (1998):

$$\delta^{13}C_{FA} = [(n_{FA} + 1) \times \delta^{13}C_{FAME} - \delta^{13}C_{MeOH}] / n_{FA}$$

where $\delta^{13}C_{FA}$ is the $\delta^{13}C$ of fatty acid, n_{FA} is the number of carbon atoms of the fatty acid, $\delta^{13}C_{FAME}$ is the $\delta^{13}C$ of the fatty acid methyl ester in the sample, and $\delta^{13}C_{MeOH}$ is the $\delta^{13}C$ of the methanol used for methylation (-38.13 ‰).

The ^{13}C incorporation into fatty acids of soil microorganisms and Collembola was assigned as ^{13}C atom percent in fatty acids in the pulse labelled samples in excess to those in the non-labelled samples as follows:

$^{13}C\text{-}FA = [(\text{atom } ^{13}C\ \%)\ FA_{\text{labelled}} - (\text{atom } ^{13}C\ \%)\ FA_{\text{unlabelled}}] \times FA$

where ^{13}C FA is the amount of ^{13}C incorporated into individual FAs (μmol ^{13}C g^{-1} soil or animal dry weight) and the (atom ^{13}C %) FA_{labelled} and (atom ^{13}C %) $FA_{\text{unlabelled}}$ the atom ^{13}C % of individual FAs in labelled and unlabelled samples, respectively. The relative abundance of ^{13}C in individual FAs ($^{13}C\text{-}FA_{\text{individual}}$) was calculated as:

$^{13}C\% = {}^{13}C\text{-}FA_{\text{individual}} / \sum {}^{13}C\text{-}FA_{\text{individual}} \times 100$

2.5.4 Root and Shoot length analyses

Images of the plant organs taken at harvest (**2.1.1** and **2.1.4**) were analysed using WinFolia and WinRhizo Pro software (Regent Instrument Inc., Canada) to determine the leaf area and root length of the oak microcuttings, respectively.

2.5.5 Nematode quantification

Nematodes were extracted from soil using a modified Baermann method described by Ruess (1995). Extraction started at room temperature (18°C) for 24 h and temperature was gradually increased hourly by 5°C starting with 20°C to 45°C. Nematodes were preserved in 4% formaldehyde and total numbers of nematodes from all treatments replicates were counted under a light microscope (Carl Zeiss Axiolab) using 50x magnification. Nematodes were identified to genus level according to Bongers (1988) and assigned to their respective trophic groups according to the feeding habits and life history characteristics (Yeates et al. 1993).

To quantify the number of plant-parasitic nematodes in roots of the oak microcuttings, roots were stained with acid fuchsin. For this, the roots were boiled for 3 min in 0.8 % acetic acid and 0.013 % acid fuchsin, washed with running tap water and then destained in acid glycerol according to Byrd et al., (1983). Quantification was done using a stereomicroscope at 50x magnification.

2.5.6 Quantification of Streptomyces sp. AcH 505

The amount of *Streptomyces sp*. AcH 505 was estimated from soil samples by quantitative real-time PCR (Smith and Osborn, 2009) according to Kurth et al. (2013) with primers targeting the intergenic region between the *gyrA* and *gyrB* genes of the AcH 505 genome. Briefly, total DNA was extracted from soil samples and DNA quantity and quality were estimated using a spectrophotometer and agarose gel electrophoresis. Real-time PCR was performed and template abundances were determined based on the Ct values.

2.6 Statistical analysis

Data were analysed using the STATISTICA package 9.0 for Windows (StatSoft, Hamburg). Prior to any analyses, the fitting of the data to a normal distribution for all assessed parameters was tested with the Shapiro-Wilks test (significance level at $P < 0.05$) and homogeneity of variance was tested using the Levene's test (significance level at $P < 0.05$).
For the first experiment (Chapter **2.1**) the effects of biotic interactors i.e. *P. penetrans* ($n = 2$) and *P. croceum* ($n = 2$) and the plant's endogenous rhythmic growth pattern (n = 2) on the oak microcuttings growth parameters, carbon and nitrogen allocation patterns and the rhizosphere microbial biomass were tested using three-way analysis of variance (ANOVA). Post hoc mean separation was performed by the Tukey's HSD test (significance level at $P < 0.05$). Multivariate analysis of variance (MANOVA) on the effects of *P. penetrans* ($n = 2$) and *P. croceum* ($n = 2$) on the dominant fatty acid concentrations was performed to determine shifts in the microbial community pattern. Discriminant function analysis (DFA) was performed with the PLFAs ($n = 15$), as response variables and the biotic treatments as groups ($n = 4$) during both RF and SF growth stages. The canonical scores of the first and second discriminant functions were correlated with the PLFAs and the Pearson coefficients are provided.
For the second experiment (Chapter **2.2**) the effects of the interrelationship between *P. penetrans* ($n = 2$), the beneficial mycorrhizal helper bacteria Streptomyces AcH 505 ($n = 2$) and the growth stage of oaks ($n = 2$) were tested by a three-way ANOVA and post hoc mean separation was performed by the Tukey's HSD test, calculated at $P < 0.05$. Data were LN-transformed to achieve a normally distributed set prior to any statistical

analyses. Parameters tested were oak growth, density of nematodes, amount of helper bacteria and the abundance of soil PLFAs. Shifts in the microbial community pattern were determined using MANOVA with *P. penetrans* (n = 2), *Streptomyces* sp. AcH 505 (n = 2) and plant growth stage as categorical predictors while the concentrations of the dominant fatty acid were the respondent variables (n = 16). Post hoc mean separation was performed by the Duncan's test (significance level at $P < 0.05$).

For the third experiment (Chapter **2.3**) the effects of soil fauna i.e. *P. penetrans* (n = 2) and *P. armata* (n = 2) and the sampling data (n = 3) on the plant biomass parameters, PLFA concentrations and ^{13}C fatty acid enrichment in soil PLFAs and Collembola TLFAs were analysed by three factorial ANOVA, while two-factor ANOVA was used to assess the effects of *P. penetrans* and *P. armata* on the PLFA concentrations of the biomarker PLFAs at individual sampling times. Post hoc mean separation was performed using Tukey's HSD test at significance level $P < 0.05$. Data for the ^{13}C enrichment of lipids were arcsine square root transformed to improve normality. MANOVA on the effects of *P. penetrans* (n = 2), *P. armata* (n = 2) and sampling time (n = 3) on the dominant soil PLFAs was performed to determine shifts in the microbial community pattern. DFA was performed with the biotic interaction treatments as groups (n = 4) and the soil PLFAs (n = 13) as variables for discrimination. The canonical scores of the first and second discriminant functions were correlated with the soil PLFAs and the Pearson coefficients are provided.

For the fourth experiment (Chapter **2.4**) data were initially Log transformed to obtain normal distribution and then subjected to ANOVA with the nematode trophic group treatments (n = 8) as the independent variables. Post hoc mean separation was performed using Tukey's HSD test at $P < 0.05$ and a Dunnett's test with significance level at $P < 0.05$ was performed to check for successful manipulation of nematode community structure. Multivariate fitting was performed by MANOVA with nematode trophic treatments as the categorical predictor (n = 8) and the dominant soil PLFAs as response variables (n = 18). DFA was carried out with the nematode trophic group treatments as groups (n = 8) and individual PLFAs (n =1 8) as the dependent variables in the model. The canonical scores of the first and second roots were correlated with the PLFAs and the Pearson correlation coefficients are presented.

CHAPTER THREE: RESULTS

3.1 Genetic, nutrient allocation and growth responses of oaks to plant-parasitic nematodes

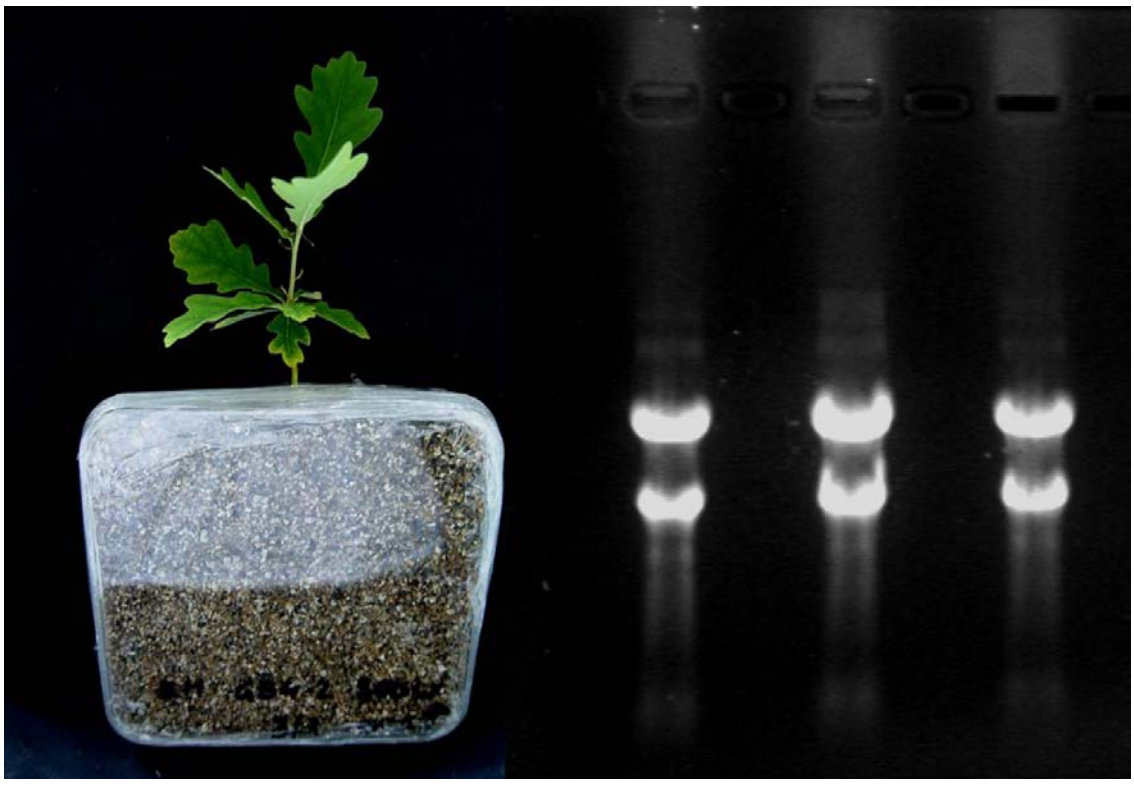

Image showing *Quercus robur* microcosm and extracted plant RNA bands on electrophoresis gel

3.1.1 Comparative gene expression profiling

An assessment of the number and the expression pattern, i.e. up- or downregulation of differentially expressed contigs (DECs), was performed to assign the systemic transcriptomic responses in leaf tissues of oak microcuttings to the plant-parasitic nematode *P. penetrans*, the ectomycorrhizal fungus *P. croceum* or both versus non-inoculated plants. The different biotic interactions provoked distinctive responses (Table 2), which were additionally modified by the oak growth stages root flush (hereinafter RF) and shoot flush (hereinafter SF).

Table 2 Overview of numbers of differentially expressed contigs (DECs), up- and downregulated, in oak microcutting leaf tissues at different plant growth stages following pairwise comparisons of plants inoculated with *Pratylenchus penetrans*, *Piloderma croceum* and co-inoculation *Pratylenchus penetrans* and *Piloderma croceum*. Data presented are for root flush and shoot flush developmental stages of oaks. Significance of differential expression was determined using a threshold of Benjamini-Hochberg adjusted $P < 0.01$ as cut off (modified from Maboreke et al., 2016)

Growth Stage	Treatment	Number of biological replicates	Total DECs	DECs upregulated	DECs downregulated
Root flush					
	P. penetrans	3	91	46	45
	P. croceum	3	118	63	55
	P. penetrans × *P. croceum*	3	543	371	172
Shoot flush					
	P. penetrans	2	895	289	606
	P. croceum	2	47	23	24
	P. penetrans × *P. croceum*	2	83	27	56

P. penetrans provoked a stronger systemic transcriptomic response in the plants as shown by a 16-fold increase in the number of DECs during SF compared to RF (Table 2). In contrast, the pattern of the oak responses to interaction with both *P. penetrans* and *P. croceum* was inverted; there was a 10-fold increase in the number of DECs during RF compared to SF (Figure 17). However, compared to the other biotic treatments the growth stage of the plants had a milder effect on the systemic response of oak microcuttings to *P. croceum*, indicated by just a single-fold increase in DECs during growth stage RF compared to SF (Table 2). Moreover, regulation of the DECs showed that during interaction with *P. penetrans* 68% of

the DECs were downregulated during SF, in comparison to 49% during RF, while in response to co-inoculation of *P. penetrans* and *P. croceum* twice as many of the total DECs (68%) were upregulated during RF compared to 32% during SF (Table 2). Irrespective of the plants growth stage, the transcriptomic response of oak to the different biotic interactions in comparison to the control was dissimilar as indicated by the apparent low overlap in co-expressed genes (Figure 17).

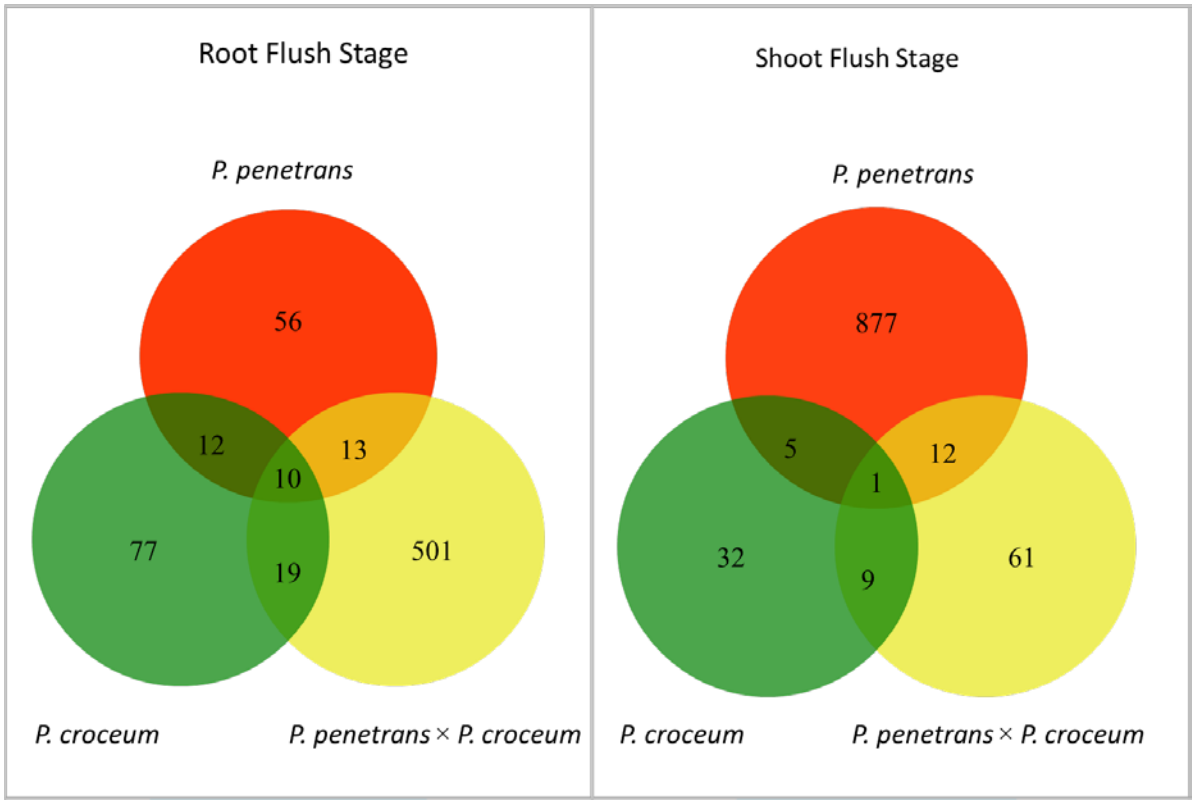

Figure 17 Venn diagrams illustrating numbers of differentially expressed contigs (DECs: Benjamini-Hochberg adjusted $P < 0.01$). The comparisons depicted are DECs on plants inoculated with *Pratylenchus penetrans*, *Piloderma croceum,* and co-inoculation of *Pratylenchus penetrans* and *Piloderma croceum* during root flush and shoot flush stages of oaks. The overlapping values correspond to the number of common DECs in comparisons (modified from Maboreke et al., 2016)

For each biotic interaction, the significantly enriched GO terms were summarized and presented as Figures 18, 19 and 20 and the top ten most significantly enriched protein families are presented in Tables 3, 4 and 5. A complimentary list of KEGG pathways enriched in up- and downregulated contigs is provided in the Appendix in table A1. The list of the contigs associated with the enriched GO terms following inoculation with *P. penetrans* and co-inoculation with *P. penetrans* and *P. croceum* is available at (https://static-

content.springer.com/esm/art%3A10.1186%2Fs12864-016-2992 8/MediaObjects/12864_2016_2992_MOESM2_ESM.xlsx), while the list of contigs associated with the enriched GO terms following inoculation with *P. croceum* solely is provided in the Appendix in table A2. A supplementary table indicating the total number of differentially expressed contigs enriching the GO categories is provided in the Appendix in Table A3.

3.1.1.1 Systemic transcriptome changes in response to *Pratylenchus penetrans*

During RF, GO terms *lipid metabolism* and *phospholipase C activity* (Figure 18a) and corresponding KEGG pathways for arachidonic acid, linoleic acid and alpha-linolenic acid metabolism (Table A1) were enriched in upregulated contigs denoting an increase in production of signalling molecules. The production of ROS was enhanced, indicated by enrichment of GO terms such as *hydroquinone oxygen oxidoreductase*, *lactoglutathione lyase activity*, *mitochondrial respiratory chain and superoxide metabolism* (Figure 18a) and Pfam terms *glutathione-S-transferase* (Table 3) for upregulated contigs. Moreover, GO terms *allene-oxide cyclase activity* a jasmonic acid pathway enzyme and *intracellular cyclic nucleotide activated cation channel activity* (Figure 18a), further point to increased signal transductions in oaks in response to *P. penetrans* during RF. Similarly, during SF GO terms such as *protein N-acetylglucosaminyltransfarase* (Figure 18c) and abundant Pfam terms *leucine rich repeats* (*LRR*) *proteins* involved in pathogen resistance signalling (Table 3) enriched in upregulated contigs indicate increased defence signalling. Consistently, KEGG pathways related to lipid metabolism and microbial metabolism in diverse environments (Table A1) all related to biosynthesis of signalling molecules and transductions were enriched in upregulated contigs during SF.

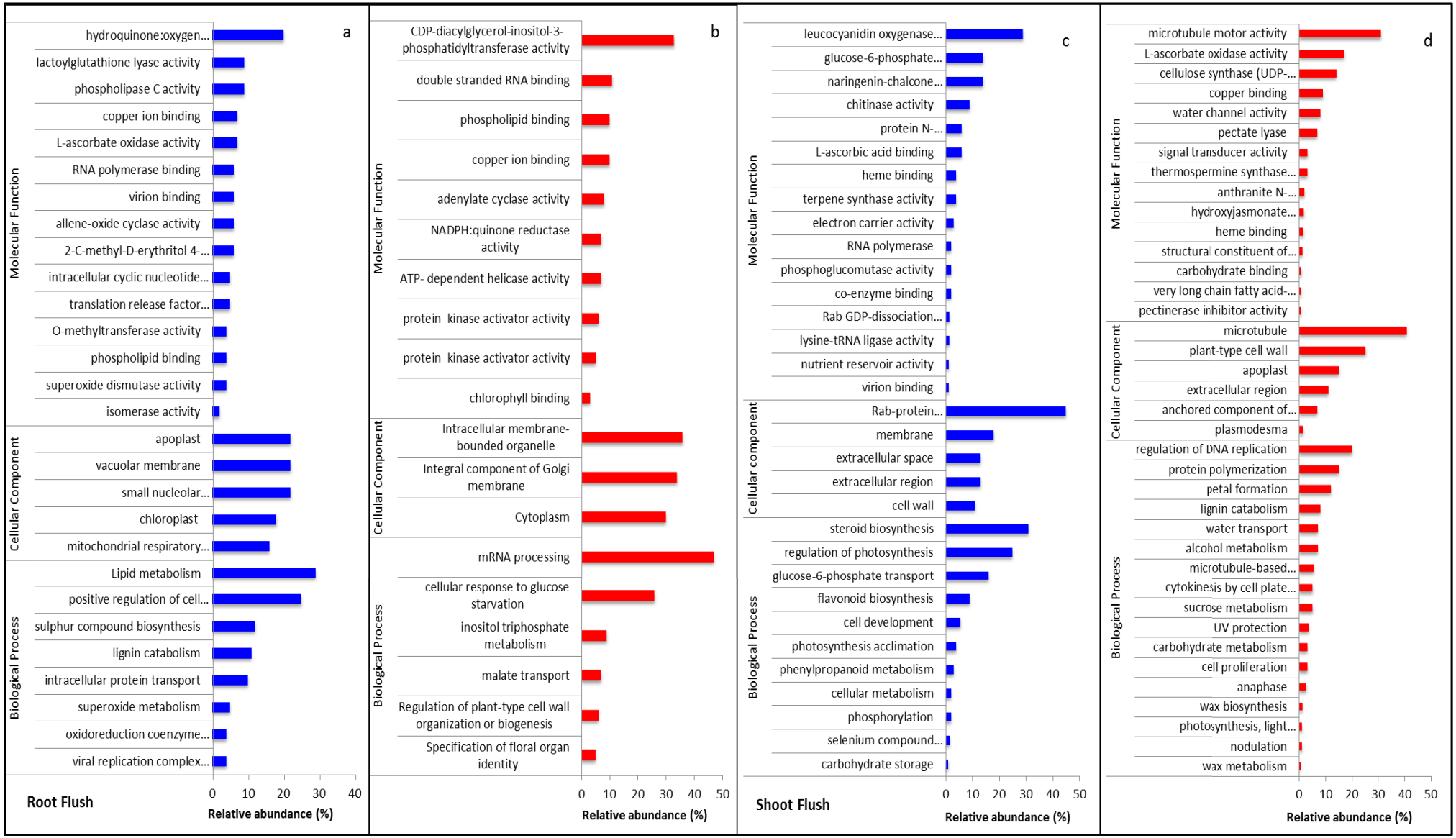
a
Molecular Function
hydroquinone:oxygen...
lactoylglutathione lyase activity
phospholipase C activity
copper ion binding
L-ascorbate oxidase activity
RNA polymerase binding
virion binding
allene-oxide cyclase activity
2-C-methyl-D-erythritol 4-...
intracellular cyclic nucleotide...
translation release factor...
O-methyltransferase activity
phospholipid binding
superoxide dismutase activity
isomerase activity
Cellular Component
apoplast
vacuolar membrane
small nucleolar...
chloroplast
mitochondrial respiratory...
Biological Process
Lipid metabolism
positive regulation of cell...
sulphur compound biosynthesis
lignin catabolism
intracellular protein transport
superoxide metabolism
oxidoreduction coenzyme...
viral replication complex...
Root Flush
0 10 20 30 40
Relative abundance (%)
b
Molecular Function
CDP-diacylglycerol-inositol-3-phosphatidyltransferase activity
double stranded RNA binding
phospholipid binding
copper ion binding
adenylate cyclase activity
NADPH:quinone reductase activity
ATP- dependent helicase activity
protein kinase activator activity
protein kinase activator activity
chlorophyll binding
Cellular Component
Intracellular membrane-bounded organelle
Integral component of Golgi membrane
Cytoplasm
Biological Process
mRNA processing
cellular response to glucose starvation
inositol triphosphate metabolism
malate transport
Regulation of plant-type cell wall organization or biogenesis
Specification of floral organ identity
0 10 20 30 40 50
Relative abundance (%)
c
Molecular Function
leucocyanidin oxygenase...
glucose-6-phosphate...
naringenin-chalcone...
chitinase activity
protein N-...
L-ascorbic acid binding
heme binding
terpene synthase activity
electron carrier activity
RNA polymerase
phosphoglucomutase activity
co-enzyme binding
Rab GDP-dissociation...
lysine-tRNA ligase activity
nutrient reservoir activity
virion binding
Cellular component
Rab-protein...
membrane
extracellular space
extracellular region
cell wall
Biological Process
steroid biosynthesis
regulation of photosynthesis
glucose-6-phosphate transport
flavonoid biosynthesis
cell development
photosynthesis acclimation
phenylpropanoid metabolism
cellular metabolism
phosphorylation
selenium compound...
carbohydrate storage
Shoot Flush
0 10 20 30 40 50
Relative abundance (%)
d
Molecular Function
microtubule motor activity
L-ascorbate oxidase activity
cellulose synthase (UDP-...
copper binding
water channel activity
pectate lyase
signal transducer activity
thermospermine synthase...
anthranite N-...
hydroxyjasmonate...
heme binding
structural constituent of...
carbohydrate binding
very long chain fatty acid-...
pectinerase inhibitor activity
Cellular Component
microtubule
plant-type cell wall
apoplast
extracellular region
anchored component of...
plasmodesma
Biological Process
regulation of DNA replication
protein polymerization
petal formation
lignin catabolism
water transport
alcohol metabolism
microtubule-based...
cytokinesis by cell plate...
sucrose metabolism
UV protection
carbohydrate metabolism
cell proliferation
anaphase
wax biosynthesis
photosynthesis, light...
nodulation
wax metabolism
0 10 20 30 40 50
Relative abundance (%)

Figure 18 Summarized GO terms enriched for differentially expressed contigs in systemic leaf tissue of oak microcuttings response to inoculation with *Pratylenchus penetrans* during root flush (RF) (a and b) and shoot flush (SF) (c and d) developmental stages of the oak microcuttings. Presented are data for the relative abundance of GO terms enriched belonging to each classification i.e. biological process, cellular component and molecular function, upregulated (blue) and downregulated (red)

Table 3 Most enriched Protein families during interaction with *Pratylenchus penetrans*. Presented are the top ten most enriched Protein families for up- and downregulated contigs in leaf tissues of oak microcuttings during root flush and shoot flush developmental stages of oaks, Protein family (Pfam) ID, Pfam term description and significance level (*P*-value) (modified from Maboreke et al., 2016)

Oak growth stage	ID	Description	*P* value
Upregulated			
Root Flush	PF05131.9	Pep3/Vps18/deep orange family	4.58E-06
	PF10433.4	Mono-functional DNA-alkylating methyl methanosulfonate N-term	1.13E-04
	PF07650.12	KH domain	9.43E-04
	PF02798.15	Glutathione S-transferase	9.85E-04
	PF00043.20	Glutathione S-transferase	1.03E-03
	PF13410.1	Glutathione S-transferase	1.05E-03
	PF07452.7	CHRD domain	1.35E-03
	PF13409.1	Glutathione S-transferase	1.35E-03
	PF02536.9	mTERF	1.64E-03
	PF13417.1	Glutathione S-transferase	1.74E-03
Shoot Flush	PF05368.8	NmrA-like family	9.92E-07
	PF13460.1	NADH(P)-binding	2.18E-06
	PF00067.17	Cytochrome P450	2.45E-06
	PF01073.14	3-beta hydroxysteroid dehydrogenase/isomerase family	4.78E-06
	PF01370.16	NAD dependent epimerase/dehydratase family	9.43E-06
	PF13504.1	Leucine rich repeat	1.04E-05
	PF00560.28	Leucine Rich Repeat	2.60E-05
	PF13855.1	Leucine rich repeat	3.79E-05
	PF13854.1	Kelch motif	4.60E-05
	PF13516.1	Leucine Rich repeat	4.96E-05
Downregulated			
Root Flush	PF14225.1	Cell morphogenesis C-terminal	1.50E-04
	PF05004.8	Interferon-related developmental regulator (IFRD)	1.85E-04
	PF08167.7	rRNA processing/ribosome biogenesis	4.64E-04
	PF06146.7	Phosphate-starvation-inducible E	9.10E-04
	PF12348.3	CLASP N terminal	1.04E-03
	PF13798.1	Protein of unknown function with PCYCGC motif	1.54E-03
	PF10248.4	Myelodysplasia-myeloid leukemia factor 1-interacting protein	2.43E-03
	PF11305.3	Protein of unknown function (DUF3107)	2.47E-03
	PF14151.1	YfhD-like protein	2.96E-03
	PF01690.12	Potato leaf roll virus readthrough protein	3.02E-03
Shoot Flush	PF07732.10	Multicopper oxidase	1.50E-14
	PF00394.17	Multicopper oxidase	1.48E-13
	PF07731.9	Multicopper oxidase	4.20E-13
	PF00225.18	Kinesin motor domain	2.17E-11
	PF00759.14	Glycosyl hydrolase family 9	2.07E-08
	PF06525.6	Sulfocyanin (SoxE)	3.46E-08
	PF00230.15	Major intrinsic protein	1.74E-07
	PF00091.20	Tubulin/FtsZ family	2.03E-07
	PF13229.1	Right handed beta helix region	4.66E-07
	PF12708.2	Pectate lyase superfamily protein	5.02E-07

Pathogen triggered defence was activated, indicated by enriched GO terms *lignin catabolism* involved in cell wall fortification during RF (Figure 18a), and *chitinase activity* and *chitinase binding* during SF (Figure 18c). Moreover, during RF the production of

secondary metabolites was induced indicated by enriched GO terms *O-methyltransferase activity* and *2-C-methyl-D-erythritol 4-phosphate cytidyltransferase activity* involved in the phenylpropanoid and isoprenoid biosynthesis pathways, respectively (Figure 18a). A large repertoire of secondary metabolites was induced, e.g. GO terms such as *steroid* and *flavonoid biosynthesis*, *leucocyanidin oxygenase activity*, *naringenin-chalcone synthase activity*, *terpene synthase activity* (Figure 18c) and Pfam term *3-beta hydroxysteroid dehydrogenase family* (Table 3). Correspondingly, KEGG pathways for biosynthesis of flavonoids and phenylpropanoid were enriched in upregulated contigs (Table A1) during SF. The enrichment of KEGG pathways for metabolism of xenobiotic cytochrome P450, drug metabolism-cytochrome P450 and aminobenzoate degradation (Table A1) in upregulated contigs during both growth stages of oak microcuttings, further points to induction of plant defence in response to *P. penetrans*.

On the other hand, some plant defence processes were repressed in response to *P. penetrans*. During RF GO terms *inositol triphosphate metabolism* and *cellular response to glucose starvation* (Figure 18b) and Pfam term *Phosphate-starvation-inducible E* (Table 3) essential for plant resistance signalling were enriched in downregulated contigs. KEGG pathways for ascorbate, aldarate and inositol phosphate metabolism (Table A1) were enriched in downregulated during RF. Similarly, during SF GO terms *pectinesterase inhibitor*, *signal transducer activity* (Figure 18d) along with Pfams *Right handed beta helix region* and *Major intrinsic protein* (Table 3) involved in pathogen elicited signalling, were enriched in downregulated contigs. KEGG pathways for linoleic acid and sphingolipid metabolism were enriched in downregulated contigs during SF (Table 1). Moreover, during RF GO terms enriched in downregulated contigs related to basal defence *mRNA processing* and *double stranded RNA binding* (Figure 18b) and corresponding Pfam *rRNA processing/ribosome biogenesis* (Table 3). While during SF GO terms *lignin catabolism* and *copper binding* (Figure 18d) and Pfam terms *Multicopper oxidase* (Table 3) were enriched in downregulated contigs indicating reduced defence responses. Consistently, KEGG pathways involved in plant defence such as glycosaminoglycan degradation, phenylpropanoid biosynthesis and phenylalanine metabolism (Table) were also enriched in downregulated contigs.

Photosynthetic processes and carbohydrate metabolism were altered in response to *P. penetrans*, yet mainly during SF. Processes related to carbohydrate metabolism were significantly altered. The enrichment of GO terms *regulation of photosynthesis* and *photosynthesis acclimation* in upregulated contigs (Figure 18 c) and the corresponding KEGG

pathways porphyrin and chlorophyll metabolism in downregulated contigs (Table A1) point to repressed photosynthesis. Moreover, during SF GO terms *glucose-6-phosphate transport*, *glucose-6-phosphate transmembrane transporter activity* and *carbohydrate storage* (Figure 18c) were enriched in upregulated contigs, while GO terms *sucrose metabolism* and *carbohydrate metabolism* (Figure 18d) were enriched in downregulated contigs. Consistently, KEGG pathways for glycolysis/gluconeogenesis, glyoxylate and dicarboxylate metabolism were enriched in upregulated contigs; while pathways such as pentose and glucuronate interconversions and galactose metabolism were enriched in downregulated contigs (Appendix 1), collectively pointing to an accumulation of glucose in terminal leaf tissues and substantial changes in carbohydrate metabolism during SF.

Additional to regulation of host defence and carbohydrate metabolism, genes related to cell growth process were differentially expressed. During RF GO term *positive regulation of cell proliferation* (Figure 18a) and corresponding Pfam term *Chordin* (CHRD) protein related to regulation of basic and vital cellular processes (Table 3) were enriched in upregulated contigs, likely an indication compensatory growth in response to *P. penetrans* infection. Contrastingly, during SF the enrichment of GO terms *protein polymerization, regulation of DNA replication* and *cell proliferation* (Figure 18d) and Pfam terms *kinesin motor domain* and *tubulin family proteins* (Table 3) in downregulated contigs points to repressed plant growth. Moreover, GO terms *cellulose synthase* (*UDP-forming*) *activity*, *plant-type cell wall* and *lignin catabolism* (Figure 18d) and the corresponding Pfam term *glycosyl hydrolase family 9* (Table 3) were also enriched in downregulated contigs. Together, all these point to repression of plant growth during SF.

3.1.1.2 Systemic transcriptome changes in response to *Piloderma croceum*

The ectomycorrhizal fungus, *P. croceum,* elicited plant signalling in leaf tissues of oak microcuttings during RF, indicated by GO terms *phospholipase C activity*, *adenylate cyclase activity* and *calcium binding* (Figure 19a) and the corresponding abundant Pfam terms *EF hand domain* and *oligopeptidase F* (Table 4) which were enriched in upregulated contigs during RF. In addition, GO terms *response to wounding*, *hydroquinone: oxygen oxidoreductase activity*, *superoxide metabolism* and *oxygen binding* induced in response to pathogens (Figure 19a) and KEGG pathways related to biosynthesis of signalling molecules such as linoleic and arachidonic acid were enriched in upregulated contigs (Table A1). Similarly, during SF signalling was enhanced via increased oxidative stress signalling

molecules indicated by the enrichment of GO terms *ATPase activity coupled* and *NADH dehydrogenase* (*ubiquinone activity*) (Figure 19c) and Pfam term *acyl-Co dehydrogenase C terminal* (Table 4) in upregulated contigs. In support, the KEGG pathway for oxidative phosphorylation was enriched in upregulated contigs during SF (Table A1).

Moreover, the enrichment of GO terms *xyloglucan: xyloglucosyltransferase* and *lignin catabolism* (Figure 19a) and the corresponding KEGG pathway for metabolism of xenobiotics by cytochrome P450 (Table A1) indicate induction of plant defence and cell wall fortification during RF. Meanwhile, during SF GO term *DNA repair*, *damaged DNA binding* and *voltage-gated potassium channel activity* (Figure 19c) and the KEGG pathway for *N-Glycan biosynthesis* (Table A1) were enriched in upregulated contigs indicating promotion of stress tolerance. Furthermore, the enrichment of Pfam term *6,7-dimethyl-8-ribityllumazine synthase,* a precursor for riboflavin biosynthesis (Table 4) and KEGG pathways for caffeine, thiamine and retinol metabolism in upregulated contigs during RF and folate biosynthesis and vitamin B6 metabolism during SF (Table A1) all point to increased antioxidant activity and stress tolerance in the oaks in response to *P. croceum*.

On the contrary, the interaction with the mycorrhizal symbiont also repressed signalling and host defence. During RF GO terms *response to stress*, *salicylic acid biosynthesis* and *phosphorylase activity* (Figure 19b) and Pfam term *carbohydrate phosphorylase* (Table 4) and the KEGG pathway for alpha-linolenic acid metabolism were enriched in downregulated contigs. While during SF, GO terms *linoleate 13 S-lipoxygenase* and *oxylipin biosynthesis* (Figure 19d) and Pfam term *lipoxygenases* (Table 4) enriched in downregulated contigs, further indicate repressed activation of host resistance responses. In support, KEGG pathways for fatty acid elongation and linoleic acid metabolism (Table A1) were enriched in downregulated contigs. Moreover, the enrichment of GO terms *mRNA processing*, *ubiquitin-protein transferase activity* and *response to herbivore* (Figure 19d) in downregulated contigs further indicates repression of oak defence in response to *P. croceum* during SF.

Generally, a repression of secondary oak defence compounds was assigned. During RF GO terms *pyridoxal phosphate binding*, *terpene synthase* and *spermidine biosynthesis* (Figure 19b) and Pfam terms *terpene synthase* and *terpene synthase family* (Table 4) and KEGG pathways for flourobenzoate, chlorocyclohexane and chlorobenzene degradation (Table A1) were enriched downregulated contigs. Similarly, during SF the enrichment of KEGG pathway for monoterpernoid biosynthesis (Table A1) in downregulated contigs indicates a repression of secondary metabolites.

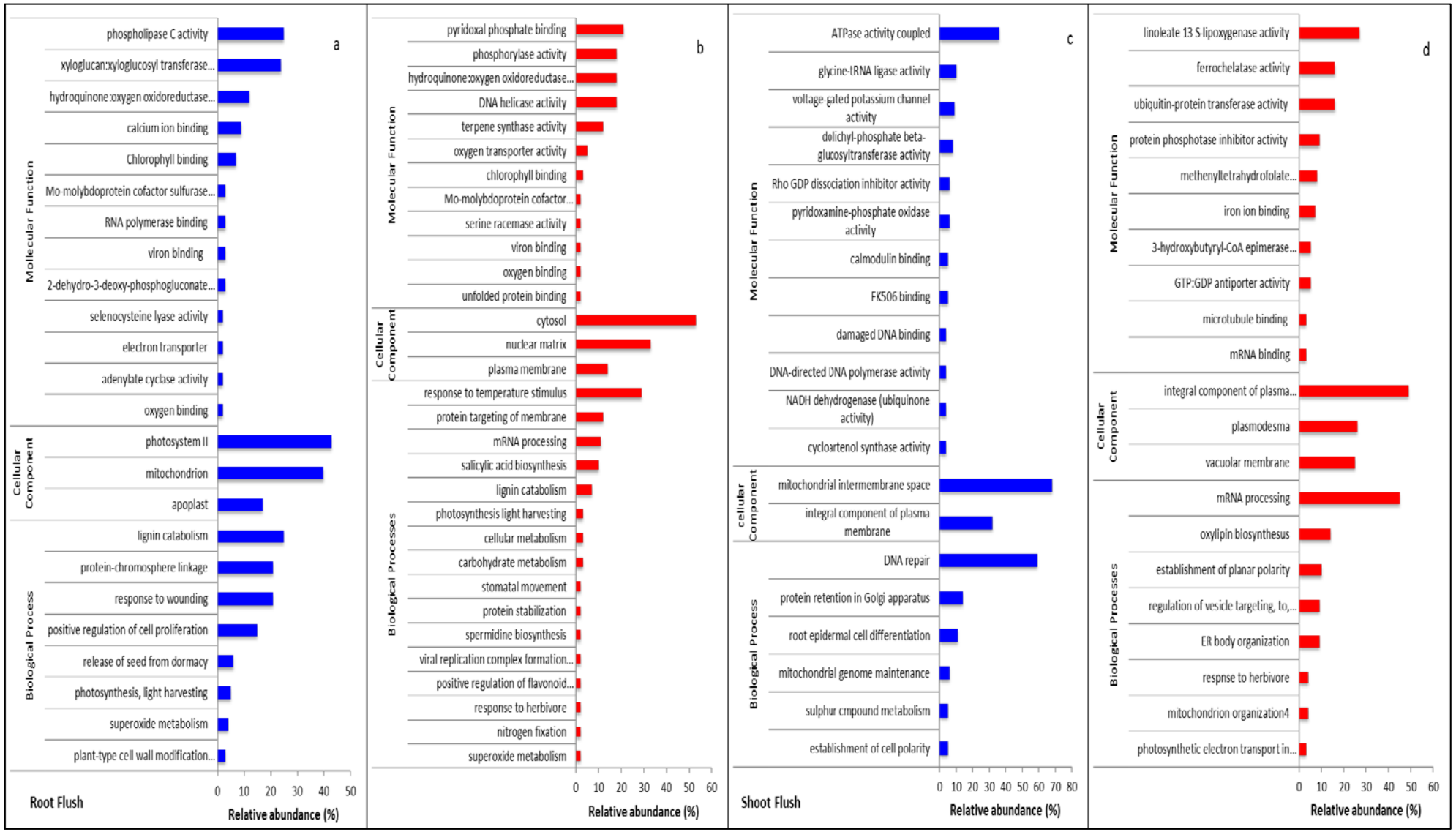
a
Molecular Function
phospholipase C activity
xyloglucan:xyloglucosyl transferase...
hydroquinone:oxygen oxidoreductase...
calcium ion binding
Chlorophyll binding
Mo molybdoprotein cofactor sulfurase...
RNA polymerase binding
viron binding
2-dehydro-3-deoxy-phosphogluconate...
selenocysteine lyase activity
electron transporter
adenylate cyclase activity
oxygen binding
Cellular Component
photosystem II
mitochondrion
apoplast
Biological Process
lignin catabolism
protein-chromosphere linkage
response to wounding
positive regulation of cell proliferation
release of seed from dormacy
photosynthesis, light harvesting
superoxide metabolism
plant-type cell wall modification...
0 10 20 30 40 50
Root Flush
Relative abundance (%)
b
Molecular Function
pyridoxal phosphate binding
phosphorylase activity
hydroquinone:oxygen oxidoreductase...
DNA helicase activity
terpene synthase activity
oxygen transporter activity
chlorophyll binding
Mo-molybdoprotein cofactor...
serine racemase activity
viron binding
oxygen binding
unfolded protein binding
Cellular Component
cytosol
nuclear matrix
plasma membrane
Biological Processes
response to temperature stimulus
protein targeting of membrane
mRNA processing
salicylic acid biosynthesis
lignin catabolism
photosynthesis light harvesting
cellular metabolism
carbohydrate metabolism
stomatal movement
protein stabilization
spermidine biosynthesis
viral replication complex formation...
positive regulation of flavonoid...
response to herbivore
nitrogen fixation
superoxide metabolism
0 10 20 30 40 50 60
Relative abundance (%)
c
Molecular Function
ATPase activity coupled
glycine-tRNA ligase activity
voltage gated potassium channel activity
dolichyl-phosphate beta-glucosyltransferase activity
Rho GDP dissociation inhibitor activity
pyridoxamine-phosphate oxidase activity
calmodulin binding
FK506 binding
damaged DNA binding
DNA-directed DNA polymerase activity
NADH dehydrogenase (ubiquinone activity)
cycloartenol synthase activity
cellular Component
mitochondrial intermembrane space
integral component of plasma membrane
Biological Process
DNA repair
protein retention in Golgi apparatus
root epidermal cell differentiation
mitochondrial genome maintenance
sulphur compound metabolism
establishment of cell polarity
0 10 20 30 40 50 60 70 80
Shoot Flush
Relative abundance (%)
d
Molecular Function
linoleate 13 S lipoxygenase activity
ferrochelatase activity
ubiquitin-protein transferase activity
protein phosphotase inhibitor activity
methenyltetrahydrofolate...
iron ion binding
3-hydroxybutyryl-CoA epimerase...
GTP:GDP antiporter activity
microtubule binding
mRNA binding
Cellular Component
integral component of plasma...
plasmodesma
vacuolar membrane
Biological Processes
mRNA processing
oxylipin biosynthesus
establishment of planar polarity
regulation of vesicle targeting, to,...
ER body organization
respnse to herbivore
mitochondrion organization4
photosynthetic electron transport in...
0 10 20 30 40 50 60
Relative abundance (%)

Figure 19 Summarized GO terms enriched for differentially expressed contigs in systemic leaf tissue of oak microcuttings in response to inoculation with *Piloderma croceum* during root flush (RF) (a and d) and shoot flush (SF) (c and d) developmental stages of the oak microcuttings. Presented are data for the relative abundance of GO terms enriched belonging to each classification i.e. biological process, cellular component and molecular function, upregulated (blue) and downregulated (red).

Table 4 Most enriched Protein families during interaction with *Piloderma croceum*. Presented are the top ten most enriched Protein families for up- and downregulated contigs in leaf tissues of oak microcuttings during root flush and shoot flush developmental stages of oaks, Protein family (Pfam) ID, Pfam term description and significance level (*P*-value)

Oak growth stage	ID	Description	*P* value
Upregulated			
Root Flush	PF03305.8	Mycoplasma MG185/MG260 protein	3.85E-03
	PF03484.10	tRNAsynthetase B5 domain	3.85E-03
	PF05131.9	Pep3/Vps18/deep orange family	3.82E-02
	PF13833.1	EF-hand domain pair	3.82E-02
	PF13202.1	EF hand	3.82E-02
	PF13405.1	EF-hand domain	3.82E-02
	PF13499.1	EF-hand domain pair	3.82E-02
	PF08439.5	Oligopeptidase F	3.82E-02
	PF00036.27	EF hand	3.82E-02
	PF02439.10	Adenovirus E3 regionprotein CR2	3.82E-02
Shoot Flush	PF02875.16	Mur ligase family	2.25E-04
	PF08245.7	Mur ligase middle domain	2.62E-04
	PF07042.6	TrfA protein	1.74E-03
	PF10013.4	Uncharacterized protein conserved in bacteria (DUF2256)	2.07E-03
	PF12432.3	Protein of unknown function (DUF3677)	2.23E-03
	PF00885.14	6,7-dimethyl-8-ribityllumazine synthase	2.54E-03
	PF11099.3	Apoptosis regulator M11L like	2.62E-03
	PF07963.7	Prokaryotic N-terminal methylation motif	2.70E-03
	PF02813.9	Retroviral M domain	2.98E-03
	PF12186.3	Acyl-CoA dehydrogenase C terminal	2.99E-03
Downregulated			
Root Flush	PF01397.16	Terpene synthase	1.67E-06
	PF06958.7	S-type Pyocin	6.55E-05
	PF12745.2	Anticodon binding domain of tRNAs	9.99E-05
	PF08507.5	COPI associated protein	1.16E-04
	PF13393.1	Histidyl-tRNAsynthetase	1.33E-04
	PF03936.11	Terpene synthase family	2.09E-04
	PF03129.15	Anticodon binding domain	3.72E-04
	PF07653.12	Variant SH3 domain	4.00E-04
	PF06241.7	Protein of unknown function (DUF1012)	5.02E-04
	PF00343.15	Carbohydrate phosphorylase	5.22E-04
Shoot Flush	PF00305.14	Lipoxygenase	7.23E-04
	PF11618.3	Protein of unknown function (DUF3250)	1.18E-03
	PF03012.9	Phosphoprotein	1.73E-03
	PF12438.3	Protein of unknown function (DUF3679)	1.89E-03
	PF12901.2	SUZ-C motif	1.92E-03
	PF02554.9	Carbon starvation protein CstA	2.45E-03
	PF10655.4	Hypothetical protein of unknown function (DUF2482)	2.63E-03
	PF09515.5	Thiamine transporter protein (Thia_YuaJ)	2.73E-03
	PF06625.6	Protein of unknown function (DUF1151)	2.74E-03
	PF02442.12	Lipid membrane protein of large eukaryotic DNA viruses	2.84E-03

Carbohydrate metabolism was altered in response to *P. croceum* indicated by the enrichment of GO terms *carbohydrate metabolism* in downregulated contigs (Figure 19c) during RF. Similarly, during SF the enrichment of Pfam term *carbon starvation protein CstA* (Table 4) and KEGG pathways for porphyrin and chlorophyll metabolism (Table A1) in downregulated contigs point to reduced carbohydrate metabolism. In addition, during SF GO terms related to

protein secretion *ER body organization*, *regulation of vesicle targeting, to, from or with Golgi* in downregulated contigs (Figure 12d) and KEGG pathway lysine degradation (Table A1), while GO term *protein retention in Golgi apparatus* was enriched in upregulated contigs (Figure 19c) pointing to repressed protein secretions.

3.1.1.3 Systemic transcriptome changes in response to *Pratylenchus penetrans* and *Piloderma croceum*

Co-inoculation of oak microcuttings with *P. penetrans* and *P. croceum* elicited defence related signalling in the leaf tissues of oak microcuttings. GO terms such as *response to biotic stimulus*, *lipid metabolism*, *inositol tetrakisphosphate-2-kinase activity* and *signal transducer* (Figure 20a) and Pfam term *probable lipid transfer* (Table 5) related to pathogen perception, were enriched in upregulated contigs. Corresponding KEGG pathways for fatty acid, linoleic and arachidonic acid as well as sphingolipid, gylcerolipid and gylcerophospholipid metabolism, all related to signalling molecules were also enriched in upregulated contigs (Table 5). Similarly, during SF the enrichment of GO terms *intracellular cyclic nucleotide activated cation channel activity* and *superoxide dismutase activity* (Figure 20c) in upregulated contigs indicates activation of signalling.

In addition, during RF GO terms *copper binding*, *plant-type cell wall organization*, *wax* and *cutin biosynthesis* (Figure 20a) and corresponding Pfam terms *multicopper oxidase* and *GDSL-like lipase/acylhydrolase* (Table 5) related to physical reinforcement of plant cell wall barrier were enriched in upregulated contigs. The induction of defence in oak microcutting was further indicated by the enrichment of KEGG pathways for metabolism of xenobiotics by cytochrome P450 and cutin in upregulated contigs (Table A1) during RF. Comparably, GO terms *aldehyde catabolism*, *quinone binding*, *aldehyde decarbonylase activity* and *triglyceride lipase activity* (Figure 20c) and Pfam terms *multi-copper polyphenol oxidoreductase laccase* and *wax 2 C-terminal domain proteins* (Table 5) were enriched in upregulated contigs also indicating enhanced defence during SF. Furthermore, during RF, GO terms *trihydroxyferuloyl spermidine O-methyltransferase activity* and polyamine metabolism (enzymes related to *spermidin*e or spermine) (Figure 20a) and related KEGG pathways for phenylpropanoid and steroid hormone biosynthesis, phenylalanine, retinol and caffeine metabolism (Table A1) were enriched in upregulated contigs pointing to an increase in production of secondary metabolites.

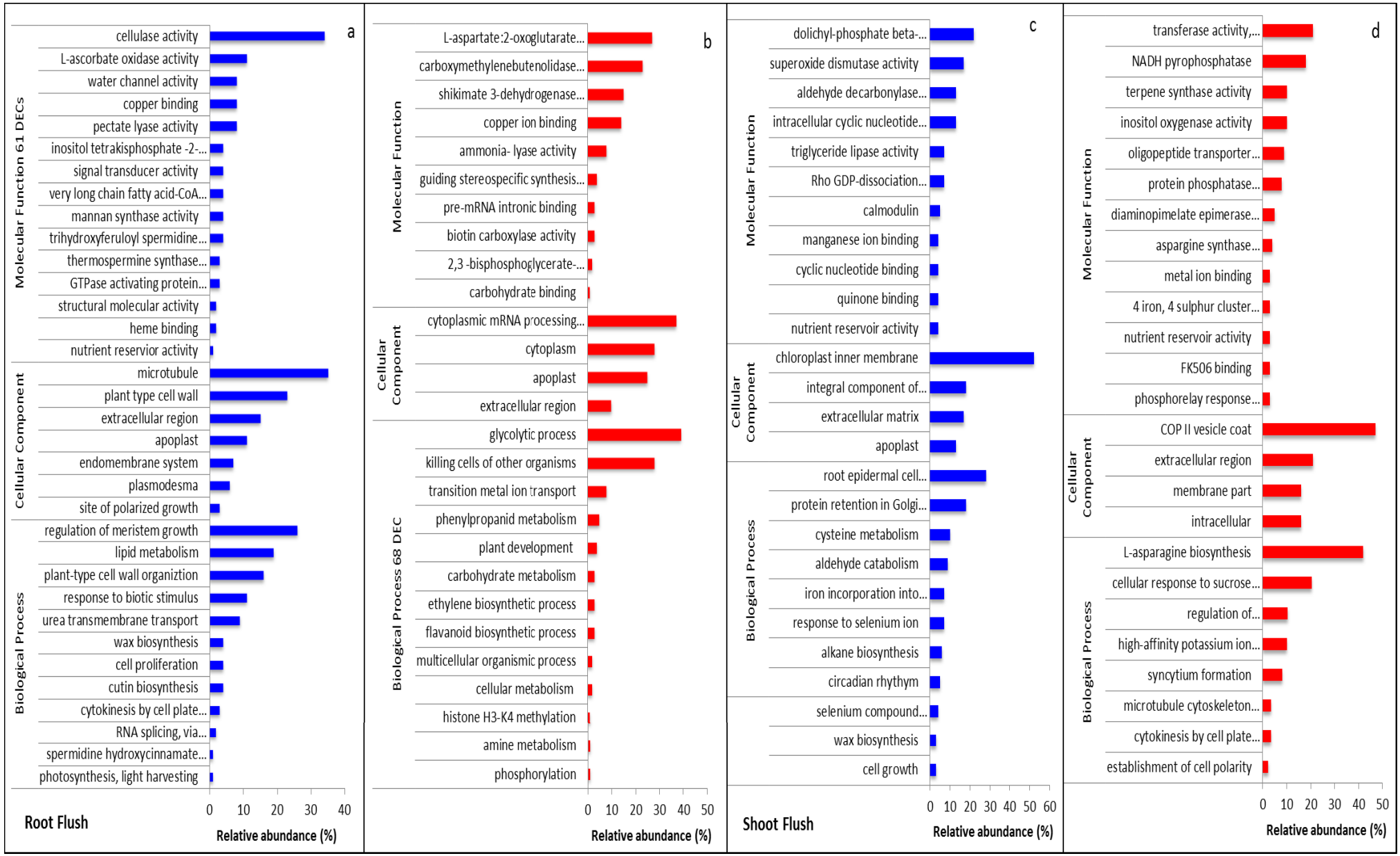
a
Molecular Function 61 DECs
cellulase activity
L-ascorbate oxidase activity
water channel activity
copper binding
pectate lyase activity
inositol tetrakisphosphate -2-...
signal transducer activity
very long chain fatty acid-CoA...
mannan synthase activity
trihydroxyferuloyl spermidine...
thermospermine synthase...
GTPase activating protein...
structural molecular activity
heme binding
nutrient reservior activity
Cellular Component
microtubule
plant type cell wall
extracellular region
apoplast
endomembrane system
plasmodesma
site of polarized growth
Biological Process
regulation of meristem growth
lipid metabolism
plant-type cell wall organiztion
response to biotic stimulus
urea transmembrane transport
wax biosynthesis
cell proliferation
cutin biosynthesis
cytokinesis by cell plate...
RNA splicing, via...
spermidine hydroxycinnamate...
photosynthesis, light harvesting
0 10 20 30 40
Root Flush
Relative abundance (%)
b
Molecular Function
L-aspartate:2-oxoglutarate...
carboxymethylenebutenolidase...
shikimate 3-dehydrogenase...
copper ion binding
ammonia- lyase activity
guiding stereospecific synthesis...
pre-mRNA intronic binding
biotin carboxylase activity
2,3 -bisphosphoglycerate-...
carbohydrate binding
Cellular Component
cytoplasmic mRNA processing...
cytoplasm
apoplast
extracellular region
Biological Process 68 DEC
glycolytic process
killing cells of other organisms
transition metal ion transport
phenylpropanid metabolism
plant development
carbohydrate metabolism
ethylene biosynthetic process
flavanoid biosynthetic process
multicellular organismic process
cellular metabolism
histone H3-K4 methylation
amine metabolism
phosphorylation
0 10 20 30 40 50
Relative abundance (%)
c
Molecular Function
dolichyl-phosphate beta-...
superoxide dismutase activity
aldehyde decarbonylase...
intracellular cyclic nucleotide...
triglyceride lipase activity
Rho GDP-dissociation...
calmodulin
manganese ion binding
cyclic nucleotide binding
quinone binding
nutrient reservoir activity
Cellular Component
chloroplast inner membrane
integral component of...
extracellular matrix
apoplast
Biological Process
root epidermal cell...
protein retention in Golgi...
cysteine metabolism
aldehyde catabolism
iron incorporation into...
response to selenium ion
alkane biosynthesis
circadian rhythm
selenium compound...
wax biosynthesis
cell growth
0 10 20 30 40 50 60
Shoot Flush
Relative abundance (%)
d
Molecular Function
transferase activity,...
NADH pyrophosphatase
terpene synthase activity
inositol oxygenase activity
oligopeptide transporter...
protein phosphatase...
diaminopimelate epimerase...
aspargine synthase...
metal ion binding
4 iron, 4 sulphur cluster...
nutrient reservoir activity
FK506 binding
phosphorelay response...
Cellular Component
COP II vesicle coat
extracellular region
membrane part
intracellular
Biological Process
L-asparagine biosynthesis
cellular response to sucrose...
regulation of...
high-affinity potassium ion...
syncytium formation
microtubule cytoskeleton...
cytokinesis by cell plate...
establishment of cell polarity
0 10 20 30 40 50
Relative abundance (%)

Figure 20 Summarized GO terms enriched for differentially expressed contigs in systemic leaf tissue of oak microcuttings in response to inoculation with *Pratylenchus penetrans* and *Piloderma croceum* during root flush (RF) (a and d) and shoot flush (SF) (c and d) developmental stages of the oak microcuttings. Presented are data for the relative abundance of GO terms enriched belonging to each classification i.e. biological process, cellular component and molecular function, upregulated (blue) and downregulated (red)

Table 5 Most enriched Protein families during interaction with *Pratylenchus penetrans* and *Piloderma croceum*. Presented are the top ten most enriched Protein families for up- and downregulated contigs in leaf tissues of oak microcuttings during root flush and shoot flush growth stages of oaks, Protein family (Pfam) ID, Pfam term description and significance level (*P*-value) (modified from Maboreke et al., 2016)

Oak growth stage	ID	Description	*P* value
Upregulated			
Root Flush	PF13229.1	Right handed beta helix region	2.73E-10
	PF14368.1	Probable lipid transfer	3.90E-09
	PF00230.15	Major intrinsic protein	4.07E-09
	PF00234.17	Protease inhibitor/seed storage/LTP family	9.65E-09
	PF00657.17	GDSL-like Lipase/Acylhydrolase	2.17E-08
	PF07731.9	Multicopper oxidase	2.48E-08
	PF12708.2	Pectate lyase superfamily protein	2.36E-07
	PF00759.14	Glycosyl hydrolase family 9	2.54E-07
	PF00394.17	Multicopper oxidase	3.01E-07
	PF07732.10	Multicopper oxidase	4.23E-07
Shoot Flush	PF07042.6	TrfA protein	9.92E-04
	PF13222.1	Protein of unknown function (DUF4030)	1.07E-03
	PF03511.9	Fanconi anaemia group A protein	1.68E-03
	PF07963.7	Prokaryotic N-terminal methylation motif	1.77E-03
	PF08412.5	Ion transport protein N-terminal	1.77E-03
	PF02041.11	Auxin binding protein	2.55E-03
	PF02578.10	Multi-copper polyphenol oxidoreductase laccase	2.63E-03
	PF12076.3	WAX2 C-terminal domain	2.86E-03
	PF07393.6	Exocyst complex component Sec10	3.02E-03
	PF02522.9	Aminoglycoside 3-N-acetyltransferase	3.05E-03
Downregulated			
Root Flush	PF03055.10	Retinal pigment epithelial membrane protein	1.44E-07
	PF00332.13	Glycosyl hydrolases family 17	2.84E-06
	PF01738.13	Dienelactone hydrolase family	1.73E-05
	PF00670.16	S-adenosyl-L-homocysteine hydrolase	3.31E-05
	PF04101.11	Glycosyltransferase family 28 C-terminal domain	5.33E-05
	PF01973.13	Protein of unknown function DUF115	6.11E-05
	PF13528.1	Glycosyl transferase family 1	1.02E-04
	PF00300.17	Histidine phosphatase superfamily (branch 1)	1.80E-04
	PF02772.11	S-adenosylmethionine synthetase	2.47E-04
	PF00221.14	Aromatic amino acid lyase	3.04E-04
Shoot Flush	PF10604.4	Polyketide cyclase / dehydrase and lipid transport	2.47E-04
	PF03169.10	OPT oligopeptide transporter protein	5.82E-04
	PF00190.17	Cupin	6.22E-04
	PF00407.14	Pathogenesis-related protein Bet VI family	8.53E-04
	PF05360.9	yia A/B two helix domain	2.28E-03
	PF03547.13	Membrane transport protein	3.25E-03
	PF02442.12	Lipid membrane protein of large eukaryotic DNA viruses	3.58E-03
	PF07963.7	Prokaryotic N-terminal methylation motif	3.80E-03
	PF05153.10	Family of unknown function (DUF706)	3.99E-03
	PF01092.14	Ribosomal protein S6e	4.35E-03

On the other hand, during RF GO terms *killing cells of other organisms* and *ethylene biosynthetic process* (Figure 20b) and KEGG pathway *microbial metabolism in diverse environments* (Table A1) all related to host defence were enriched in downregulated contigs. Similarly, during SF GO terms such as *regulation of phosphoprotein phosphatase activity* and

protein phosphatase inhibitor (Figure 20d) and corresponding Pfam terms *pathogenesis-related protein Bet VI family* and *polyketide cyclase/dehydrase* involved in signal transductions (Table 5) were enriched in downregulated contigs. Production of secondary metabolites was also repressed indicated by GO terms such as *carboxymethylene butenolidase activity*, *phenylpropanoid metabolism* and *shikimate 3- dehydrogenase activity* (Figure 20b) as well as Pfams terms *aromatic amino acid lyase* and *S-adenosylmethionine synthase* (Table 5) enriched in downregulated contigs during RF. Comparably during SF, the GO term *terpene synthase activity* (Figure 20d) was enriched in downregulated contigs. Further, repression of oak defence responses was indicated by the enrichment of KEGG pathways such as flavonoid and novobiocin metabolism and terpenoid biosynthesis during RF and steroid hormone biosynthesis, biosynthesis of secondary metabolites and ascorbate aldarate during SF in downregulated contigs (Table A1).

Furthermore, during RF GO terms regulation of meristem growth, cell replication and cytokinesis by cell plate formation as well as cellulase and pectate lyase activity (Figure 20a) and Pfams terms glycosyl hydrolase family 9 and pectate lyase superfamily protein (Table 5) enriched in upregulated contigs indicate promotion of cell growth. Similarly, enrichment of Pfam term Auxin binding protein linked to control of growth and development processes (Table 5) and GO terms root epidermal cell differentiation and Rho GDP-dissociation inhibitor activity in upregulated contigs (Figure 20c) and GO terms syncytium formation and high affinity potassium ion import (Figure 20d) and the auxin efflux carrier Pfam Membrane transport protein (Table 6) enriched in downregulated contigs during SF all point to promotion of lateral root growth process over apical growth.

Besides plant signalling, nutrient metabolism of oaks was altered. Carbohydrate metabolism was downregulated during RF, GO term *glycolytic process* (Figure 20b) and corresponding KEGG pathways for glycolysis/gluconeogenesis, carbon fixation in photosynthetic organisms, pyruvate, fructose, mannose, starch and sucrose metabolisms (Table A1) were enriched in downregulated contigs. Meanwhile during SF, the GO term *cellular response to sucrose starvation* (Figure 20d) and related KEGG pathway for ascorbate and aldarate metabolism (Table A1) were enriched in downregulated contigs indicating repressed sugar induced signal transductions. For nitrogen, the enrichment of GO terms *urea transmembrane transport* and *water channel activity* (Figure 20c) involved in remobilizing amino acids and KEGG pathways for cyanoamino acid, tryptophan and beta-alanine metabolism (Table A1) in upregulated contigs indicate enhanced metabolism and transport of proteins during RF. In

contrast, during SF GO terms *protein retention in Golgi apparatus* and *dolichyl-phosphate beta-glucosyltransferase activity* (Figure 20c) and Pfam *Exocyst complex 3 component Sec10* (Table 5) were enriched in upregulated contigs, while GO terms *L-asparagine biosynthesis*, *asparagine synthase* and *oligopeptide transporter activity* (Figure 20d) and corresponding Pfams *ribosomal protein S6* and *OPT oligopeptide transporter protein* (Table 5) were enriched in downregulated contigs. Together these are indicative of repressed mobilization of proteins in systemic leaf tissues of oak microcuttings during SF.

3.1.2 Effect of *Pratylenchus penetrans* and *Piloderma croceum* on allocation of ^{13}C and ^{15}N in total plant, shoot and root compartments

3.1.2.1 Carbon allocation

The effects of the biotic interactions on oak carbon and nutrient metabolisms were assigned using $^{13}CO_2$ and ^{15}N labelling of plants. The total amount of ^{13}C excess in oak microcutting across the different treatments ranged between 0.13 - 0.20 and 0.15 - 0.4 mg during RF and SF oak microcutting growth stages, respectively (Figure 21). The growth stage of the oak microcuttings impacted the total amount of ^{13}C excess in plants ($F_{1, 60} = 6.08$, $P = 0.017$), and that allocated to shoots ($F_{1, 60} = 27.91$, $P < 0.001$) or roots ($F_{1, 60} = 12.99$, $P < 0.001$) (Figure 21). The relative allocation of carbon to the shoot and root tissues expressed as the R/S ratio of ^{13}C excess was significantly higher during RF compared to SF ($F_{1, 60} = 33.48$, $P < 0.001$). Inoculation of plants with *P. croceum* enhanced the total amount of carbon in the oak microcuttings in comparison to the control plants by 50% and 40% during RF and SF, respectively, ($F_{1, 60} = 33.95$, $P < 0.001$) (Figure 21).

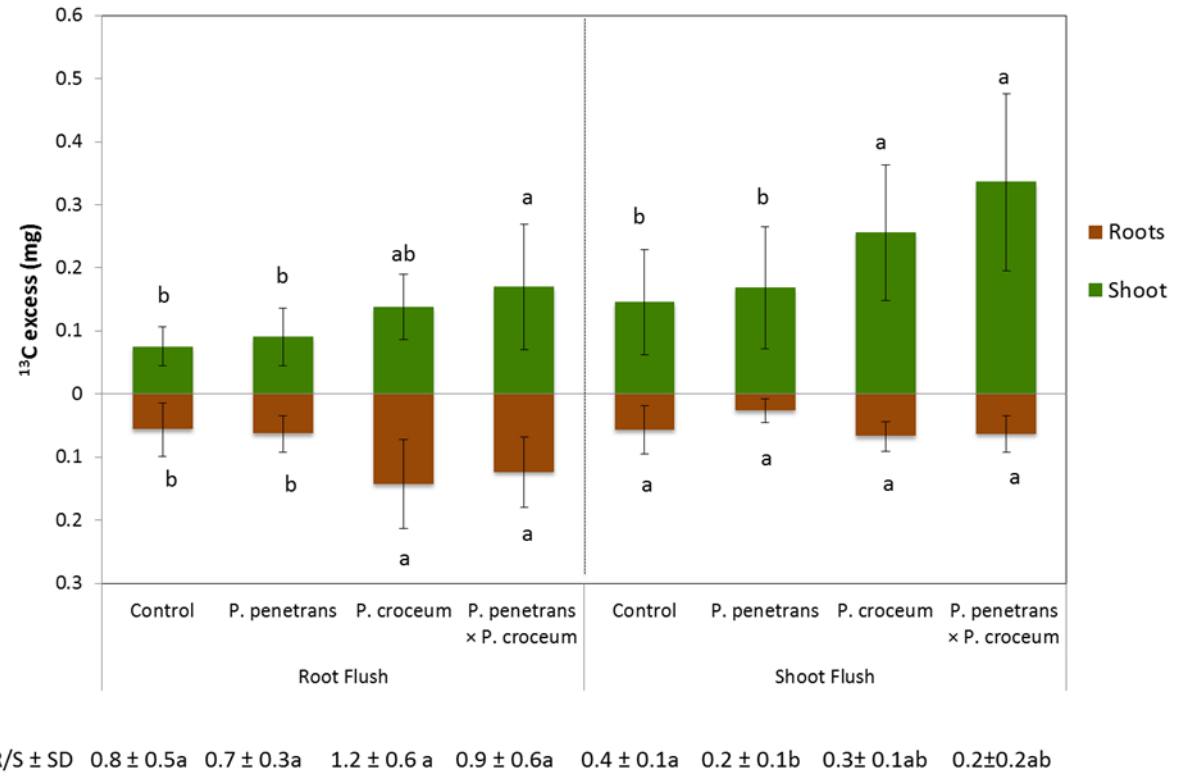

Figure 21 Effect of the plant-parasitic nematode *Pratylenchus penetrans* and the ectomycorrhizal fungus *Piloderma croceum* on total amount of ^{13}C excess (mg ± s.d.) in oak microcuttings. Presented are data for ^{13}C excess in shoot and root compartments, root to shoot ratios (R/S) of ^{13}C excess (mean ± s.d.) determined for plants harvested during root flush and shoot flush developmental stages of oaks. For each oak growth stage, data with the same letters are not significantly different according to Tukey's HSD test at $P < 0.05$

In addition, two-way ANOVA showed that *P. croceum* doubled the amount of ^{13}C excess in total plant ($F_{1, 42} = 27.61$, $P < 0.001$) and for both shoot ($F_{1, 42} = 15.08$, $P = 0.001$) and root ($F_{1, 42} = 23.19$, $P < 0.001$) compared to control plants during RF (Figure 14). Similarly, *P. croceum* enhanced total amount of ^{13}C excess in total plant ($F_{1, 18} = 10.31$, $P = 0.005$) and shoot ($F_{1, 18} = 33.95$, $P = 0.008$) during SF (Figure 21). On the other hand, *P. penetrans* had no effect on the total amount of ^{13}C excess or amount of carbon allocated to shoot and roots compartments in oak microcuttings during either growth stage. However, *P. penetrans* reduced the R/S of ^{13}C excess by 50% in comparison to the control, during SF ($F_{1, 18} = 6.97$, $P = 0.017$).

3.1.2.2 Nitrogen allocation

The total amount of ^{15}N excess ranged between 2.6 - 5.6 and 1.7 - 6.8 µg during growth stages RF and SF, respectively. In contrast to carbon allocation, the growth stage had no effect on the total amount of nitrogen acquired by the plant. However, three-way ANOVA showed that the growth stage influenced the allocation of nitrogen to shoot ($F_{1, 60} = 8.88$, $P = 0.004$) and root ($F_{1, 60} = 12.71$, $P < 0.001$) tissues, higher amounts of nitrogen were allocated to shoots and roots during SF and RF, respectively compared to the control (Figure 22). Consequently, plants at SF had comparably lower ^{15}N excess R/S ratio ($F_{1, 60} = 18.40$, $P < 0.001$) than during RF (Figure 22). Three-way ANOVA also showed that *P. croceum* enhanced the total amount of nitrogen acquired by the plant ($F_{1, 60} = 36.84$, $P < 0.001$) and allocated to the shoot ($F_{1, 60} = 34.66$, $P < 0.001$) in comparison to the control, while *P. penetrans* reduced the amount of ^{15}N excess in shoots compared to *P. croceum* ($F_{1, 60} = 5.33$, $P < 0.024$) (Figure 22).

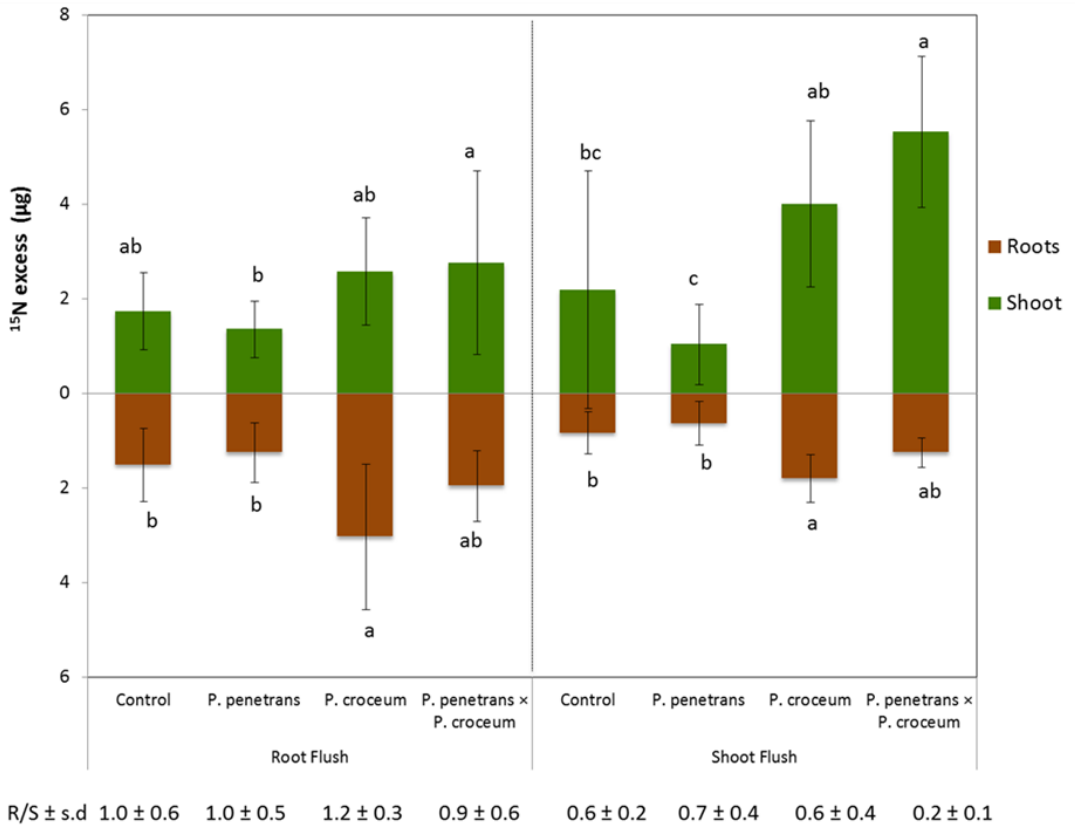

Figure 22 Effect of the plant-parasitic nematode *Pratylenchus penetrans* and the ectomycorrhizal fungus *Piloderma croceum* on total amount of ^{15}N excess (in µg ± s.d.) in oak microcuttings. Presented is data for ^{15}N excess in shoot and roots compartments, root to shoot ratios (R/S) of ^{15}N excess (mean ± s.d.) determined for plants harvested during root flush and shoot flush developmental stages of oaks. For each oak growth stage, data with the same letters are not significantly different according to Tukey's HSD test at $P < 0.05$

Two-way ANOVA showed that positive effect on the total amount of nitrogen acquired by the microcuttings was consistent regardless of the oak growth stage ($F_{1, 42} = 15.29$, $P < 0.001$ and $F_{1, 18} = 21.10$, $P < 0.001$, for growth RF and SF, respectively) (Figure 22). Similarly, *P. croceum* boosted the amount of nitrogen allocated to shoots and roots of oaks at both growth stages (shoot: $F_{1, 42} = 9.68$, $P = 0.003$ and roots: $F_{1, 42} = 14.26$, $P < 0.001$ during RF, and shoot: $F_{1, 18} = 17.98$, $P < 0.001$ and roots: $F_{1, 18} = 17.631$, $P < 0.001$ during SF) (Figure 22).
On the contrary, interaction of *P. croceum* and *Pratylenchus penetrans* hampered allocation of nitrogen to the roots ($F_{1, 42} = 5.13$, $P = 0.029$) during RF as demonstrated by a 35% decrease of ^{15}N excess in roots compared to plants inoculated with only *P. croceum* (Figure 22).

3.1.2.3 Relative allocation of ^{13}C and ^{15}N to terminal leaves

Similar to the transcriptomic responses above (Chapter **3.1.1**), three-way ANOVA showed that the growth stage of oaks strongly increased the allocation of recent photoassimilated carbon ($F_{1, 60} = 158.05$, $P < 0.001$) and nitrogen ($F_{1, 60} = 147.31$, $P < 0.001$) in terminal leaves (Figure 23; Table A4). Three-way ANOVA showed that *P. penetrans* independently enhanced the amount of ^{13}C ($F_{1, 60} = 7.15$, $P < 0.001$) and ^{15}N ($F_{1, 60} = 11.22$, $P = 0.001$) allocated to leaves as well as *P. penetrans* in interaction with the oak growth stage (^{13}C: $F_{1, 60} = 10.61$, $P = 0.002$ and ^{15}N: $F_{1, 60} = 21.47$, $P < 0.001$) during SF compared to RF (Figure 23). Comparably, *P. croceum* increased the proportion of nitrogen allocated to terminal leaves compared to the control ($F_{1, 60} = 5.13$, $P = 0.027$) (Figure 23) however, with no effect on the ^{13}C flux. Similarly, interaction of *P. croceum* and oak growth stage influenced allocation of nitrogen to terminal leaves ($F_{1, 60} = 7.48$, $P = 0.008$) with more ^{15}N excess allocated during SF and compared to RF (Figure 23; Table A4).

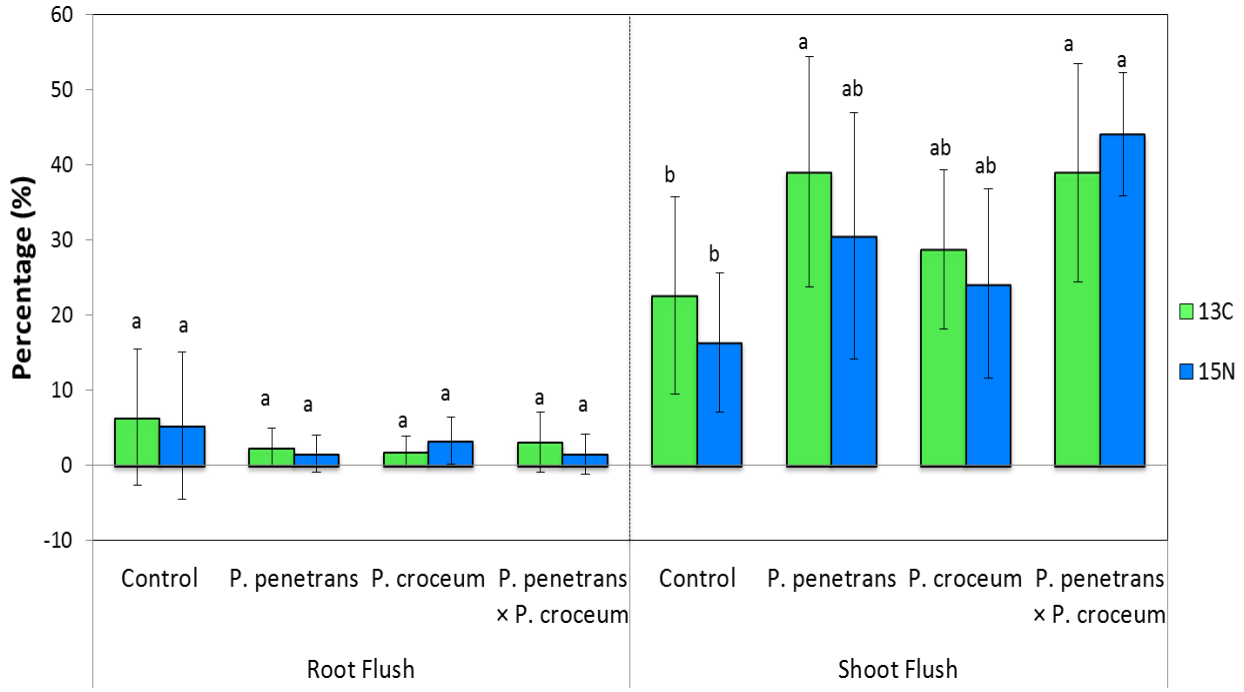

Figure 23 Effect of the plant-parasitic nematode *Pratylenchus penetrans* and the ectomycorrhizal fungus *Piloderma croceum* on the percentage of total ^{13}C and ^{15}N excess (% mean ± s.d.) allocated to terminal leaves of oak microcuttings. Presented are data for root flush and shoot flush developmental stages of oaks. For each oak growth stage, data with the same letters are not significantly different according to Tukey's HSD test at $P < 0.05$

3.1.3 Plant growth response

3.1.3.1 Plant Biomass

The total plant biomass of the oak microcuttings ranged between 0.31 ± 0.07 – 0.42 ± 0.14 and 0.27 ± 0.14 – 0.49 ± 0.11 g DW during RF and SF, respectively (Figure 24) with no effect of growth stage.

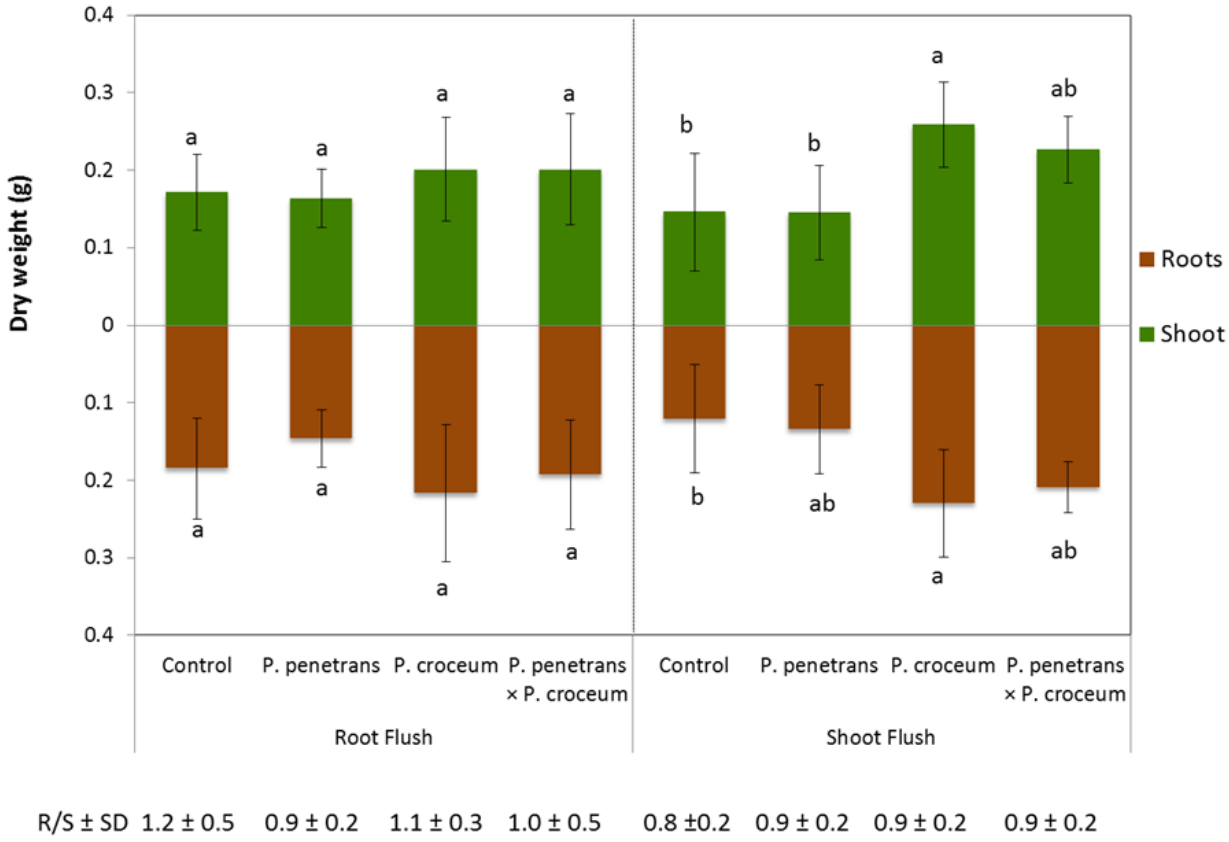

Figure 24 Effect of the plant-parasitic nematode *Pratylenchus penetrans* and the ectomycorrhizal fungus *Piloderma croceum* on total amount of plant biomass (g ± SD) in oak microcuttings. Presented is data for biomass of shoot and roots compartments, root to shoot ratios (R/S) of plant biomass (mean ± s.d.) determined for plants harvested during root flush and shoot flush developmental stages of oaks. For each oak growth stage, data with the same letters are not significantly different according to Tukey's HSD test at $P < 0.05$

Three-way ANOVA showed that *P. croceum* enhanced the biomasses of the total plant ($F_{1, 60} = 20.59$, $P < 0.001$), shoot ($F_{1, 60} = 18.34$, $P < 0.001$) and root ($F_{1, 60} = 14.65$, $P = 0.001$) (Figure 24). Correspondingly, two-way ANOVA showed that *P. croceum* enhanced the total plant biomass during RF ($F_{1, 42} = 5.11$, $P = 0.029$) and SF ($F_{1, 18} = 14.83$, $P = 0.001$) (Figure 24). Similarly, *P. croceum* increased the biomass of roots ($F_{1, 18} = 12.82$, $P = 0.002$) and shoot ($F_{1, 18} = 14.32$, $P = 0.001$) during RF (Figure 24). In contrast, *P. penetrans* had no effect on the plant biomass.

3.1.3.2 Leaf area and root length

Neither *P. penetrans* nor *P. croceum* had an effect on the leaf area. However, three-way ANOVA showed that *P. croceum* significantly reduced the root length of the oak

microcuttings ($F_{1, 60}$ = 13.84, P < 0.001) across the growth stages (Table 6). This was particularly noticeable during RF ($F_{1, 42}$ = 20.88, P < 0.001), roots of plants inoculated with *P. croceum* were 30% shorter compared to control (Table 6).

Table 6 Effect of the plant-parasitic nematode *Pratylenchus penetrans* and the ectomycorrhizal fungus *Piloderma croceum* on average leaf area (leaf area/ number of leaves (cm^2 ± s.d.)) and root length of oak microcuttings. Presented are data for root flush and shoot flush developmental stages of oaks. ANOVA with *** for P < 0.001. Data with the same letters are not significantly different (Tukey's HSD test, P <0.05). Pp: *Pratylenchus penetrans*, Pc: *Piloderma croceum*, PpPc: co-inoculation with *Pratylenchus penetrans* and *Piloderma croceum*

	Control	*P. penetrans*	*P. croceum*	PpPc	ANOVA
Root Flush					
Leaf area (cm^2)	5.78 ± 1.37	7.01 ± 3.83	6.42 ± 1.90	5.92 ± 2.43	
Root Length (cm)	304.7 ± 41.4a	282.1 ± 51.8a	218.5 ± 52.3b	234.5 ± 52.5b	Pc***
Shoot Flush					
Leaf area (cm^2)	3.98 + 1.95	3.38 ± 2.23	3.33 ± 1.80	3.87 ± 1.85	
Root Length (cm)	262.1 ± 58.6	260.9 ± 33.6	235.2 ± 26.9	240.7 ± 34.5	

Figure 25 Images showing *Quercus robur* microcuttings harvested during root flush and shoot flush

3.1.4 Effects of *P. penetrans* and *P. croceum* on the rhizosphere microbial biomass and dominant groups

The microbial biomass as assessed by the total amount of PLFAs in the rhizosphere soils was strongly affected by the growth stage of the oak microcuttings ($F_{1, 60} = 111.75$, $P < 0.001$) indicated by generally higher amounts of total amount PLFAs during RF compared to SF (Figure 26). Due to the observed strong effect of the plants endogenous growth stage on transcriptomic and nutrient allocation responses, the following results present data for individual growth stages i.e. RF and SF, respectively.

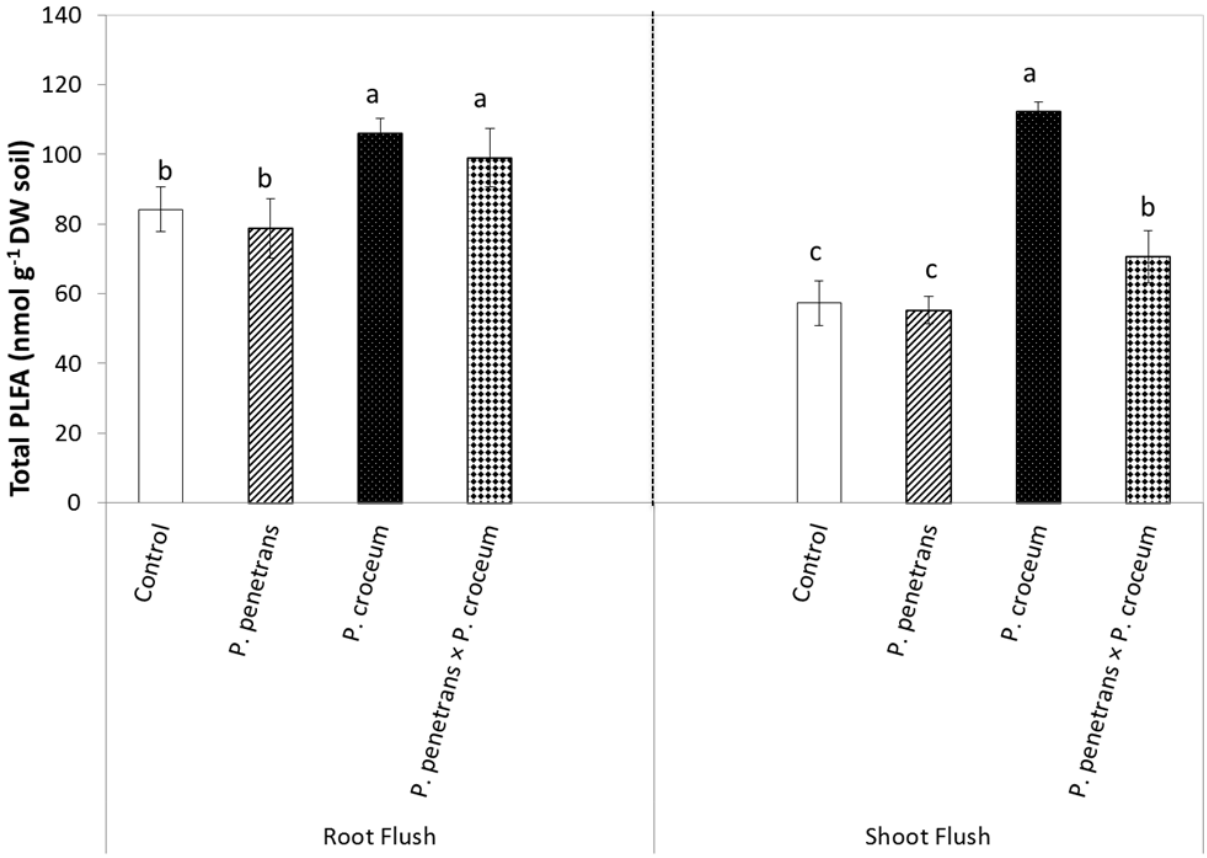

Figure 26 Effects of the plant-parasitic nematode *Pratylenchus penetrans* and the ectomycorrhizal fungus *Piloderma croceum* on total amounts of phospholipid fatty acids (PLFAs)(in nmol/g DW soil ± s.d.) in the rhizosphere of *Quercus robur* microcuttings. Presented are data for root flush and shoot flush developmental stages of oaks. For each growth stage, data with the same letters are not significantly different (Tukey's HSD test, $P < 0.05$)

During RF, *P. croceum* strongly increased ($F_{1, 42}$ = 102.41, P < 0.001) the total amount of PLFAs, as measure for microbial biomass, by 20% and 25% compared to the control and *P. penetrans* treatments, respectively, (Figure 26). During SF, the effect of the biotic interactions was stronger and the symbiont *P. croceum* increased biomass of microorganisms by almost 50% compared to the control ($F_{1, 18}$ = 245.83, P < 0.001). In contrast, *P. penetrans* either solely ($F_{1, 18}$ = 94.16, P < 0.001) or in co-inoculation with *P. croceum* ($F_{1, 18}$ = 78.23, P < 0.001) resulted in a drastic decline by 41% compared to singular *P. croceum* inoculation (Figure 26).

Table 7 Effects of the plant-parasitic nematode *Pratylenchus penetrans* and the ectomycorrhizal fungus *Piloderma croceum* on the occurrence of Gram-positive, Gram-negative and Actinobacteria, and fungi (phospholipid fatty acids in nmol g^{-1} DW soil ± s.d.) in the rhizosphere of *Quercus robur* microcuttings. Presented are data for the developmental stages root flush and shoot flush. For each oak growth stage, data with the same letters are not significantly different according to Tukey's HSD test at P < 0.05. F/B: fungal to bacterial biomass Pp: *Pratylenchus penetrans*, Pc: *Piloderma croceum*, PpPc: co-inoculation with *Pratylenchus penetrans* and *Piloderma croceum.*

	Control	*P. penetrans*	*P. croceum*	Pp × Pc	Anova
Root Flush					
Gram + bacteria	22.32 ± 2.18bc	20.32 ± 2.12c	27.06 ± 1.89a	24.33 ± 2.07ab	Pp**; PpPc***
Gram- bacteria	10.39 ± 1.89b	10.51 ± 2.52b	14.54 ± 2.11a	13.73 ± 2.90a	Pc***
Actinobacteria	11.75 ± 1.64b	11.33 ± 1.21b	13.52 ± 0.66a	12.08 ± 1.52ab	Pp*, Pc**
Fungi	3.41± 0.38b	3.57 ± 0.45b	6.45 ± 1.28a	6.13 ± 1.11a	Pc***
F/B[e]	0.06 ± 0.01b	0.07 ± 0.01b	0.09 ± 0.02a	0.09 ± 0.02a	Pc***
Shoot Flush					
Gram + bacteria	15.07 ± 1.57b	14.68 ± 0.68b	27.53 ± 1.79a	16.34 ± 0.86ab	Pp***, Pc***, P Pc***
Gram- bacteria	8.17 ± 2.35b	7.10 ± 1.10b	16.70 ± 2.27a	10.20 ± 2.76b	Pp**, Pc*, PpPc***
Actinobacteria	6.72 ± 0.91b	7.21 ± 0.67b	15.07 ± 0.43a	8.30 ± 1.91b	Pp***, Pc***, PpPc***
Fungi	2.88 ± 0.19c	2.75 ± 1.52c	6.48 ± 0.45a	4.039 ± 1.07b	Pp***, Pc***, PpPc***
F/B[e]	0.08 ± 0.01a	0.07 ± 0.00a	0.08 ± 0.01a	0.09 ± 0.03a	

Irrespective of the plant's growth stage, the microbial community in the soil of the mesocosms was predominantly composed of Gram-positive, Gram-negative, Actino- and general bacteria, as well as fungi PLFA markers (Table 7). During RF, the plant parasite *P.penetrans* repressed the biomass of Gram-positive bacteria ($F_{1, 42}$ = 12.0, P = 0.001) and Actinobacteria ($F_{1, 42}$ = 5.71, P = 0.021). In contrast, the presence of the symbiont *P. croceum* enhanced the abundance of all microbial groups compared to the control (Gram-positive

bacteria: $F_{1,\ 42}$ = 41.10, P < 0.001, Gram-negative bacteria: $F_{1,\ 42}$ = 27.70, P < 0.001; Actinobacteria: $F_{1,\ 42}$ = 10.64, P = 0.002 and Fungi: $F_{1,\ 42}$ = 111.27, P < 0.001). The fungal biomass in soils inoculated with *P. croceum* was twice as much as that of soils without, this was further highlighted by the significantly higher F/B ratios in these soils compared to the control ($F_{1,\ 42}$ = 34.90, P < 0.001).

During SF, the effect of *Pratylenchus penetrans* and *Piloderma croceum* on the predominant microbial groups in the rhizosphere of the oak microcuttings was even stronger (Table 7). *P. croceum* significantly increased the biomass of all microbial groups in comparison to the control (Gram-positive bacteria: $F_{1,\ 18}$ = 143.90, P < 0.001; Gram-negative bacteria: $F_{1,\ 18}$ = 35.15, P < 0.001; Actinobacteria: $F_{1,\ 18}$ = 94.28, P < 0.001 and Fungi: $F_{1,\ 18}$ = 96.73, P < 0.001). In contrast, *P. penetrans* reduced the biomass of all microbial groups in comparison to sole inoculation with *P. croceum* (Gram-positive bacteria: $F_{1,\ 18}$ = 97.16, P < 0.001; Gram-negative bacteria: $F_{1,\ 18}$ = 14.31, P = 0.002; Actinobacteria: $F_{1,\ 18}$ = 41.86, P < 0.001 and Fungi: $F_{1,\ 18}$ = 27.54, P = 0.001). This negative impact of *P. penetrans* remained pronounced during interaction with *P. croceum* (Gram-positive bacteria: $F_{1,\ 18}$ = 84.55, P < 0.001; Gram-negative bacteria: $F_{1,\ 18}$ = 7.02, P = 0.017; Actinobacteria: $F_{1,\ 18}$ = 55.82, P < 0.001 and Fungi: $F_{1,\ 18}$ = 22.14, P < 0.001).

3.1.5 Effect of *P. penetrans* and *P. croceum* on the rhizosphere microbial community structure

MANOVA revealed that *P. penetrans* ($F_{16,\ 27}$ = 3.88, P < 0.001), *P. croceum* ($F_{16,\ 27}$ = 28.59, P < 0.001) and their co-inoculation ($F_{16,\ 27}$ = 2.44, P = 0.020) were responsible for the changes in the predominant PLFAs in the rhizosphere of the oaks during RF. A stepwise discriminant function of analysis (DFA) showed significant differences among the soil microbial communities depending on the different biotic interactions (Figure 27a; whole model: $F_{\ 24,\ 102}$ = 12.98, P < 0.001). The first two discriminant functions significantly accounted for 95% of the total variances (root 1: P < 0.001and root 2: < 0.001). The first discriminant function showed a clear separation (eigenvalue = 12.37) of microbial communities in soils inoculated with *P. croceum* (*P. croceum* vs. Control: $F_{\ 8,\ 35}$ = 35.96, P < 0.001; *P. penetrans* × *P. croceum* vs. Control: $F_{\ 8,\ 35}$ = 21.21, P < 0.001; *P. croceum* vs. *P. penetrans*: $F_{\ 8,\ 35}$ = 37.72, P < 0.001; *P. penetrans* × *P. croceum* vs. *P. penetrans*: $F_{\ 8,\ 35}$ = 19.87, P < 0.001) (Figure 27a).

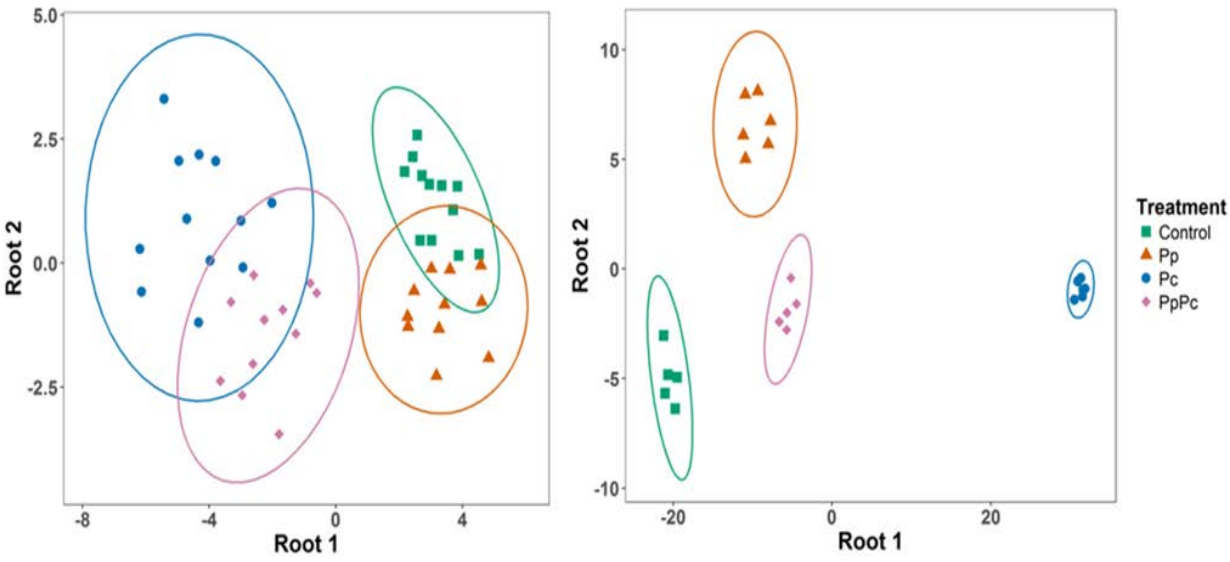

Figure 27 Discriminant functional analysis of the phospholipid fatty acids identified in the rhizosphere soil of *Quercus robur* microcuttings inoculated with *Pratylenchus penetrans*, *Piloderma croceum* and co-inoculation with *Pratylenchus penetrans* and *Piloderma croceum* (groups, n = 4), during (a) root flush and (b) shoot flush. Pp: *Pratylenchus penetrans*, Pc: *Piloderma croceum* and PpPc: co-inoculation with *Pratylenchus penetrans* and *Piloderma croceum*

Correlation of the PLFAs with the extracted axes indicated significant effects of PLFAs i14:0, a15:0, i16:0, i17:0, a17:0, 16:1ω5c, 16:1ω7c, 17:0-10 meth, 18:2ω6, 18:1ω9c and cy19:0 in the discrimination of microbial communities along root 1 (Table 8). This corresponds to the increased amounts of these PLFAs in soils inoculated with *P. croceum* compared to control or *P. penetrans* treatments during RF (Table 9). Discrimination along root 2 indicated subtle separation (eigenvalue = 1.49) of rhizosphere microbial communities in soils inoculated with *P. penetrans* (*P. penetrans* vs. Control: $F_{8, 35} = 4.74$, $P = 0.001$ and *P. penetrans* × *P. croceum* vs. *P. croceum*: $F_{8, 35} = 7.57$, $P < 0.001$) (Figure 27a). PLFAs i14:0, i16:0, i17:0, 17:0-10 meth and 18:0-10 meth were positively correlated root 2, whilst 18:1ω9c had a negative correlation (Table 8). Consistently, *P. penetrans* reduced the amounts of most PLFAs in the soil during RF (Table 9).

Table 8 Pearson's coefficients of correlation between the different phospholipid fatty acids and the extracted roots of the discriminant function analyses. Presented are data for root flush and shoot flush growth stages of the oak microcuttings. Canonical scores for the first and second roots were used for the correlation. *, ** and *** refer to P <0.05, 0.01, and 0.001, respectively

		Root Flush		Shoot Flush	
Fatty acids	Organism	ROOT_1	ROOT_2	ROOT_1	ROOT_2
i14:0	Gram-positive bacteria	-0.530***	0.555***	0.668**	-0.362
i15:0		-0.21	-0.105	0.869***	-0.136
a15:0		-0.746***	0.162	0.880***	-0.276
i16:0		-0.701***	0.557***	0.860***	-0.218
i17:0		-0.545***	0.546***	0.886***	-0.12
a17:0		-0.740***	0.131	0.900***	-0.239
cy 17:0	Gram-negative bacteria	-0.0745	0.129	0.871***	-0.213
cy 19:0		-0.702***	-0.143	0.801***	-0.283
16:0-10 Meth	Actinobacteria	-0.485**	0.185	0.957***	-0.108
17:0-10 Meth		-0.311*	0.468**	0.820***	-0.191
18:0-10 Meth		-0.394**	0.450**	0.867***	-0.110
16:1ω7c	Bacteria in general	-0.337*	0.170	0.632***	-0.456*
16:1ω5c		-0.620***	0.225	0.788***	-0.133
18:1ω9t		-0.868***	-0.124	0.919***	-0.078
18:2ω6c	Fungi	-0.909***	0.180	0.957***	0.051
18:1ω9c		-0.847***	-0.392**	0.842***	-0.395

Meanwhile, during SF MANOVA showed that *P. penetrans* ($F_{3, 16}$ = 17.85, P = 0.018), *P. croceum* ($F_{3, 16}$ = 68.73, P = 0.002) and their interaction ($F_{3, 16}$ = 48.96, P = 0.004) provoked significant changes in the soil PLFA profiles in the rhizosphere of oak microcuttings, which is supported by a subsequent DFA (Figure 27b; whole model: $F_{39, 18}$ = 24.63, P < 0.001). The first two roots significantly accounted for 98% of the variance (root 1: P < 0.001 and root 2: P < 0. 001). The first discriminant function distinctly separated (eigenvalue = 482.0) the PLFA pattern of soils inoculated with singular *P. croceum* from those of the other treatments (*P. croceum* vs. control: $F_{6, 13}$ = 188.33, P < 0.001; *P. croceum* vs. *P. penetrans*: $F_{6, 13}$ = 133.60, P < 0.001 and *P. croceum* vs. *P. penetrans* × *P. croceum*: $F_{6, 13}$ = 97.60, P < 0.001) (Figure 27b). In addition, microbial communities in rhizosphere soils inoculated with *P. penetrans* were also separated from the control treatment along root 1 (*P. penetrans* vs. Control: $F_{7, 12}$ =

17.71, $P = 0.001$ and *P. penetrans* × *P. croceum* vs. Control: $F_{7, 12} = 18.90$, $P < 0.001$) (Figure 27b).

Correlation of the PLFAs with the extracted axes indicated significant effects of all predominant fatty acids in the discrimination of microbial communities along root 2 (Table 8). Correspondingly, the highest amount of PLFAs was extracted from soils from the singular *P. croceum* treatment, whereas the lowest amounts of PLFAs i15:0, 16:1w5, 18:2ω6, 18:1ω9t and 18:0-10 meth were extracted from rhizosphere soils of the control treatment (Table 9). Meanwhile along root 2, *P. penetrans* evidently (eigenvalue = 22.62) altered the PLFA profiles of soils compared to the other treatments during SF (*P. penetrans* vs. Control: $F_{7, 12} = 17.71$, $P = 0.001$; *P. penetran*s vs. *P. croceum*: $F_{6, 13} = 133.60$, $P < 0.001$ and *P. penetrans* vs. *P. penetrans* × *P. croceum*: $F_{6, 13} = 8.61$, $P = 0.007$). In contrast to root 1, only 16:1ω7 and 18:1ω9c showed significant correlation (negative) with root 2 (Table 8) indicating that these two PLFAs contributed to the second discriminant function. Consistently, the lowest amounts of 16:1ω7 and 18:1ω9c were extracted from soils of the singular *P. penetrans* treatment (Table 9).

Table 9 Effects of the plant-parasitic nematode *Pratylenchus penetrans* and the ectomycorrhizal fungus *Piloderma croceum* on amounts of individual phospholipid fatty acids (PLFAs)(in nmol/g DW± s.d.) of the rhizosphere of *Quercus robur* microcuttings. Presented are oak growth stages root flush and shoot flush. Values in a row followed by the same letter are not significantly different (Tukey's HSD test, $P < 0.05$). Pp: *Pratylenchus penetrans*, Pc: *Piloderma croceum*, PpPc: co-inoculation with *Pratylenchus penetrans* and *Piloderma croceum*

		Root Flush				Shoot Flush			
Fatty acid	Organism	Control	*P. penetrans*	*P. croceum*	PpPc	Control	*P. penetrans*	*P. croceum*	Pp Pc
i14:0	Gram-positive bacteria	0.49 ± 0.08b	0.47 ± 0.04b	0.59 ± 0.05a	0.51 ± 0.12ab	0.47 ± 0.01b	0.38 ± 0.25b	0.60 ± 0.10a	0.40 ± 0.08b
i15:0		6.02 ± 0.83	6.42 ± 3.88	6.66 ± 0.82	6.30 ± 0.80	4.32 ± 0.69b	4.32 ± 0.37b	7.48 ± 1.04a	4.48 ± 0.82b
a15:0		4.29 ± 0.50b	3.88 ± 0.72b	5.92 ± 0.87a	5.22 ± 0.98a	3.21 ± 0.49b	2.88 ± 0.22b	5.73 ± 0.43a	3.73 ± 0.89b
i16:0		6.62 ± 0.91b	5.13 ± 1.55c	8.07 ± 0.95a	7.19 ± 1.10ab	4.30 ± 0.33b	4.00 ± 0.48b	7.38 ± 1.25a	4.59 ± 0.67b
i17:0		1.33 ± 0.28ab	1.10 ± 0.29b	1.58 ± 0.18a	1.28 ±0.18b	0.84 ± 0.21b	0.88 ± 0.02b	1.54 ± 0.18a	0.99 ± 0.18b
a17:0		1.62 ± 0.35bc	1.54 ± 0.42c	2.21 ± 0.71a	2.11 ± 0.32ab	1.13 ± 0.32b	0.97 ± 0.12b	2.51 ± 0.37a	1.24 ± 0.14b
16:0-10 Meth	Actinobacteria	7.95 ± 1.15b	7.77 ± 0.81b	9.40 ± 1.10a	8.32 ± 1.00ab	4.43 ± 0.45b	4.93 ± 0.38b	10.55 ± 0.60a	5.71 ± 1.35b
17:0-10 Meth		1.93 ± 0.41ab	1.70 ± 0.50b	2.19 ± 0.31a	1.90 ± 0.28ab	1.21 ± 0.30b	1.14 ± 0.20b	2.28 ± 0.44a	1.35 ± 0.37b
18:0-10 Meth		1.87 ± 0.38a	1.87 ± 0.15a	2.20 ± 0.29a	1.86 ± 0.29a	1.08 ± 0.19b	1.14 ± 0.13b	2.23 ± 0.45a	1.24 ± 0.26b
cy 17:0	Gram-negative	4.00 ± 1.00a	3.39 ± 1.70a	3.80 ± 0.55a	3.73 ± 1.26a	2.90 ± 0.41c	2.94 ± 0.59c	6.01 ± 0.80a	4.32 ± 0.65b
cy 19:0		6.41 ± 1.34b	7.12 ± 1.82b	11.41 ± 2.16a	10.00 ± 2.88a	5.23 ± 2.09b	4.16 ± 1.01b	10.69 ± 1.75a	5.88 ± 2.16b
16:1ω7c	Bacteria in general	3.63 ± 0.42a	3.19 ± 1.29a	4.02 ± 0.60a	3.63 ± 0.53a	3.69 ± 0.06b	2.28 ± 0.43b	5.19 ± 1.49a	3.07 ± 0.85ab
16:1ω5c		0.95 ± 0.13b	0.99 ± 0.12b	1.28 ± 0.20a	1.07 ± 0.17b	0.72 ± 0.41b	0.72 ± 0.20b	1.57 ± 0.33a	0.83 ± 0.23b
18:1ω9t		6.49 ± 1.13b	5.34 ± 2.00b	10.48 ± 1.33a	10.84 ± 0.67a	2.76 ± 0.35c	4.03 ± 1.00c	9.39 ± 0.84a	6.33 ± 1.10b
18:2ω6c	Fungi	0.90 ± 0.32b	0.67 ± 0.12b	2.67 ± 1.49a	1.94 ± 0.66a	0.59 ± 0.02c	0.94 ± 0.03b	2.22 ± 0.28a	0.75 ± 0.26bc
18:1ω9c		2.51 ± 0.24b	2.90 ± 0.41b	4.02 ± 0.85a	4.19 ± 0.58a	2.29± 0.21c	1.81 ± 0.13c	4.25 ± 0.48a	3.29 ± 0.81b

3.2 Interrelationships between plant-parasitic nematodes and beneficial rhizosphere microorganisms

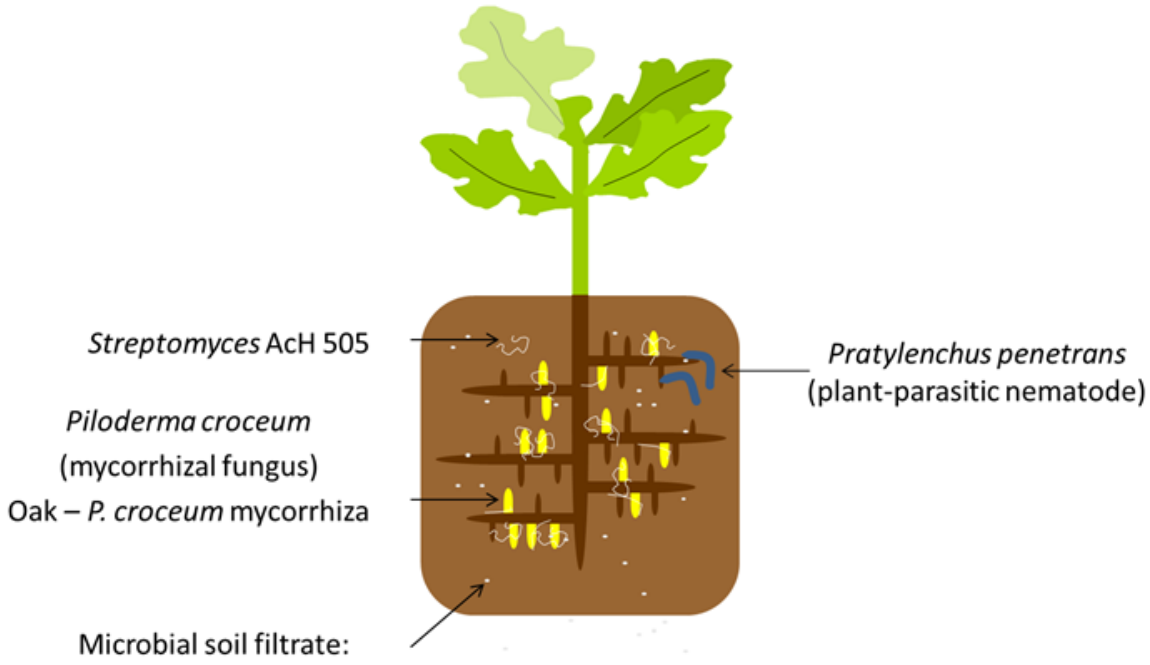

Schematic illustration of the rhizosphere interactions between the mycorrhizal oak microcutting and the plant-parasitic nematodes as well as the mycorrhizal helper bacteria (courtesy of M. Tarkka)

3.2.1 Effect of *Pratylenchus penetrans* and *Streptomyces* sp. AcH 505 on plant growth parameters

MANOVA revealed that sampling time had a strong effect (whole model: $F_{3, 67} = 17.96$, $P < 0.001$) on the oak microcuttings growth parameters, i.e. the total plant biomass, shoot and root biomass, as well as root: shoot ratio (Figure 28 and 29). At the first sampling, the total plant biomass ranged between 0.26 ± 0.06 and 0.33 ± 0.08 during bud rest stage (hereinafter BR) and 0.20 ± 0.07 - 0.31 ± 0.07 during root flush stage (hereinafter RF) (Figure 28). The growth stage of the oak microcuttings ($F_{1, 40} = 4.44$, $P = 0.041$) and interaction with *P. penetrans* ($F_{1, 40} = 4.92$, $P = 0.032$) increased plant biomass during BR in comparison to than RF (Figure 28). In contrast, the mycorrhizal the helper bacterial *Streptomyces sp*. AcH 505 had no effect on the plant biomass at the first sampling.

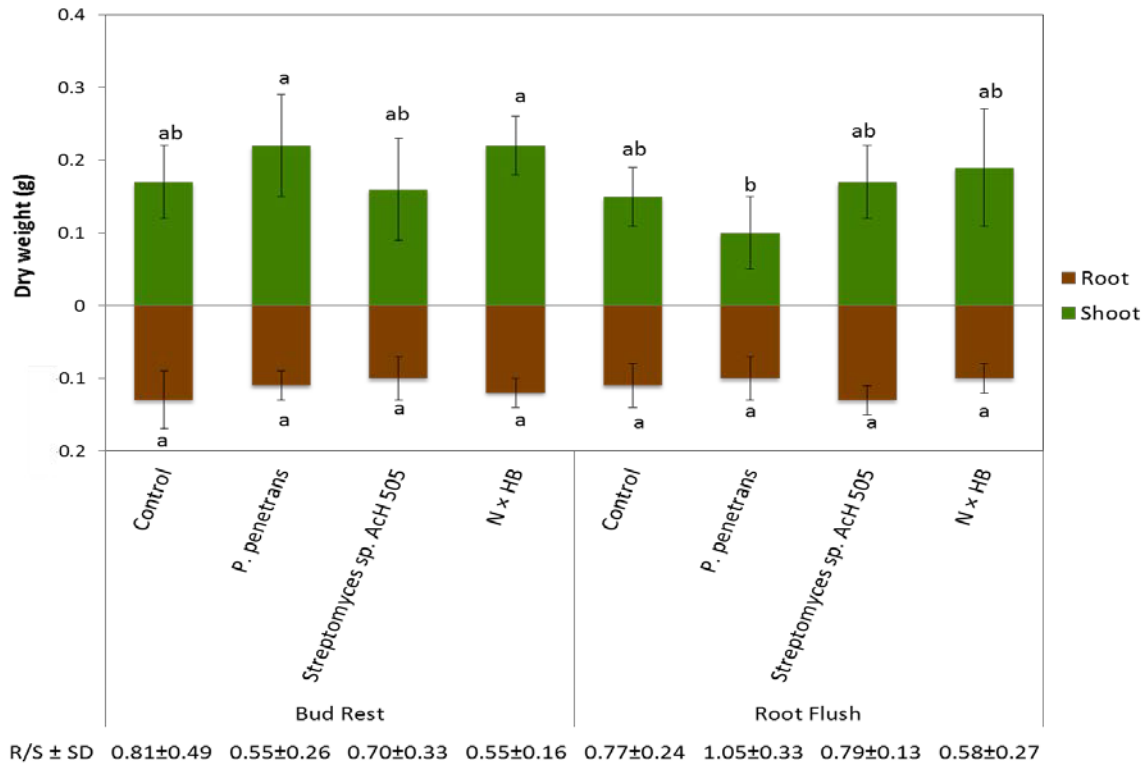

Figure 28 Effects of the plant-parasitic nematode *Pratylenchus penetrans* and the mycorrhizal helper bacteria *Streptomyces* sp. AcH 505 on growth of *Quercus robur* microcuttings. Presented are the biomass data (in g dry weight ± s.d.) of root and shoot compartments and root/shoot ratios (R/S) of the biomass of microcuttings during bud rest and root flush growth stages at 7 (first sampling) weeks after the establishment of the microcosms, data with the same letters are not significantly different according to Tukey's HSD test at $P < 0.05$. N: nematodes, HB: *Streptomyces* sp. AcH 505

At the second sampling the total plant biomass ranged between 0.32 ± 0.08 - 0.43 ± 0.09 and 0.33 ± 0.14 - 0.58 ± 0.06 during BR and RF, respectively (Figure 29) *Streptomyces* sp. AcH 505 enhanced total plant ($F_{1, 29}$ = 6.45, P = 0.0167) and shoots biomass ($F_{1, 29}$ = 6.00, P = 0.021) of oak microcuttings at stage BR in comparison to control soil (by 35%) and inoculated with *P. penetrans* (by 55%)(Figure 29). The growth stage of oak microcuttings had a significant effect on the root biomass ($F_{1, 29}$ = 6.70, P = 0.015) during RF the microcuttings had significantly higher root biomass compared to plants during BR (Figure 29). In contrast, the plant-parasitic nematode reduced the root biomass ($F_{1, 29}$ = 6.00, P = 0.021) by 33 and 48% compared to control and *Streptomyces* sp. AcH 505 inoculated soil, respectively during RF (Figure 29).

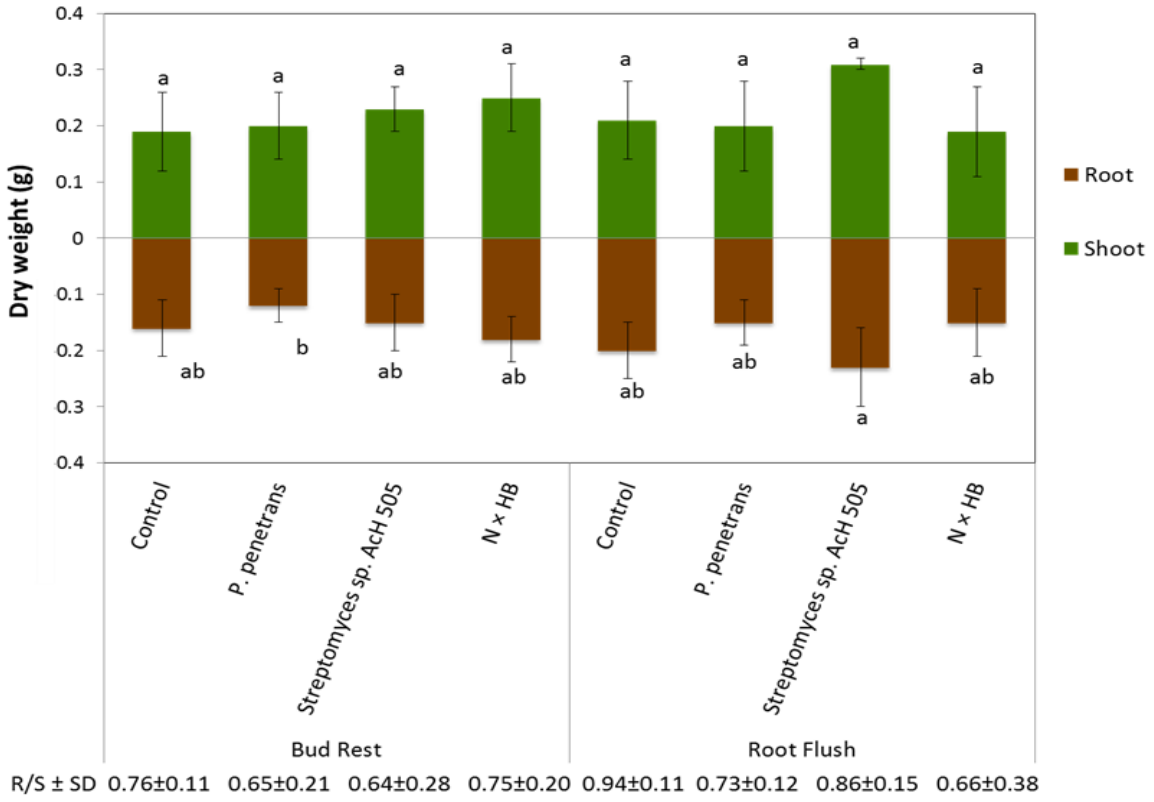

Figure 29 Effects of plant-parasitic nematode *Pratylenchus penetrans* and the mycorrhizal helper bacteria *Streptomyces* sp. AcH 505 on the growth of *Quercus robur* microcuttings. Presented are the biomass data (in g dry weight ± s.d.) of root and shoot compartments and root/shoot ratios (R/S) of the biomass of microcuttings during bud rest and root flush growth stages at 9 (second sampling) weeks after the establishment of the microcosms, data with the same letters are not significantly different according to Tukey's HSD test at $P < 0.05$. N: nematodes, HB: *Streptomyces* sp. AcH 505

3.2.2 Interactions between *Pratylenchus penetrans* and *Streptomyces* sp. AcH505

The population density of *P. penetrans* individuals retrieved from the soil at both sampling times was not affected by the presence of *Streptomyces* sp. AcH 505 (Table 10). Instead, sampling time ($F_{1, 32}$ = 4.97, P = 0.028) and growth stage ($F_{1, 32}$ = 2.05, P = 0.049) of the oak microcuttings affected the number of nematodes, with more *P. penetrans* being extracted from the soil at the second sampling (28 days after inoculation (DAI)) compared to the first sampling (14 DAI) (Table 10).

Table 10 Biotic interactions in the rhizosphere of *Quercus robur* microcuttings: effect of the mycorrhizal helper bacteria *Streptomyces* sp. AcH 505 on *Pratylenchus penetrans* (individuals g^{-1} soil fresh weight ± s.d.) and effect of *P. penetrans* on the relative abundance (in terms of delta Ct values) of *Streptomyces* sp. AcH 505. Presented are oak stages bud rest (BR) and root flush (RF) at 7 (first sampling) and 9 (second sampling) weeks after establishment of the microcosms. For each sampling time, applying to both growth stages ANOVA with *for P < 0.05. N: nematodes (*Pratylenchus penetrans*), HB: mycorrhizal helper bacteria (*Streptomyces* sp. AcH 505) and S: oak growth stage

		First Sampling	Second Sampling
	Nematode numbers g^{-1} soil		
Stage BR	N	4.94 ± 2.21	5.08 ± 1.56
	N × HB	3.52 ± 1.85	6.00 ± 2.61
Stage RF	N	3.51 ± 0.90	4.83 ± 1.95
	N × HB	2.7 ± 0.37	3.45 ± 0.80
	ANOVA	S*	S*
	Abundance of *Streptomyces* sp. ΔCt		
Stage BR	HB	1.07 ± 2.09	5.47 ± 1.63
	N × HB	1.12 ± 0.77	3.98 ± 1.58
Stage RF	HB	3.28 ± 1.92	3.21 ± 1.59
	N × HB	0.68 ± 0.40	3.99 ± 1.02
	ANOVA	N*, S×N*	S*, S×N*

The sampling time ($F_{1, 64}$ = 49.67, P < 0.001) affected the abundance of *Streptomyces* sp. AcH505, higher abundances of the mycorrhizal helper bacteria were detected in rhizosphere soils of the oak microcuttings during the second sampling (25 DAI) in comparison to the first sampling (39 DAI) (Table 10). Inoculation of *P. penetrans* reduced the abundance of

Streptomyces sp. AcH505. At first sampling, this negative impact ($F_{1, 32}$ = 5.54, P = 0.025) was depending on the growth stage of the microcuttings ($F_{1, 32}$ = 6.00, P = 0.020) with a decline during RF compared BR (Table 10). At second sampling the growth stage of the plants ($F_{1, 32}$ = 4.92, P = 0.034) and its interaction with *P. penetrans* ($F_{1, 32}$ = 5.01, P = 0.032) resulted in lower abundances of *Streptomyces* sp. AcH 505 in soils of oak microcuttings during BR compared to RF (Table 10).

3.2.3 Effect of *P. penetrans* and *Streptomyces* sp. AcH 505 on the rhizosphere microbial biomass and dominant groups

The microbial biomass in the rhizosphere soil of oak microcosms ranged between 14.6-51.9 and 10.1-46.0 nmol g^{-1} DW at the first and second sampling, respectively (Table 11). Irrespective of sampling time, *P. penetrans* reduced the amount of PLFAs during RF but increased it during BR relative to the control (Table 11). Meanwhile, *Streptomyces* sp. AcH 505 lowered ($F_{1, 40}$ = 4.63, P = 0.037) the microbial biomass particularly during growth stage B at the first sampling; however, it had no impact at second sampling (Table 11).

Table 11 Effects of plant-parasitic nematode *Pratylenchus penetrans* and the mycorrhizal helper bacteria *Streptomyces* sp. AcH 505 on the amount of actinobacteria, Gram+ and Gram- bacteria, fungi and total amounts of phospholipid fatty acids (amount in nmol g^{-1} ± s.d.), and the fungi/bacteria ratio in the rhizosphere soil of *Quercus robur* microcuttings. Presented are data during bud rest and root flush of oak developmental stages at 7 (first sampling) and 9 (second sampling) weeks after the establishment of the microcosms. For each sampling time, ANOVA with *, ** and *** for $P < 0.05$, $P < 0.01$ and $P < 0.001$, respectively. Values in a row followed by the same letter are not significantly different (Tukey's HSD test, $P < 0.05$). N: nematodes, HB: helper bacteria and S: oak growth stage

	Bud Rest				Root Flush				
	Control	*Pratylenchus penetrans* (N)	*Streptomyces* sp. AcH 505 (HB)	N × HB	Control	*Pratylenchus penetrans* (N)	*Streptomyces* sp. AcH 505 (HB)	N × HB	ANOVA
First Sampling									
Actinobacteria	2.0 ± 1.6a	7.0 ± 5.8a	2.1 ± 2.5ab	4.2 ± 3.4ab	4.6 ± 2.5ab	3.6 ± 3.1ab	1.4 ± 1.3b	1.7 ± 1.9b	HB*, S × N*
Gram+	4.0 ± 3.2ab	11.6 ± 9.1a	3.9 ± 3.9b	8.1 ± 6.0ab	8.2 ± 4.0ab	6.4 ± 4.9ab	3.3 ± 2.7b	3.5 ± 3.7b	HB*, S × N*
Gram-	1.5 ± 0.8	5.3 ± 4.4	3.1 ± 5.0	6.2 ± 6.3	5.0 ± 3.6	3.4 ± 3.6	1.5 ± 0.8	1.8 ± 1.4	S × N*
Fungi	0.8 ± 0.6b	4.2 ± 4.6a	1.1 ± 0.9ab	2.5 ± 3.0ab	1.5 ± 0.9ab	1.5 ± 1.1ab	0.6 ± 0.2b	1.1 ± 1.2b	N*
F/B	0.09 ± 0.03	0.13 ± 0.06	0.14 ± 0.10	0.10 ± 0.06	0.06 ± 0.01	0.12 ± 0.08	0.09 ± 0.04	0.17 ± 0.16	
Total amount of PLFAs	15.8 ± 11.4a	51.9 ± 42.5a	18.5 ± 21.0a	36.4 ± 30.4a	36.7 ± 19.0a	27.8 ± 22.3a	12.5 ± 8.3a	14.6 ± 14.0a	HB*, S × N*
Second Sampling									
Actinobacteria	1.0 ± 0.5b	5.8 ± 2.8ab	3.6 ± 3.7ab	5.8 ± 1.6a	4.4 ± 3.0ab	2.7 ± 2.3ab	2.9 ± 2.2ab	2.3 ± 1.8ab	S × N**
Gram+	2.3 ± 0.7b	10.7 ± 4.8ab	7.8 ± 7.5ab	10.6 ± 3.1a	7.2 ± 5.1ab	5.2 ± 4.8ab	6.7 ± 5.3ab	4.3 ± 3.5ab	S × N**
Gram-	1.1 ± 0.4b	5.2 ± 3.6ab	5.2 ± 5.6ab	7.0 ± 3.9a	5.0 ± 3.4ab	2.7 ± 2.6ab	3.7 ± 1.7ab	2.0 ± 1.2ab	S × N**
Fungi	0.7 ± 0.1a	2.4 ± 1.4a	2.3 ± 3.2a	2.8 ± 1.3a	1.7 ± 3.4a	1.3 ± 0.9a	5.0 ± 6.1a	1.4 ± 0.8a	S × N*
F/B	0.13 ± 0.06ab	0.09 ± 0.02ab	0.10 ± 0.04ab	0.10 ± 0.02ab	0.07 ± 0.02b	0.10 ± 0.03ab	0.22 ± 0.20a	0.14 ± 0.03ab	HB*, S × HB*
Total amount of PLFAs	10.1 ± 1.2a	43.1 ± 21.6a	34.6 ± 33.5a	46.0 ± 16.2a	33.9 ± 22.3a	21.1 ± 17.4a	34.5 ± 27.9a	18.4 ± 13.6a	S × N**

At first sampling, irrespective of plant growth stage *Streptomyces* sp. AcH 505 reduced the amount of actinobacteria ($F_{1, 40}$ = 5.65, P = 0.022) and Gram-positive bacteria ($F_{1, 40}$ = 4.34, P = 0.044) in soil (Table 11). In contrast, the presence of *P. penetrans,* particularly during BR stage, enhanced the amount of actinobacteria ($F_{1, 40}$ = 4.73, P = 0.036), Gram-positive bacteria ($F_{1, 40}$ = 4.94, P = 0.032) and Gram-negative bacteria ($F_{1, 40}$ = 4.39, P = 0.043) compared to RF (Table 11). In addition, *P. penetrans* enhanced the amount of fungi in the soil ($F_{1, 40}$ = 4.37, P = 0.043), this was more pronounced relative to the control during BR of the microcuttings (Table 11). Neither oak growth stage nor *P. penetrans* and *Streptomyces* sp. AcH505 had any effect on the fungal to bacterial ratio.

Similarly, at the second sampling time the interaction between *P. penetrans* and the growth stage of the plants resulted in an increase in the amounts of all dominant groups during BR relative to the control (actinobacteria: $F_{1, 29}$ = 10.11, P = 0.004; Gram-positive bacteria: $F_{1, 29}$ = 8.09, P = 0.008; Gram-negative bacteria: $F_{1, 29}$ = 7.87, P = 0.009 and fungi: $F_{1, 29}$ = 5.19, P = 0.030) during RF (Table 12). Contrastingly, the impact of *Streptomyces* sp. AcH 505 was restricted to an enhanced fungal to bacterial ratio in the soil ($F_{1, 29}$ = 4.88, P = 0.035) independently and in interaction with the growth stage of the oaks ($F_{1, 29}$ = 8.46, P = 0.007) (Table 11).

3.2.4 Effect of *Pratylenchus penetrans* and *Streptomyces* sp. AcH 505 on rhizosphere microbial community structure

At first sampling MANOVA revealed that both *P. penetrans* ($F_{17, 24}$= 2.23, P = 0.035) and *Streptomyces* sp. AcH 505 ($F_{14, 27}$= 2.11, P = 0.046) prompted significant changes in the predominant fatty acids in the rhizosphere of oak. *P. penetrans* modified the lipid profiles in the rhizosphere of oak compared to the control during BR, shifts were accompanied by increases in the amounts of PLFAs i14:0, i15:0 and i16:0, 16:0-10 meth, 17:0 10-meth, 18:0-10 meth, 18:2ω6,9 and 18:1ω9c (Table 12).

In contrast, the microbial community structure of soils inoculated with *Streptomyces* sp. AcH 505 distinctly differed from the control during RF, at first sampling (Table 12). Soils inoculated with the mycorrhizal helper bacteria had significantly lower amounts of PLFAs i15:0, i16:0, 16:0-10 meth, 17:0 10-meth, 18:0-10 meth, 18:2ω6,9 and 18:1ω9c (Table 12).

At second sampling time, MANOVA showed that the interaction between *P. penetrans* and the growth stage of the oaks ($F_{12, 18}$ = 2.80, P = 0.037) was primarily responsible for the shifts

in the microbial community structures. The lipid profiles of soils inoculated with *P. penetrans* distinctly shifted from the control during BR (Table 13). These shifts were attributed to increases in the amounts of PLFAs i15:0, a15:0, 16:0, i17:0, 16:1ω7, 16:0 10-meth, 17:0 10-meth, 18:0 10-meth, cy17:0 and cy19:0 in *P. penetrans* solely and co-inoculation with *Streptomyces* sp. AcH 505 treated soils compared to control (Table 13).

Table 12 Phospholipid fatty acids (PLFAs)(in nmol/g DW± s.d.) patterns in rhizosphere soil of *Quercus robur* microcuttings inoculated with the plant-parasitic nematode *Pratylenchus penetrans* and the mycorrhizal helper bacteria *Streptomyces* sp. AcH 505. Presented are data during bud rest and root flush developmental stages of oaks at 7 weeks (first sampling) after the establishment of the microcosms. ANOVA with *, ** and *** for $P < 0.05$, $P < 0.01$ and $P < 0.001$, respectively. For each oak growth stage values in a row followed by the same letter are not significantly different (Duncan test, $P < 0.05$). N: nematodes, HB: helper bacteria and S: oak growth stage. G+: Gram-positive bacteria, G-: Gram-negative bacteria, A: Actinobacteria, B: Bacteria in general and F: Fungi (modified from Caravaca et al., 2015)

		Bud rest				Root flush			
Fatty Acids	Origin	Control	*P. penetrans* (N)	*Streptomyces* sp. (HB)	N x HB	Control	*P. penetrans* (N)	Streptomyces sp. (HB)	N × HB
i14:0	G+	0.00 ± 0.00b	0.2 1± 0.26a	0.03 ± 0.10b	0.08 ± 0.16ab	0.00 ± 0.00a	0.00 ± 0.00a	0.00 ± 0.00a	0.00 ± 0.00a
i15:0		0.94 ± 0.83b	3.02 ± 2.46a	1.01 ± 1.07b	2.09 ± 1.73ab	2.20 ± 1.14a	1.61 ± 1.42a	0.78 ± 0.70b	0.83 ± 0.84b
a15:0		0.79 ± 0.59a	2.39 ± 1.97a	0.82 ± 0.76a	1.71 ± 1.33a	1.55 ± 0.65a	1.13 ± 0.80a	0.78 ± 0.51a	0.79 ± 0.72a
i16:0		1.66 ± 1.39b	4.47 ± 3.15a	1.44 ± 1.45b	2.96 ± 2.01ab	3.29 ± 1.77a	2.64 ± 2.14ab	1.12 ± 1.13b	1.25 ± 1.50b
i17:0		0.17 ± 0.21a	0.63 ± 0.65a	0.20 ± 0.27a	0.50 ± 0.38a	0.51 ± 0.25a	0.40 ± 0.33a	0.19 ± 0.15a	0.19 ± 0.23a
a17:0		0.46 ± 0.25a	0.86 ± 0.68a	0.43 ± 0.32a	0.77 ± 0.48a	0.69 ± 0.24a	0.58 ± 0.27a	0.43 ± 0.23a	0.42 ± 0.37a
cy 17:0	G-	0.55 ± 0.41a	2.04 ± 1.95a	1.58 ± 2.94a	2.00 ± 2.04a	2.78 ± 2.33a	1.72 ± 2.07a	0.60 ± 0.27a	0.69 ± 0.47a
cy 19:0		0.93 ± 0.46a	3.22 ± 2.49a	1.56 ± 2.09a	4.17 ± 4.46a	2.26 ± 1.31a	1.65 ± 1.54a	0.92 ± 0.69a	1.06 ± 0.94a
16:0 10-meth	A	1.34 ± 1.05b	4.67 ± 3.86a	1.48 ± 1.74b	2.89 ± 2.38ab	3.07 ± 1.69a	2.41 ± 2.03ab	0.94 ± 0.81b	1.12 ± 1.17b
17:0 10-meth		0.34 ± 0.28b	1.17 ± 0.94a	0.34 ± 0.42b	0.68 ± 0.54ab	0.78 ± 0.45a	0.62 ± 0.53ab	0.23 ± 0.23b	0.25 ± 0.33a
18:0 10-meth		0.32 ± 0.25b	1.18 ± 0.98a	0.27 ± 0.40b	0.66 ± 0.53ab	0.75 ± 0.39a	0.56 ± 0.49a	0.24 ± 0.23a	0.28 ±0 .36b
16:1 ω7		0.55 ± 0.62a	1.96 ± 1.74a	0.79 ± 0.88a	1.22 ± 1.14a	1.35 ± 0.80a	1.10 ± 1.02ab	0.38 ± 0.29b	0.45 ± 0.42b
16:1ω5		0.00 ± 0.00a	0.45 ± 0.58a	0.07 ± 0.20a	0.25 ± 0.36a	0.17 ± 0.28a	0.20 ± 0.27a	0.00 ± 0.00a	0.00 ± 0.00a
18:1ω9t		1.64 ± 1.73a	5.31 ± 4.91a	1.68 ± 2.41a	3.11 ± 3.11a	4.86 ± 3.08a	2.74 ± 2.68a	1.26 ± 0.83a	1.42 ± 1.62a
18:2ω6,9	F	0.12 ± 0.21b	0.86 ± 0.93a	0.16 ± 0.21b	0.70 ± 1.23a	0.16 ± 0.30ab	0.27 ± 0.36ab	0.04 ± 0.07b	0.27 ± 0.34a
18:1ω9c		0.72 ± 0.39b	3.32 ± 3.67a	0.91 ± 0.69b	1.79 ± 1.82ab	1.29 ± 0.66a	1.26 ± 0.82ab	0.57 ± 0.19b	0.82 ± 0.87ab

Table 13 Phospholipid fatty acids (PLFAs)(in nmol/g DW± s.d.) patterns in rhizosphere soil of *Quercus robur* microcuttings inoculated with the plant-parasitic nematode *Pratylenchus penetrans* and the mycorrhizal helper bacteria *Streptomyces* sp. AcH 505. Presented are data during bud rest and root flush developmental stages of oaks at 9 weeks (second sampling) after the establishment of the microcosms. ANOVA with *, ** and *** for $P < 0.05$, $P < 0.01$ and $P < 0.001$, respectively. For each oak growth stage values in a row followed by the same letter are not significantly different (Duncan test, $P< 0.05$) N: nematodes, HB: helper bacteria and S: oak growth stage. G+: Gram-positive bacteria, G-: G ram-negative bacteria, A: Actinobacteria, B: Bacteria in general and F: Fungi (modified from Caravaca et al., 2015)

		Bud Rest				Root Flush			
Fatty acid	Origin	Control	*P. penetrans* (N)	*Streptomyces* sp. (HB)	N × HB	Control	*P. penetrans* (N)	*Streptomyces* sp. (HB)	N × HB
i14:0	G+	0.00 ± 0.00a	0.06 ± 0.14a	0.09 ± 0.16a	0.07 ± 0.12a	0.11 ± 0.13a	0.05 ± 0.11a	0.00 ± 0.00a	0.00 ± 0.00a
i15:0		0.59 ± 0.21b	2.60 ± 1.25a	2.10 ± 2.12ab	2.82 ± 1.04a	2.22 ± 1.57a	1.37 ± 1.18a	1.77 ± 1.59a	1.12 ± 0.96a
a15:0		0.54 ± 0.14b	2.10 ± 1.16a	1.45 ± 1.32ab	1.82 ± 0.66ab	1.34 ± 0.84a	1.04 ± 0.73a	1.35 ± 1.03a	0.85 ± 0.66a
i16:0		0.74 ± 0.25b	4.40 ± 1.77a	2.91 ± 2.85ab	4.30 ± 0.97a	2.29 ± 2.56a	1.95 ± 2.14a	2.52 ± 2.02a	1.62 ± 1.47a
i17:0		0.13 ± 0.05b	0.67 ± 0.31a	0.50 ± 0.47ab	0.68 ± 0.19a	0.55 ± 0.37a	0.23 ± 0.35a	0.39 ±0 .31a	0.27 ± 0.21a
a17:0		0.33 ± 0.06a	0.89 ± 0.38a	0.76 ± 0.61a	0.88 ± 0.28a	0.73 ± 0.34a	0.51 ± 0.28a	0.64 ± 0.36a	0.42 ± 0.18a
cy 17:0	G-	0.51 ± 0.26b	2.40 ± 1.76a	1.46 ± 1.18ab	2.48 ± 1.29a	1.23 ± 0.67a	0.92 ± 0.47a	1.19 ± 0.09a	0.68 ± 0.36a
cy 19:0		0.59 ± 0.20b	2.77 ± 1.84a	3.70 ± 4.39ab	4.51 ± 2.98a	3.73 ± 2.80a	1.81 ± 2.19a	2.49 ± 1.80a	1.29 ± 0.86a
16:0 10-meth	A	0.71 ± 0.30b	3.86 ± 1.92a	2.20 ± 2.24ab	3.90 ± 1.07a	2.97 ± 2.00a	1.81 ± 1.56a	1.91 ± 1.22a	1.53 ± 1.16a
17:0 10-meth		0.14 ± 0.07b	0.99 ± 0.46a	0.66 ± 0.63ab	0.97 ± 0.25a	0.75 ± 0.50a	0.44 ± 0.40a	0.46 ± 0.32a	0.39 ± 0.32a
18:0 10-meth		0.12 ± 0.10b	0.91 ± 0.43a	0.70 ± 0.67ab	0.91 ± 0.27a	0.72 ± 0.47a	0.41 ± 0.34a	0.58 ± 0.47a	0.38 ± 0.28a
16:1ω7	B	0.35 ± 0.11b	1.64 ± 0.99a	1.15 ± 1.10ab	1.63 ± 0.60a	1.22 ± 0.82a	0.77 ± 0.53a	0.98 ± 0.78a	0.69 ± 0.60a
16:1ω5		0.03 ± 0.06a	0.32 ± 0.32a	0.31 ± 0.35a	0.37 ± 0.22a	0.30 ± 0.33a	0.10 ± 0.18a	0.19 ± 0.07a	0.19 ± 0.27a
18:1ω9t		1.02 ± 0.16a	3.61 ± 1.94a	3.02 ± 3.06a	3.46 ± 1.26a	2.05 ± 1.10a	1.83 ± 1.05a	3.06 ± 2.17a	1.62 ± 1.24a
18:2ω6,9	F	0.13 ± 0.03b	0.51 ± 0.31ab	0.42 ± 0.52ab	0.66 ± 0.28a	0.32 ± 0.37a	0.28 ± 0.21a	1.10 ± 1.28a	0.13 ± 0.18a
18:1ω9c		0.55 ± 0.12b	1.93 ± 1.11a	1.86 ± 2.67ab	2.10 ± 1.07a	1.33 ± 1.18a	0.99 ± 0.75a	3.94 ± 1.80a	1.25 ± 1.01a

3.3 Rhizosphere carbon dynamics modulated by plant-parasitic nematodes and fungivorous Collembola

Image of Collembola foraging on algae (courtesy of T. Buse)

3.3.1 Effects of Pratylenchus penetrans and Protaphorura armata on oak growth parameters

The total biomass of the oak microcuttings ranged between 0.35 ± 0.15 and 0.48 ± 0.16 g DW and was not influenced by the sampling time (Figure 30). Neither singular inoculation of *P. penetrans* nor *P. armata* had any effect on the plant biomass. The interaction between *P. penetrans* and *P. armata* marginally reduced total plant ($F_{1, 28}$ = 4.44, P = 0.044) and shoot biomass ($F_{1, 28}$ = 4.20, P = 0.049) compared to singular *P. penetrans* or *P. armata* at 5 days post-labelling (DPL) plants with $^{13}CO_2$ (Figure 30).

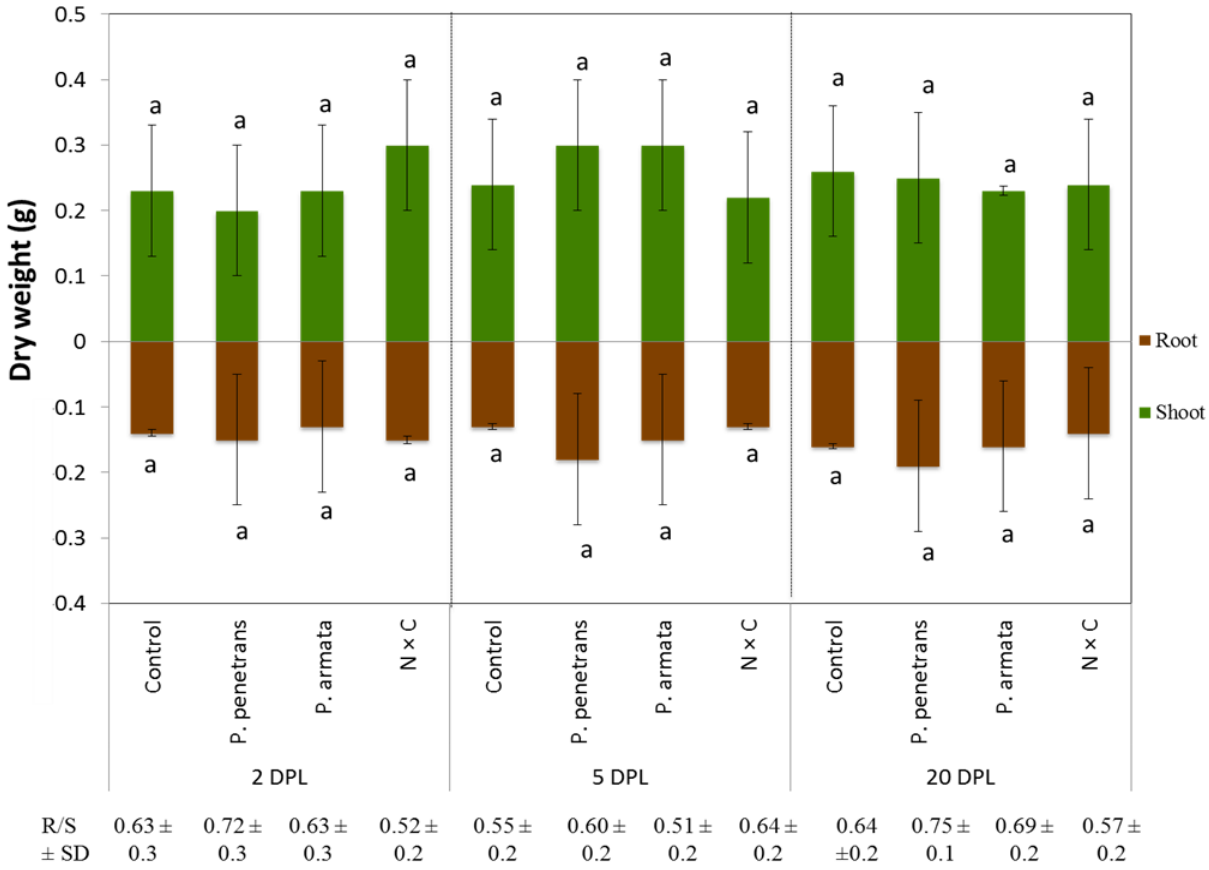

Figure 30 Effects of the plant-parasitic nematode *Pratylenchus penetrans* and the Collembola *Protaphorura armata* on growth of *Quercus robur* microcuttings. Presented are the biomass data (in g dry weight ± s.d.) of root and shoot compartments at 2, 5 and 20 days post labelling (DPL). N: nematodes; C: Collembola. Bars with the same letter are not significantly different Tukey test at P < 0.05

3.3.2 Effect of *Protaphorura armata* on abundance and activity of *P. penetrans*

The number of nematode individuals detected in oak root increased over time ($F_{2, 42}$= 8.82, P < 0.001) (Figure 31). The presence of *P. armata* enhanced the number of nematodes in root tissue ($F_{1, 47}$ = 13.30, P < 0.001), demonstrated by a 100% increase compared to singular *P. penetrans* treatment during the third sampling (20 DPL). On the other hand, the numbers of nematodes extracted from the rhizosphere soil declined significantly by >50% in the presence of *P. armata* ($F_{1, 40}$ = 22.92, P < 0.001) regardless of sampling time (Figure 31).

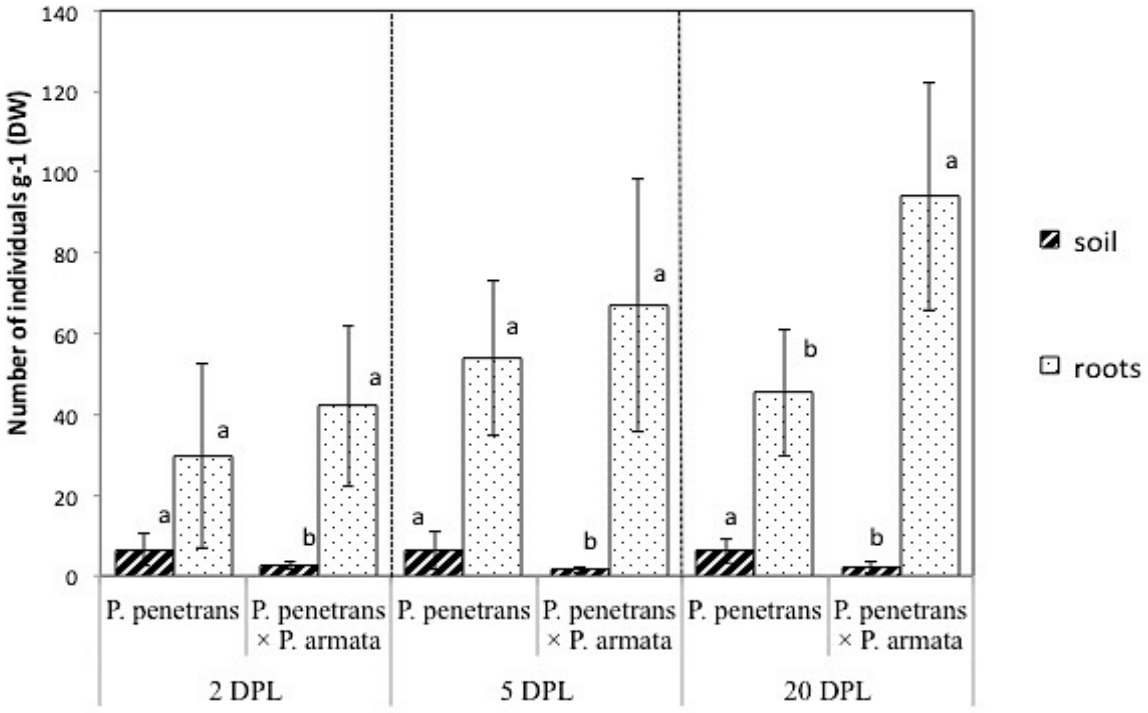

Figure 31 Numbers of *Pratylenchus penetrans* (ind. g-^{1} DW) in the microcosm soil or inside the roots of oak microcuttings. Mesocosms were inoculated with the nematode *Pratylenchus penetrans* solely or in combination with the *Protaphorura armata* (*P. penetrans* × *P. armata*). Presented are data of the first (2 DPL), second (5 DPL) and third (20 DPL) sampling times of the oak microcuttings. Data with the same or no letters are not significantly different according to Tukey's HSD test at P < 0.05. DPL: days post labelling

3.3.4 Effect of *P. penetrans* and *Protaphorura armata* on the rhizosphere microbial biomass and dominant groups

The total amount of soil PLFAs ranged between 46.5 - 65.5 nmol g^{-1} DW (Table 14) and showed no significant variation with time. Irrespective of sampling time or treatment, bacteria dominated the rhizosphere microbial community accounting for 64- 72 % of the total biomass, while fungal biomass was relatively low with 7-18 %. Consequently, the fungal to bacterial ratios were low, with values < 0.16 and showed minor variations due to treatments or sampling time. The effects of the plant-parasitic nematode *P. penetrans* and the fungal grazer *P. croceum* on the rhizosphere microbial biomass increased with time, and distinctions between the treatments became more apparent at 20 DPL, where the presence of the *P. armata* increased the total microbial biomass ($F_{1, 27}$ = 5.35, P = 0.029) (Table 14).

P. penetrans and *P. armata* differentially affected the bacterial community at 20 DPL. *P. armata* increased the bacterial biomass ($F_{1, 27}$ = 5.57; P = 0.026), whereas its interaction with *P. penetrans* promoted the abundance of Gram-positive bacteria in the rhizosphere soil compared to sole inoculation with *P. penetrans* ($F_{1, 27}$ = 7.74, P = 0.001). *P. penetrans* contrastingly lowered the bacterial biomass ($F_{1, 27}$ = 4.61; P = 0.041), particularly of Gram-negative taxa (and $F_{1, 27}$= 7.40, P = 0.011) (Table 14).

Table 14 Effects of the plant-parasitic nematode *Pratylenchus penetrans* and the fungivorous Collembola *Protaphorura armata* on the occurrence of Gram-positive and Gram-negative bacteria, and fungi (phospholipid fatty acids in nmol g^{-1} DW soil ± s.d.) in the rhizosphere of *Quercus robur* microcuttings. Presented are data of the first (2 DPL), second (5 DPL) and third (20 DPL) sampling times of oak microcuttings. Data with the same or no letters are not significantly different according to Tukey's HSD test at $P < 0.05$. DPL - days post labelling. N: nematodes, C: Collembola, Gram+/Gram: Gram-positve to Gram-negative bacteria ratio, f/b: fungal to bacterial ratio

	Control	*P. penetrans*	*P. armata*	N × C
2 DPL				
Gram +	16.7 ± 5.5	17.0 ± 5.4	18.6 ± 4.1	19.3 ± 4.3
Gram -	10.1 ± 6.8	11.0 ± 5.4	10.3 ± 3.8	9.7 ± 4.5
Fungi	3.9 ± 2.4	4.1 ± 3.2	4.3 ± 2.5	5.8 ± 1.4
Bacteria (total)	37.3 ± 16.8	38.9 ± 14.9	38. 3 ±7.9	41.7 ± 9.7
f/b	0.10 ± 0.05	0.10 ± 0.05	0.11 ± 0.05	0.14 ± 0.04
Gram+/Gram-	2.14 ± 1.2	1.69 ± 0.55	2.06 ± 1.0	2.35 ± 1.0
Total PLFA amount	57.8 ± 26.9	60.5 ± 24.9	60.7 ± 14. 6	65.3 ± 13.3
5 DPL				
Gram +	16.2 ± 4.9	13.8 ± 3.7	16.0 ± 4.4	16.8 ± 2.8
Gram -	11.9 ± 7.4	8.2 ± 1.7	7.4 ± 2.2	8.9 ± 2.1
Fungi	3.8 ± 1.9	4.3 ± 1.7	5.2 ± 2.3	4.0 ± 2.1
Bacteria (total)	39.1 ± 17.0	31.1 ± 6.2	31.9 ± 7.4	34.4 ± 6.3
f/b	0.11 ± 0.08	0.14 ± 0.05	0.16 ± 0.07	0.12 ± 0.06
Gram+/Gram-	1.62 ± 0.7	1.76 ± 0.7	2.28 ± 0.8	1.95 ± 0.3
Total PLFA amount	60.8 ± 23.1	49.6 ± 9.4	51.6 ± 11.6	54.5 ± 9.5
20 DPL				
Gram +	15.4 ± 3.7ab	13.0 ± 3.9b	19.2 ± 5.0a	17.0 ± 4.3ab
Gram -	12.8 ± 2.2ab	8.7 ± 4.6b	13.7 ± 3.1a	11.4 ± 2.5ab
Fungi	3.6 ± 2.5	3.0 ± 1.5	3.6 ± 1.4	3.9 ± 1.6
Bacteria (total)	37.8 ± 10.0ab	27.3 ± 12.4b	44.3 ± 10.3a	38.6 ± 8.6ab
f/b	0.10 ± 0.08	0.10 ± 0.05	0.10 ± 0.09	0.10 ± 0.03
Gram+/Gram-	1.24 ± 0.3	1.64 ± 0.5	1.43 ± 0.3	1.49 ± 0.2
Total PLFA amount	57.5 ± 14.2ab	46.5 ± 17.1b	65.6± 13.1a	59.8± 13.1ab

3.3.5 Effect of *Pratylenchus penetrans* and *Protaphorura armata* on rhizosphere microbial community structure

The microbial community structure as indicated by the soil PLFA patterns strongly differed with sampling time, presence of *P. armata* and their interaction (MANOVA: $F_{15, 67} = 107.75$, $P < 0.001$; sampling times: $F_{30, 134} = 4.65$, $P < 0.001$, *P. armata*: $F_{15, 67} = 2.39$, $P = 0.008$, sampling date × *P. armata*: $F_{30, 134} = 1.61$, $P = 0.036$). At individual sampling times the microbial community structure was mainly affected by the presence of *P. penetrans* at 2 DPL ($F_{15, 12} = 3.06$, $P = 0.029$) while the impact of *P. armata* was most pronounced at 20 DPL ($F_{15, 13} = 4.02$, $P = 0.008$). Treatment effects on the amount of individual PLFAs were not significant at the first two sampling times (2 and 5 DPL) (Table A5 and A6) but became evident at the third sampling time at 20 DPL (Table 15).

Table 15 Effects of the nematode *Pratylenchus penetrans* and the Collembola *Protaphorura armata* on the amounts of individual phospholipid fatty acids (in nmol g^{-1} DW soil ± s.d.) in the rhizosphere of *Quercus robur* microcuttings. Presented are data of third (20 DPL) sampling time of oak microcuttings. ANOVA with *, ** and *** for P < 0.05, P < 0.01 and P < 0.001, respectively. Values in a row followed by the same letter are not significantly different (Tukey's HSD test, $P < 0.05$). N: nematodes, C: Collembola. DPL - days post labelling

		Control	*P.penetrans*	*P. armata*	N × C	ANOVA
Fatty acid	Organism					
i15:0	Gram-positive bacteria	5.0 ± 1.1 ab	3.9 ± 1.6 b	6.6 ± 1.9 a	5.90 ± 1.41ab	C**
a15:0		2.88 ± 0.94ab	1.96 ± 0.72b	3.53 ± 1.11a	2.95 ± 0.77ab	N*, C*
i16:0		5.02 ± 1.10ab	4.27 ± 1.36b	6.06 ± 1.19a	5.79 ± 1.36ab	C**
i17:0		1.42 ± 0.35ab	1.05 ± 0.61b	1.76 ± 0.54a	1.56 ± 0.48ab	C*
a17:0		1.03 ± 0.59	0.76 ± 0.52	1.28 ± 0.64	0.94 ± 0.66	
cy17:0	Gram-negative bacteria	7.02 ± 2.34ab	4.08 ± 2.65b	7.61 ± 2.02a	6.12 ± 1.38ab	N**
cy19:0		5.82 ± 1.39	3.98 ± 2.12	6.04 ± 1.54	5.30 ± 1.39	N*
16:1ω7c	Bacteria in general	4.22 ± 0.90	3.10 ± 1.92	5.13 ± 2.06	5.01 ± 1.30	C*
18:1ω7c		5.35 ± 2.50	4.23 ± 2.12	6.28 ± 2.37	5.14 ± 1.34	
18:1ω9c	Fungi	2.01 ± 0.75	1.76 ± 1.00	2.85 ± 1.13	2.97 ± 1.14	C*
18:2ω6c		1.54 ± 1.79	0.85 ± 0.98	0.76 ± 0.52	0.97 ± 0.74	

A corresponding stepwise DFA of the predominant PLFAs showed significant differences among the soil microbial communities at 20 DPL (Figure 32; whole model: $F_{24, 58} = 2.75$, $P < 0.008$). Only the first discriminant function was significant ($P < 0.001$) and accounted for 78% of the variance. There was a separation (eigenvalue: 3.4) of microbial communities in soils inoculated with *P. croceum* from those without (*P. armata* vs. Control: $F_{8, 20} = 5.54$, $P < 0.001$; *P. armata* vs. *P. penetrans*: $F_{8, 20} = 6.07$, $P < 0.001$; *P. penetrans* × *P. armata* vs. Control: $F_{8, 20} = 4.07$, $P = 0.005$ and *P. penetrans* × *P. armata* vs. *P. penetrans*: $F_{8, 20} = 3.37$, $P = 0.013$) (Figure 32). Correlation of the PLFAs with the extracted axis indicated the relevance of PLFAs i15:0, a15:0, i16:0, i17:0, cy17:0, 16:1ω7 and 18:1ω9c (Table 16) in the discrimination of rhizosphere microbial communities along root 1. Correspondingly, significantly higher amounts of these PLFAs were extracted from soils inoculated with *P. armata* compared to singular inoculation with *P. penetrans* at 20 DPL (Table 15).

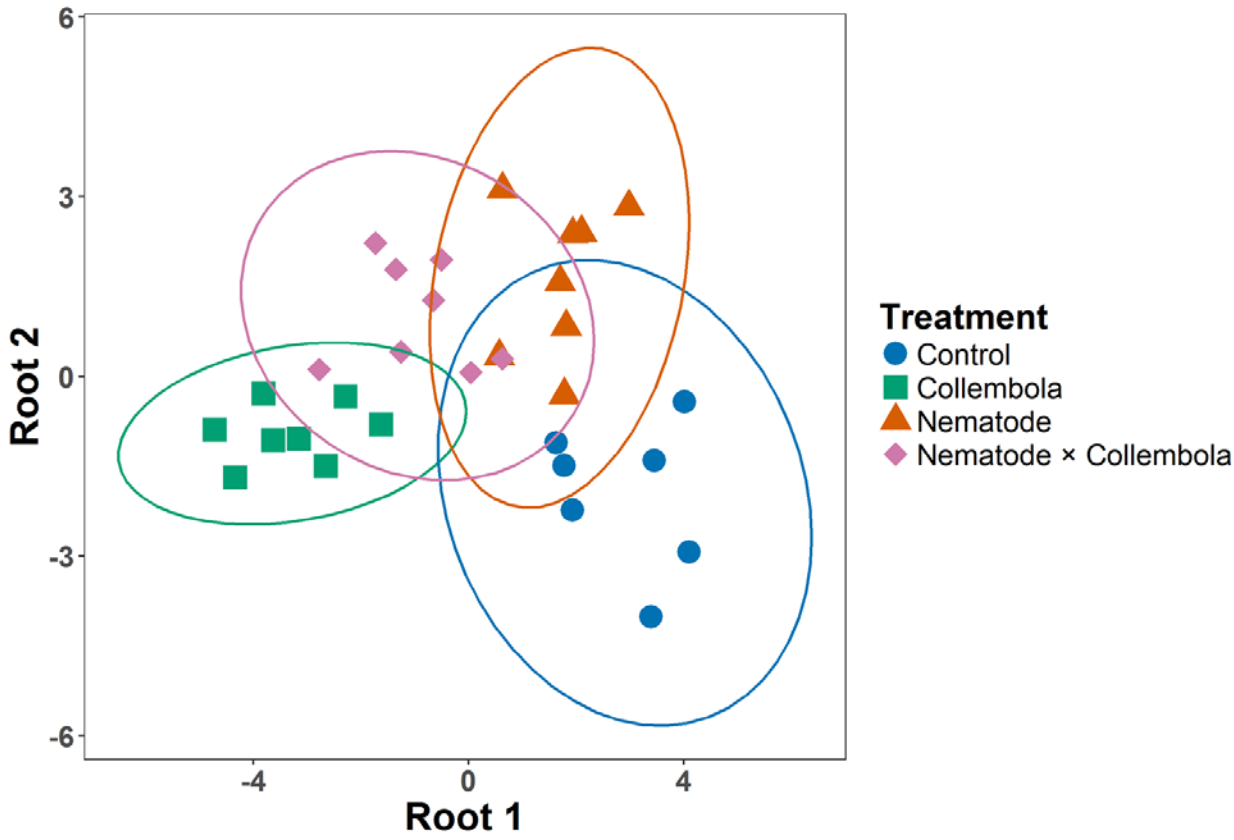

Figure 32 Discriminant plot for the first and second functions of the phospholipid fatty acids identified in the rhizosphere of *Quercus robur* microcuttings inoculated with Nematodes, Collembola or both (groups, n = 4), at 20 days post labelling (DPL) (whole model: $F_{24, 58} = 2.75$, $P < 0.008$)

Table 16 Pearson's coefficients of correlation between concentrations of phospholipid fatty acids and the extracted roots of the discriminant function analyses. Presented are data at third (20 DPL) sampling time of oak microcuttings. The four treatments (Control, *Pratylenchus penetrans*, *Protaphorura armata,* and *P. penetrans* × *P. armata*) were used as groups (n = 4) in the model. Canonical scores for the first and second roots were used for correlation. *, **, and *** refer to $P <$ 0.05, 0.01, and 0.001, respectively. DPL - days post labelling

		20 DPL	
Fatty acid	Organism	ROOT 1	ROOT 2
i15:0	Gram-positive bacteria	0.59***	-0.35*
a15:0		0.52**	-0.41*
i16:0		0.51**	-0.25
i17:0		0.48**	-0.36*
a17:0		0.26	-0.26
cy17:0	Gram-negative bacteria	0.37*	-0.69***
cy19:0		0.3	-0.58***
16:1ω7	Bacteria in general	0.45*	-0.24
18:1ω7		0.28	-0.34
18:1ω9c	Fungi	0.52**	-0.02
18:2 ω6		-0.12	-0.08
14:00	Miscellaneous origin	0.26	-0.3
15:00		0.14	-0.34

3.3.6 Allocation of recent photoassimilates into soil microorganisms

The $^{13}CO_2$ pulse labelling of oaks resulted in the enrichment of plant shoot and root tissue with $\delta^{13}C$ values of 69.0 ± 61.5‰ and 75.4 ± 44.1‰, respectively. Recent photoassimilated carbon was incorporated into seven microbial PLFA markers, which were indicative for Gram-positive bacteria (i15:0, a15:0, i16:0, i17:0), Gram-negative bacteria (cy17:0), general bacteria (16:1ω7) and the ectomycorrhiza fungus *P. croceum* (18:1ω9) (Figure 33). In addition, plant-derived carbon was incorporated into 16:0 a major PLFA present in all organisms in the experiment. However, due to the indiscriminate origin of 16:0, the amount of

incorporation of plant carbon is given for the specific microbial markers, as assessed by the relative abundance (%) of ^{13}C excess (µmol ^{13}C g^{-1} soil dry weight) in individual soil PLFAs.

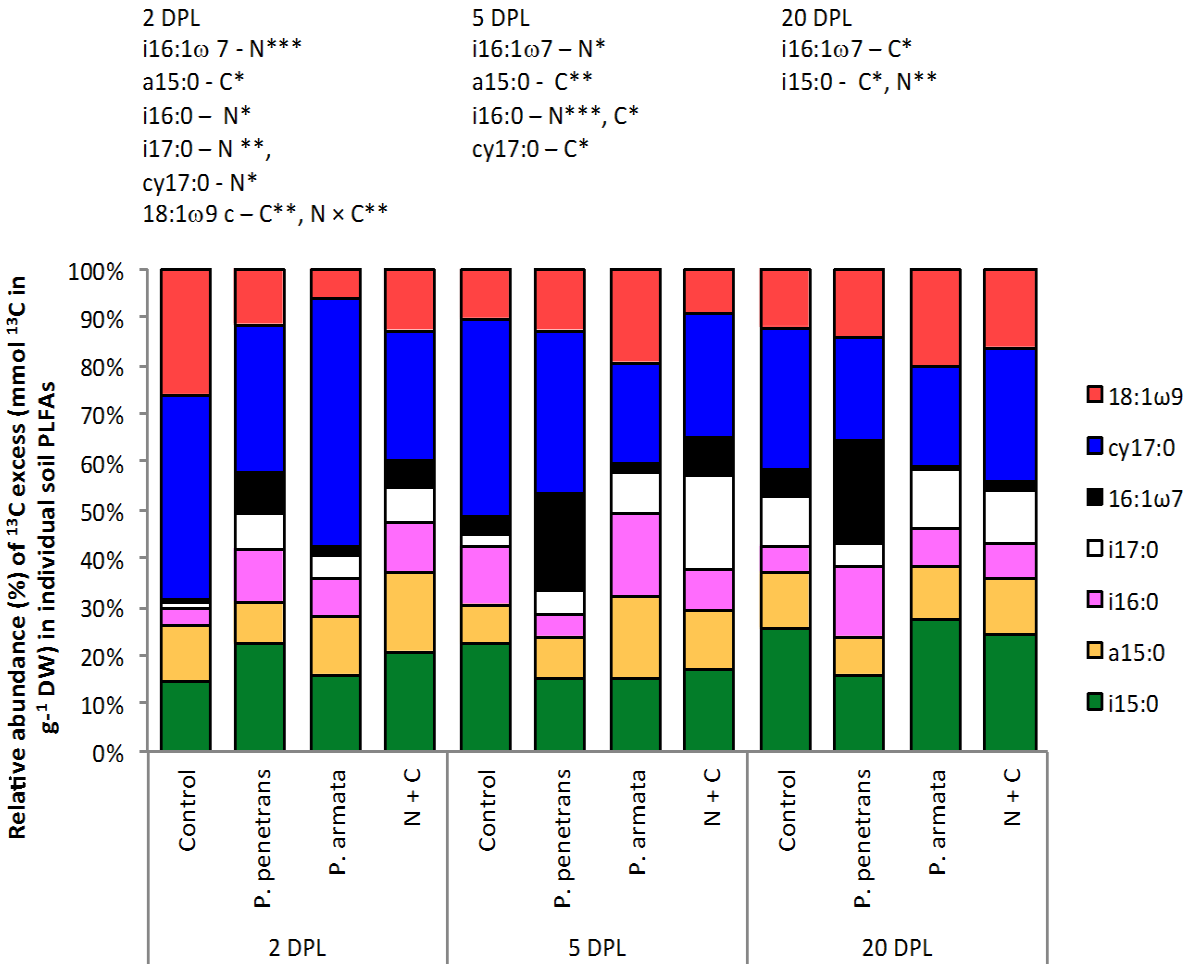

Figure 33 Relative abundance (%) of ^{13}C excess (µmol^{13}C g-^{1} soil dry weight) in individual PLFAs in the rhizosphere of *Quercus robur* microcuttings inoculated with *Pratylenchus penetran*s and the Collembola *Protaphorura armata* sampled at 2, 5 and 20 days post 13CO2 labelling of plants. For each harvest date, ANOVA with *, ** and *** for $P< 0.05$, $P< 0.01$ and $P< 0.001$, respectively. DP: days post labelling, N: nematodes, C: Collembola

In general, plant-derived carbon was largely incorporated into bacteria with amounts ranging between 80-92% of the total ^{13}C allocated in PLFAs across treatments (Figure 33). Gram-positive bacteria markers with methyl branching (iso/anteiso) assimilated most of the plant carbon. Two-way ANOVA revealed that the impact of the soil fauna on microbial carbon allocation pattern (i.e. the number of marker PLFAs significantly affected) decreased progressively from 2 to 20 DPL (Figure 33).

At 2 DPL, *P. penetrans* enhanced assimilation of plant-derived carbon by Gram-positive bacteria and bacteria in general (i16:0: $F_{1, 10} = 7.27$, $P = 0.023$; i17:0: $F_{1, 10} = 13.00$, $P = 0.005$ and 16:1ω7: $F_{1, 10} = 24.65$, $P < 0.001$), while reducing assimilation by Gram-negative bacteria (cy17:0: $F_{1, 10} = 9.61$, $P = 0.011$) (Figure 33). Similarly, *P. armata* stimulated incorporation of plant-derived carbon into Gram-positive bacteria (a15: $F_{1, 10} = 6.46$, $P = 0.029$), while less carbon was assimilated by *P. croceum* (18:1ω9c: $F_{1, 10} = 14.58$, $P = 0.003$). However, this effect was less obvious if *P. penetrans* was also present ($F_{1, 10} = 17.92$, $P = 0.002$).

At 5 DPL, *P. penetrans* continued to enhance assimilation of plant carbon by bacteria in general (16:1ω7: $F_{1, 12} = 8.39$ $P = 0.013$) but reduced assimilation by Gram-positive taxa (i16:0: $F_{1, 12} = 18.81$, $P = 0.001$) (Figure 33). Contrariwise, *P. armata* enhanced incorporation of ^{13}C into Gram-positive bacteria (a15: $F_{1, 12} = 10.14$, $P = 0.008$ and i16:0: $F_{1, 12} = 5.19$, $P = 0.042$), whereas ^{13}C allocation by Gram-negative bacteria declined (cy17:0: $F_{1, 12} = 8.03$, $P = 0.015$).

Contrary to the trend observed at the first two sampling times, at 20 DPL *P. penetrans* lowered incorporation of recently photoassimilated carbon into Gram-positive bacteria (i15:0: $F_{1, 11} = 13.24$, $P = 0.004$), whereas with presence of *P. armata* ^{13}C assimilation by Gram-positive bacteria (i15:0: $F_{1, 11} = 8.63$, $P = 0.0135$ and i17:0: $F_{1, 11} = 7.22$, $P = 0.0212$) increased, while that of bacteria in general (16:1ω7: $F_{1, 11} = 6.45$, $P = 0.028$) decreased (Figure 33).

3.3.7 Collembola feeding behaviour

The accumulation of body fat in Collembola was negatively affected by the presence of nematodes, although not statistically significant. The amount of TLFAs ranged between 288 and 407 nmol g^{-1} DW when only *P. armata* was present in the microcosms, whereas in combination with *P. penetrans* it only ranged between 206 and 290 nmol g^{-1} DW (Table 17). The lipid profile of Collembola consisted of six TLFAs: 16:0, 16:1ω7, 18:0, 18:1ω9c, 18:2ω6,9 and 20:4ω6,9,12,15. The major fatty acids in *P. armata* were oleic (18:1ω9c) and linoleic (18:2ω6,9) acid contributing 42-47% and 15-19% of total fatty acids, respectively. The relative abundance of the individual TLFAs was similar between treatments and sampling dates, with the exception for 16:1ω7 which decreased with time ($F_{2, 37} = 13.85$, $P < 0.001$).

Table 17 Total lipid fatty acids (TLFAs in nmol g^{-1} DW ± s.d.) and relative abundance of individual Collembola fatty acids in the soil of oak microcosms inoculated with *Protaphorura armata* solely (C) or in combination with the nematode *Pratylenchus penetrans* (N + C) after $^{13}CO_2$ labelling of oaks. Presented are data of the first (2 DPL), second (5 DPL) and third (20 DPL) sampling times of oak microcuttings. Data with the same or no letters are not significantly different according to Tukey's HSD test at $P < 0.05$. DPL – days post labelling

	2 DPL		5 DPL		20DPL	
	Collembola	N + C	Collembola	N + C	Collembola	N + C
16:1ω7	2.8 ± 1.3ab	3.5 ± 1.9a	2.9 ±2.4ab	2.9 ± 2.4ab	0.1 ± 0.3c	0c
16:0	18.4 ± 5.3	14.3 ± 2.9	15.3 ± 3.9	16.1 ± 3.1	19.6 ± 5.8	17.9 ± 3.1
18:1ω9c	47.0 ± 4.6	43.8 ± 4.7	44.7 ± 5.3	45.1 ± 3.3	45.1 ± 8.2	41.6 ±4.5
18:2ω6	15.2 ± 3.2	19.2 ± 2.8	18.6 ± 5.2	16.8 ± 3.1	16.5 ± 4.3	18.1 ± 3.9
18:0	10.2 ± 1.8	10.6 ± 1.5	10.0 ± 1.0	10.5 ± 1.5	12.3 ± 1.0	12.0 ± 0.9
20:4ω6,9,12,15c	6.3 ± 3.0	8.6 ± 3.0	8.5 ± 3.2	8.6 ± 1.9	6.4 ± 3.9	10.5 ± 3.6
Total TLFAs (nmol g^{-1} DW)	407 ± 267	219 ± 201	373 ± 346	290 ± 113	288 ± 147	206 ± 645

Recently photoassimilated carbon from oak microcuttings was incorporated into all dominant Collembola TLFAs, and this did not differ significantly between sampling times (Figure 34). Plant-derived carbon was mainly incorporated into 18:1ω9c and 18:2ω6,9 with 42-57 % and 7-19 % of the total ^{13}C excess, respectively, indicating ingestion of fungal tissue by Collembola. Three-way ANOVA showed that the incorporation of ^{13}C into 18:2ω6,9 lessened ($F_{2, 16}$ = 9.55, P = 0.0019) over time with detection only at the first two sampling times (Figure 34). In contrast, the relative abundance of ^{13}C excess in arachidonic acid (20:4ω6,9,12,15) increased over the experimental period ($F_{2, 16}$ = 12.51, $P < 0.000$), likely due to dispersal of the isotopically marked carbon molecules by lipid metabolism of the Collembola (Figure 34).

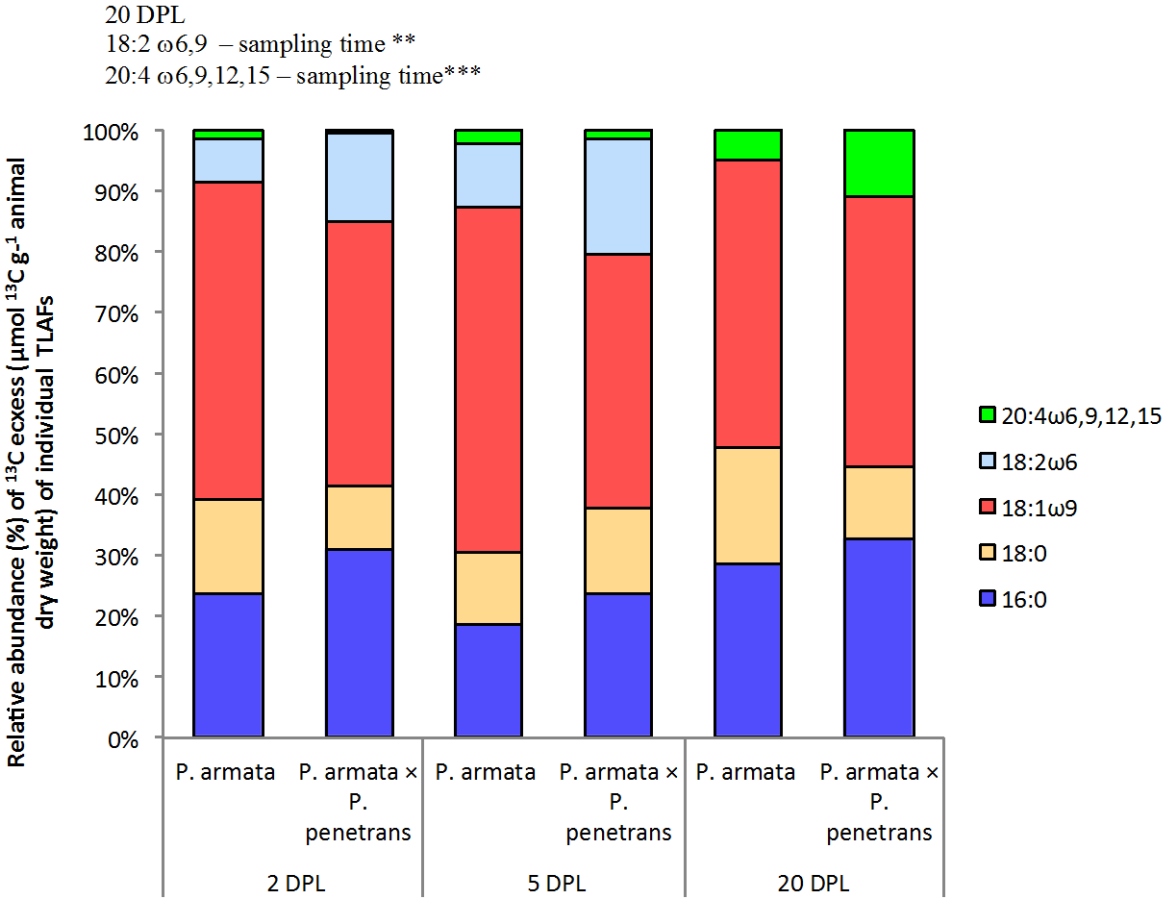

Figure 34 Effects of *Pratylenchus penetrans* on the ^{13}C enrichment of the TLFAs of *Protaphorura armata*. Presented are the relative abundances (%) of ^{13}C excess (µmol ^{13}C g^{-1} animal DW) in individual fatty acids of P. armata at 2, 5 and 20 DPL $^{13}CO_2$ labelling of plants. ANOVA with *, ** and *** for $P < 0.05$, 0.01 and 0.001, respectively. DPL – days post labelling

3.4 Impact of multitrophic interactions on oak growth and rhizosphere microbial communities

Bacterial feeder
Acrobeloides buetschlii

Fungal feeder
Aphelenchoides saprophilus

Plant feeder
Pratylenchus penetrans

Image courtesy of V. Bartel

3.4.1 Effect of nematode functional group amendments on nematode community composition

Nematode population densities in amended soils were comparable to the control, ranging between 8-18 and 7-20 Ind. g^{-1} DW soil after four and eight weeks, respectively (Figure 35). One-way ANOVA showed that amendments had no effect on the nematode density at the first sampling time; while at the second sampling time nematode density differed significantly ($F_{7, 40} = 3.57$, $P = 0.004$) with higher numbers in soils amended with BF + PF in comparison to the FF (Figure 35).

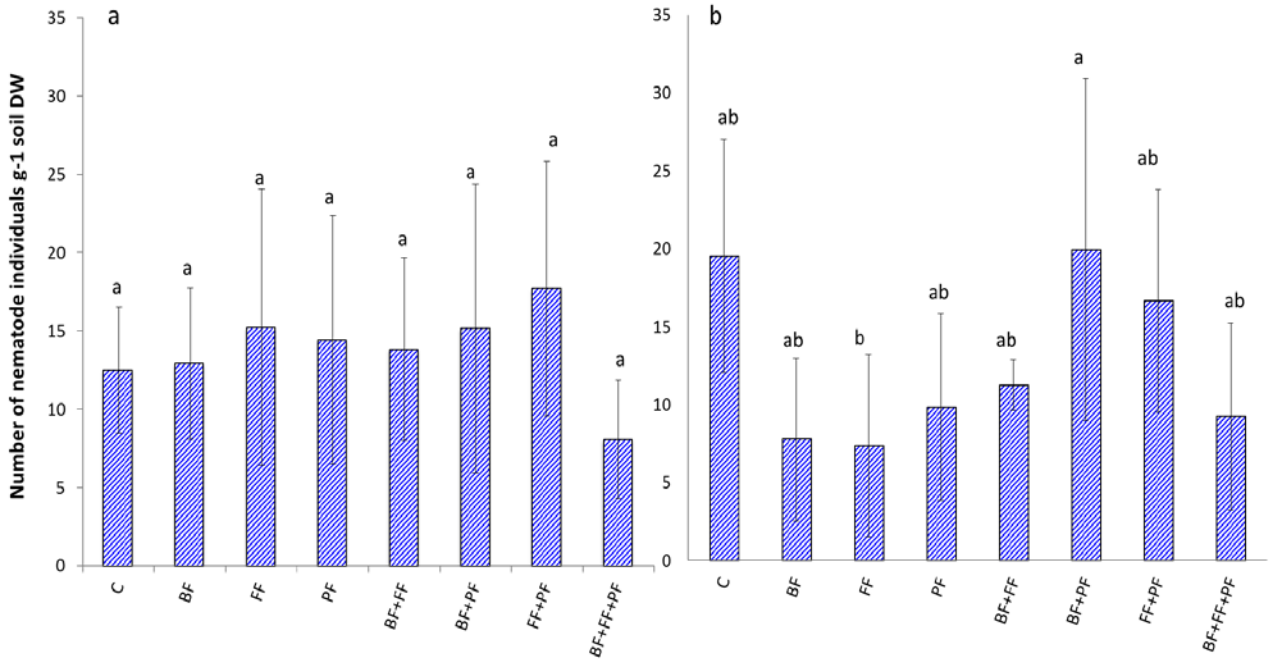

Figure 35 Numbers of nematodes (ind. g^{-1}soil DW± s.d.) after amendment with *Acrobeloides buetschlii* (BF), *Aphelenchoides saprophilus* (FF) and *Pratylenchus penetrans* (PF) and their combinations at first (a - 4 weeks) and second (b - 8 weeks) sampling. Data with the same letter are not significantly different according to Tukey's HSD test, $P < 0.05$

Irrespective of amendment, the nematode communities in the soil were primarily composed of bacterial feeders, fungal feeders and plant feeders (Figure 36). Across all treatments and sampling times, bacterial feeders were the most abundant trophic group accounting for 60-90%, while fungal and plant feeders accounted for 3-26 % and 7-35 % respectively, of the nematode populations (Figure 36).

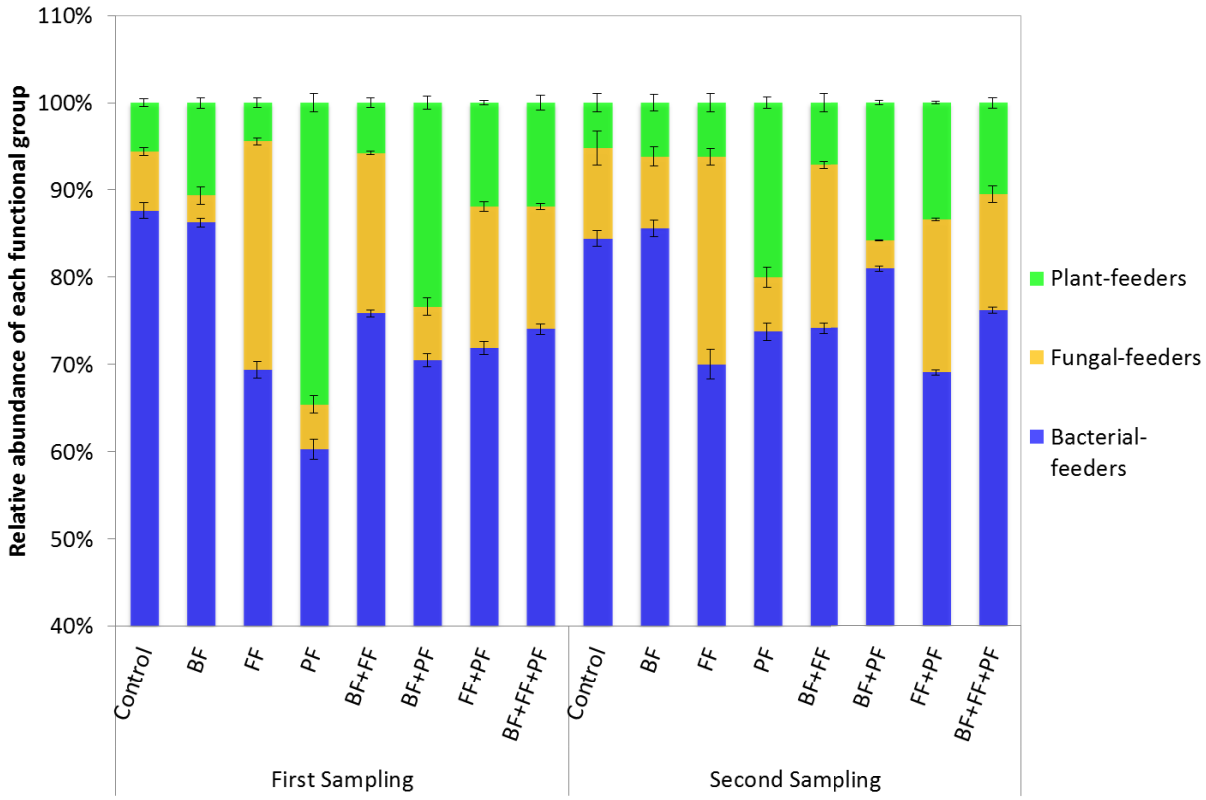

Figure 36 Effect of nematode trophic group amendments on the nematode trophic structure (proportion in % ± s.d.). Soil was amended with *Acrobeloides buetschlii* (BF), *Aphelenchoides saprophilus* (FF), and *Pratylenchus penetrans* (PF) and their combinations. Data presented for 4 (first sampling) and 8 (second sampling) weeks post inoculation

At first sampling, one-way ANOVA revealed the amendments significantly altered the abundance of bacterial feeders ($F_{7, 16} = 247.7$, $P < 0.001$), fungal feeders ($F_{7,16} = 406.5$, $P < 0.001$) and plant feeders ($F_{7,16} = 372.7$, $P < 0.001$), changing the nematode community structure relative to the control. Dunnett's test showed that amending the soil with FF and PF resulted in increased the density of fungal and plant feeders relative to the control.

The treatment effect on the relative abundance of nematode functional groups in the soil remained detectable over time with significant enhancement in the proportion of bacterial feeders ($F_{7, 16} = 147.2$, $P < 0.001$), fungal feeders ($F_{7, 16} = 142.1$, $P < 0.001$) and plant feeders ($F_{7, 16} = 136.7$, $P < 0.001$) at the second sampling. Comparably, inoculation with FF and PF enhanced the density of their respective functional groups while BF did not change abundance of bacterial feeders relative to the control (Figure 36).

3.4.2 Effects of the nematode trophic structure on microbial biomass

The microbial biomass in the pot soil of oaks as assessed by the total amounts of PLFAs ranged between 30.6 and 39.0 nmol g^{-1} DW (Table 18). Two-way ANOVA revealed that the total microbial biomass decreased over time (sampling time × treatment: $F_{7, 76}$ =16.5, P < 0.001), with a significant treatment effect on biomass ($F_{7, 37}$= 16.21, P < 0.001 and $F_{7, 39}$ = 83.9, P < 0.001 at first and second sampling, respectively). Generally, increasing the density of two or more nematode functional groups had a stimulatory effect at both samplings. The application of FF + PF and BF + FF + PF at the first sampling enhanced microbial biomass, whilst FF at the second sampling suppressed total microbial biomass relative to the control (Table 18).

At the first sampling, increasing the dominance of specific nematode trophic groups significantly impacted on the occurrence of microbial groups. Gram-positive ($F_{7, 37}$ = 39.5, P < 0.001) and Gram-negative bacteria ($F_{7, 37}$ = 52.2, P < 0.001) increased in soils amended with BF + FF, FF + PF and BF + FF + PF in comparison to the control, whereas BF + PF reduced the biomass of Gram-positive bacteria (Table 18). In addition the amendments affected the occurrence of Actinobacteria ($F_{7, 37}$ = 6.1, P < 0.001) and bacteria in general $F_{7, 37}$ = 6.4, P < 0.001).

Table 18 Effects of increasing relative abundance of nematode trophic groups in soil on the amounts of Gram+, Gram-, General bacteria, Actinobacteria, Fungi and total PLFAs, (nmol g^{-1} ± s.d.), and the fungi/bacteria ratio in the rhizosphere of *Quercus robur* seedlings. Presented are data at first (4 weeks) and second (eight weeks) sampling times after application of amendments i.e. C: control; BF: *Acrobeloides buetschlii*; FF: *Aphelenchoides saprophilus* and PF: *Pratylenchus penetrans*. Values in a row with the same letters are not significantly different (Tukey's HSD test, $P< 0.05$)

	C	**BF**	**FF**	**PF**	**BF+FF**	**BF+PF**	**FF+PF**	**BF+FF+PF**	**ANOVA**	
1st Sampling									$F_{7,37}$	**P**
Gram +	8.57 ± 0.21cd	8.67 ± 0.11bcd	8.47 ± 0.37d	8.67 ± 0.19bcd	9.08 ± 0.37ab	7.07 ± 0.22e	9.28 ± 0.36a	9.02 ± 0.04abc	39.53	0.000
Gram -	3.41 ± 0.12cd	3.34 ± 0.03cd	3.27 ± 0.03d	3.48 ± 0.12c	3.69 ± 0.06b	3.26 ± 0.04d	3.95 ± 0.12a	3.80 ± 0.04ab	52.17	0.000
Bacteria	6.78 ± 0.63ab	6.73 ± 0.10ab	6.28 ± 0.04bc	6.49 ± 0.49abc	6.71 ± 0.10ab	6.06 ± 0.32bc	7.07 ± 0.08a	6.96 ± 0.02a	6.40	0.000
Actinobacteria	4.43 ± 0.31abc	4.32 ± 0.08bc	4.26 ±0.05bc	4.40 ± 0.36abc	4.70 ± 0.08ab	4.19 ± 0.38c	4.79 ± 0.18a	4.84 ± 0.08a	6.11	0.000
Fungi	3.91 ± 0.59	3.67 ± 0.45	3.69 ± 0.37	3.91 ± 0.59	4.05 ± 0.19	3.91± 0.49	4.20 ± 0.13	4.34 ± 0.06	n.s	n.s
Sum	36.06 ± 2.04cd	35.74 ± 0.46cd	34.90 ± 0.70de	36.49 ±1.52bcd	37.72 ± 1.27abc	32.71 ± 1.49de	39.00 ± 0.64a	38.86 ± 0.64ab	16.21	0.000
F/B ratio	0.17 ± 0.02	0.16 ± 0.02	0.17 ± 0.01	0.17 ± 0.02	0.17 ± 0.01	0.19 ± 0.02	0.17 ± 0.01	0.18 ± 0.00	n.s	n.s
2nd Sampling									$F_{7,39}$	**P**
Gram +	7.91 ± 0.07c	7.55 ± 0.22d	7.15 ± 0.16e	8.17 ± 0.18bc	8.33 ± 0.22b	8.84 ± 0.11a	8.29 ± 0.05b	8.73 ± 0.04a	83.00	0.000
Gram -	3.29 ± 0.05d	3.34 ± 0.02d	3.08 ± 0.04e	3.52 ± 0.04c	3.70 ± 0.07b	3.72 ± 0.08b	3.56 ± 0.03c	4.01 ± 0.05a	178.90	0.000
Bacteria	5.89 ± 0.05c	5.54 ± 0.08d	5.13 ± 0.12e	5.62 ± 0.08d	6.28 ± 0.12b	5.99 ± 0.14c	6.34 ± 0.05 b	6.94 ± 0.10a	190.20	0.000
Actinobacteria	4.19 ± 0.05e	4.29 ± 0.06de	3.81 ± 0.08f	4.26 ± 0.07e	4.50 ± 0.04b	4.45 ± 0.05bc	4.38 ± 0.06 cd	4.82 ± 0.07a	132.20	0.000
Fungi	3.55 ± 0.13d	3.81 ± 0.07c	3.14 ± 0.09e	3.79 ± 0.07c	4.02 ± 0.07b	4.13 ± 0.08b	5.03 ± 0.11a	4.19 ± 0.07b	227.66	0.000
Sum	33.36 ± 0.81d	33.70 ± 0.77d	30.59 ± 0.51e	34.00± 0.25d	35.40 ± 0.77c	36.25 ± 0.69bc	36.83 ± 0.40b	38.05 ± 0.43a	83.90	0.000
F/B ratio	0.167 ± 0.01e	0.184 ± 0.00b	0.164 ± 0.00e	0.176 ± 0.00cd	0.176 ± 0.00bcd	0.179 ±0.00bc	0.223 ± 0.01a	0.171 ± 0.00de	120.83	0.000

At the second sampling, combination treatments, i.e. BF+ FF, BF + PF, FF + PF and BF + FF + PF generally enhanced the growth of Gram-positive bacteria ($F_{7, 39}$ = 83.0, P < 0.001), Gram-negative bacteria ($F_{7, 39}$ = 178.9, P < 0.001), Actinobacteria ($F_{7, 39}$ = 132.2, P < 0.001) and fungi ($F_{7, 39}$ = 227.7, P < 0.001) relative to the control (Table 18). In addition, with time, sole PF amendment stimulated growth of Gram-negative bacteria and fungi. In contrast, singular treatments of BF and FF both reduced the biomass of Gram-positive and general bacteria and FF that of Gram-negative and Actinobacteria as well as fungi.

3.4.3 Effects of the nematode amendment on microbial community structure

Multivariate analysis of PLFA profiles revealed that manipulation of the density of nematode trophic groups provoked significant changes in the predominant fatty acids in the soil at both sampling times (first: $F_{126, 142}$ = 4.85, P < 0.001; second: $F_{126, 155}$ = 23.89, P < 0.001). Discriminant function of analyses of the PLFAs patterns indicated large differences among the microbial communities at the first sampling (whole model: $F_{112, 151}$ = 5.70, P < 0.00; Figure 37). The first two discriminant functions were both significant (root 1: P < 0.001; root 2: P < 0. 001), and explained 84.9% of the total variance. The first discriminant function clearly separated (eigenvalue: 30.3) microbial communities in soils amended with BF + FF, FF + PF, BF + FF+ PF predominantly from the single trophic group treatments along root 1. Correlation of the PLFAs with the extracted axes indicated significant effects of PLFAs i15:0, a15:0, i16:0, 16:1w5, 16:1ω7, 16:0 10-meth, i17:0, a17:0, cy17:0, cy19:0, 18:1ω9c, 18:2ω6,9, 16:0 and 18:0 in the discrimination of microbial communities in soils amended with the different nematode functional groups (Table 20). Correspondingly, the highest levels of the respective PLFAs were in soils amended with BF + FF, FF + PF, BF + FF+ PF at the first sampling time (Table A7).

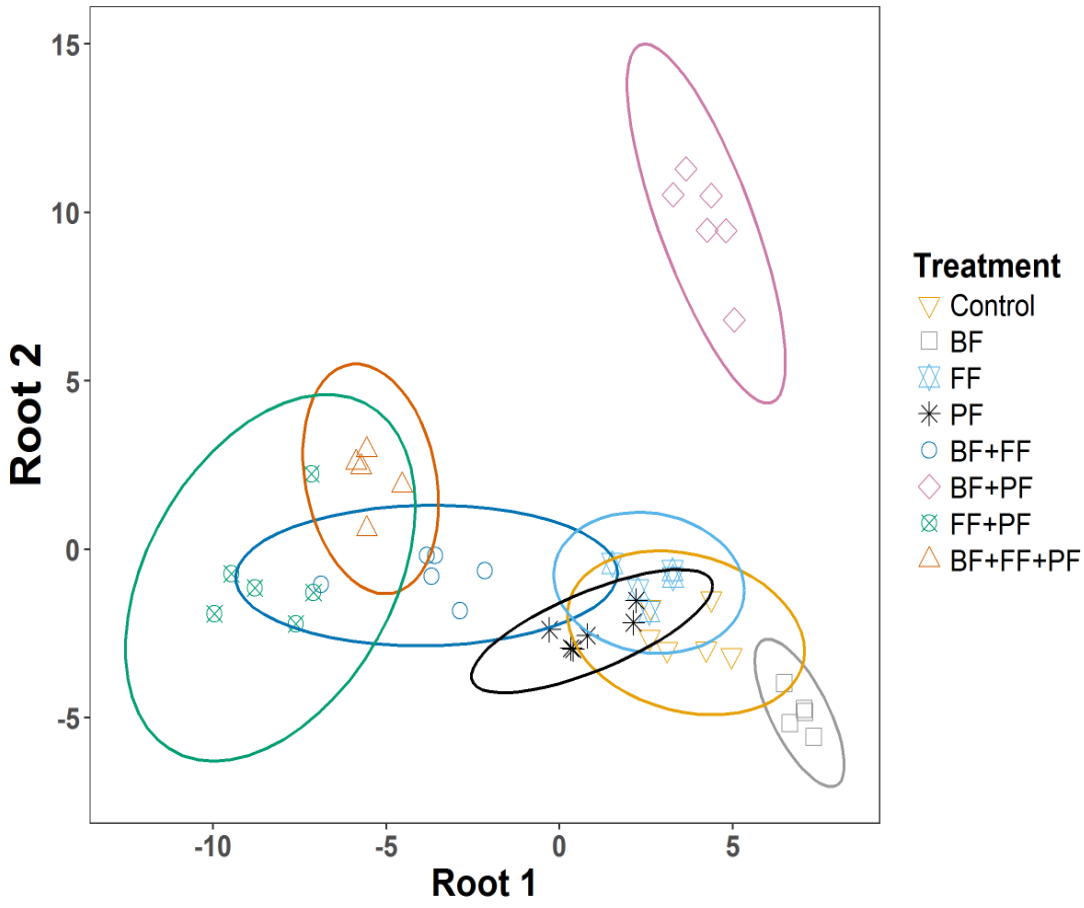

Figure 37 Discriminant function analysis (DFA) of the phospholipid fatty acid pattern (PLFA in nmol g^{-1} DW soil) with bacterial, fungal and plant feeders and their combinations as groups (n=8) and individual PLFAs as variables (n = 18). Analysed were soils at 4 weeks after inoculation with C - no nematodes, BF – the bacterial feeder *Acrobeloides buetschlii*, FF – the fungal feeder *Aphelenchoides saprophilus*, and PF – the plant feeder *Pratylenchus penetrans*

Discrimination along root 2 resulted in a clear distinction (eigenvalue: 21.3) of BF + PF from the other treatments, and in addition microbial communities of soils inoculated with BF were also distinguished from FF along root 2. Bacterial PLFAs (i15:0, a15:0, i17:0, 16:0-10 meth) and non-specific PLFAs (14:0, 15:0, 16:0) were significantly correlated with root 2, thereby contributed considerably to this separation. Correspondingly, with the least amounts of these PLFAs were in BF + PF at the first sampling (Table A7).

Table 19 Pearson's coefficients of correlation between concentrations of phospholipid fatty acids and the extracted roots of the discriminant function analyses. Presented are data of the first (4 weeks) and second sampling of oak amended with *Acrobeloides buetschlii*, *Aphelenchoides saprophilus* and *Pratylenchus penetrans* and their combinations as groups (n=8) in the model. Canonical scores for the first and second roots were used for correlation. *, **, and *** refer to P <0.05, 0.01, and 0.001, respectively. DPL - days post labelling. G+: Gram-positive bacteria, G-: Gram-negative bacteria, A: Actinobacteria, B: Bacteria in general, F: Fungi

	1st Sampling		2nd Sampling	
	Root 1	Root 2	Root 1	Root 2
i15:0 (G+)	-0.540***	-0.806***	0.865***	0.014
a15:0 (G+)	-0.519***	-0.804***	0.779***	0.189
i16:0 (G+)	-0.607***	-0.275	0.756***	-0.120
i17:0 (G+)	-0.407**	-0.343*	0.643***	-0.165
a17:0 (G+)	-0.462**	-0.282	0.902***	0.187
cy17:0 (G-)	-0.935***	-0.176	0.902***	0.163
cy19:0 (G-)	-0.736***	-0.092	0.806***	-0.066
16:1ω7 (B)	-0.430**	-0.442	0.914***	0.237
16:1ω5 (B)	-0.238	-0.531	0.871***	-0.141
18:1ω9t (B)	-0.454**	-0.155	0.793***	-0.271
16:0 10-meth (A)	-0.589***	-0.308*	0.874***	-0.042
18:0 10- meth (A)	-0.590***	0.097	0.805***	0.033
18:2ω6,9 (F)	-0.224	0.183	0.486**	-0.822***
18:1 ω9c (F)	-0.4186**	0.072	0.864***	-0.371*
14:0	-0.225	-0.408**	0.389	0.240
15:0	0.145	-0.561***	0.349	0.355*
16:0	-0.645***	-0.416**	0.364	-0.457**
18:0	-0.496**	0.117	0.000	-0.334*

At the second sampling time, the discriminant analysis of the PLFA profiles clearly distinguished microbial communities of soils treated with more than one nematode group from the control and singular amendments (whole model: $F_{112, 164}$ = 27.95, P < 0.001; Figure 38). The first two discriminant functions significantly accounted for 77.2 % of the variation in the data (root 1: P < 0.001; root 2: P < 0. 001). The microbial communities in soils of the different treatments distinctly separated from each other along root 1 (eigenvalue: 131.2). Microbial communities in soils amended with singular BF and FF greatly differed from the

combination amendment treatments, also BF + FF+ PF showed dissimilarity to the other combination treatments along root 1 (Figure 38).

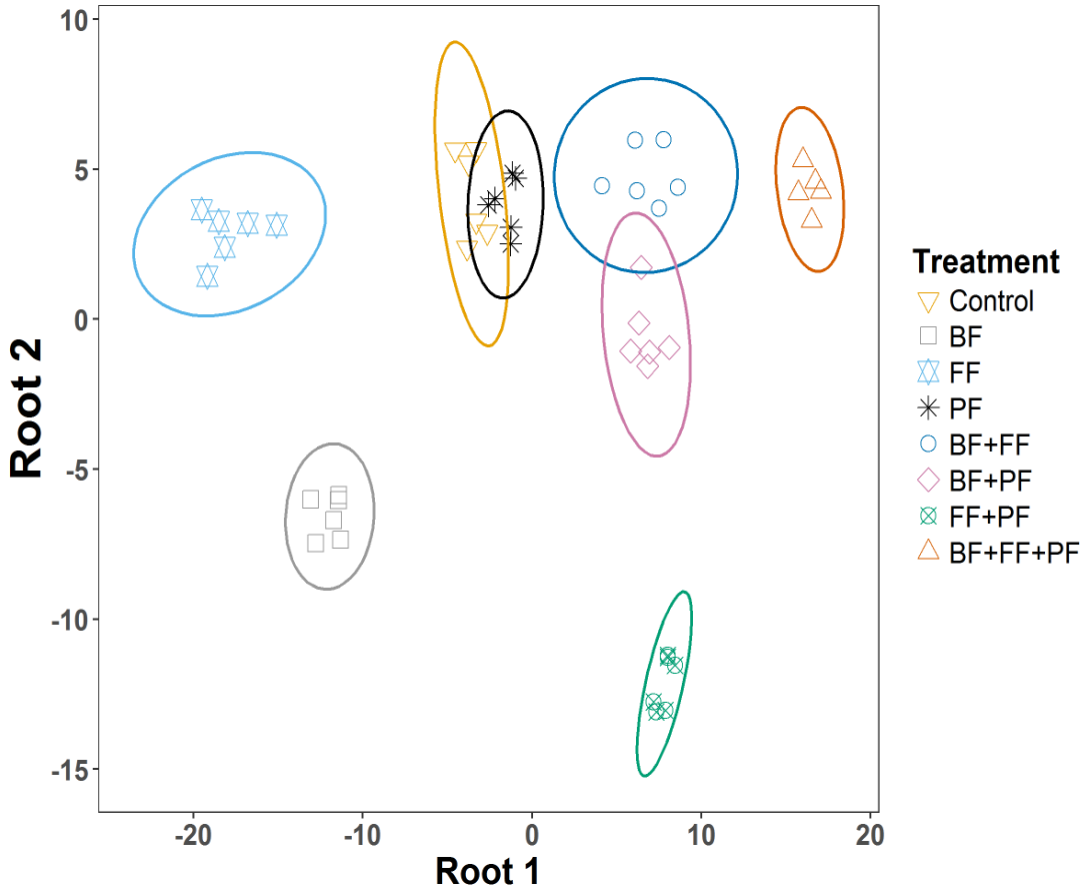

Figure 38 Discriminant function analysis (DFA) of the phospholipid fatty acid pattern (PLFA in nmol g^{-1} DW soil) with bacterial, fungal and plant feeders and their combinations as groups (n=8) and individual PLFAs as variables (n = 18). Analysed were soils at 8 weeks after inoculation with C - no nematodes, BF – the bacterial feeder *Acrobeloides buetschlii*, FF – the fungal feeder *Aphelenchoides saprophilus*, and PF – the plant feeder *Pratylenchus penetrans*

PLFAs i15:0, a15:0, i16:0, 16:1ω5, 16:1ω7, 16:0 10-meth, i17:0, a17:0, cy17:0, cy19:0, 18:1ω9c, 18:2ω6,9, 14:0, 16:0 and 18:0 showed significant positive correlation with root 1 (Table 19), thereby all contributed to the first discriminant function. Correspondingly, significantly higher amounts of these PLFAs were extracted in soils amended with BF + FF, BF + PF, FF + PF and BF + FF + PF compared to the control (Table A8). Meanwhile, the second discriminant function largely separated microbial communities in soils amended with BF and FF + PF along root 2 (eigen value: 41.6) (Figure 38). Correlation of the PLFAs with the extracted axis showed that fungal PLFAs and the saturated forms 16:0 and 18:0 were

largely responsible for the discrimination (Table 19). In support, at the second sampling FF + PF had significantly higher amounts of fungal PLFAs compared to the other treatments, while BF had higher amounts of 18:0 (Table A8).

3.4.4 Effects of the nematode amendment on plant performance

The effect of the nematode amendments on the plant performance became apparent over time. No differences in the performance of the oak seedlings (shoot and root weights, root/shoot ratio; Table 5) were observable among treatments at first sampling time. In contrast, at the second sampling time altering the relative abundance of each trophic group of nematodes had an impact on the root/shoot ratio of the oak seedlings ($F_{7, 40} = 25.14$, $P < 0.001$) demonstrated by an increased in response to amendment with BF + FF + PF, and a decline in response to PF and FF + PF (Table 20).

Table 20 Effects of increasing relative abundance of trophic groups of soil nematodes on the root length (cm ± s.d), root and shoot biomass (g ± s.d. DW) and the root/shoot ratio ± s.d.in the rhizosphere of Quercus robur seedlings. Presented is data at first (4 weeks) and second (eight weeks) sampling times after application of amendments. C - no nematodes, BF – the bacterial feeder *Acrobeloides buetschlii*, FF – the fungal feeder *Aphelenchoides saprophilus*, and PF – the plant feeder *Pratylenchus penetrans*. ANOVA with *, **, and *** at P <0.05, 0.01, and 0.001, respectively. Values in a row with the same letters are not significantly different (Tukey's HSD test, $P < 0.05$)

	C	BF	FF	PF	BF+FF	BF+PF	FF+PF	BF+FF+PF	ANOVA
1st Sampling									
Root length [cm]	38.75 ± 8.07	42.83 ± 21.50	37.50 ± 13.81	37.50 ± 10.10	37.17 ± 15.01	38.33 ± 13.66	35.67 ± 11.57	45.67 ± 10.63	
Root biomass [g]	3.80 ± 0.74	3.13 ± 1.39	3.15 ± 0.66	3.21 ± 0.67	3.18 ± 0.65	3.19 ± 0.87	3.82 ± 1.05	3.93 ± 0.87	
Shoot biomass [g]	2.62 ± 0.55	2.43 ± 0.46	2.65 ± 0.34	2.58 ± 0.29	2.89 ± 0.69	2.54 ± 0.8	2.56 ± 0.29	2.67 ± 0.61	
root / shoot ratio	1.50 ± 0.36	1.29 ± 0.59	1.21 ± 0.30	1.28 ± 0.37	1.15 ± 0.36	1.27 ± 0.17	1.51 ± 0.43	1.52 ± 0.47	
2nd Sampling									
Root length [cm]	39.00 ± 10.22	30.33 ± 9.95	35.33 ± 13.69	41.67 ± 9.35	46.50 ± 5.75	35.50 ± 12.88	35.00 ± 11.51	43.83 ± 9.41	
Root biomass [g]	6.67 ± 0.72	5.83 ± 1.33	5.54 ± 0.89	4.66 ± 1.048	6.33 ± 2.11	5.78 ± 0.67	4.82 ± 0.60	6.82 ± 2.71	
Shoot biomass [g]	3.00 ± 0.81	3.24 ± 0.58	3.15 ± 0.42	3.04 ± 0.48	3.11 ± 0.71	3.00 ± 0.60	3.24 ± 0.52	2.85 ± 0.47	
root / shoot ratio	2.36 ± 0.19ab	1.91 ± 0.14c	1.79 ± 0.26cd	1.54 ± 0.12d	2.06 ± 0.11bc	1.95 ± 0.20c	1.52 ± 0.09d	2.39 ± 0.08a	***

CHAPTER FOUR: DISCUSSION

4.1 The genetic, nutrient allocation and growth responses of oaks to plant-parasitic nematodes

This study investigated the transcriptomic and physiological responses of pedunculate oak to infection with the plant-parasitic nematode *P. penetrans*. It further addressed how these responses were impacted by the endogenous rhythmic growth pattern of oak, and the presence of the ectomycorrhizal fungus *P. croceum*, taking into account carbon and nutrient allocation and fitness of the plant.

4.1.1 Response to the plant-parasitic nematode *Pratylenchus penetrans*

Ten days after inoculation, the systemic response of oak microcuttings to *P. penetrans* showed that transcriptional reprogramming occurred in sink and source leaves. Migratory plant-parasitic nematodes cause physical damage to root tissues and employ a suite of effectors to facilitate mobility within root tissues triggering systemic host response (Kyndt et al., 2012, 2014). Till now most research has focused on annual agricultural crops, reporting that plants generally respond to nematode infection by differential regulation of genes involved in signal transductions, hormonal signalling, stress and defence, cell wall alterations and nutrient allocation (Li et al., 2008; Escobar et al., 2011). This study showed that *P. penetrans* induced a comparable response in pedunculate oak, a perennial tree.

P. penetrans as a belowground pathogen systemically activated oak defence such as elicitation of signalling by induction of reactive oxygen species (ROS) production in the leaf tissue microcuttings. Upregulation of ROS has previously been reported in roots of *A. thaliana* upon infection with the nematodes *Heterodera glycines* and *Meliodogyne incognita* (Waetzig et al., 1999; Melillo et al., 2006). ROS play a signalling role mediating plant defence genes activation over long distances following pathogen infection leading to priming of different plant tissues (Miller et al., 2009, Levine et al., 1994; Torres et al., 2006). Consistent with increased ROS homeostasis, elicitation of host defence was assigned by induction of transmembrane receptor-like kinases (RLKs), receptor-like proteins (RLPs), and

proteins containing the LRR kinase class. Previous studies reported that the *Mi*-1 gene which contains an LRR region confers resistance to root-knot nematodes in tomato plants (Milligan et al., 1998; Vos et al., 1998).

Hormonal signalling pathways were activated in response to *P. penetrans*, particularly induction of genes related to the biosynthesis of salicylic acid, jasmonic acid and ethylene. These plant hormones are known to regulate induced systemic defence against pathogens (Delaney et al., 1994; Pieterse et al., 2012) and their induction has been shown for migratory endoparasitic nematodes in rice (Nahar et al., 2012; Kyndt et al., 2014). Proteins involved in biosynthesis of brassinosteroids and flavonoids as well as in the shikimate pathway were upregulated, which are important players in pathogen-triggered immunity (Maeda and Dudareva, 2012; Albrecht et al., 2012) and also alter the motility and hatching of nematodes (Wuyts et al., 2006). The distinct and diverse changes in metabolic profiles of leaf tissues in the present study point to a priming effect of aboveground tissues of oak, which can enhance systemic resistance against insect leaf herbivores as reported previously (Wurst and van der Putten, 2007; Wondafrash et al., 2013).

On the other hand, transcripts encoding enzymes involved in synthesis of signalling molecules such as *probable CDP-diacylglycerol-inositol 3 phosphatidyltransferase 2* and *inositol 1,3,4-trisphosphate 5/6-kinase family proteins,* which play a key role in immune response signalling and mediate plant defence responses to herbivory (Jones and Dangl, 2006; Gillaspy, 2010; Mosblech et al., 2011) were repressed. This is likely due to secretion of immune-modulatory effectors by *Pratylenchus* spp. as strategy to hijack host-signalling pathways in aide of parasitism (Quentin et al., 2013; Bellafiore and Briggs, 2010; Jones and Fuso-Nyarko, 2014). In addition, transcripts encoding pectin methylesterase inhibitors were repressed in response to *P. penetrans*, which activate signalling cascades triggering plant immunity upon detection of compromised cell wall integrity (Hamman, 2012). Overall, *P. penetrans* hampered oak immune reaction, likely a strategy to support its establishment in the roots.

Significantly higher relative abundances of nitrogen were detected in leaf tissues of oaks inoculated with *P. penetrans* in comparison to control plants. Nitrogen is essential for production of defence compounds such as alkaloids and glucosinolates (Baldwin et al., 1994; Chen et al., 2001), consistent with the present findings of enhanced production of secondary metabolites. Kohl et al., (2012) reported that nitrogen-demanding tissues are capable of signalling their need for nitrogen, and transcription factors such as the *AP2/ethylene-*

responsive family involved in abscisic acid signalling pathway and glucosinolates metabolism were induced, pointing to high nitrogen demand in the oak terminal leaves.

In addition, the nematode altered carbon metabolism in oak microcuttings, mediated by three predominant processes. Firstly, pathogen elicited host defence linked to the levels of sugar in plant cells, glucose triggers expression of resistance genes while sucrose functions as a signalling molecule (Hey et al., 2010; Morkunas and Ratajczak, 2014; Wind et al., 2010). During the infection with *P. penetrans* sucrose non-fermenting-1 related protein kinase a key metabolic regulator altering defence mechanisms against biotic and abiotic stress (Morkunas et al., 2011) was downregulated. Secondly, transcripts encoding for enzymes such as sucrose and raffinose synthases were downregulated. This points to an accumulation of fructose and glucose in leaf tissues of microcuttings, and is supported by the high relative abundance of recent photoassimilated carbon assigned by ^{13}C labelling of oaks. Thirdly, transcriptome analyses indicated repressed photosynthesis a common plant response during incompatible pathogen interaction in order to allow induction of processes required for respiration and defence (Bonfig et al., 2006; Berger et al., 2007). Previous studies on plant-nematode interactions revealed reductions in the amount of chlorophyll in systemic tissues of rice by *H. oryzae,* photosynthesis in tomato by *M. javanica* and carbon fixation in coffee by *Pratylenchus coffeae* (Nahar et al., 2012; Bird, 1974, Mazzafera et al., 2004). In sum, these alterations in carbon source and sink metabolism induced by *P. penetrans* are likely to be part of the oak's strategy in enhancing defence referred to as "to gain fuel for the fire" by Bolton (2009).

Smith and Stitt (2007) proposed that the consumption of carbon for defence related processes prompts the plant to adjust growth. In contrast, the present study found that the nematode had no effect on total amount of plant carbon and growth pattern of the oak, suggesting a time lag between transcription and physiological changes. A significant correlations between the initial density of nematodes and the extent of damage to host plants exists (e.g. Castillo and Vovlas, 2007; Sato et al., 2009), therefore 2300 nematode individuals might have been too few to cause significant damage during the short infection period (10 days). Besides, although *P. penetrans* has a wide host range including oak (Ruehle, 1973), it is predominantly observed on grasses and annual crops (CABI, 2015), and oak may not be the plant it is best adapted to. Nevertheless, the distinct systemic response of oak microcuttings to *P. penetrans* assigns a strong host-parasite interaction, and changes in transcriptomic pattern likely would have been followed by changes in growth pattern given enough time.

4.1.2 Response to the ectomycorrhizal fungus *Piloderma croceum*

The development of ectomycorrhiza symbiosis is a highly regulated process involving morphological and physiological changes (Le Quéré et al., 2005; Duplessis et al., 2005). Previous studies reported extensive reprogramming of the oak transcriptome during pre-symbiotic development and in mature symbiotic ectomycorrhiza with *P. croceum* (Krüger et al., 2004; Frettinger et al., 2007; Tarkka et al., 2013). However, the overall response of oak microcuttings to *P. croceum* was small indicated by the low number of DECs. Transcripts encoding *cyclic nucleotide-gated ion channel 1-like* and *calmodulin binding proteins* were induced, that play a vital intracellular signalling role during the initiation of plant symbiotic gene reprogramming (Harrison, 2005; Martin et al., 2007) and also mediate plant defence response (Kang et al., 2006; Clough et al., 2000). In addition, transcripts encoding LRR resistance proteins were upregulated as reported in cork oak in response to an ectomycorrhizal fungus (Sebastiana et al., 2014). Together, these findings show that oak employs the same proteins to respond to pathogens and symbionts.

On the other hand, downregulation of transcripts encoding enzymes participating in salicylic acid pathway and biosynthesis of jasmonic acid in response to *P. croceum* point to a repression of host defence, which is in agreement with previous studies (Durrant and Dong 2004, Sebastiana et al., 2014; Plett et al., 2014). Furthermore, transcripts encoding proteins related to increased stress tolerance such as recA DNA recombination family protein were upregulated indicating enhanced repair of damage induced by *P. croceum* (Manova and Gruska, 2015). Together these findings correspond with Tarkka et al. (2013) who showed that *P. croceum* attenuated host defence and enhanced stress tolerance in oak microcuttings.

Several studies showed that mycorrhization with *P. croceum* increases sink strength of roots, which is stabilized by higher photosynthetic activity (Branzanti et al., 1999; Quoreshi, 2003; Herrmann et al., 2004). In agreement with these findings, the ^{13}C excess increased in *P. croceum* inoculated the oak microcuttings, pointing to enhanced photosynthetic efficiency by the ectomycorrhizal fungus. In addition, in a recent study Herrmann et al. (2015) showed that the high carbohydrate status in oak microcuttings inoculated with *P. croceum* is balanced by increased nitrogen acquisition. Comparably, the present study showed higher nitrogen acquisition in oak microcuttings following inoculation with *P. croceum,* as indicated by the upregulation of ammonium transporters and ^{15}N excess signature in the plant.

Microbial biomass increased in the rhizosphere of oak microcuttings inoculated with *P. croceum* pointing to enhanced rhizodeposition. Ectomycorrhiza fungi modify the quality and chemical composition of carbon components in the rhizosphere (Johansson et al., 2004; Barea et al., 2005; Rineau and Garbaye, 2010) and thus induce competitive pressure on the inhabiting bacteria (de Boer et al., 2015). While root exudates predominantly contain labile low molecular weight compounds such as organic acids, sugars, and amino acids the hyphal exudates contain pigments, proteins, polyols, i.e. complex organic compounds that require a suite of extracellular enzymes for degradation (Walker et al., 2003; Read and Perez-Moreno 2003; van Hees et al., 2006; Johansson et al., 2009). Consistent with this, the biomass of gram-positive bacteria and actinobacteria was favoured by *P. croceum* in the rhizosphere of oak microcuttings. These microbial groups can be classified in general as *K*-strategists according to Andrew and Harris (1986), capable of utilizing recalcitrant substrates. In sum, the altered conditions in the mycorrhizosphere of *P. croceum* fostered a specific microbial community, which in turn also promoted plant fitness, as indicated by the higher biomass of mycorrhized oak microcuttings.

4.1.3 Effect of plant growth stage on biotic interactions

The two major growth stages of pedunculate oak, i.e. RF and SF, coincide with predominant allocation of photoassimilates to belowground and aboveground compartments in the plant, respectively (Herrmann et al., 2015; Herrmann et al., 2016). During plant-pathogen interactions, the plant carbohydrate status affects the defence reaction as under limited resource conditions a plant is faced with a carbon and energy allocation decision, for either defence or growth (Steppuhn and Baldwin, 2008). In agreement, the present study showed that systemic response of oak to *P. penetrans* appears to be greatly influenced by the plant's developmental stage. Defence was much stronger during SF, demonstrated by the 16-fold increase of differentially expressed genes ~~as~~ compared to RF. This finding is consistent with Kurth et al. (2015), who using the same oak model system reported a larger systemic transcriptomic response during SF to the mycorrhiza helper bacterium *Streptomyces* sp. AcH 505.

The observed weak response of oak microcuttings to *P. penetrans* during RF likely mirrors their endogenous nutrient allocation pattern. Generally, plant parasitic nematodes create a strong carbon and nutrient sink to roots (Kaplan et al., 2011). However, in the present study

the influx of nutrients into oak roots in the presence of *P. penetrans* was not altered, instead, processes related to cell generation, lipid metabolism and lignin catabolism were activated, with the former being vital for membrane biogenesis and the latter for mediating cytoskeleton rearrangements (Schmid and Ohlrogge, 2002; Wang et al., 2013). Overall, these processes point to repair and compensatory growth as oak´s strategy in response to *P. penetrans*, as reported in crops and grass (Bardgett et al., 1999b; Haase et al., 2007). However, enhanced oak growth did not take place after 10 days plant-nematode interaction.

Meanwhile, during SF when oak endogenously allocates photoassimilates predominantly to aboveground tissues, the feeding by *P. penetrans* induced a vast and diverse pattern of defence mechanisms. During this growth stage, feeding activity of the nematode apparently led to sink competition between the roots and shoots, indicated by the reduced root to shoot ratio of ^{13}C allocation in infected plants and enhanced activity of sugar transporters in terminal leaves. Correspondingly, during SF 40% of the plants recently photoassimilated carbon was allocated to terminal leaves in comparison to 2% during RF. Obviously, the competition between the nematode belowground and the plant aboveground carbon sinks upset the balance and triggered the stronger defence responses against the pathogen during SF. This is supported by a repression of enzymes related to carbohydrate metabolism such cellulose, raffinose and sucrose synthases, that point to the accumulation of sugars in terminal leaves to trigger the host defence responses (Koch, 1996; Bolton, 2009). Pathways activated were phenylpropanoid and isoprenoid producing defence metabolites as well as PR-proteins and callose deposition, pointing to a major flow of carbon from primary into secondary metabolism (Bolton 2009). These defence compounds created in one compartment, here terminal leaves, can be transported over long distances to, here roots (Arnold and Schultz, 2002; Appel et al., 2012).

In summary, the response of oaks to *P. penetrans* was greatly modulated by the plant growth stage. During RF the plant-nematode relationship was evidently quite harmonius, whereas during SF *P. penetrans* triggered a strong systemic defence response and altered primary metabolism including reprogramming of photosynthesis and physiological mechanisms. This was further reflected in altered allocation patterns of nutrients in the plants and carbon flux into the rhizosphere. This clearly shows that resource allocation pattern related to endogenous rhythmic growth determines host response to pathogens, which should be considered in future investigations with regards to plant-nematode interactions.

The study found that in contrast to the plant-nematode interaction, the interaction between the oak microcuttings and the mycorrhizal symbiont *P. croceum* was mildly affected by the growth stage of the plant. Previous studies report that *P. croceum* has a high demand for carbohydrates and acts as a strong sink for photoassimilates (Gibson and Deacon, 1990; Herrmann et al., 1998). Consistently, more carbon was allocated to roots of oaks inoculated with *P. croceum* confirming that the ectomycorrhizal fungus induced a stronger sink for carbon during RF. Further supporting this, transcripts encoding genes related to enhanced photosynthesis were upregulated consistent with reports from previous studies (Högberg et al., 2002; van Hees et al., 2005) and likely a mechanism to compensate for carbon demand of *P. croceum*. However, *P. croceum* also triggered a greater host defence response demonstrated by a stronger induction of transcripts encoding proteins related to enhanced signalling and reinforcement of cell wall integrity. This finding indicates that the carbon burden of the ectomycorrhizal fungus was strong enough to offset the balance, resulting in the plant favouring activation of defence mechanisms over growth.

In contrast, during SF the ectomycorrhizal fungus had no effect on the carbon allocation patterns and a subtle induction of defence responses. Instead, there was a general enhancement of total amount of carbon in the plant, likely indicating cooperation between carbon sinks (Schultz et al., 2013).

In summary, these findings show that the response of oaks to *P. croceum* mirrored the plant growth stage. During RF, there was an increase in the sink strength of roots which trigged a competition for carbon between the plants' own needs and that of *P. croceum*. Ultimately, the oak microcuttings predominantly invested in defence during RF but in growth during SF.

4.1.3 Effects of interaction of *P. penetrans* and *P. croceum*

The presence of ectomycorrhizal fungus *P. croceum* modified the transcriptomic response to *P. penetrans* in oaks at both growth stages. Interestingly, the magnitude of genes expressed was vice versa, high and low during RF and SF, respectively. During RF the presence of both *P. penetrans* and *P. croceum* resulted in higher amounts of carbon allocated to the roots. This increase in root sink strength triggered enhanced pathogen perception as demonstrated by the enrichment in upregulated contigs of GO terms *response to biotic stimulus* and *wax biosynthesis*. However numerous plant defence mechanisms were also repressed indicated by enrichment of GO terms such as *killing cells of other organisms* and *flavonoid, ethylene* and

phenylpropanoid metabolism for downregulated contigs. In addition, processes related to primary metabolism such as glycolysis and cellular and carbohydrate metabolism were repressed. Overall, this gene expression pattern points to impaired host defence and pathogen resistance in the presence of both biotic interactors resulting in increased the susceptibility of microcuttings during RF which is consistent with Caravaca et al. (2015). However, plants co-inoculated with *P. penetrans* and *P. croceum* showed a higher biomass compared to sole *P. penetrans* inoculation, likely due to the enhanced microbial biomass in those soils, which can have a growth stimulating effect oaks (Bonkowski et al., 2000; Zhu et al., 2014).

During SF the very low number of DECs shows that *P. croceum* strongly repressed oak's response to *P. penetrans*. This finding is consistent with Kurth et al. (2015) who reported similar effects for the interaction of oak with *P. croceum* and the mycorrhiza helper bacterium *Streptomyces* sp. AcH 505. The enrichment of GO terms for downregulated contigs involved in triggering hypersensitive response and accumulation of pathogenesis related proteins indicated a repression of oak defence responses. Similar findings of host defence repression by ectomycorrhizal fungi have been reported for the host trees *Quercus suber* and *Populus sp.* and their respective symbiotic fungi *Pisolithus tinctorius* and *Laccaria bicolor* (Sebastiana et al., 2014; Plett et al., 2014). The repressed host defence could be directly linked to the increased carbon status of oaks with a mycorrhizal symbiont and hence enough resources for all the biotic interaction partners. Furthermore, the microbial biomass and community composition was altered, resulting in stimulated plant growth in comparison to plants inoculated with only *P. penetrans*.

Together, these findings show that during SF the presence of *P. croceum* improved oak stress tolerance to *P. penetrans* indicated by attenuation of host defence response, while during RF the susceptibility to the plant-parasitic nematode was increased. The latter is likely due to the fact that both the nematode and ectomycorrhiza draw their nutrients from the roots and their combined effects created a stronger sink particularly for carbon.

4.2 Interrelationships between plant-parasitic nematodes and beneficial rhizosphere microorganisms on oaks

The present study investigated the impact of the interrelationship between the migratory endoparasitic nematode *P. penetrans* and the mycorrhizal rhizosphere helper bacteria *Streptomyces sp*. AcH 505 on the performance of mycorrhized microcuttings and rhizosphere microorganisms during bud rest (BR) and root flush (RF) developmental stages of oak.

4.2.1 Effect of *Pratylenchus penetrans* and *Streptomyces* sp. AcH505 on plant growth parameters

Comparable to the differences between RF and SF discussed above (chapter 4.1.), the pronounced decline in shoot biomass during RF compared to BR showed that the response of oak to *P. penetrans* is directly linked to the differential resource allocation pattern governed by the plants' endogenous rhythmic growth. Photoassimilates are primarily channelled into belowground tissues during RF (Herrmann et al., 1998; 2015), and the presence of plant-parasitic nematodes imposes an additional nutrient sink (Poll et al., 2007; Kaplan et al., 2011), thus diminishing available resources for the sustenance of aboveground tissues. The reduction of root biomass, largely evident during RF at second sampling, further showed that also the belowground negative impact of migratory endoparasitic nematodes via damage to cells, removal of cell contents and disruption of physiological processes (Williamson and Gleason, 2003; Davis et al., 2004) was modified by the oak's developmental stage.

The mycorrhizal helper bacteria Streptomyces sp. AcH 505 enhanced the production of shoot biomass during RF at the second sampling indicating growth-promoting activity (Nassar et al., 2003; Tarkka et al., 2008; Verma et al., 2011). This benefit, however, did not contribute to an improvement in plant growth in soils co-inoculated with *P. penetrans* nor did it suppress nematode population in the soil during RF. This finding contradicts reports stating that *Streptomyces* sp. prime the plant basal immune response system (Conn et al., 2008) and provide protection against plant-parasitic nematodes (Siddiqui and Ehteshamul-Haque, 2001; Ruanpanun et al., 2011). This discrepancy could be that due to an increase in susceptibility of

oak to *P. penetrans* during RF (Caravaca et al., 2015; Maboreke et al., 2016) therefore more nematodes entered the roots and evaded the mitigating effect of mycorrhizal helper bacteria.
The nematode markedly repressed the population of *Streptomyce*s sp. AcH 505 in oaks during RF at the first sampling and during BR at the second sampling although at a lesser magnitude. Two propositions can be put forward; i.e. *P. penetrans* may have promoted proliferation of antagonistic bacteria (Garbaye, 1994) or altered the effectiveness of mycorrhizal helper bacteria in rhizosphere colonisation, which is discussed below.

4.2.2 Effect of *Pratylenchus penetrans* and *Streptomyces* sp. AcH505 on rhizosphere microbial community structure

The feeding activity of plant-parasitic nematodes has a profound influence on microbial community structure attributed to the ability of nematodes to alter the quantity and quality of root exudations (Haase et al., 2007; Poll et al., 2007). During BR *P. penetrans* increased the microbial biomass in the rhizosphere indicating an increase in exudation, which shifted the rhizosphere microbial community composition in favour of Gram-positive bacteria, actinobacteria and fungi at first sampling and actinobacteria and Gram-negative bacteria at second sampling. This finding is consistent with previous reports stating that plant-parasitic nematodes contribute to the regulation of microbial communities (Yeates et al., 1998, Poll et al., 2007).
In contrast, with presence of *Streptomyces* sp. AcH 505 the amount of Gram-positive bacteria, actinobacteria and fungi declined at first sampling. This indicates that the introduced helper bacteria effectively colonized the rhizosphere outcompeting native populations, and such competition between bacteria in the rhizosphere is a common phenomenon (Hibbing et al., 2010). Kurth et al. (2013) demonstrated that *Streptomyces* AcH 505 had a competitive advantage against the microbial filtrate in the soil of oak mesocosms. This has been attributed to their ability to utilize recalcitrant substrates as well as production of antagonistic secondary metabolites possessing anti-microbial activity that inhibit the growth of competitors (Chater et al., 2010).
Despite the antagonistic effect of *P. penetrans* on the mycorrhizal helper bacteria, *Streptomyces* sp. AcH 505 counteracted the negative effect of the nematode on shoot biomass during RF at first sampling. *Streptomyces* sp. are known to produce chitinases or nitric oxide which have been linked to induced systemic resistance to plant-parasitic nematodes in their

host plants (Siddiqui and Mahmood, 1999). However, given that *Streptomyces* sp. AcH 505 had no effect on the abundance of nematodes in the soil, it is likely that changes in rhizosphere microbial community composition rather than antibiosis were the driving mechanisms involved in its antagonistic activity. Such shifts in rhizosphere microbial community composition are necessary for soil suppressiveness promoting plant growth (Mazzola, 2002).

In addition, Streptomyces increased the growth of *P. croceum* in oaks during RF, as indicated by higher amounts of specific PLFA biomarkers for the respective symbiont (18:1ω9c and 18:2ω6,9) at second sampling. This finding corresponds with studies showing that vital processes related to fungal development such as germination rate, foraging behaviour, hyphal growth, reproduction growth and development, exudates composition and antibacterial metabolites production that can be heavily influenced by bacteria (Krishna et al., 1982, Barea et al., 2005; de Boer et al., 2005; Kesba and Al-Sayed, 2006; Franco-Correa et al., 2010). Similar studies showed that simultaneous presence of *Streptomyces* and ectomycorrhizal fungus *P. croceum* promotes the mycorrhizal growth via enhanced production of auxofuran and foster mycorrhizal colonization by the bacteria hence earning *Streptomyces* the name "mycorrhizal helper bacteria" (Riedlinger et al., 2006; Tarkka and Frey-Klett, 2008; Kurth et al., 2013). Despite, this strong evidence for positive synergism between *Streptomyces* and *P. croceum* this study could not demonstrate a beneficial impact on plant growth in the presence of nematodes. Instead, a significant reduction of the fungal PLFA 18:2ω6,9 occurred in soils co-inoculated with nematodes and mycorrhizal helper bacteria. Previous studies showed that the establishment and beneficial effects of ectomycorrhizal colonization of roots is negatively modulated by plant-parasitic nematodes (Brussaard et al., 2001; Villenave and Duponnois, 2002).

4.3 Rhizosphere carbon dynamics modulated by plant-parasitic nematodes and fungivorous Collembola

The aim of this study was to investigate the changes in the allocation of carbon induced by soil animals i.e. the migratory endoparasitic nematode *P. penetrans* and the fungal grazer Collembola *P. armata*, and the carbon flow into the belowground food chain. Stable isotope labelling was used to trace ^{13}C flux from plants into soil microorganisms and Collembola.

4.3.1 Feeding behaviour of *Protaphorura armata*

Collembola are generally referred to as fungal feeders (Hopkin, 1997; Rusek, 1998), although some recent studies have suggested they are generalists (Endlweber et al., 2009, Ngosong et al., 2011, Fiera, 2014) while others report a pronounced niche differentiation (Chahartaghi et al., 2005, Potapov and Tiunov, 2016) or a preference for dead ectomycorrhizal hyphae (Kaneda and Kaneko, 2004). Therefore, due to a lack of consensus the present study sought to determine the dietary source of *P. armata* in the oak microcosm system.

Some studies have reported that Collembola feed on nematodes (Gilmore and Potter, 1993; Hopkins, 1997), and indeed the density of nematode individuals in the soil was lower in the presence of *P. armarta*. However, the lipid profile of *P. armata* does not indicate nematode feeding, as the dominant fatty acids were oleic acid (42-47%) followed by linoleic acid (15-19%). Both are relative markers that can be synthesised in the consumer lipid metabolism, but increase in abundance if resources rich in these components are fed upon, with oleic acid indicative for plant and linoleic acid for fungal feeding (Ruess and Chamberlain, 2010). However, their proportion can vary according to fungal species (Ruess et al., 2002). The fatty acid profile of *P. croceum*, the symbiotic partner of oaks in the present study, was dominated by 43% oleic acid. This points to fungal and/or root feeding by *P. armata*, and the negative interaction between *P. armata* and *P. penetrans* to be non-trophic.

These results based on trophic biomarker fatty acids were further supported by their ^{13}C signal after pulse labelling oaks. The highest ^{13}C allocation in the Collembola lipid profile was detected in oleic acid, the most dominant fatty acid of *P. croceum*. This finding is consistent with reports by Pollierer et al. (2012) stating that recent photoassimilates enter fungivores via grazing on ectomycorrhizal hyphae. However, it is difficult to disentangle whether fungal hyphae in soil or those associated with oak roots were taken as diet. Stumpe et al. (2005) demonstrated that the level of fungal specific fatty acids increased in mycorrhized roots compared to non-mycorrhized roots. Taking into account the ^{13}C signature in unlabelled and labelled samples, the average shift in $\delta^{13}C$ was 100‰ for bulk oak tissue but only 3‰ for the soil PLFA 18:1ω9, whereas it was 90‰ in the Collembola TLFA 18:1ω9. Considering dietary routing, i.e. the fact that fatty acids derived from the diet are directly transferred to consumer tissue without change in the isotopic signal (Ruess et al., 2005), indicates that *P. armata* fed on mycorrhizae associated with roots as opposed to fungal hyphae in soil.

4.3.2 Effect of *Pratylenchus penetrans* and *Protaphorura armata* on oak growth

In the present study neither *P. penetrans* nor *P. armata* alone did alter oak biomass parameters, whereas in comparison to single inoculation, their interaction lowered shoot and total plant biomass. This finding points to a synergistic mode of action between the rhizosphere fauna. Generally, nematodes reduce the habitable sites for the ectomycorrhizal colonization and disrupt the fungal mantle (Marks et al., 1987; Francl, 1993), while grazing on ectomycorrhizal fungi by Collembola reduces fungal biomass and impairs nutrient uptake via the fungal channel, thereby reducing tree growth (Finlay 1985; Ek et al., 1994; Johnson et al., 2005). However, in the present study there was an increase in biomass of the fungal marker (18:1ω9c) in the presence of Collembola with time. Therefore, it is unlikely that the decline in plant growth was a result of a negative impact on the ectomycorrhizal fungus. Recent studies reported that grazing of Collembola results in thinner and longer roots with more root tips in herbaceous plants (Endlweber and Scheu, 2006, 2007). Cohn et al. (2002) reported that plant-parasitic nematodes preferentially enter host roots at the root tips. Thus Collembola may have facilitated nematode entry to host roots, resulting in the significantly higher numbers of individuals in root tissues of oaks in the presence of *P. armata*, subsequently leading to a reduction in growth**.**

4.3.3 Effects of *Pratylenchus penetrans* and *Protaphorura armata* on the rhizosphere microbial biomass

Exudates from forest trees are estimated to represent 5-10 % of the photoassimilates of trees (Jones et al., 2004), and their quantity and quality significantly affect microorganisms in the ectomycorhizosphere (Fransson et al., 2015). *P. penetrans* reduced microbial biomass in particular that of bacteria indicating that the nematodes directly altered the quality and/or quantity of root exudates in oak microcuttings. The decline in Gram-negative bacteria biomass further indicates an alteration in the composition of root exudates, as these fast growing *r*-strategists specifically benefit from labile carbon substrates (Vandenkoornhuyse et al., 2007; Philippot et al., 2013; Kivlin and Hawkes, 2011). These findings are in agreement

with previous studies showing that the feeding activity of plant-parasitic nematodes alters the quantity and quality of root exudates (Haase et al., 2007; Kaplan et al., 2011).

In contrast, *P. armata* enhanced total microbial biomass in the rhizosphere of oak microcuttings consistent with results of Bardgett and Chan (1999). Some studies suggest that Collembola influence microbial biomass production by triggering compensatory growth of the fungi on which they graze (Hanlon, 1981; Hedlund et al., 1991). It is well acknowledged that the outcome of this interaction is species and density dependent, with high Collembola densities reducing whilst low densities increasing fungal biomass (Fitter and Sanders, 1992; Ek et al., 1994; Setälä, 1995; Setälä et al., 1998). Moreover, although *P. armata* primarily fed on *P. croceum*, its grazing activity stimulated hyphal growth in the oak microcosms likely the fungus became resilient to feeding over time (Tlalka et al., 2007; Kanters et al., 2015). In addition, Collembola enhanced bacterial biomass suggesting that *P. armata* indirectly facilitated nutrient accessibility to bacteria as reported previously (Hanlon and Anderson, 1979; Kaneda and Kaneko, 2004; Steinaker and Wilson, 2008).

4.3.4 Effects of *Pratylenchus penetrans* and *Protaphorura armata* on the rhizosphere microbial community structure

Shifts in rhizosphere microbial community structure due to feeding of plant-parasitic nematode or Collembola are attributed to changes in root exudation (Denton et al., 1999; Yeates, 1999; Bardgett and Chan, 1999; Endlweber and Scheu, 2006). Both *P. penetrans* and *P. armata* caused shifts in the community structure of rhizosphere microorganisms of oak microcuttings, however, their effects varied with time. The effect of *P. penetrans* was prominent at the first sampling, consistent with Poll et al. (2007), who reported a short-term impact of plant-parasitic nematodes on the community structure of rhizosphere microorganisms. In contrast, the effect of Collembola increased with time and at the third sampling the shift in microbial community structure was accompanied by an increase in Gram-positive bacteria, bacteria in general and the ectomycorrhizal fungus. The ectomycorrhizal hyphal tips fed upon by Collembola are active sites for root exudation and re-adsorption of compounds (Sun et al., 1999); hence grazing presumably reduced the acquisition of organic compounds by the fungus thereby favouring bacteria. In addition, grazing on ectomycorrhizal fungi increases the release of polymer degradation enzymes into the rhizosphere, enhancing decomposition of complex soil organic matter into more readily

accessible nutrients for soil microbes including bacteria thereby stimulating bacterial biomass growth (Crowther et al., 2011; Philipps et al., 2014). The shift to Gram-positive bacteria likely is due to the fact that, in contrast to root exudates that are primarily composed of simple sugars (Toal et al., 2000), hyphal exudates contain pigments, proteins, polyols and siderophores, and complex organic compounds (Read and Perez-Moreno 2003; van Hees et al., 2006; Johansson et al., 2009). Gram-positive bacteria were shown to be efficient at utilizing such complex substrates in rhizosphere (Waldrop et al., 2000; Bell et al., 2009), as indicated by their proliferation in the rhizosphere of microcuttings inoculated with *P. armata*. Overall, this suggests synergistic interaction between soil microorganisms and Collembola, where the enhanced activity of the fungus by *P. armata* facilitates growth of bacteria.

4.3.5 Utilization of plant-derived carbon in rhizosphere organisms

Stable isotope labelling of forest trees has shown that root derived C is quickly incorporated in high amounts into virtually all decomposer species (Pollierer et al., 2007). Ectomycorrhizal fungi are reported to form strong sinks for plant carbon, receiving up to 30% of the plant-assimilated carbon (Smith and Read 2008; Jones et al., 2009; de Deyn et al., 2011). However, findings from this study show that bacteria acquired the most of the plant carbon (72-95% of the plant-assimilated carbon), as indicated by the relative abundance of ^{13}C concentration in general, Gram-positive and Gram-negative bacterial marker PLFAs. This corresponds to the low fungal-to-bacterial ratio in the soil, thus indicating a dominance of the bacterial carbon and energy channel (Joergesen and Wichern, 2008). In line with this, the extraradical hyphae of the ectomycorrhizal fungus *P. croceum* in the soil sequestered less photoassimilates from oaks as indicated by relative abundance of ^{13}C excess below 25%.

Similar to effects on microbial biomass and community structure, both *P. penetrans* and *P. armata* significantly influenced the incorporation of root-derived carbon into rhizosphere microorganisms, which is consistent with previous studies (Yeates et al., 1999b; Johnson et al., 2005). This impact was pronounced at 2 DPL and later declined due to the loss of ^{13}C via respiration. Interestingly, the effect of root feeders and fungivores was largely independent of each other with only a single interaction being significant, i.e. the effect of *P. armata* on the incorporation of plant carbon into the ectomycorrhizal fungus at 2 DPL was less evident when *P. penetrans* was also present.

The impact of *P. penetrans* was strongest at the first sampling date and later weakened. This indicates leakage of root cell content mainly at the time when nematode enters the host, which is in agreement with Yeates et al. (1998, 1999). However, this nematode impact on carbon allocation differed in major microbial groups, with incorporation being high in Gram-positive but low in Gram-negative bacteria. The latter quickly assimilate root-derived carbon whilst utilizing simple organic compounds in the rhizosphere (Vandenkoornhyse et al., 2007; Bahn et al., 2013; Philippot et al., 2013), and *P. penetrans* probably modified the transport and distribution of labile carbon in roots (e.g. sucrose, Mazzafera et al., 2004). This highlights that nematode induced changes in the physiology of host plants can distinctly alter belowground carbon pathways in trees similar to herbaceous plants (Davis et al., 2004).
In sum, the enhanced incorporation of the recent photoassimilated carbon by bacteria in the presence of *P. armata* indicates that grazing by Collembola facilitated the acquisition of plant carbon that otherwise would have been transferred into fungal biomass.

4.4 Multitrophic interaction on oak growth and soil microbial community biomass and structure

This study investigated the role of different nematode trophic groups in influencing soil microbial activity and growth of oak seedlings. To achieve this aim, multitrophic soil environments, comprising increased numbers of specific trophic groups solely and in all possible combinations was employed.

4.4.1 Effect of treatments on the abundance and community structure of nematodes

As the objective of this study was to quantify the collective contribution of different trophic groups, a modified freeze-thaw method was used to reduce the pre-existing nematode population in the soil (Poll et al., 2007). This method is reported to have little effect on the soil microbial community and nutrient status of the soil (Stenberg et al., 1998), and further ensures the presence of a viable native background nematode community, hence is ideal for studying processes under semi-natural conditions.

Manipulation of the relative abundances of the nematode functional groups in the soil was successful, predominantly for fungal and plant feeders, as the model nematodes *Pratylenchus* and *Aphelenchoides* were infrequent in the control soil, likely due to the longer time period required for re-establishment due to their low colonization ability (Bongers 1990). Sole inoculations enhanced the relative abundance of fungal feeders (by 20%) and plant feeders (by 30%), respectively, resulting in a stable and dominant fraction within the nematode population of the respective treatments. In contrast, inoculation with the bacterial feeder *A. buetschlii* did not affect the abundance of bacterial feeders in the soil and over time the nematode community structure shifted towards that of non-inoculated control soils. Cephalobidae family members dominated the bacterial-feeding functional group, which are resilient to disturbance such as freezing (Bongers 1990; Bongers and Bongers 1998).

4.4.2 Impact of multitrophic interactions on microbial communities and oak growth

4.4.2.1 Effect of bacterial feeders

Bacterial feeding nematodes consume a diverse variety of bacteria in soils thus regulating the abundance, community composition, activity and phenotype of bacteria (Djigal et al., 2010; Xu et al., 2015). In this study, the effect of the BF treatment was more pronounced at 8 weeks ANI where it reduced the abundance bacteria, predominantly of Gram-positive taxa, in comparison to the control. A number of studies report that effect of bacterial feeders on bacterial biomass varies according to nematode species (Ingham et al., 1985; Postma-Blaauw et al., 2005), incubation time (Elliott et al., 1980), and identity of bacterial taxa (Glücksman et al. 2010; Griffiths et al., 1999; Rønn et al., 2002; Xiao et al. 2010). The observed reduction of Gram-positive bacteria points to a distinct top-down control by *A. buetschlii*. Bacterial feeders change the relative abundance of dominant bacterial populations in the soil (Djigal et al., 2004), often increasing the relative abundance of bacteria that are grazing-protected, either by physical means, such as Gram-positive bacteria (Griffiths et al., 1999; Rønn et al., 2002) or filamentous growth such as actinomycetes (Rosenberg et al., 2009), or by chemical compounds (Mazzola et al., 2007, Jousset et al., 2010). Ackermann et al., (2016) showed that *A. buetschlii* preferentially feeds on Gram-negative bacteria consistent with previous studies that found bacterial-feeding nematodes to prefer Gram-negative over Gram-positive bacteria (Salinas et al., 2007; Abada et al., 2009). However, in this study the neutral effect of *A.*

buetschlii on Gram-negative bacteria and the reduced abundance of Gram-positive bacteria suggests a food preference for the latter.

On the other hand the enhanced abundance of bacterial feeders increased the biomass of fungi in the soil demonstrated by a higher fungal to bacteria ratio. Bacteria and fungi are often reported as antagonists in soil (de Boer et al., 2005; Schrey *et al.*, 2012) and the competition between these groups has been shown to inhibit fungal growth (Mille-Lindblom et al., 2006; Meidute et al., 2008), therefore it is likely that the grazing on bacteria indirectly facilitated growth of fungi. Additionally, enhanced abundance of bacterial feeders reduced the oak biomass root to shoot ratio, suggesting an indirect facilitation of root colonisation by the mycorrhizal fungi resulting in less investment in roots by the plant as previously reported (Ditengou et al., 2000; Smith and Read, 2008).

4.4.2.2 Effect of fungal feeders

Fungal feeders are considered the main drivers of fungal abundance and decomposition processes (Filser et al., 2002; Tordoff et al., 2008). In this study, increasing the relative abundance of fungal feeders by sole inoculation of *A. saprophilus* significantly reduced the microbial biomass of all major microbial taxa in the soil including fungi, suggesting a strong top-down effect. Moreover, the fungal to bacterial ratio declined, indicating a dominance of the bacterial energy channel. This finding confirms the strong top-down control of the microorganisms due to the grazing pressure of the fungal feeders (Ingham et al., 1985; Setälä et al., 1997). Grazing by nematodes on ectomycorrhizal fungi can lead to reduced mycorrhizal biomass and consequently reduced plant fitness and growth (Ek et al., 1994; Setälä et al., 1997). However, no negative impact of *A. saprophilus* on oak growth was observed consistent with Chapter **3.3** where Collembola grazing had no independent effect on plant growth. Previous studies showed that the effect of fungal grazing on plants by nematodes was conditionally determined by the nutrition status of the soil (Ek et al., 1994; Setälä et al., 1995, 1997, 1998). Since the oak seedlings received supplementary nitrogen fertilizer application this could have buffered the negative effect of fungal feeders on the overall fitness of the plant.

4.4.2.3 Effect of plant feeders

In the present study, increasing the relative abundance of only plant feeders promoted the growth the amount of Gram-negative bacteria and fungi, whilst reducing that of Gram-positive bacteria likely due to an increased influx of labile root exudates consistent with Chapter **3.2** where the presence of *P. penetrans* stimulated microbial growth (Caravaca et al., 2015). Gram-negative bacteria multiply rapidly multiply and have a competitive advantage for labile exudates (Waldrop et al., 2000) thus directly negatively impacting the growth of Gram-positive taxa. Maboreke et al. (2016) showed that *P. penetrans* act as strong terminal nutrient sinks in oak roots and thus indirectly promote carbon flow to rhizosphere microorganisms. Correspondingly, plant-feeders enhanced growth of ectomycorrhiza fungi compared to sole fungal feeders. Considering the ubiquity of this nematode species, these results provide evidence that it widely modulates rhizosphere microbial communities as well as mutualistic interactions not only in agricultural but also in woody plants.

4.4.3 Effect of multitrophic interactions

Irrespective of sampling time, the increase in trophic complexity by inoculating soil with more than one functional group had a general stimulatory effect on microorganisms in comparison to singular inoculations and control treatments. In addition, the microbial communities diversified and were separated from each other. As the population amendment by nematode inoculation did not result in a significant increase of the overall nematode population density, this validates that the observed changes are related to differences in trophic structure. Unlike in the singular nematode inoculation treatments where effects became apparent at 8 weeks ANI, the impact of increasing trophic complexity was already pronounced at 4 weeks ANI and, moreover, shifts in microbial community compositions were provoked over time.

Nematode impact was particularly evident for the interaction of fungal and plant feeders, which increased the total microbial biomass and altered community structure compared to soils inoculated with singular fungal and plant feeder treatments. This separation was stronger at 8 weeks ANI and showed a correlation with fungal PLFAs, which were significantly higher. Plant feeders are reported to induce the degradation of cellulose and indirectly increase the fungal biomass (Denton et al., 1999; Tu et al., 2003). Therefore, the negative effect of fungal grazers was likely counteracted by the positive impact of plant

feeders on rhizosphere microbial communities as discussed above for the synergistic interaction of Collembola and plant parasitic nematodes (Chapter 4.3). The facilitation of the fungal symbiont likely resulted in less belowground investment of oaks as indicated by a decline in the root to shoot ratio. Overall, when trophic diversity of faunal grazers is considered as functional component of forest soils, their effects on the ectomycorrhiza play a key role in the context of plant production.

Similarly, the interaction of bacterial feeders and plant feeders increased total microbial biomass in comparison to singular nematode trophic group inoculations. DFA separated microbial communities from other treatments along root 2, this correlated with Gram-negative bacteria (i15:0 and a15:0) at 4 weeks ANI and with the fungal PLFA markers (18:2ω6) at 8 weeks ANI. Additionally, the presence of bacterial feeders increased the oak root to shoot ratio in comparison with sole inoculation of plant feeders. Thus, the combination of bacteria and plant feeders, both primary modulators of rhizosphere bacterial biomass and activity resulted in a positive impact on oak performance. Plant feeders stimulated growth of bacteria, while grazing activity of the bacterial feeders counteracted the negative impact caused by feeding on root tissue by plant feeders. Previous studies demonstrated that nitrogen fertilization offset nematode damage as bacterial feeders increase microbial turnover leading to improved nutrient availability (Yeates, 1987; Bardgett and Chan, 1999; Gebremikael et al., 2016). This work shows that multitrophic interactions can have a comparable stimulatory effect.

The interaction of bacterial and fungal feeders altered the microbial community structure indicated by the DFA separation along root 1 at both sampling times. The abundance of bacteria and fungi in the soil increased compared to sole nematode inoculations as well as control. Grazing by fungal feeders may have given bacteria a competitive advantage resulting in a higher turnover of nutrients via the bacterial pathway that could otherwise have been immobilized in fungal biomass consistent with findings from the above study above where grazing by Collembola indirectly promoted growth of bacteria (Chapter **4.3**). The presence of bacterial feeders regulated the bacterial biomass (Wardle and Yeates, 1993) thus indirectly facilitating growth of fungi.

Finally, inoculation with all three trophic nematode groups significantly increased the total microbial biomass compared to singular and dual inoculation treatments. DFA further disentangled these treatments from the dual interactions of bacterial feeders with either fungal or plant feeders with a distinct separation along root 1 at 8 weeks ANI. This shift was

attributed to an increase in abundance of Gram-negative bacteria and Actinobacteria, and a reduced fungal biomass. In sum, these findings show that in soil with diversified nematode interactions, the different trophic groups counteract the negative effects of each other to the benefit of the plant. In line with this, Setälä and Huhta (1990) reported that simple fauna communities to be less effective in promoting plant production than complex ones. Although, in the present study this did not lead to enhanced plant biomass, the root to shoot ratio of the plant biomass was significantly more than singular or dual inoculations pointing towards a healthier plant in an environment with multitrophic interactions.

CHAPTER FIVE: GENERAL DISCUSSION

This thesis has led to a deep insight how plant-parasitic nematodes, major players in the rhizosphere, interact with a temperate forest tree, pedunculate oak. In nature the roots of oak are engaged in mutualistic, neutral and pathogenic associations with soil microorganisms and fauna, that are directly or indirectly connected, generating a diversity of outcomes with regards to plant fitness (Plomion and Fievet, 2013). Further adding to the complexity of these biotic interactions is the endogenous rhythmic growth pattern of oak, since primary metabolism (i.e. the carbohydrate status) also regulates defence responses and overall plant performance (Berger et al., 2007; Hulsmans et al., 2016). This thesis reconstructs the soil food web starting from a simple ecosystem (first experiment) and gradually increasing diversity by introducing mycorrhizal helper bacteria (second experiment), Collembola grazers (third experiment) to a multitrophic system (last experiment). The experimental approach used in the first experiment, employing RNA sequencing, isotope labelling, and lipid profiling, laid a strong foundation towards understanding of how oak responds to plant-parasitic nematodes. Most importantly it showed that *P. penetrans* acted as a strong carbon and nutrient sink (Chapter **3.1**), with major consequences for the biotic interactions in the rhizosphere of oaks.

The first main hypothesis for this thesis study stated that plant-parasitic nematodes induce genes associated with plant defence. These responses are modulated by the ectomycorrhizal fungus, which primes oak against pathogen infection as well as oak´s growth stage, with a stronger impact when shoots are the main C-sink.

The transcriptomic profile of oak showed that the plant-parasitic nematode provoked systemic responses, that can be classified into three main processes: i) elicitation of plant defence and production of secondary metabolites with defence properties, ii) repression of host defence, and iii) modulation of primary metabolism. These responses of oak varied greatly depending on the endogenous growth stage of the oak microcuttings indicating the outcomes were a direct result of nutrient sink competition. During RF the interaction between oak and *P. penetrans* was generally harmonious as this coincides with the predominant allocation of photoassimilates belowground (Angay et al., 2014; Herrmann et al., 2015). Contrastingly, during SF with plant carbon retained aboveground a large defence response was initiated against the plant parasite. This indicates that the life strategy of plants, i.e.

resource allocation related to endogenous rhythmic growth in perennial trees, influences costs and benefits investment in plant defence and should be taken into consideration in future studies.

The ectomycorrhizal fungus modified the transcriptomic responses of oak, predominantly related to tolerance of biotic stress and primary metabolism (Chapter **3.1**). Its beneficial nature increased plant fitness and subsequently tolerance of oak to *P. penetrans*, a finding also observed in the third and fourth experiment (Chapter **3.3** and **3.4**). *P. croceum* altered the rhizosphere microbial biomass and community structure, consistent with previous reports (Rineau and Garbaye, 2010; de Boer et al., 2015), which likely improved mineralization processes and thereby indirectly counteracted the negative effects of plant-parasites. Together these findings show that, beside the well-known symbiotic function, the ectomycorrhizal fungus plays a significant role in enhancing overall plant stress tolerance towards pathogenic nematodes. This biotic interaction was also governed by the plant's endogenous growth pattern, and the transcriptomic profile indicated oaks to be more vulnerable to nematode damage during RF due to the weakened host defence by the ectomycorrhizal fungus; this was confirmed in the second experiment (Chapter **3.2**).

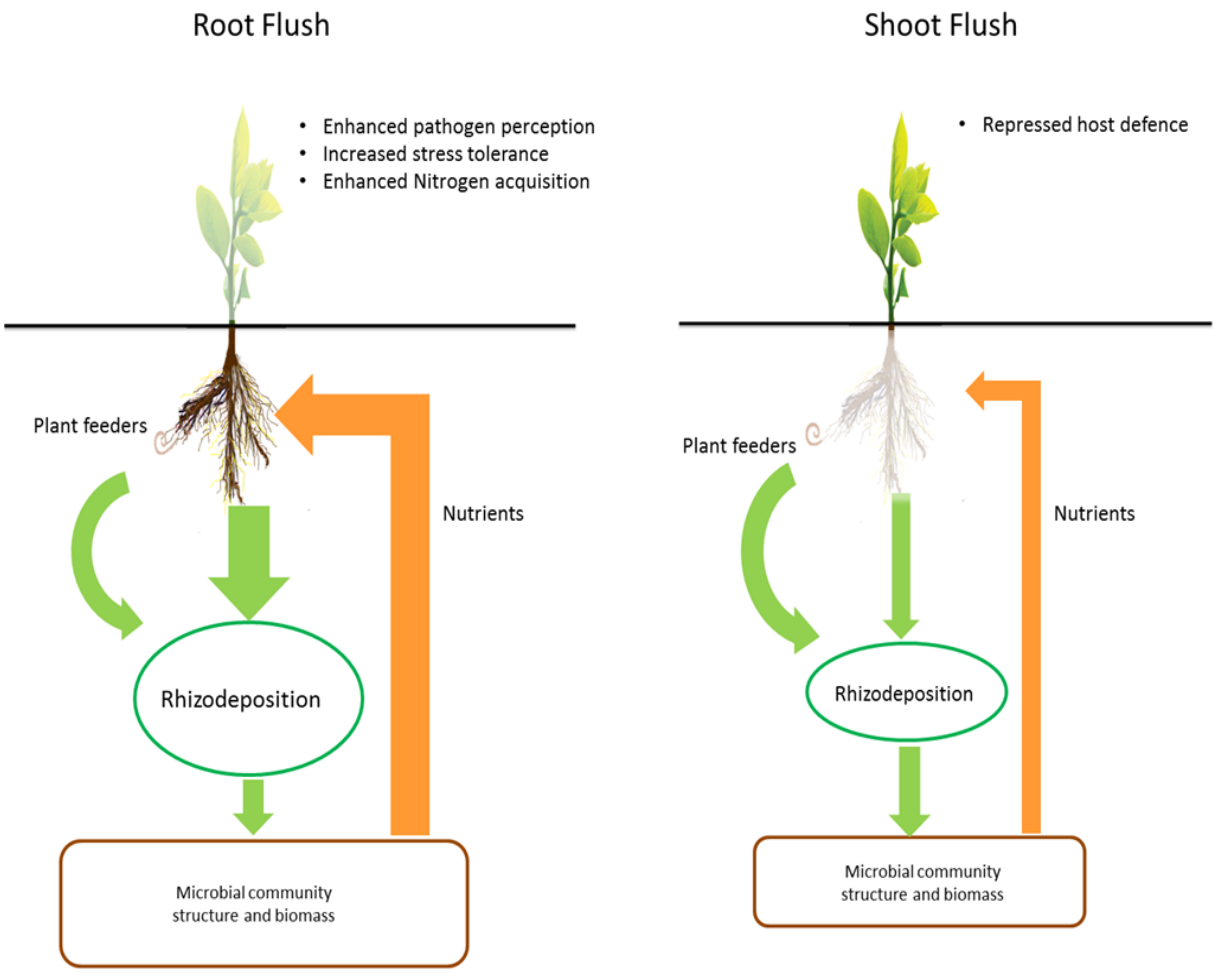

Figure 39 Schematic illustration summarizing the outcomes of the interaction between mycorrhized *Quercus robur* microcuttings and the plant-parasitic nematode *Pratylenchus penetrans* during different the endogenous growth stage of the microcutting. Presented is an overview on the transcriptomic response of *Quercus robur* to the plant-parasitic nematode and the effect of the interaction on the rhizosphere microbial community and the reciprocal effect of the rhizosphere microorganisms on the plant during root flush and shoot flush growth stages. The width of the arrows depicts the magnitude of the effect.

The second main hypothesis for this thesis study stated that the protecting strength of rhizosphere helper bacteria is weakened by root infection by plant-parasitic nematodes; the reciprocal effects in the rhizosphere create dynamic feedbacks that are not simply additive but antagonistic.

Rhizosphere helper bacteria such as *Streptomyces* sp. AcH 505 are well known to promote mycorrhizal colonization of oak, thereby indirectly enhancing plant growth (Kurth et al., 2013). However, this thesis showed that *Streptomyces* sp. AcH 505 had no growth priming

effect during the interaction with *P. penetrans* (Chapter **3.2**), neither did it have any negative effect on the density of nematodes as previously reported (Meng et al., 2012). Instead, *P. penetrans* had an antagonistic effect on the helper bacteria and its associated plant growth promotion properties. This may be due to altered quality and quantity of rhizodeposits by the nematode indirectly diminishing the positive effect of *P. croceum* on the oak microcuttings generally observed in the study (Chapters **3.1, 3.3** and **3.4**). Moreover, direct interference by plant-parasitic nematode is likely, through damage of root tissue, thereby deterring the colonization by the ectomycorrhizal fungi as previously reported (Francl, 1993). In support of this the first study (Chapter **3.1**) showed that *P. penetrans* had an antagonistic effect on the abundance *P. croceum*. In sum, the findings on this tripartite association show that, although beneficial rhizosphere microorganisms modulate the interaction between oak and *P. penetrans*, the plant-parasite also indirectly affects the microbial plant-beneficial interactions with oak.

The third main hypothesis for this thesis study stated the interaction between the two functional groups, root-feeding nematodes and fungal grazing Collembola, would increase plant carbon allocation to roots and soil microorganisms, favouring bacteria in particular opportunistic species exploiting rhizodeposits (Gram-negative bacteria).

The thesis showed that both the plant-parasitic nematode and fungal grazing Collembola independently regulated microbial biomass and activity in the rhizosphere. Collembola grazing enhanced microbial biomass and altered the rhizosphere community composition towards saprophytic bacteria by facilitating nutrient accessibility as confirmed by ^{13}C enrichment of bacterial PLFAs (Chapter **3.3**). In contrast, *P. penetrans* reduced the overall microbial biomass in the rhizosphere, whereas the additive effect of nematodes and Collembola stimulated the growth of microbial biomass as well as the utilization of plant-derived carbon by the microorganisms. This was particularly evident for Gram-positive bacteria that are better adapted to utilizing hyphal exudates, suggesting the presence of specific, resource adapted, microbial community in the myco-rhizosphere of oak.

The fourth main hypothesis for this thesis study stated increasing trophic diversity in the soil micro-food web counteracts negative effects of plant-parasitic nematodes on plant growth due to fostering of the soil microbial communities that participate in nutrient mineralization.

The results showed that the interaction of functionally diverse nematode trophic groups with the plant-feeding nematodes had a general stimulatory effect of the microbial activity in the soil (Chapter **3.4**). This counteracted the negative impact on oak performance induced by the enhanced presence of individual functional groups. Such increasing trophic diversity is particularly important in woody plants as this can also alleviate effects of fungal grazers on ectomycorrhiza, which play a pivotal role in plant productivity of trees such as oak.

CHAPTER SIX: CONCLUSION

This thesis work was quite innovative as it is the first of this kind to investigate the responses of a perennial tree, oak, at both genetic and physiological level to major players of a natural forest rhizosphere ecosystem. Knowledge about the mechanisms underlying plant-nematode interactions has been derived from a limited number of model annual plant species in very highly artificial simple experiments resulting in fragmented knowledge about the mechanisms with regards to natural ecosystems. Consequently, extrapolations into ecologically representative scenarios have been a great challenge, as previous studies often do not take into account the effects of the plant's developmental stage or the complexity of natural rhizosphere ecosystems.

The study showed that plant-parasitic nematodes are indeed major players in the rhizosphere interactions of forest trees via their direct and indirect effects on the tree and soil microorganisms. This study found that the outcome of these rhizosphere interactions was strongly governed by the endogenous rhythmic growth pattern of the tree. It has long been acknowledge that plant-parasitic nematodes induce nutrient sinks in the root; however, the effect of the endogenous resource allocation pattern of plants has not been explored as this produces varying outcomes with regards to plant-nematode interactions. For the future studies, I recommend that these consider investigating the responses of plants to nematodes during different plant developmental stages. This resource allocation pattern observed in the present study can also be applicable to studies involving annual plants that do not typically display the rhythmic growth pattern but undergo developmental stages that require more investments of photoassimilates in certain organs during a particular time for instance when a tomato plant is fruiting as opposed to when its undergoing vegetative growth.

The study showed plant-parasitic nematodes can negatively affect the interaction between plants and beneficial microorganisms such as mycorrhizal helper bacteria thereby undermining their beneficial contributions towards plant fitness. On the other hand I found that increasing soil fauna trophic diversity counteracted the negative effects of plant-parasitic nematodes on oaks. These findings show the importance of indirect effects of nematodes on plants and thus further emphasize the importance of conducting studies in an experimental set-up emulating the real ecosystem to study the fitness effects.

By integrating mechanistic studies with experiments in complex systems as well as taking into account the resource allocation pattern of plants this thesis was able to provide a better understanding of how long-lived plants such as trees optimally adapt to rhizosphere multitrophic biotic interactions. Given the effects of these tree-microbe-fauna interactions, it is likely that studies investigating interactions between plant and plant-parasitic nematodes that do not take into account the other rhizosphere players will remain limited in their capacity to explain plant fitness in an environment where the plant interacts with multiple biotic partners at any given time point. The experimental set–up used in this thesis study paves the way for a more holistic understanding of rhizosphere interactions and can be adopted for future studies to enable realistic appraisals of the roles played by the different rhizosphere players contributing to plant fitness. There is need to quantify the roles of the entire rhizosphere communities, accounting for crucial interactions amongst the soil microbial and fauna communities with plants which is critical to plant growth and biogeochemical cycles in forested ecosystems.

REFERENCES

Abad, P., Williamson, V.M. (2010). Plant Nematode Interaction: A Sophisticated Dialogue. In: Kader JCDM (Ed) Advances in Botanical Research 53, 147-192

Abada, E.A., Sung, H., Dwivedi, M, Park, B.J., Lee S.K., Ahnn, J. (2009). *C. elegans* behavior of preference choice on bacterial food. Molecules and Cells 28, 209–213. doi: 10.1007/s10059-009-0124-x

Abraham, W.R, Hesse, C., Pelz, O. (1998). Ratios of carbon isotopes in microbial lipids as an indicator of substrate usage. Applied and Environmental Microbiology 64, 4202-4209

Ackermann, M., Prill, P., Ruess, L. (2016). Disentangling nematode-bacteria interactions using a modular soil model system and biochemical markers. Nematology18, 403-415

Alaoui Sossé, B., Parmentier, C., Dizengremel, P., Barnola, P. (1994). Rhythmic growth and carbon allocation in *Quercus robur*. 1. Starch and sucrose. Plant Physiology and Biochemichemistry 32, 331–9

Albrecht, C., Boutrot, F., Segonzac, C., Schwessinger, B., Gimenez-Ibanez, S., Chinchilla, D., et al. (2012). Brassinosteroids inhibit pathogen-associated molecular pattern-triggered immune signaling independent of the receptor kinase BAK1. Proceedings of the National Academy of Science of the United States of America 109, 303-308

Andrássy, I., and Zombori, L. (1976). Evolution as a basis for the systematization of nematodes. London: Pitman. 3

Andrews JH *&* Harris RF *(*1986*) r* and *K*-selection and microbial ecology. Advances in Microbial Ecology*,* Vol. 9 (MarshallKC, ed.), Plenum Press, New York pp. 99–144.

Angay, O., Fleischmann, F., Recht, S., Herrmann, S., Matyssek, R., Oßwald, W., Buscot, F., and Grams, T.E.E. (2014). Sweets for the foe–effects of non-structural carbohydrates on the susceptibility of *Quercus robur* against *Phytophthora quercina*. New Phytologist 203,1282-1290.doi: 10.1111/nph.12876

Bonkowski, M., Cheng, W., Griffiths, B.S., Alphei, J., Scheu, S. (2000). Microbial–faunal interactions in the rhizosphere and effects on plant growth. European Journal of Soil Biology 36, 135–147

Anwar, S.A.,Van Gundy, S.D. (1989). Influence of the interaction of *Meloidogyne incognita* and *Pratylenchus vulnus* on root-shoot growth parameters in grape. Afro-Asian Journal of Nematology 3: 5-11

Appel H. M., Arnold T. A., Schultz J. C. (2012). JA responses reconfigure the long-distance of carbon but not nitrogen in poplar. New Phytol. 2 419–42610.1111/j.1469-8137.2012.04171.x

Arnold T. M., Schultz J. C. (2002). Induced sink strength as a prerequisite for tannin biosynthesis in *Populus*. Oecologia 2, 585–59310.1007/s00442-001-0839-7

Back, M., Haydock, P., and Jenkinson, P. (2002). Disease complexes involving plant parasitic nematodes and soilborne pathogens. Plant Pathology 51, 683-697

Baermann, G. (1917). Eine einfache Methode zur Auffindung von Anklyostomum (Nematoden) Larven in Erdproben. Geneesk, Tijdschr. Ned Ind 57, 900-904

Bahn, M., Lattanzi, F. A., Hasibeder, R., Wild, B., Koranda, M., Danese, V., Brüggemann N., Schmitt M., Siegwolf R., Richter, A. (2013). Responses of belowground carbon allocation dynamics to extended shading in mountain grassland. The New Phytologist, 198(1), 116–126. http://doi.org/10.1111/nph.12138

Baldwin I. T., Karb M. J., Ohnmeiss T. E. (1994). Allocation of 15N from nitrate to nicotine: production and turnover of a damage-induced mobile defense. Ecology 6

Baldwin, J.G., Nadler, S.A., Adams, B.J. (2004). Evolution of plant parasitism among nematodes. Annual Review of Phytopathology 42, 83-105

Bardgett, R.D., Chan, K.F. (1999). Experimental evidence that soil fauna enhance nutrient mineralization and plant nutrient uptake in montane grassland ecosystems. Soil Biology and Biochemistry 31, 1007–1014

Bardgett, R.D., Cook, R. (1998). Functional aspects of soil animal diversity in agricultural grasslands. Applied Soil Ecology 10, 263-276

Bardgett, R.D., Denton, C.S., and Cook, R. (1999a). Belowground herbivory promotes soil nutrient transfer and root growth in grassland. Ecology Letters 2, 357–360

Bardgett, R.D., Cook, R., Yeates, G.W., Denton, C.S. (1999b). The influence of nematodes on belowground processes in grassland ecosystems. Plant Soil 212, 23-33

Bardgett, R.D., van der Putten, W.H. (2014). Belowground biodiversity and ecosystem functioning. Nature 515, 505–511. doi:10.1038/nature13855

Barea, J.M., Pozo, M.J., Azcon, R., Azcon-Aguilar, C. (2005) Microbial co-operation in the rhizosphere. Journal of Experimental Botany 56, 1761-1778

Bell, C.W., Acosta-Martinez, V., McIntyre, N.E., Cox, S., Tissue, D.T., Zak, J.C. (2009). Linking microbial community structure and function to seasonal differences in soil

moisture and temperature in a Chihuahuan desert grassland. Microbial Ecology 58, 827–842

Bellafiore, S., Briggs, S.P. (2010). Nematode effectors and plant responses to infection. Current Opinion in Plant Biology 13, 442-448

Berger, S., Sinha, A.K., Roitsch, T. (2007). Plant physiology meets phytopathology: plant primary metabolism and plant-pathogen interactions. Journal of Experimental Botany 58, 4019-4026. doi: 10.1093/jxb/erm298

Bernard, E.C. (1992). Soil nematode biodiversity. Biology and Fertility of Soils 14, 99-103. doi:10.1007/BF00336257

Bird, A.F. (1974). Plant response to root-knot nematode. Annual Review of Phytopathology 12, 69-85

Bird, D.M., Jones, J.T., Opperman, C.H., Kikuchi, T., Danchin, E.G.J. (2015). Signatures of adaptation to plant parasitism in nematode genomes. Parasitology, 142 (Suppl 1), S71-S84.http://doi.org/10.1017/S0031182013002163

Bird, J.A., Herman, D.J., Firestone, M.K., (2011). Rhizosphere priming of soil organic matter by bacterial groups in a grassland soil. Soil Biology and Biochemistry 43,

Björsell, P., Edin, E., Viketoft, M. (2017). Interactions between some plant-parasitic nematodes and Rhizoctonia solani in potato fields. Applied Soil Ecology 113, 151–154

Blaxter, M. (1998). *Caenorhabditis elegans* is a nematode. Science, 282, 2041-2016.

Blaxter, M. (2011). Nematodes: The Worm and Its Relatives. PLoS Biology 9, e1001050. doi:10.1371/journal.pbio.1001050

Blumenthal, T. and Davis, R.E. (2004). Exploring nematode diversity. Nature Genetics 12, 1246-124

Bolton, M.D. (2009). Primary metabolism and plant defence - fuel for the fire. Molecular Plant-Microbe Interactions 22, 487–497. doi: 10.1094/MPMI-22-5-0487.

Bonfig, K.B., Schreiber, U., Gabler, A., Roitsch, T., Berger, S. (2006). Infection with virulent and avirulent P. syringae strains differentially affects photosynthesis and sink metabolism in *Arabidopsis* leaves. Planta 225, 1-12

Bongers, T. (1990). The maturity index – an ecological measure of environmental disturbance based on nematode species composition. Oecologia 83, 14–19

Bongers, T., Bongers, M. (1998). Functional diversity of nematodes. Applied Soil Ecology 10, 239–251.

Bongers, T., Ferris H. (1999). Nematode community structure as a bioindicator in environmental monitoring. Trends in Ecology and Evolution 14, 224–228

Brandle, M., Brandl, R. (2001). Species richness of insects and mites on trees: expanding Southwood. Journal of Animal Ecology 70, 491-504

Branzanti, M.B., Rocca, E., Pisi, A. (1999). Effect of ectomycorrhizal fungi on chestnut ink disease. Mycorrhiza 9, 103–109

Brussaard, L., Kuyper, T.W., de Goede, R.G.M. (2001). On the relationships between nematodes, mycorrhizal fungi and plants: functional composition of species and plant performance. Plant Soil 232,155-165.

Byrd, D.W., Kirkpatrick, T., Barker, K.R. (1983) An improved technique for clearing and staining plant tissues for detection of nematodes. Journal of Nematology 15, 142-145

CABI (2015). *Pratylenchus penetrans* (nematode, northern root lesion) basic datasheet. http://www.cabi.org/isc/datasheet/43900

Caravaca, F., Maboreke, H., Kurth, F., Hermann, S., Tarkka, T.M., Ruess, L. (2015) Synergists and antagonists in the rhizosphere modulate microbial communities and growth of *Quercus robur* L. Soil Biology and Biochemistry 82, 65-73

Castillo, P., Volvas, N. (2007). *Pratylenchus* (Nematoda: Pratylenchidae); Diagnosis, Biology, Pathogenicity and Management. Nematology Monographs and Perspectives 6. Leiden: Brill

Chahartaghi, M., Langel, R., Scheu, S., and Ruess, L. (2005) Feeding guilds in Collembola based on nitrogen stable isotope ratios. Soil Biology and Biochemistry 37, 1718-1725

Chater, K.F., Biro, S., Lee K.J., Palmer, T., Schrempf, H. (2010) The complex extracellular biology of Streptomyces. FEMS Microbiology Reviews 34,171–198

Chen S., Petersen B. L., Olsen C. E., Schulz A., Halkier B. A. (2001). Long-distance phloem transport of glucosinolates in Arabidopsis. Plant Physiol. 127 194–20110.1104/pp.127.1.194

Chitwood, D.J. (2003). Research on plant parasitic nematode biology conducted by the United States Department of Agricultural Research Service. Pest Management Science 59, 748-753

Clough, S.J., Fengler, K.A., Yu, I.C., Lippok, B., Smith, R.K. Jr., Bent, A.F. (2000). The Arabidopsis dnd1 “defense, no death” gene encodes a mutated cyclic nucleotide-gated ion channel. Procedings of the National Academy of Science of the United States of America 97, 9323–9328

Cobb, N.A. (1915). Nematodes and their relationships. USDA Yearbook of Agriculture, 1914, 457–490

Cohn, E., Koltai, H., Sharon, E., Spiegel, Y. (2002). Root-nematode interactions: recognition and pathogenicity. In: Waisel, J. Eshel, A., Kalkaf, U. (Eds) Plant roots – the hidden half. Marcel Dekker, New York. pp. 783-796.

Conn, V.M., Walker, A.R., Franco, C.M.M. (2008). Endophytic Actinobacteria Induce Defense Pathways in Arabidopsis thaliana. Molecular Plant-Microbe interactions 21, 208-218

Crow, W.T., Luc, J.E. (2014). Field efficacy of furfural as a nematicide on turf. Journal of Nematology 46, 8-11

Crowther, T.W., Jones, T.H., Boddy, L., Baldrian, P. (2011). Invertebrate grazing determines enzyme production by basidiomycete fungi. Soil Biology and Biochemistry 43, 2060–2068

Davis, E., Haegeman, A., Kikuchi, T. (2011). Degradation of the plant cell wall by nematodes. In: Jones J., Gheysen G., Fenoll C (Eds), Genomics and Molecular Genetics of Plant-Nematode Interactions eds., editors. Springer, Berlin. pp 225–272

Davis, E.L., Hussey, R.S., Baum, T.J. (2004). Getting to the roots of parasitism by nematodes. Trends in Parasitology 20, 134–141

de Boer W, Hundscheid MPJ, Klein Gunnewiek PJA, de Ridder-Duine AS, Thion C, van Veen JA, van der Wal A. (2015). Antifungal Rhizosphere Bacteria Can increase as Response to the Presence of Saprotrophic Fungi. PLoS ONE 10(9): e0137988. doi:10.1371/journal.pone.0137988

de Boer, W., Folman, L.B., Summerbell, R.C., Boddy, L. (2005). Living in a fungal world: impact of fungi on soil bacterial niche development. FEMS Microbiology Reviews 29, 795-811

De Deyn, G.B. et al. 2004. Plant community development is affected by nutrients and soil biota. Journal of Ecology 92, 824-834

De Deyn, G.B., Quirk, H., Oakley, S., Ostle, N., Bardgett, R.D., 2011. Rapid transfer of photosynthetic carbon through the plant–soil system in differently managed species-rich grasslands. Biogeosciences 8, 1131–1139

De Ley, P. (2006). A quick tour of nematode diversity and the backbone of nematode phylogeny. In: WormBook: The Online Review of C. elegans Biology [Internet].

Pasadena (CA): WormBook; 2005-. Available from: https://www.ncbi.nlm.nih.gov/books/NBK19684/

De Ruiter, P.C., Van Veen, J.A., Moore, J.C., Brussaard, L., Hunt, H. (1993). Calculation of nitrogen mineralization in soil food webs. Plant and Soil 157, 263–273

Delaney, T.P., Uknes, S., Vernooij, B., Friedrich, L. Weymann K., Negrotto, D., Graff,T. (1994) A central role of salicylic acid in plant disease resistance. Science 266, 1247-1250

Denton, C.S., Bardgett, R.D., Cook, R., Hobbs, P.J. (1999) Low amounts of root herbivory positively influence the rhizosphere microbial community in a temperate grassland soil. Soil Biology and Biochemistry 31, 155–165

Dighton, J., Mason, P. (1985). Mycorrhizal dynamics during forest tree development. Developmental biology of higher fungi, pp 117-139

Ditengou, F.A., Beguiristain, T., Lapeyrie, F. (2000). Root hair elongation is inhibited by hypaphorine, the indole alkaloid from the ectomycorrhizal fungus Pisolithus tinctorius, and restored by indole-3-acetic acid. Planta 211: 722–728

Djigal, D., Baudoin, E., Philippot, L., Brauman, A., Villenave, C. (2010). Shifts in size,genetic structure and activity of the soil denitrifier community by nematodegrazing. European Journal of Soil Biology 46, 112-118.

Djigal, D., Brauman, A., Diop, T.A., Chotte J.L., Villenave, C. (2004). Influence of bacterial-feeding nematodes (*Cephalobidae*) on soil microbial communities during maize growth. Soil Biology and Biochemistry 36, 323–331

Ducousso, A., Bordacs, S. (2003). EUFORGEN Technical Guidelines for genetic conservation and use for pedunculate and sessile oaks (*Quercus robur*/*Quercus petraea*) Bioversity International

Duncan LW. (2005). Nematode parasites of citrus. In: Luc M, Sikora RA, Bridge J, (Eds) Plant Parasitic Nematodes in Subtropical and Tropical Agriculture.. CAB International, Wallingford, UK pp. 437-466

Duplessis, S., Courty, P., Tagu, D., Martim, F. (2005). Transcript patterns associated with ectomycorrhiza development in *Eucalyptus globus* and *Pisolithus microcarpus*. New Phytologist 165, 599-611

Durrant, W.E., Dong, X. (2004). Systemic aquired resistance. Annual Review of Phytopathology 42, 185–209

Ek, H., Sjögren, M., Arnebrant, K., Söderström, B. (1994). Extra matrical mycelial growth, biomass allocation and nitrogen uptake in ectomycorrhizal systems in response to collembolan grazing. Applied Soil Ecology 1, 155–169

Elliott, E.T., Anderson, R.V., Coleman, D.C., Cole C.V. (1980). Habitable pore space and microbial trophic interactions. Oikos 35, 327–335

Endlweber, K., Scheu, S., (2006). Effects of Collembola on root properties of two competing ruderal plant species. Soil Biology and Biochemistry 38, 2025-2031

Endlweber, K., Scheu, S. (2007). Interactions between mycorrhizal fungi and collembola: effects on root structure of competing plant species. Biology and Fertility of Soils 43, 741-749

Endlweber, K., Ruess, L., Scheu, S. (2009). Collembola switch diet in presence of plant roots thereby functioning as herbivores. Soil Biology and Biochemistry 41, 1151-1154

Escobar, C., Brown, S., Mitchum, M.G. (2011). Transcriptomic and proteomic analysis of plant response to nematode infection. In: Gheysen, G., Fenoll, C., Jones, J.T., (Eds). Genomics and molecular genetics of plant–nematode interactions. London, UK: Springer Science and Business Media, B.V., pp 157–175

Escobar, C., Barcala, M., Cabrera, J., Fenoll, C. (2015). Overview of root-Knot Nematodes and giant cells. In: Escobar C., Fenoll C. (Eds), Advances in Botanical Research 73 (Oxford: Elsevier Academic Press) pp 1–32

Ferris, H. (2010). Form and function: metabolic footprints of nematodes in the soil food web. European Journal of Soil Biology 46, 97–104

Ferris, H., Venette, R.C., Lau, S.S. (1997). Population energetics of bacterial-feeding nematodes: Carbon and nitrogen budgets. Soil Biology and Biochemistry 29, 1183–1194

Fiera, C. (2014). Application of stable isotopes and lipid analysis to understand trophic interactions in springtails. North-Western Journal of Zoology 10, 227-235

Filser, J., Mebes, K.-H., Winter, K., Lang, A., Kampichler, C. , 2002: Long-term dynamics and interrelationships of soil Collembola and microorganisms in an arable landscape following land use change, Geoderma, 105, 201–221.

Finlay, R.D. (1985). Interactions between soil micro-arthropods and endomycorrhizal associations of higher plants. In: Fitter, A.H., Atkinson, D., Read D.J., Usher, M.B. (Eds). Ecological interactions in soil; plants, microbes and animals. Blackwell Scientific, Oxford, England. pp. 319-331

Fitter, A.H., Sanders, I.R. (1992). Interactions with soil fauna. In: Allen M.F. (Ed) Mycorrhizal Functioning. Routledge, Chapman and Hall, New York, pp. 333-354

Fraedrich, S.W., Cram, M.M. (2002). The association of a *Longidorus* species with stunting and root damage of loblolly pine (*Pinus taeda* L.) seedlings. Plant Disease 86, 803-807

Francl, L.J. (1993). Interactions of nematodes with mycorrhizae and mycorrhizal fungi. In: Kahn, M.W. (Ed.) Nematode Interactions. Chapman & Hall, New York, pp. 203-216

Franco-Correa, M., Quintana, A., Duque, C., Suarez, C., Rodriguez, M.X., Barea, J.M. (2010). Evaluation of actinomycete strains for key traits related with plant growth promotion and mycorrhiza helping activities. Applied Soil Ecology 45, 209-217

Fransson, P., Andersson A., Norström, S., Bylund, D., Bent, E. (2015). Ectomycorrhizal exudates and pre-exposure to elevated CO_2 affects soil bacterial growth and community structure. Fungal Ecology 20, 211-224

Frettinger, P., Derory, J., Herrmann, S., Plomion, C., Lapeyrie, F., Oelmüller, R., Martin, F., Buscot, F. (2007). Transcriptional changes in two types of pre-mycorrhizal roots and inectomycorrhizas of oak microcuttings inoculated with *Piloderma croceum*. Planta 225, 331-340

Frostegard, A., Baath, E. (1996). The use of phospholipid fatty acid analysis to estimate bacterial and fungal biomass in soil. Biology and Fertility of Soils 22, 59-65

Frostegard, A., Tunlid, A., and Baath, E. (1993). Phospholipids fatty acid composition, biomass and activity of microbial communities from two soil types experimentally exposed to different heavy metals. Applied Environmental Microbiology 59, 3605-3617

Garbaye, J. (1994). Interactions between mycorrhizal fungi and other soil organisms. Plant Soil 159, 123-132

Gebremikael, M.T., Steel, H., Buchan, D., Bert, W., de Neve, S. (2016). Nematodes enhance plant growth and nutrient uptake under C and N-rich conditions. Nature Scientific Reports 6, 32862

Gentleman, R.C., Carey, V.J., Bates, D.M., Bolstad, B., Dettling, M., Dudoit, S., et al. (2004) Bio conductor: open software development for computational biology and bioinformatics. Genome Biology 5, R80. doi.org/10.1186/gb-2004-5-10-r80

Gheysen G., Mitchum M.G. (2011). How nematodes manipulate plant development pathways for infection. Current Opinion in Plant Biology 14, 415-421. 10.1016/j.pbi.2011.03.012

Gibbs, D.S., Anderson, G.L., Beuchat, L.R., Cartra, L.K., Williams, P.L. (2005). Potential role of Diploscapter sp. strain LKC25, a bacterivorous nematode from soil, as a vector of food-bourne pathogenic bacteria to preharvest fruits and vegetables. Applied and Environmental Microbiology 71, 2433-2437

Gibson, F., Deacon, J.W. (1990). Establishment of ectomycorrhizas in aseptic culture: effects of glucose, nitrogen and phosphorus in relation to successions. Mycological Research 94,166-172

Gilbert, G.S. (2002). Evolutionary ecology of plant diseases in natural ecosystems. Annual Review of Phytopathology 40, 13-43

Gillaspy, G. (2010). Signaling and the polyphosphoinositide phosphatases. In: Munnik T, (Ed). Lipid signalling in plants. Berlin, Germany: Springer. pp. 117–130

Gilmore S.K., Potter, D.A (1993). Potential role of Collembola as biotic mortality agents for entomopathogenic nematodes. Pedobiologia 37, 30-38

Glücksman, E., Bell, T., Griffiths, R. I. and Bass, D. (2010). Closely related protist strains have different grazing impacts on natural bacterial communities. Environmental Microbiology, 12: 3105–3113. doi:10.1111/j.1462-2920.2010.02283.x

Gowen, S.C., Quénéhervé, P., Fogain, R. (2005). Nematode parasites of bananas and plantains. In: Luc M, Sikora RA, Bridge J (Eds). Plant parasitic nematodes in subtropical and tropical agriculture, 2nd edn. CABI Publishing, Wallingford. pp 611–643

Griffiths BS, Bonkowski M, Dobson G, Caul S (1999). Changes in soil microbial community structure in the presence of microbial-feeding nematodes and protozoa. Pedobiologia 43, 297–304

Haase, S., Ruess, L., Neumann, G., Marhan, S., Kandeler, E. (2007). Low-level herbivory by root-knot nematodes (*Meloidogyne incognita*) modifies root hair morphology and rhizodeposition in host plants (*Hordeum vulgare*). Plant and Soil 301, 151-164

Haegeman, A., Mantelin, S., Jones, J.T., Gheysen, G. (2012). Functional roles of effectors of plant-parasitic nematodes. Gene 492, 19–31

Hamann, T. (2012). Plant cell wall integrity maintenance as an essential component of biotic stress response mechanisms. Frontiers in Plant Science 3, 77. http://doi.org/10.3389/fpls.2012.00077

Hanlon, R.D.G. (1981). Influence of grazing by Collembola on the activity of senescent fungal colonies grown on media of different nutrient concentration. Oikos 36, 362–367

Hanlon, R.D.G., Anderson, J.M. (1979). Effects of collembola grazing on microbial activity in decomposing leaf litter. Oecologia 38, 93–99

Harmer, R. (1990). Relation of shoot growth phases in seedling oak to development of the tap root, lateral roots and fine root tips. New Phytologist 115, 23-37

Harris, M.A., Clark, J., Ireland, A., Ashburner, M., et al. (2004). Gene Ontology (GO) database and informatics resource. Nuclei Acids Research 32, D258-261

Harrison, R.D. (2005). Figs and the diversity of tropical rain forests. Bioscience 55, 1053–1064

Hedlund, K., Boddy, L., Preston, C. (1991). Mycelial responses to soil fungus *Mortierella isabellina*, to grazing by *Onychiurus armatus* (Collembola). Soil Biology and Biochemistry 23, 361-366

Helder, J., Vervoort, M., van Megen, H., Rybarczyk-Mydłowska, K., Quist, C., Smant, G., Bakker, J. (2015). Phytopathogenic Nematodes. In: Lugtenberg, B. (Ed). Principles of Plant-Microbe Interactions. Springer International Publishing. pp.91-102 doi: 10.1007/978-3-319-08575-3_11

Herrmann, S., Munch, J.C., Buscot, F. (1998). A gnotobiotic culture system with oak microcuttings to study specific effects of mycobionts on plant morphology before and in the early phase of ectomycorrhiza formation by Paxillus involutus and Piloderma croceum. New Phytologist 138, 203-212

Herrmann, S., Oelmuller, R., Buscot, F. (2004). Manipulation of the onset of ectomycorrhiza formation by indole-3-acetic acid, activated charcoal or relative humidity in the association between oak microcuttings and Piloderma croceum: influence on plant development and photosynthesis. Journal of Plant Physiology 61, 509-517

Herrmann, S., Buscot F. (2008). Why and how using micropropagated trees rather than germinations for controlled synthesis of ectomycorrhizal associations? In: Varma, A., (Ed). Mycorrhiza. Berlin: Springer, 439–465

Herrmann, S., Recht, S., Boenn, M., Feldhahn, L., Angay, O., Fleischmann, F., Tarkka, M.T., Grams, T.E.E., Buscot, F. (2015). Endogenous rhythmic growth in oak trees is regulated by internal clocks rather than resource availability. Journal of Experimental Botany 66, 7113-7127. doi: 10.1093/jxb/erv408

Herrmann, S., Grams, T.E.E.,Tarkka, M.T., Anga,y O., Bacht, M., Bonn, M., Feldhahn, L., Graf, M., Kurth, F., Maboreke, H., Mailander, S., Recht, S., Fleischman, F., Ruess, L., Schadler, M., Scheu, S., Schrey, S.D., and Buscot, F. (2016). Endogenous rhythmic growth, a trait suitable for the study of interplays between multitrophic interactions and tree development. Perspectives in Plant Ecology, Evolution and Systematics 19, 40-48.DOI: http://dx.doi.org/doi:10.1016

Hey, S.J., Bryne, E., Halford, N.G. (2010). The interface between metabolic and stress signaling. Annals of Botany 105, 197-203. doi: 10.1093/aob/mcp285

Hibbing, M.E., Fuqua, C., Parsek, M.R., Peterson, S.B. (2010). Bacterial competition: surviving and thriving in the microbial jungle. Nature Reviews. Microbiology 8, 15–25. http://doi.org/10.1038/nrmicro2259

Hofmann, J., Wieczorek, K., Blochl, A., Grundler, F.M.W. (2007). Sucrose supply to nematode-induced syncytia depends on the apoplasmic and symplasmic pathways. Journal of Experimental Botany 58, 1591–1601 doi:10.1093/jxb/erl285

Hofmann, J., El Ashry, A. E. N., Anwar, S., Erban, A., Kopka, J., Grundler, F. (2010). Metabolic profiling reveals local and systemic responses of host plants to nematode parasitism. The Plant Journal 62, 1058–1071 http://doi.org/10.1111/j.1365-313X.2010.04217.x

Högberg, P., Nordgren, A., Buchmann, N., Taylor, A.F.S., Ekblad, A., Högberg, M.N., Nyberg, G., Ottosson-Löfvenius, M., Read, D.J. (2001). Large-scale forest girdling shows that current photosynthesis drives soil respiration. Nature 411, 789–792

Högberg, P., Nordgren, A., Aren, G. (2002). Carbon allocation between tree root growth and root respiration in boreal pine forest, Oecologia, 132, 579-581

Hopkin, S.P. (1997). Biology of the springtails - Insecta: Collembola. Oxford University Press, Oxford

Hunt, H.W., Wall, D.H., DeCrappeo, N.M., Brenner, J.S. (2001). A model for nematode locomotion in soil. Nematology. 3, 705-716

Ingham, R.E., Trofymow, J.A., Ingham, E.R., Coleman, D.C. (1985). Interactions of bacteria, fungi, and their nematode grazers:effects on nutrient cycling and plant growth. Ecology Monograms 55, 119–140

Irshad, U., Villenave, C., Brauman, A., Plassard, C. (2011). Grazing by nematodes on rhizosphere bacteria enhances nitrate and phosphorus availability to *Pinus pinaster* seedlings. Soil Biology and Biochemistry 43, 2121-2126

Joergensen, R.G., Wichern, F. (2008). Quantitative assessment of the fungal contribution to microbial tissue in soil. Soil Biology and Biochemistry 40, 2977–2991

Johansson, E.M., Fransson, P.M.A., Finlay, R.D., van Hees, P.A.W. (2009). Quantitative analysis of soluble exudates produced by ectomycorrhizal roots as a response to ambient and elevated CO_2. Soil Biology and Biochemistry 41, 1111–1116

Johansson, J., Paul, L., Finlay, R.D. (2004). Microbial interactions in the mycorrhizosphere and their significance for sustainable agriculture, FEMS Microbiology Ecology 2004, 48, 1-12

Johansson, T., Le Quéré, A., Ahren, D., Soderttrom, B., Erlandson, R., Lunderberg, J., Uhlen, M., Tunlid, A. (2004). Transcriptional responses of *Paxillus involutus* and *Betula pendula* during formation of ectomycorrhizal root tissue. Molecular Plant-Microbe interactions 17, 202-205

Johnson, D., Krsek, M., Wellington, M.H., Stott, A.W., Cole, L., Bardgett, R.D., Read, D.J., Leake, J. (2005). Soil invertebrates disrupt carbon through fungal networks. Science 309, 1047

Jones, D.L., Hodge, A., Kuzyakov, Y. (2004). Plant and mycorrhizal regulation of rhizodeposition. New Phytologist 163, 459–480

Jones, D.L., Nguyen, C., Finlay, R.D. (2009). Carbon flow in the rhizosphere: carbon trading at the soil-root interface. Plant and Soil 321, 5-33.

Jones, J.D.G., and Dangl, J.L. (2006). The plant immune system. Nature 444, 323-329

Jones, J.T., Haegeman, A., Danchin, E. G. J., Gaur, H. S., Helder, J., Jones, M. G. K., Kikuchi, T., Manzanilla-López, R., Palomares-Rius, J. E., Wesemael, W. M. L., Perry, R. N. (2013). Top 10 plant-parasitic nematodes in molecular plant pathology. Molecular Plant Pathology, 14: 946–961. doi:10.1111/mpp.12057

Jones, M.G.K., Fuso-Nyarko, J. (2014). Molecular biology of rot lesion nematodes (*Pratylenchus* spp.) and their interaction with host plants. Annals of Applied Biology 164, 168-181

Jousset, A., Rochat, L., Scheu, S., Bonkowski, M. & Keel, C. (2010). Predator–prey chemical warfare determines the expression of antifungal genes by rhizosphere pseudomonads. Applied Environmental Microbiology 76, 5263–5268

Kaneda, S., Kaneko, N. (2004). The feeding preference of a collembolan (*Folsomia candida* Willem) on ectomycorrhiza (*Pisolithus tinctorius* (Pers.)) varies with the mycelial growth. Applied Soil Ecology 27, 1-5

Kaneda, S., Kaneko, N. (2008). Collembolans feeding on soil affect carbon and nitrogen mineralization by their influence on microbial and nematode activities. Biology and Fertility of Soils 44, 435-442. doi: 10.1007/s00374-007-0222-x

Kanehisa, M., Goto, S., Sato, Y., Kawashima, M., Furumichi, M., Tanabe, M. (2014). Data, information, knowledge and principle: Back to metabolism in KEGG. Nucleic Acids Research 42, D199–D205

Kang, C.H, Jung, W.Y., Kang, Y.H., Kim, J.Y., Kim, D.G., Jeong, J.C., Baek, D.W., Jin, J.B., Lee, J.Y., Kim, M.O.,Chung, K.W.S, Mengiste, T., Koiwa, H.,Kwak,S.S. Bahk, J.D., Lee, S.Y., Nam, J.S., Yun, D.J., Cho, M.J. (2006). AtBAG6, a novel calmodulin-binding protein, induces programmed cell death in yeast and plants. Cell Death Differentiation 13, 84–95

Kanters, C., Anderson, I.C., Johnson, D. (2015). Chewing up the Wood-Wide Web: Selective Grazing on Ectomycorrhizal Fungi by Collembola. Forests 6, 2560-2570

Kaplan, I., Sardanelli, S., Rehill, B.J., Denno, R.F. (2011). Toward a mechanistic understanding of competition in vascular-feeding herbivores: an empirical test of the sink competition hypothesis. Oecologia 166, 627–636

Kesba, H.H., and Al-Sayed, A.-SA. (2006). Interactions of three species of plant-parasitic nematodes with arbuscular mycorrhizal fungus, Glomus macrocarpus, and their effect on grape. Biochemistry 7, 945-952

Kivlin, S., Hawkes, C. (2010). Differentiating between effects of invasion and diversity: Impacts of aboveground plant communities on belowground fungal communities. New Phytologist 189, 526-535

Knox, O.G.G., Killham, K., Mullins, C.E., Wilson, M.J. (2003). Nematode-enhanced microbial colonization of the wheat rhizosphere. FEMS Microbiology Letters 225, 227-233

Koch, K.E. (1996). Carbohydrate-modulated gene expression in plants. Annual Review of Plant Physiology and Plant Molecular Biology 47,509–540

Kohl, S., Hollmann J., Blattner, F. R., Radchuk, V., Andersch, F., Steuernagel, B., Schmutzer, T., Scholz, U., Krupinska, K., Weber, H., Weschke, W. (2012). A putative role for amino acid permeases in sink-source communication of barley tissues uncovered by RNA-seq. BMC Plant Bioogy 12:154–17210.1186/1471-2229-12-154

Krishna, K.R., Balakrishna, A.N., Bagyaraj, D.J. (1982). Interaction between vesicular arbuscular mycorrhizal fungus and *Streptomyces cinnamomeus* and their effects on finger millet. New Phytologist 93, 401-405

Krüger, A., Peskan-Berghofer, T., Frettinger, P., Herrmann, S., Buscot, F., Oelmüller, R. (2004). Identification of premycorrhiza-related plant genes in the association between *Quercus robur* and *Piloderma croceum*. New Phytologist 163, 149-157

Kurth, F., Feldhahn, L., Bönn, M., Herrmann, S., Buscot, F., Tarkka, M. (2015). Large scale transcriptome analysis reveals interplay between development of forest tress and a beneficial mycorrhiza helper bacterium. BMC Genomics 16, 658

Kurth, F., Zeitler, K., Feldhahn, L., Neu, T.R., Weber, T., Krištůfek, V., Wubet, T., Herrmann, S., Buscot, F., Tarkka, M.T. (2013). Detection and quantification of a mycorrhization helper bacterium and a mycorrhizal fungus in plant-soil microcosms at different levels of complexity. BMC Microbiology 13, 205-214

Kyndt, T, Nahar, K., Haegeman, D., De Vleesschauwer, M., Höfte, M., Gheysen, G. (2012). Comparing systemic defence-related gene expression changes upon migratory and sedentary nematode attack in rice. Plant Biology 14, 73-82

Kyndt, T., Denil, S., Bauters, L., Van Criekinge, W., De Meyer, T. (2014). Systemic suppression of shoot metabolism upon rice root nematode infection. PLoS One 9:e0106858

Langmead, B., Trapnell, C., Pop, M., Salzberg, S.L. (2009). Ultrafast and memory-efficient alignment of short DNA sequences to the human genome. Genome Biology 10: R25

Lavarenne, S. (1966). Croissance rythmique de quelques espèces de chênes cultivés en chambres climatisée. Comptes Rendus de l'Académie des Sciences 3, 358-361

Le Quéré, C., Harrison, S.P., Pretence, I.,Buitenhuis, E.T., Aumonts, O., Bopp, L., Claustre, H., Cunha, L.C., Geider, R., Giraud, X., Klass, C., Kohfeld, K.E., Legendre, L., Manizza, M., Platt, T., Rivkin, R.B., Sathyendranath, S., Uitz, J., Watson, A.J., Wolf-Gladrow, D. (2005). Ecosystem dynamics based on plankton functional types for global ocean biogeochemistry models, Global Change Biology11, 2016–2040, doi:10.1111/j.1365-2486.2005.01004.x.

Lee, Q., Widden, P. (1996). *Folsomia candida*, a "fungivorous" Collembolan, feeds preferentially on nematodes rather than soil fungi. Soil Biology and Biochemistry 28, 689-690

Levine, A., Tenhaken, R., Dixon, R., Lamb, C.J. (1994). H_2O_2 from the oxidative burst orchestrates the plant hypersensitive disease resistance response. Cell 79, 583–593

Li, B., Dewey, C.N. (2011). RSEM: accurate transcript quantification from RNASeq data with or without a reference genome. BMC Bioinformatics 12, 323

Li, Y., Fester, T., Taylor, C.G. (2008). Transcriptomic analysis of nematode infestation. In: Howard, R., Christopher, G.T. (Eds) Cell biology of plant nematode parasitism. Springer-Verlag, Berlin

Lindroth, R.L. (2010). Impacts of elevated atmospheric CO_2 and O_3 on forests: phytochemistry, trophic interactions, and ecosystem dynamics. Journal of Chemical Ecology 36, 2–21

Maboreke, H.R., Feldhahn, L., Bonn, M., Tarkka, M.T., Buscot, F., Herrmann, S., Menzel, R., Ruess, L. (2016). Transcriptome analysis in oak uncovers a strong impact of endogenous rhythmic growth on interaction with plant-parasitic nematodes. BMC Genomics 17, 627

Mackey, B. (2014). Counting trees, carbon and climate change. Significance 11, 19–23

Maeda, H., Dudareva, N. (2012). The shikimate pathway and aromatic amino acid biosynthesis in plants. Annual review of plant biology 63, 73–105

Maggenti, A.R., Allen, M.W. (1959). Nematode structure and life: Wide range of life habits requires combination of characters for identification of parasites classified among nematodes. California Agriculture 13, 5-12

Maier, A., Riedlinger, J., Fiedler, H.P., Hampp, R. (2004). Actinomycetales bacteria from a spruce stand: characterization and effects on growth of root symbiotic, and plant parasitic soil fungi in dual culture. Mycological Progress 3, 129-136

Manova, V., & Gruszka, D. (2015). DNA damage and repair in plants – from models to crops. *Frontiers in Plant Science*, *6*, 885. http://doi.org/10.3389/fpls.2015.00885

Marks, G.C., Winoto-Suatmadji, R., Smith, I.W. (1987). Effects of nematode control on shoot, root and mycorrhizal development of *Pinus radiata* seedlings growing in a nursery soil infested with *Pratylenchus penetrans*. Australian Forestry Research 17, 1-10

Martin, F. (2007) Fair trade in the underworld: the ectomycorrhizal symbiosis. In: Howard R.J., Gow N.A.R. (Eds) Biology of the fungal cell. The Mycota VIII. Springer, Berlin, pp 291–30

Marx, D.H. (1969). Influence of ectotrophic mycorrhizal fungi on resistance of pine roots to pathogenic infections. I. Antagonsim of mycorrhizal fungi to pathogenic fungi and soil bacteria. Phytopathology 59, 153-163

Mazzafera, P., Kubo, R.K., Inomoto, M.M. (2004). Carbon fixation and partitioning in coffee seedlings infested with *Pratylenchus coffeae*. European Journal of Plant Pathology 110, 861–865. doi: 10.1007/s10658-004-4839-4.

Mazzola, M. (2002). Mechanisms of natural soil suppressiveness to soilborne diseases. Antonie van Leeuwenhoek 81, 557-564

Mazzola, M. (2007). Manipulation of rhizosphere bacterial communities to induce suppressive soils. Journal of Nematology 39, 213-220

Meidute, S., Demoling, F., Bååth, E. (2008) Antagonistic and synergistic effects of fungal and bacterial growth in soil after adding different carbon and nitrogen sources. Soil Biology and Biochemistry 40, 2334-2343

Melillo, M.T., Leonetti, P., Bongiovanni, M., Castagnone-Sereno, P., Bleve-Zacheo, T. (2006). Modulation of reactive oxygen species activities and H_2O_2 accumulation during compatible and incompatible tomato–root-knot nematode interactions. New Phytologist 170, 501–512.doi:10.1111/j.1469-8137.2006.01724.x

Meng, Q.X., Yin, J.F., Rosenzweig, N., Douches, D., Hao, J.J. (2012). Culture based assessment of microbial communities in soil suppressive to potato common scab. Plant Disease 96, 712-717

Mille-Lindblom, C., Fischer, H., Tranvik, L.J. (2006). Antagonism between bacteria and fungi: substrate competition and a possible tradeoff between fungal growth and tolerance toward bacteria. *Oikos* 113, 233–242.

Miller, G., Schlauch, K., Tam, R., Cortes, D., Torres, M.A., Shulaev, V., Dangl, J.L., Mittler, R. (2009). The plant NADPH oxidase RBOHD mediates rapid systemic signaling in response to diverse stimuli. Science Signaling 2, 45

Milligan, S.B., Bodeau, J., Yaghoobi, J., Kaloshian, I., Zabel, P., Williamson, V.M. (1998). The root-knot nematode resistance gene *Mi* from tomato is a member of the leucine zipper, nucleotide binding, leucine-rich repeat family of plant genes. Plant Cell 10, 1307-1319

Mitchell, C.E., Power, A.G. (2006). Plant communities and disease ecology. In: Collinge, S.K., Ray, C. (Eds) Disease Ecology: Community Structure and Pathogen Dynamics. Oxford University Press, Oxford, pp. 58–72

Mitchum, M.G., Hussey, R.S., Baum, T.J., Wang, X., Elling, A.A., Wubben, M., Davis E.L. (2013). Nematode effector proteins: an emerging paradigm of parasitism. New Phytologist 199, 879–894 10.1111/nph.12323

Morkunas, I., Narozna, D., Nowak, W., Samardakiewicz, W., Remlein-Starosta, D. (2011). Cross-talk interactions of sucrose and *Fusarium oxysporum* in the phenylpropanoid pathway and the accumulation and localization of flavonoids in embryo axes of yellow lupine. Journal of Plant Physiology 168, 424-433

Morkunas, I., Ratajczak, L. (2014). The role of sugar signalling in plant defence responses against fungal pathogens. Acta Physiologiae Plantarum 36, 1607-1619

Mosblech, A., Thurow, C., Gatz, C., Feussner, I., Heilmann, I. (2011). Jasmonic acid perception by COI1 involves inositol polyphosphates in *Arabidopsis thaliana*. Plant Journal 65, 949-957. doi: 10.1111/j.1365-313X.2011.04480.x.

Müller, M. (2000). Waldbaurahmenrichtlinie der Landesforstverwaltung Brandenburg.AFZ/Der Wald 5, 239-243

Nahar, K., Kyndt, T., Nzogela, Y.B., Gheysen, G. (2012). Abscisic acid interacts antagonistically with classical defence pathways in rice-migratory nematode interaction. New Phytologist 196, 901-913

Nassar, A.H., El-Tarabily, K.A., Sivasithamparam, K. (2003). Growth promotion of bean (*Phaseolus vulgaris* L.) by a polyamine producing isolate of *Streptomyces griseoluteus*. Plant Growth Regulation 40, 97–106. doi: 10.1023/A:1024233303526.

Neher, D.A. (2010). Ecology of plant and free-living nematodes in natural and agricultural soil. Annual Review of Phytopathology 48, 371-394

Ngosong, C., Raupp, J., Richnow, H.H., Ruess, L. (2011). Tracking Collembola feeding strategies by the natural C-13 signal of fatty acids in an arable soil with different fertilizer regimes. Pedobiologia 54, 225–233

Nicol, J.M., Turner, S.J., Coyne, D.L., den Nijs, L., Hockland, S., Maafi, Z.T. (2011). Current nematode threats to world agriculture. In: Jones, J.T., Gheysen, G. and Fenoll, C., (Eds) Genomics and Molecular Genetics of Plant–Nematode. Heidelberg: Springer. pp. 21–44

O'Bannon, J.H., Taylor, A.L. (1968). Migratory endoparasitic nematodes reared on carrot discs. Phytopathology 58, 385

Pachlewska, J. (1968). Pr. Inst. Badaw Lens. 245, 3-76

Partsch, S., Milcu, A., Scheu, S. (2006). Decomposers (Lumbricidae, Collembola) affect plant performance in model grasslands of different diversity. Ecology 87, 2548–2558

Percy, K.E., Awmack, C.S., Lindroth, R.L., Kubiske, M.E., Kopper, B.J., Isebrands, J.G., Pregitzer, K.S., Hendrey, G.R., Dickson, R.E., Zak, D.R., Oksanen, E., Sober, J., Harrington, R., Karnosky, D.F., (2002). Altered performance of forest pests under CO_2 and O_3 enriched atmospheres. Nature 420, 403-407

Perry, R.N., Moens, M. (2006). Plant Nematology. CABI Publishing: Wallingford, UK. 447. ISBN-10: 1-84593-056-8; ISBN-13: 978-1-84593-056-1.

Perry, R.N., Moens, M. (2011). Introduction to plant-parasitic nematodes; modes of parasitism. In: In: Jones, J.T., Gheysen, G. and Fenoll, C., (Eds) Genomics and Molecular Genetics of Plant–Nematode Interactions, Heidelberg: Springer. pp. 3–20.

Peterson, B.J., Fry, B. (1987). Stable isotopes in ecosystem studies. Annual Review of Ecology, Evolution, and Systematics 18, 293– 32

Philippot, L., Raaijmakers, J.M., Lemanceau, P., Van Der Putten, W.H. (2013). Going back to the roots: the microbial ecology of the rhizosphere. Nature Reviews Microbiology 11, 789-799

Pieterse, C.M.J., van der Does D., Zamioudis C., Leon-Reyes, A., van Wees, S.C.M. (2012). Hormonal modulation of plant immunity. Annual Review of Cell Developmental Biology 28, 489-521

Plett, J.M., Daguerre, Y., Wittulsky, S., Vayssières, A., Deveau, A., Melton, S.J., Kohler, A., Morrell-Falvey, J.L., Brun, A., and Veneault-Fourrey, C. (2014). Effector MiSSP7 of the mutualistic fungus *Laccaria bicolor* stabilizes the *Populus* JAZ6 protein and represses jasmonic acid (JA) responsive genes. Proceedings of the National Academy of Sciences of the United States of America 111, 8299-8304

Plomion, C., Fievet, V. (2013). Oak genomics take off ... and enters the ecological genomics era. New Phytologist 199, 308-310

Poll, J., Marhan, S., Haase, S., Hallmann, J., Kandeler, E., Ruess, L., (2007). Low amounts of herbivory by root-knot nematodes affect microbial community dynamics and carbon allocation in the rhizosphere. FEMS Microbiology Ecology 62, 268-279

Pollierer, M. M., Dyckmans, J., Scheu, S. and Haubert, D. (2012). Carbon flux through fungi and bacteria into the forest soil animal food web as indicated by compound-specific ^{13}C fatty acid analysis. Functional Ecology 26, 978–990

Postma-Blaauw, M.B., de Vries, F.T., de Goede, R.G.M., Bloem, J., Faber, J.H., Brussaaerd, L. (2005). Within-trophic group interactions of bacterivorous nematode species and their effects on the bacterial community and nitrogen mineralization. Oecologia142, 428–439

Potapov, A.M., Tiunov, A.V. (2016). Stable isotope composition of mycophagous collembolans versus mycotrophic plants: Do soil invertebrates feed on mycorrhizal fungi? Soil Biology and Biochemistry 93, 115-118

Praciak A., Pasiecznik N.M., Sheil, D., van Heist, M., Sassen, M., Correia, C.S., Dixon, C., Fyson, G.E., Rushforth, K. Teeling, C. (2013). The CABI encyclopedia of forest trees. Wallingford, Oxfordshire, United Kingdom; Boston, Massachusetts: CABI

Prescott, C.E., Grayston, S.J. (2013). Tree species influence on microbial communities in litter and soil: current knowledge and research needs. Forest Ecology and Management 309, 19–27

Punta, M., Coggill, P.C., Eberhardt, R.Y., Mistry, J., Tate, J., Boursnell, C., Pang N, Forslund K, Ceric G, Clements J, Heger A, Holm L, Sonnhammer EL, Eddy SR, Bateman A, Finn, R. D. (2012). The Pfam protein families database. Nucleic Acids Research, 40 (Database issue), D290–D301. http://doi.org/10.1093/nar/gkr1065

Quentin, M., Abad, P., Favery, B. (2013). Plant parasitic nematode effectors target host defense and nuclear functions to establish feeding cells. Frontiers in Plant Science 4, 53. http://doi.org/10.3389/fpls.2013.00053

Quoreshi, A.M. (2003). The Role of mycorrhiza in forest ecosystems under CO_2-enriched atmosphere. Eurasian Journal of Forest Research 6, 171–176

Rabatin, S.C., Stinner, B.R. (1988). Indirect effects of interactions between VAM fungi and soil-inhabiting invertebrates on plant processes. In: Edwards, C.A., Stinner, B.R., Stinner, D., Rabatin, S. (Eds) Biological Interactions in Soil. Elsevier, Amsterdam.pp. 135–146.

Rahman-Khan, M., Khan, S.M., Mohide, F. (2005). Root-knot nematode problem of some winter ornamental plants and its biomanagement, Journal of Nematology 37, 198-206

Read, D.J., Perez-Moreno, J. (2003). Mycorrhizas and nutrient cycling in ecosystems - a journey towards relevance? New Phytologist 157, 475–492

Riedlinger, J., Schrey, S.D., Tarkka, M.T., Hampp, R., Kapur, M., Fiedler, H.P. (2006). Auxofuran, a novel metabolite stimulating growth of fly agaric, produced by the mycorrhiza helper bacterium *Streptomyces* AcH 505. Applied Environmental Microbiology 72, 3550-7

Rineau F, Garbaye J. (2010). Effects of liming on potential oxalate secretion and iron chelation of beech ectomycorrhizal root tips. Microbial Ecology 60, 331-9 doi: 10.1007/s00248-010-9697-3

Robinson, M.D., McCarthy, D.J., Smyth, G.K. (2010). Bioconductor package for differential expression analysis of digital gene expression data. Bioinformatics 26, 139-140

Rønn, R., McCaig, A.E., Griffiths, B.S., Prosser, J.I. (2002). Impact of protozoan grazing on bacterial community structure in soil microcosms. Applied Environment Microbiology 68, 6094–6105

Rosenberg, K., Bertaux, J., Krome, K., Hartmann, A., Scheu, S., Bonkowski, M. (2009). Soil amoebae rapidly change bacterial community composition in the rhizosphere of Arabidopsis thaliana. The ISME Journal 3, 675-684

Rosenfeld, J.M. (2002). Application on analytical derivatizations to the quantitative and qualitative determination of fatty acids. Analytica Chimica Acta 465, 93–100

Rúa, M. A., Wilson, E. C., Steele, S., Munters, A. R., Hoeksema, J. D., Frank, A. C. (2016). Associations between Ectomycorrhizal Fungi and Bacterial Needle Endophytes in *Pinus radiata*: Implications for Biotic Selection of Microbial Communities. Frontiers in Microbiology, 7, 399. http://doi.org/10.3389/fmicb.2016.00399

Ruanpanun, P., Laatsch, H., Tangchitsomkid, N., Lumyong, S. (2011). Nematicidal activity of fervenulin isolated from a nematicidal actinomycete, *Streptomyces* sp. CMU-MH021, on *Meloidogyne incognita*. World Journal of Microbiology and Biotechnology 27, 1373-1380

Ruehle, J.L. (1967). Distribution of plant-parasitic nematodes associated with forest trees of the world. U.S. Department of Agriculture; S.B. Forest Experiment Station; Asheville, North Carolina, 1, pp 56

Ruehle, J.L. (1973). Nematodes and forest trees-types of damage to tree roots. Annual Review of Phytopathology 11, 99-118

Ruess, L. (1995). Studies on the nematode fauna of an acid forest soil: spatial distribution and extraction. Nematologica 41, 229-239

Ruess, L., Chamberlain, P.M. (2010). The fat that matters: Soil food web analysis using fatty acids and their carbon stable isotope signature. Soil Biology and Biochemistry 42, 1898-1910

Ruess, L., Häggblom, M.M., Garzía Zapata, E.J., Dighton, J. (2002). Fatty acids of fungi and nematodes - possible biomarkers in the soil food chain? Soil Biology and Biochemistry 34, 745-756

Ruess, L., Tiunov, A., Haubert, D., Richnow, H.H., Häggblom, M.M., Scheu, S. (2005). Carbon stable isotope fractionation and trophic transfer of fatty acids in fungal based soil food chains. Soil Biology and Biochemistry 37, 945-954

Ruess, L., Zapata, E.J.G., Dighton, J. (2000) Food preferences of a fungal-feeding *Aphelenchoides species*. Nematology 2, 223-230

Rusek, J. (1998). Biodiversity of Collembola and their functional role in the ecosystem. Biodiversity and Conservation 7, 1207-1219

Rybarczyk-Mydłowska, K., Maboreke, H.R., Van Megen, H., Van Den Elsen, S., Mooyman, P., Smant, G., Bakker, J., Helder, J. (2012). Rather than by direct acquisition via lateral gene transfer, GHF5 cellulases were passed on from early *Pratylenchidae* to root-knot and cyst nematodes. BMC Evolutionary Biology 12, 221

Salinas, K.A., Edenborn, S.L., Sexstone, A.J., Kotcon, J.B. (2007). Bacterial preferences of the bacterivorous soil nematode *Cephalobus brevicauda* (*Cephalobidae*): effect of bacterial typeand size. Pedobiologia 51, 55–64

Sato, E., Min, Y.Y., Toyota, K., Takada, A. (2009). Relationships between the damage to radish caused by the root-lesion nematode Pratylenchus penetrans, its density prior to cultivation and the soil nematode community structure evaluated by polymerase chain reaction-denaturing gradient gel electrophoresis. Soil Science and Plant Nutrition 55, 478–484

Savill, P. (2013). The silviculture of trees used in British forestry. The silviculture of trees used in British forestry (Ed.2), p. viii + 280 pp

Savin, M.C., Görres, J.H., Neher, D.A., Amador, J.A. (2001). Uncoupling of carbon and nitrogen mineralisation: Role of microbivorous nematodes. Soil Biology and Biochemistry 33, 1463–1472

Schmid, K.M., Ohlrogge, J.B. (2002). Lipid metabolism in plants. In: Vance D.E. and Vance J.E. (Eds) Biochemistry of lipids, lipoproteins and membranes 4th edn. Elsevier Science B.V. pp 93-126

Schouteden, N., De Waele, D., Panis, B., Vos, C.M. (2015). Arbuscular Mycorrhizal Fungi for the Biocontrol of Plant-Parasitic Nematodes: A Review of the Mechanisms Involved. Frontiers in Microbiology 6, 1280.http://doi.org/10.3389/fmicb.2015.01280

Schrey, S.D., Erkenbrack, E., Früh, E., Fengler, S., Hommel, K.,Horlacher, N., Schulz,D., Ecke, M., Kulik, A., Fiedler, H.-P., Hampp, R., Tarkka, M. (2012). Production of fungal and bacterial growth modulating secondary metabolites iswidespread among mycorrhiza-associated streptomycetes. BMC Microbiology 12,164

Schultz, J. C., Appel, H. M., Ferrieri, A. P., Arnold, T. M. (2013). Flexible resource allocation during plant defense responses. Frontiers in Plant Science 4, 324. http://doi.org/10.3389/fpls.2013.00324

Sebastiana M, Vieira B, Lino-Neto T, Monteiro F, Figueiredo A, Sousa, L., Pai M.S. (2014) Oak Root Response to Ectomycorrhizal Symbiosis Establishment: RNA-Seq Derived Transcript Identification and Expression Profiling. PLOS ONE 9(5): e98376. doi: 10.1371/journal.pone.0098376

Setälä, H. (1995). Growth of Birch and Pine seedlings in relation to grazing by soil fauna on ectomycorrhizal fungi. Ecology 76, 1884-1851

Setälä, H., Huhta, V. (1990). Evaluation of the soil fauna impact on decomposition in a simulated coniferous forest soil. Biology and Fertility of Soils 10, 163

Setälä, H., Laakso, J., Mikola, J., Huhta, V. (1998). Functional diversity of decomposer organisms in relation to primary production. Applied Soil Ecology 9, 25–31

Setälä, H., Rissanen, J., Markkola, A.M. (1997). Conditional outcomes in the relationship between pine and ectomycorrhizal fungi in relation to biotic and abiotic environment. Oikos 80, 112–122

Shirling, E.B., Gottlieb, D. (1966). Methods for characterization of *Streptomyces* species. International Journal of Systematic and Evolutionary Bacteriology 16, 313-340

Shurtleff, M,C., Averre, C.W. (2000). Diagnosing plant diseases caused by nematodes. American Phytopathological Society Press, Minnesota

Siddiqui, I.A., Ehteshamul-Haque, S. (2001). Suppression of the root rot–root knot disease complex by *Pseudomonas aeruginosa* in tomato: The influence of inoculum density,

nematode populations, moisture and other plant-associated bacteria. Plant and Soil 237, 81-89

Siddiqui, Z.A., Mahmood, I. (1999). Role of bacteria in the management of plant parasitic nematodes. A review. Bioresource Technology 69, 167-179

Smith, A. M., Stitt, M. (2007). Coordination of carbon supply and plant growth. Plant Cell Environment 30, 1126–1149. doi: 10.1111/j.1365-3040.2007.01708.x

Smith, C.J., Osborn, A.M. (2009). Advantages and limitations of quantitative PCR (Q-PCR)-based approaches in microbial ecology. FEMS Microbiology and Ecology 67, 6-20

Smith, S.E., Read, D.J. (2008). Mycorrhizal symbiosis 3rd Edition. Academic Press, London. ISBN: 978-0-12-370526-6

Sohlenius, B. (1980). Abundance, Biomass and Contribution to Energy Flow by Soil Nematodes in Terrestrial Ecosystems. Oikos 34, 186-194 DOI: 10.2307/3544181

StatSoft, (2010). Statistica. Version 9.1 for Windows. StatSoft, Tusla, USA.

Steinacker, D.F., Wilson, S.D. (2008). Scale and density dependent relationship among roots, mycorrhizal fungi and collembola on grassland and forest. Oikos 117, 703-710

Stenberg, B., Johansson, M., Pell, M., Sjodahl-Svensson, K.,Stenstrom, J., Torstensson, L. (1998). Microbial biomass and activities in soil as affected by frozen and cold storage. Soil Biology and Biochemistry 30, 393–402

Steppuhn, A., Baldwin, I. T. (2008). Induced defenses and the cost-benefit paradigm. In A. Schaller (Ed.) Induced Plant Resistance to Herbivory Berlin: Springer-Verlag. pp. 61-83

Stromberger, M.E., Keith, A.M., Schmidt, O., (2012). Distinct microbial and faunal communities and translocated carbon in *Lumbricus terrestris* drilospheres. Soil Biology and Biochemistry 46, 155-162

Stumpe, M., Carsjens, J.G., Stenzel, I., Göbel, C., Lang, I., Pawlowski, K., Hause, B., Feussner, I. (2005). Lipid metabolism in arbuscular mycorrhizal roots of *Medicago trunculata*. Phytochemistry 66, 781-791

Sun,Y.P., Unestam, T., Lucas, S.D., Johanson K.J., Kenne L., Finlay, R.D., (1999). Exudation-reabsorption in mycorrhizal fungi, the dynamic interface for interaction with soil and other microorganisms. Mycorrhiza 9, 137-144

Supek, F., Bošnjak, M., Škunca, N., and Šmuc, T. (2011). REVIGO summarizes and visualizes long lists of gene ontology terms. PLoS One 6, e21800

Tarkka, M.T., Frey-Klett, P. (2008). Mycorrhiza helper bacteria. In: Varma, A. (Ed.), Mycorrhiza. Springer-Verlag, Berlin Heidelberg, pp. 113-132.

Tarkka, M.T., Herrmann, S., Wubet, T., Feldhahn, L., Recht, S., Kurth, F., Mailander, S., Bonn, M., Neef, M., Angay, O., Bacht, M., Graf, M., Maboreke, H., Fleischmann, F., Grams T.E.E., Ruess L., Schadler M., Brandl R., Scheu, S., Schrey, S.D., Grosse, I., and Buscot, F. (2013). OakContigDF159.1, a reference library for studying differential gene expression in *Quercus robur* during controlled biotic interactions: use for quantitative transcriptomic profiling of oak roots in ectomycorrhizal symbiosis. New Phytologist 199, 529-540

Tlalka, M., Bebber, D., Darrah, P.R., Watkinson, S.C., Fricker, M.D. (2007). Emergence of self-organised oscillatory domains in fungal mycelia. Fungal Genetics and Biology 44, 1085–1095

Toal, M.E., Yeomans, C., Killham, K., Meharg, A.A. (2000). A review of rhizosphere carbon flow modelling. Plant and Soil 222, 263–281

Tordoff, G.M., Boddy, L., Jones, T.H. (2008). Species-specific impacts of collembola grazing on fungal foraging ecology. Soil Biology and Biochemistry 40, 434-422

Torres, M.A., Jones, J.D.G., Dangl, J.L. (2006). Reactive Oxygen Species Signaling in Response to Pathogens. Plant Physiology 141, 373–378. http://doi.org/10.1104/pp.106.079467

Tu, C., Koenning, S.R., Hu, S. (2003) Root-parasitic nematodes enhance soil microbial activities and nitrogen mineralization. Microbial Ecological 46, 134–144

Tytgat, T., De Meutter, J., Gheysen, G., Coomans, A. (2000). Sedentary endoparasitic nematodes as a model for other plant parasitic nematodes. Nematology 2, 113–121

Umesh, K.C., Krishnappak, K., Bag-Yaraj. D.J. (1988). Interaction of burrowing nematode *Radophulus similis* (Cobb 1893) Thorne 1949 and VA mycorrhiza, *Glomus fasciculatum* (Thaxt) Gerd and Trappe in banana (*Musa acuminate* Colla.). Indian Journal of Nematology I8, 6-l l

Van der Putten, W.H., (2003). Plant defense belowground and spatiotemporal processes in natural vegetation. Ecology 84, 2269-2280

van Hees, P., Jones, D., Finlay, R., Godbold, D., Lundstrom, U. (2005). The carbon we do not see—the impact of low molecular weight compounds on carbon dynamics and respiration in forest soils: a review. Soil Biology and Biochemistry 37, 1–13

van Hees, P.A.W., Rosling, A., Essén, S., Godbold, D.L., Jones, D.L., Finlay, R.D. (2006) Oxalate and ferricrocin exudation by the extramatrical mycelium of an ectomycorrhizal fungus in symbiosis with *Pinus sylvestris*. New Phytologist 169, 367–377

Vandenkoornhuyse, P., Mahé, S., Ineson, P., Staddon, P., Ostle, N., Cliquet, J.B., Francez, A.J., Fitter, A.H., Young, J.P.W. (2007). Active root-inhabiting microbes identified by rapid incorporation of plant-derived carbon into RNA. Proceedings of the National Academy of Science of the United States of America 104, 16970–16975

Verma, V.C., Singh, S.K., and Prakash, S. (2011). Bio-control and plant growth promotion potential of siderophore producing endophytic Streptomyces from *Azadirachta indica*. A. Juss. Journal of Basic Microbiology 51, 550-556

Villenave, C., Duponnois, R. (2002). Interactions between ectomycorrhizal fungi, plant-parasitic and free-living nematodes and their effects on seedlings of the hardwood Afzelia africana Sm; Pedobiologia 46, 176–187

von Lutzow M., Kogel-Knabner, I., Ekschmitt, K., Matzner, E., Guggenberger, G., Marschner, B., Flessa, H. (2006). Stabilization of organic matter in temperate soils: mechanisms and their relevance under different soil conditions - a review. European Journal of Soil Science 5, 426–445

Vos, P., Simons, G., Jesse, T., Wijbrandi, J., Heinen, L., Hogers, R., Frijters, A., Groenedijk, J., Diegaarde, P., Reijans, M. (1998). The tomato *Mi*-1 gene confers resistance to both root-knot nematodes and potato aphids. Nature Biotechnology 16, 1365-1369

Waetzig, G.H., Sobczak, M., Grundler, F.M.W. (1999). Localization of hydrogen peroxide during the defence response of *Arabidopsis thaliana* against the plant-parasitic nematode *Heterodera glycines*. Nematology 1, 681-686

Waldrop, M.P., Balser, T.C., Firestone, M.K. (2000). Linking microbial community composition to function in a tropical soil. Soil Biology and Biochemistry 32, 1837–1846

Walker, T.H., Bais, H.P., Grotewold, E., Vivanco, J.M. (2003). Root exudation and rhizosphere biology. Plant Physiology 132, 44-51

Wang, Y., Chantreau, M., Sibout, R., Howkins, S. (2013). Plant cell wall lignification and monolignol metabolism. Frontiers in Plant Science 4, 220

Wardle D A and Yeates G W (1993). The dual importance of competition and predation as regulatory forces in terrestrial ecosystems-evidence from decomposer food-webs. Oecologia 93, 303–306.

Wardle, D.A. (2006). The influence of biotic interactions on soil biodiversity. Ecology Letters 9, 870–886. doi:10.1111/j.1461-0248.2006.00931.

Willaume, M., Pagès, L. (2011). Correlated responses of root growth and sugar concentrations to various defoliation treatments and rhythmic shoot growth in oak tree seedlings (*Quercus pubescens*). Annals of Botany 107, 653–662. http://doi.org/10.1093/aob/mcq270

Williamson, V.M., Gleason, C.A. (2003) Plant-nematode interactions. Current Opinion in Plant Biology 6, 327-333

Wind, J., Smeekens, S., Hanson, J. (2010). Sucrose: metabolite and signalling molecule. Phytochemistry 71, 1610-1614

Wisz, M.S., Pottier, J., Kissling, W.D., Pellissier, L., Lenoir, J., Damgaard, C.F., Dormann, C. F., Forchhammer, M.C., Grytnes, J.-A., Guisan, A., Heikkinen, R.K., Høye, T.T., Kühn, I., Luoto, M., Maiorano, L., Nilsson, M.C., Normand, S., Öckinger, E., Schmidt, N.M., Termansen, M., Timmermann, A., Wardle, D.A., Aastrup, P., Svenning, J.C. (2013). The role of biotic interactions in shaping distributions and realised assemblages of species: implications for species distribution modelling. Biological Reviews 88, 15–30. doi:10.1111/j.1469-185X.2012.00235.x

Wondafrash, M., Van Dam, N.M., Tytgat, T.O.G. (2013). Plant systemic induced responses mediate interactions between root parasitic nematodes and aboveground herbivorous insects. Frontiers in Plant Science 4, 87. http://doi.org/10.3389/fpls.2013.00087

Wurst, S., van der Putten, W.H. (2007). Root herbivore identity matters in plant-mediated interactions between root and shoot herbivores. Basic and Applied Ecology 8, 491–499. 10.1016/j.baae.2006.09.015

Wuyts, N., Swennen, R., and De Waele, D. (2006) Effects of plant phenylpropanoid pathway products and selected terpenoids and alkaloids on the behaviour of the plant parasitic nematodes *Radopholus similis*, *Pratylenchus penetrans* and *Meloidogyne incognita*. Nematology 8, 89-101

Xiao, H., Griffiths, B., Chen, X., Liu, M., Jiao, J., Hu, F., Li, H. (2010). Influence of bacterial-feeding nematodes on nitrification and the ammonia-oxidizing bacteria

(AOB) community composition. Applied Soil Ecology 45, 131–137, doi: 10.1016/j.apsoil.2010.03.011

Xu L, Xu W, Jiang Y, Hu F, Li H (2015). Effects of Interactions of Auxin-Producing Bacteria and Bacterial-Feeding Nematodes on Regulation of Peanut Growths. PLoS ONE 10(4): e0124361.doi:10.1371/journal.pone.0124361

Yeates, G.W, Bongers, T., De Goede, R.G.M., Freckman, D.W. Georgieva, S.S. (1993). Feeding habits in soil nematode families and genera—an outline for soil ecologists. Journal of Nematology 25, 315–331

Yeates, G.W. (1987). How plants affect nematodes. Advances in Ecological Research 17, 61-113

Yeates, G.W. (1998). Feeding in free-living soil nematodes: a functional approach. In: Perry, RN, Wright, DJ (Eds.), The Physiology and Biochemistry of Free-living and Plant-parasitic Nematodes, CABI, Wallingford, pp 245-269

Yeates, G.W. (1999). Effects of plants on nematode community structure. Annual Reviews in Phytopathology 37, 127-149

Yeates, G.W. (2003). Nematodes as soil indicators: functional and biodiversity aspects. Biology and Fertility of Soils 37,199-210

Yeates, G.W. (2010). "Nematodes in ecological webs," in Encyclopedia of Life Science Chichester: John Wiley & Sons, Ltd. pp 1–10. doi: 10.1002/9780470015902.a0021913

Yeates, G.W., Saggar, S., Denton, C.S., and Mercer, C.F. (1998). Impact of clover cyst nematode (*Heterodera trifolii*) infection on soil microbial activity in the rhizosphere of white clover (*Trifolium repens*) - a pulse-labelling experiment. Nematologica 44, 81-90

Yeates, G.W., Saggar, S., Hedley C.B., and Mercer, C.F. (1999b). Increase in ^{14}C-carbon translocation to soil microbial biomass when five species of plant-parasitic nematodes infect roots of white clover. Nematology 1, 295-300

Yeates, G.W., Wardle, D.A. (1996). Nematodes as predators and prey: relationships to biological control and soil processes. Pedobiologia 40, 43–50

Young, M.D., Wakefield, M.J., Smyth, G.K., Oshlack, A. (2010). Gene ontology analysis for RNA-seq: accounting for selection bias. Genome Biology 11, R14

Zelles, L., (1999). Fatty acid patterns of phospholipids and lipopolysaccharides in the characterization of microbial communities in soil: a review. Biology and Fertility of Soils 29, 111-129

Zhu, B., Gutknecht, J.L.M., Herman, D.J., Keck, D.C., Firestone, M.K., Cheng, X. (2014). Rhizosphere priming effects on soil carbon and nitrogen mineralization. Soil Biology and Biochemistry 76, 183-192

Zunke, U. (1990). Observations on the invasion and endoparasitic behaviour of the root lesion nematode *Pratylenchus penetrans*. Journal of Nematology 22, 309–320

Zunke, U., and Perry, R.N. (1997) Nematodes: Harmful and beneficial organisms. In: Benckiser, G. (Ed.), Fauna in Soil Ecosystems: Recycling Processes, Nutrient Fluxes and Agricultural Production. Marcel Dekker, New York, pp. 85-133

APPENDIX

Table A1 Enriched KEGG pathways for up- and downregulated contigs in leaf tissues of oak microcuttings during root flush and shoot flush stages treated with *Pratylenchus penetrans*, *Piloderma croceum* and co-inoculation of *P. penetrans* and *P. croceum*. KEGG ID, KEGG term description and significance level (*P*-value) are provided

Upregulated				
Treatment	**Oak growth stage**	**KEGG ID**	**Description**	***P* value**
P. penetrans	Root Flush	path:ec00590	Arachidonic acid metabolism	0.0129376594
		path:ec00591	Linoleic acid metabolism	0.0159379389
		path:ec00592	alpha-Linolenic acid metabolism	0.0169384108
		path:ec00053	Ascorbate and aldarate metabolism	0.0195854887
		path:ec00980	Metabolism of xenobiotics by cytochrome P450	0.0288501779
		path:ec00982	Drug metabolism - cytochrome P450	0.0311547044
		path:ec00620	Pyruvate metabolism	0.0367677367
		path:ec00627	Aminobenzoate degradation	0.0451323495
	Shoot Flush	path:ec01110	Biosynthesis of secondary metabolites	0.0000000000
		path:ec00941	Flavonoid biosynthesis	0.0000000000
		path:ec01100	Metabolic pathways	0.0000015589
		path:ec01120	Microbial metabolism in diverse environments	0.0000951627
		path:ec00350	Tyrosine metabolism	0.0002277759
		path:ec00643	Styrene degradation	0.0002521265
		path:ec00944	Flavone and flavonol biosynthesis	0.0014537165
		path:ec00980	Metabolism of xenobiotics by cytochrome P450	0.0015907729
		path:ec00740	Riboflavin metabolism	0.0018227250
		path:ec00500	Starch and sucrose metabolism	0.0032805394
		path:ec00010	Glycolysis / Gluconeogenesis	0.0033400225
		path:ec00627	Aminobenzoate degradation	0.0035543116
		path:ec00984	Steroid degradation	0.0084958178
		path:ec00982	Drug metabolism - cytochrome P450	0.0087350364
		path:ec00592	alpha-Linolenic acid metabolism	0.0118703311
		path:ec00940	Phenylpropanoid biosynthesis	0.0147319083
		path:ec00520	Amino sugar and nucleotide sugar metabolism	0.0162006024
		path:ec00626	Naphthalene degradation	0.0171467655
		path:ec00943	Isoflavonoid biosynthesis	0.0251391491
		path:ec00625	Chloroalkane and chloroalkene degradation	0.0286606815
		path:ec00565	Ether lipid metabolism	0.0325207182
		path:ec00830	Retinol metabolism	0.0339362223
		path:ec00071	Fatty acid metabolism	0.0380916184
		path:ec00630	Glyoxylate and dicarboxylate metabolism	0.0386430309
		path:ec00930	Caprolactam degradation	0.0488055455
P. croceum				
	Root Flush	path:ec01100	Metabolic pathways	0.00149336
		path:ec00591	Linoleic acid metabolism	0.001837375
		path:ec00232	Caffeine metabolism	0.006685651
		path:ec00730	Thiamine metabolism	0.010736333
		path:ec00770	Pantothenate and CoA biosynthesis	0.011064258
		path:ec00514	Other types of O-glycan biosynthesis	0.013021898
		path:ec00830	Retinol metabolism	0.017546044
		path:ec00590	Arachidonic acid metabolism	0.022558704
		path:ec00140	Steroid hormone biosynthesis	0.026394202

		path:ec00071	Fatty acid metabolism	0.040035879
		path:ec00980	Metabolism of xenobiotics by cytochrome P450	0.049427748
	Shoot Flush	path:ec00190	Oxidative phosphorylation	0.007545373
		path:ec00510	N-Glycan biosynthesis	0.029684714
		path:ec00790	Folate biosynthesis	0.043760254
		path:ec00750	Vitamin B6 metabolism	0.0441455
		path:ec00100	Steroid biosynthesis	0.045547404
P. penetrans × *P. croceum*				
	Root Flush	path:ec00500	Starch and sucrose metabolism	0.0000000000
		path:ec01100	Metabolic pathways	0.0000000002
		path:ec00040	Pentose and glucuronateinterconversions	0.0000000009
		path:ec00983	Drug metabolism - other enzymes	0.0000005594
		path:ec00053	Ascorbate and aldarate metabolism	0.0000610462
		path:ec00940	Phenylpropanoid biosynthesis	0.0001196381
		path:ec00071	Fatty acid metabolism	0.0005854107
		path:ec00073	Cutin	0.0013617016
		path:ec00360	Phenylalanine metabolism	0.0016692340
		path:ec00591	Linoleic acid metabolism	0.0017785512
		path:ec00650	Butanoate metabolism	0.0018663099
		path:ec00232	Caffeine metabolism	0.0021918703
		path:ec00627	Aminobenzoate degradation	0.0024177240
		path:ec00140	Steroid hormone biosynthesis	0.0026254399
		path:ec00830	Retinol metabolism	0.0042567314
		path:ec00062	Fatty acid elongation	0.0125036597
		path:ec00600	Sphingolipid metabolism	0.0146888407
		path:ec00980	Metabolism of xenobiotics by cytochrome P450	0.0150391208
		path:ec00460	Cyanoamino acid metabolism	0.0158343649
		path:ec00564	Glycerophospholipid metabolism	0.0166651725
		path:ec00380	Tryptophan metabolism	0.0172956688
		path:ec00982	Drug metabolism - cytochrome P450	0.0214554869
		path:ec00561	Glycerolipid metabolism	0.0248281910
		path:ec00590	Arachidonic acid metabolism	0.0256352823
		path:ec00410	beta-Alanine metabolism	0.0434347821
	Shoot Flush	path:ec00510	N-Glycan biosynthesis	0.0328949783

Downregulated

		KEGGID	Description	P-values
P. penetrans				
	Root Flush	path:ec00053	Ascorbate and aldarate metabolism	0.0172306411
		path:ec00562	Inositol phosphate metabolism	0.0202364940
	Shoot Flush	path:ec00500	Starch and sucrose metabolism	0.0000000000
		path:ec01100	Metabolic pathways	0.0000000000
		path:ec00040	Pentose and glucuronateinterconversions	0.0000000000
		path:ec00053	Ascorbate and aldarate metabolism	0.0000000003
		path:ec00531	Glycosaminoglycan degradation	0.0000000046
		path:ec00600	Sphingolipid metabolism	0.0000000300
		path:ec00604	Glycosphingolipid biosynthesis - ganglio series	0.0000001133
		path:ec00511	Other glycan degradation	0.0000002333
		path:ec00983	Drug metabolism - other enzymes	0.0000100132
		path:ec00052	Galactose metabolism	0.0000175530
		path:ec00591	Linoleic acid metabolism	0.0020969693
		path:ec00940	Phenylpropanoid biosynthesis	0.0066671373
		path:ec00360	Phenylalanine metabolism	0.0199095152
		path:ec00121	Secondary bile acid biosynthesis	0.0306798295
		path:ec00534	Glycosaminoglycan biosynthesis - heparin sulfate / heparin	0.0308762836
		path:ec00520	Amino sugar and nucleotide sugar metabolism	0.0428761333
		path:ec00532	Glycosaminoglycan biosynthesis - chondroitin sulfate / dermatansulfate	0.0440883588
		path:ec00860	Porphyrin and chlorophyll metabolism	0.0448550686

P. croceum				
	Root Flush	path:ec01100	Metabolic pathways	0.002805569
		path:ec00592	alpha-Linolenic acid metabolism	0.024686725
		path:ec00053	Ascorbate and aldarate metabolism	0.029695614
		path:ec00364	Fluorobenzoate degradation	0.034543056
		path:ec01120	Microbial metabolism in diverse environments	0.043587826
		path:ec00361	Chlorocyclohexane and chlorobenzene degradation	0.045835108
	Shoot Flush	path:ec00592	alpha-Linolenic acid metabolism	0.000222555
		path:ec00310	Lysine degradation	0.003435201
		path:ec00720	Carbon fixation pathways in prokaryotes	0.004967768
		path:ec00591	Linoleic acid metabolism	0.006165045
		path:ec00860	Porphyrin and chlorophyll metabolism	0.007191332
		path:ec00120	Primary bile acid biosynthesis	0.015356075
		path:ec00281	Geraniol degradation	0.0276533
		path:ec00362	Benzoate degradation	0.030252285
		path:ec00930	Caprolactam degradation	0.031588133
		path:ec00062	Fatty acid elongation	0.031898601
		path:ec00903	Limonene and pinene degradation	0.034700349
		path:ec00623	Toluene degradation	0.034879619
		path:ec00902	Monoterpenoid biosynthesis	0.048166633
P. penetrans × *P. croceum*				
	Root Flush	path:ec01110	Biosynthesis of secondary metabolites	0.0000000000
		path:ec01100	Metabolic pathways	0.0000000000
		path:ec01120	Microbial metabolism in diverse environments	0.0000000000
		path:ec00400	Phenylalanine	0.0000000001
		path:ec00364	Fluorobenzoate degradation	0.0000000035
		path:ec00270	Cysteine and methionine metabolism	0.0000000065
		path:ec00361	Chlorocyclohexane and chlorobenzene degradation	0.0000000185
		path:ec00941	Flavonoid biosynthesis	0.0000000191
		path:ec00710	Carbon fixation in photosynthetic organisms	0.0000000377
		path:ec00623	Toluene degradation	0.0000001579
		path:ec00360	Phenylalanine metabolism	0.0000005397
		path:ec00401	Novobiocin biosynthesis	0.0000036759
		path:ec00960	Tropane	0.0000184782
		path:ec00940	Phenylpropanoid biosynthesis	0.0000274601
		path:ec00010	Glycolysis / Gluconeogenesis	0.0000313544
		path:ec00680	Methane metabolism	0.0000344688
		path:ec00130	Ubiquinone and other terpenoid-quinone biosynthesis	0.0000389560
		path:ec00950	Isoquinoline alkaloid biosynthesis	0.0000838692
		path:ec00620	Pyruvate metabolism	0.0000986864
		path:ec00720	Carbon fixation pathways in prokaryotes	0.0001736390
		path:ec00350	Tyrosine metabolism	0.0002677796
		path:ec00740	Riboflavin metabolism	0.0003764540
		path:ec00250	Alanine	0.0007410400
		path:ec00627	Aminobenzoate degradation	0.0012006523
		path:ec00330	Arginine and proline metabolism	0.0012978615
		path:ec00300	Lysine biosynthesis	0.0027173943
		path:ec00340	Histidine metabolism	0.0079036909
		path:ec00945	Stilbenoid	0.0124506026
		path:ec00984	Steroid degradation	0.0271413295
		path:ec00020	Citrate cycle (TCA cycle)	0.0298905516
		path:ec00630	Glyoxylate and dicarboxylate metabolism	0.0299851187
		path:ec00640	Propanoate metabolism	0.0318320927
		path:ec00260	Glycine	0.0339821597
		path:ec00500	Starch and sucrose metabolism	0.0344390146
		path:ec00051	Fructose and mannose metabolism	0.0433729949
	Shoot Flush	path:ec00860	Porphyrin and chlorophyll metabolism	0.0026954519

	path:ec00140	Steroid hormone biosynthesis	0.0281674237
	path:ec01110	Biosynthesis of secondary metabolites	0.0328805910
	path:ec00053	Ascorbate and aldarate metabolism	0.0337214137

Table A2 Differentially expressed contigs associated with enriched GO terms presented in Fig. 11-13. Gene description and the significant differential expression (Log_2 of FC) determined by edgeR with a threshold Benjamini-Hochberg adjusted $P < 0.01$ as cut-off indicated by FDR, are provided. Control versus *Piloderma croceum* during root flush (RF Co-Pc) and Control versus *Piloderma croceum* during shoot flush (SF Co-Pc)

Treatment	Oak Contig	*A. thaliana* homologue	Description	Log_2FC
RF Co-Pc	comp42530_c1_seq8	AT5G37360	Ammonium transporter	7.5
RF Co-Pc	comp43571_c0_seq34	AT2G44480	Beta glucosidase 17	8.8
RF Co-Pc	comp38015_c1_seq6	AT5G65780	Branched-chain amino acid	7.1
RF Co-Pc	comp42018_c0_seq5	AT5G58200	Calcineurin-like metallo-phosphoesterase superfamily protein	5.7
RF Co-Pc	comp17244_c0_seq1	AT1G24620	Calmodulin-like protein 1-like	4.7
RF Co-Pc	comp43459_c0_seq12	AT5G51430	Conserved oligomeric golgi complex subunit	7.5
RF Co-Pc	comp43757_c1_seq42	AT5G53130	Cyclic nucleotide-gated ion channel 1-like	6.8
RF Co-Pc	comp39803_c1_seq7	AT2G29080	FTSH protease 3	8.5
RF Co-Pc	comp35200_c1_seq9	AT4G24740	FUS3-complementing gene 2	4.3
RF Co-Pc	comp33885_c0_seq2	AT1G27600	Glycosyl transferase	7.3
RF Co-Pc	comp43517_c0_seq1	AT3G07180	GPI transamidase component PIG-S-related	5.0
RF Co-Pc	comp41845_c1_seq8	AT2G43980	Inositol-tetrakisphosphate 1-kinase 4-like	4.5
RF Co-Pc	comp42746_c0_seq5	AT5G49960	Ion channel dmi1- chloroplast expressed	6.7
RF Co-Pc	comp43363_c0_seq2	AT3G47570	Leucine-rich repeat protein kinase family protein	6.7
RF Co-Pc	comp38272_c0_seq2	AT3G22400	Lipoxygenase 5	2.0
RF Co-Pc	comp43794_c0_seq60	AT5G48740	LRR receptor-like serine threonine-protein kinase	7.6
RF Co-Pc	comp42806_c1_seq2	AT1G17260	Magnesium-translocating p-type atpase AHA10	7.0
RF Co-Pc	comp41227_c1_seq16	AT2G38330	Mate efflux family protein	4.8
RF Co-Pc	comp43449_c1_seq17	AT1G66760	Mate efflux family protein	7.9
RF Co-Pc	comp43419_c0_seq3	AT5G66930	Meiotically up-regulated gene 66 protein	7.2
RF Co-Pc	comp42239_c0_seq1	AT4G21580	NADPH quinone oxidoreductase	8.6
RF Co-Pc	comp43617_c1_seq8	AT5G55810	Nicotina/nicotinamide mononucleotide adenyltransferase	8.0
RF Co-Pc	comp43330_c0_seq13	AT3G44320	Nitrilase3	6.6
RF Co-Pc	comp42299_c0_seq7	AT5G18860	Nucleoside hydrolase 3	8.3
RF Co-Pc	comp42708_c0_seq6	AT2G01220	Nucleotidyl transferase domain-containing protein	5.4
RF Co-Pc	comp40133_c0_seq5	AT1G38065	O-fucosyltransferase family protein	2.1
RF Co-Pc	comp43007_c0_seq7	AT2G01460	P-loop containing nucleoside triphosphate hydrolases superfamily protein	5.0
RF Co-Pc	comp43050_c0_seq2	AT3G27730	Pentatricopeptide repeat-containing	6.5
RF Co-Pc	comp38978_c2_seq2	AT1G03000	Peroxin 6	7.7
RF Co-Pc	comp35313_c0_seq10	AT5G64390	Poly -binding protein	9.2
RF Co-Pc	comp30456_c0_seq2	AT2G25690	Protein	7.8
RF Co-Pc	comp43811_c0_seq12	AT2G24960	Protein	9.6
RF Co-Pc	comp43811_c0_seq8	AT4G02210	Protein	10.0
RF Co-Pc	comp37558_c0_seq3	AT2G30170	Protein phosphatase 2c 26	5.8
RF Co-Pc	comp43164_c0_seq6	AT1G11340	S-locus lectin protein kinase family protein	8.2
RF Co-Pc	comp38053_c0_seq1	AT2G43810	Small nuclear ribonucleoprotein family protein	7.9

RF Co-Pc	comp39673_c0_seq2	AT4G34430	swi snf complex subunit swi3d	7.0
RF Co-Pc	comp31863_c0_seq2	AT5G57230	Thioredoxin-like domain-containing protein	8.1
RF Co-Pc	comp42344_c7_seq3	AT1G08500	early nodulin-like protein 18Transcription elongation regulator 1-like	8.8
RF Co-Pc	comp42754_c0_seq2	AT2G30140	UDP-glycosyltransferase 87a1-like	9.0
RF Co-Pc	comp40340_c0_seq4	AT5G24750	UDP-glycosyltransferase superfamily protein	7.2
RF Co-Pc	comp40412_c0_seq2	AT1G02270	Uncharacterized calcium-binding protein At1g02270-like	6.9
RF Co-Pc	comp42785_c0_seq16	AT1G12470	Vacuolar protein sorting-associated protein 18 homolog	9.0
RF Co-Pc	comp36742_c0_seq6	AT1G14530	Virion binding	4.3
RF Co-Pc	comp43120_c0_seq2	AT4G25810	Xyloglucan endotransglucosylase/hydrolase 23	7.4
RF Co-Pc	comp43108_c0_seq19	AT2G40140	Zinc finger ccch domain-containing protein	11.0
RF Co-Pc	comp35274_c0_seq1	AT1G19690	AD(P)-binding Rossmann-fold superfamily protein	-7.3
RF Co-Pc	comp43354_c0_seq8	AT3G48000	Aldehyde dehydrogenase 2	-3.2
RF Co-Pc	comp40088_c0_seq6	AT3G29320	Alpha-glucan phosphorylase 1	-7.8
RF Co-Pc	comp40088_c0_seq4	AT3G29320	Alpha-glucan phosphorylase 2	-7.0
RF Co-Pc	comp40668_c1_seq15	AT3G23600	Alpha/beta-Hydrolases superfamily protein	-9.2
RF Co-Pc	comp33288_c1_seq3	AT4G31020	Alpha/beta-Hydrolases superfamily protein	-7.2
RF Co-Pc	comp41856_c1_seq2	AT3G59410	Arabidopsis thaliana general control non-repressible 2	-7.4
RF Co-Pc	comp41856_c1_seq5	AT3G59410	Arabidopsis thaliana general control non-repressible 2	-7.3
RF Co-Pc	comp43061_c0_seq4	AT2G20190	ATCLASP cell expansion CLIP-associated protein	-7.5
RF Co-Pc	comp43571_c0_seq3	AT2G44480	Beta glucosidase 17	-9.5
RF Co-Pc	comp42244_c0_seq5	AT3G12290	c-1-tetrahydrofolate cytoplasmic	-9.1
RF Co-Pc	comp31014_c0_seq1	AT5G54160	Caffeate O-methyltransferase 1 lignin biosynthesis	-2.9
RF Co-Pc	comp42908_c0_seq22	AT3G13860	Chaperonin cpn60-like mitochondrial-like	-9.3
RF Co-Pc	comp40383_c1_seq5	AT1G65020	Conserved hypothetical protein	-7.4
RF Co-Pc	comp42202_c0_seq3	AT4G23180	Cysteine -richlike RLK 10 defence response	-4.7
RF Co-Pc	comp40413_c0_seq5	AT5G04895	DEA(D/H)-box RNA helicase family protein	-8.0
RF Co-Pc	comp42746_c0_seq3	AT5G49960	Dmi1 protein	-7.6
RF Co-Pc	comp41121_c1_seq3	AT2G01970	Endomembrane protein 70	-4.6
RF Co-Pc	comp43515_c0_seq2	AT5G10770	Eukaryotic aspartyl protease family protein	-2.1
RF Co-Pc	comp43517_c0_seq2	AT3G07180	GPI transamidase component PIG-S-related	-9.3
RF Co-Pc	comp43256_c0_seq3	AT5G42830	HXXXD-type acyl-transferase family protein	-8.5
RF Co-Pc	comp37882_c0_seq2	AT3G21760	Hypostain resistance 1	-8.3
RF Co-Pc	comp41845_c1_seq6	AT2G43980	Inositol-tetrakisphosphate 1-kinase 4-like	-8.9
RF Co-Pc	comp39930_c0_seq1	AT3G47980	Integral membrane HPP family protein	-6.7
RF Co-Pc	comp42746_c0_seq6	AT5G49960	Ion channel dmi1- chloroplast expressed	-6.7
RF Co-Pc	comp39773_c5_seq4	AT5G09360	Laccase 14	-8.5
RF Co-Pc	comp43363_c0_seq10	AT3G47570	Leucine-rich repeat protein kinase family protein	-6.6
RF Co-Pc	comp43664_c0_seq9	AT1G67560	lipoxygenase	-8.6
RF Co-Pc	comp42806_c1_seq13	AT1G17260	Magnesium-translocating p-type atpase	-6.7
RF Co-Pc	comp40525_c0_seq5	AT1G26180	Membrane protein	-8.5
RF Co-Pc	comp40483_c0_seq1	AT2G03120	Minor histocompatibility antigen h13 signal peptidase peptidase	-7.0
RF Co-Pc	comp43771_c1_seq1	AT5G07900	Mitochondrial transcription termination factor family protein	-7.6

RF Co-Pc	comp42239_c0_seq4	AT4G21580	NADPH quinone oxidoreductase	-8.6
RF Co-Pc	comp43330_c0_seq16	AT5G22300	Nitrilase 4	-8.3
RF Co-Pc	comp39050_c0_seq3	AT5G57120	Nucleolar and coiled-body phosphoprotein	-8.6
RF Co-Pc	comp40844_c0_seq1	AT3G60450	Phosphoglycerate mutase family protein	-2.0
RF Co-Pc	comp40857_c0_seq1	AT1G59520	Protein cw7	-8.0
RF Co-Pc	comp42415_c1_seq1	AT1G80010	Protein far1-related sequence 6-like	-9.0
RF Co-Pc	comp43466_c0_seq3	AT5G47070	Protein kinase superfamily protein	-9.3
RF Co-Pc	comp38369_c0_seq2	AT1G10510	Protein nlrc3-like	-6.8
RF Co-Pc	comp43604_c1_seq1	AT3G11410	Protein phosphatase 2c	-7.9
RF Co-Pc	comp42456_c1_seq3	AT1G79950	RAD3-like DNA-binding helicase protein	-8.6
RF Co-Pc	comp36158_c0_seq2	AT5G64930	Regulator of expression of pathogenesis-related (PR) genes	-7.3
RF Co-Pc	comp43807_c0_seq2	AT5G04050	rna binding	-6.8
RF Co-Pc	comp42134_c0_seq4	AT3G63470	Serine carboxypeptidase-like 40	-5.4
RF Co-Pc	comp40124_c1_seq21	AT2G17700	Serine/threonine/tyrosine kinase 8	-5.2
RF Co-Pc	comp43737_c0_seq4	AT4G16730	Terpene synthase 02 not translated	-4.1
RF Co-Pc	comp31863_c0_seq4	AT5G57230	Thioredoxin-like domain-containing protein	-7.4
RF Co-Pc	comp36210_c0_seq1	AT2G29070	Ubiquitin fusion degradation UFD1 family protein	-6.5
RF Co-Pc	comp39822_c0_seq9		Zinc finger ccch domain-containing protein 66-like	-7.2
SF Co-Pc	comp36621_c0_seq1	AT1G15690	ATAVP1	8.9
SF Co-Pc	comp43571_c0_seq14	AT2G44480	Beta glucosidase 17	8.9
SF Co-Pc	comp43571_c0_seq13	AT2G44480	Beta glucosidase 17	9.4
SF Co-Pc	comp43109_c0_seq4	AT5G62570	Calmodulin binding protein-like	10.0
SF Co-Pc	comp42225_c2_seq46	AT2G07050	Cycloartenol synthase	9.5
SF Co-Pc	comp43826_c1_seq12	AT3G14460	LRR and NB-ARC domains-containing disease resistance protein	9.2
SF Co-Pc	comp34284_c0_seq3	AT2G39630	Dolichyl-phosphate β-glucosyltransferase	10.0
SF Co-Pc	comp43459_c0_seq4	AT5G51430	Embryo yellow	9.5
SF Co-Pc	comp37458_c0_seq4	AT1G48360	FANCONI/FANCD2 associated nuclease 1	8.7
SF Co-Pc	comp41119_c0_seq1	AT3G10160	Folypolyglutamate synthetase 2	10.4
SF Co-Pc	comp43517_c0_seq1	AT3G07180	GPI transamidase component PIG-S-related	8.9
SF Co-Pc	comp43313_c1_seq4	AT2G19070	Hydroxycinnamoyl-coenzyme a shikimate quinate hydroxycinnamoyltransferase-like	8.8
SF Co-Pc	comp40225_c0_seq2	AT4G05090	Inositol monophosphatase family protein	8.8
SF Co-Pc	comp39930_c0_seq9	AT1G73200	Integral membrane hpp family protein	9.0
SF Co-Pc	comp40202_c0_seq4	AT1G73200	Integral membrane protein conserved region	9.8
SF Co-Pc	comp35600_c2_seq8	AT1G22280	Phytochrome-associated protein phosphatase type 2C	10.0
SF Co-Pc	comp42858_c0_seq3	AT1G79050	recA DNA recombination family protein;	8.9
SF Co-Pc	comp36556_c0_seq2	AT3G55580	Regulator of chromosome condensation (RCC1) family protein	9.2
SF Co-Pc	comp36977_c0_seq2	AT4G29010	Abnormal inflorescence meristem	-5.2
SF Co-Pc	comp39810_c0_seq2	AT2G38660	Amino acid dehydrogenase family protein	-8.9
SF Co-Pc	comp43159_c0_seq6	AT4G38120	ARM repeat superfamily protein	-8.6
SF Co-Pc	comp41169_c0_seq12	AT3G26950	Conserved hypothetical protein	-8.5
SF Co-Pc	comp39888_c0_seq8	AT3G15520	Cyclophilin-like peptidyl-prolyl cis-trans isomerase family protein	-5.5
SF Co-Pc	comp43500_c0_seq13	AT5G41480	Dihydrofolate synthetase	5.7
SF Co-Pc	comp34284_c0_seq1	AT2G39630	Dolichyl-phosphate β-glucosyltransferase	-9.5
SF Co-Pc	comp41726_c0_seq3	AT1G13980	Embryo defective 30	-8.6
SF Co-Pc	comp37458_c0_seq9	AT1G48360	FANCONI/FANCD2 associated nuclease 1	-9.5
SF Co-Pc	comp41194_c0_seq7	AT3G15850	Fatty acid desaturase 5	-9.8
SF Co-Pc	comp41119_c0_seq4	AT3G10160	Folypolyglutamate synthetase 2	-9.9
SF Co-Pc	comp41222_c1_seq6	AT1G75750	GAST1 Protein homolog 1,	-6.9

SF Co-Pc	comp41014_c2_seq2	AT2G36750	UDP-glucosyl transferase 73C1	-8.8
SF Co-Pc	comp38571_c0_seq3	AT1G15380	Glyoxylase 14	6.0
SF Co-Pc	comp29219_c0_seq4	AT4G02450	HSP20-like chaperones superfamily protein	-9.0
SF Co-Pc	comp37882_c0_seq2	AT3G21760	Hypostain resistance 1	-9.5
SF Co-Pc	comp30321_c0_seq6	AT5G52200	Inhibitor-2	-8.6
SF Co-Pc	comp43664_c0_seq9	AT1G67560	Lipoxygenase	-9.1
SF Co-Pc	comp32951_c0_seq3	AT4G34440	Proline-rich extensine-like receptor kinase 5	-6.8
SF Co-Pc	comp36556_c0_seq1	AT3G55580	Regulator of chromosome condensation (RCC1) family protein	-9.0
SF Co-Pc	comp42876_c0_seq3	AT5G53020	Ribonuclease P protein subunit P38-related	-8.6
SF Co-Pc	comp43391_c0_seq3	AT3G14350	Strubbelig-receptor family 6	-8.9
SF Co-Pc	comp22965_c0_seq3	AT4G22890	PGR5-like A	-11.1

Table A3 Number of differentially expressed contigs enriching the Gene Ontology terms belonging to biological process, cellular component and molecular function categories. Presented are data for up- and down regulated contigs in leaf tissues of oak microcuttings treated with *Pratylenchus penetrans*, *Piloderma croceum* and co-inoculation of *Pratylenchus penetrans* and *Piloderma croceum* during root flush and shoot flush

			Gene Ontology Categories		
Growth Stage	Treatment	Regulation	Biological Process	Cellular Component	Molecular Function
Root Flush					
	P. penetrans	Up	24	5	16
		Down	25	3	24
	P. croceum	Up	44	3	41
		Down	52	4	43
	P. *penetrans* × *P. croceum*	Up	99	23	61
		Down	68	13	71
Shoot Flush					
	P. penetrans	Up	69	8	80
		Down	178	27	102
	P. croceum	Up	28	3	23
		Down	34	5	24
	P. penetrans × *P. croceum*	Up	36	6	22
		Down	41	6	29

Table A4 Effects of *Pratylenchus penetrans* and *Piloderma croceum* on the relative allocation of carbon and nitrogen in the oak microcuttings organs. Present are data for the proportions of ^{13}C excess and ^{15}N excess (% of total ± s.d.) in plant organs harvested during root and shoot flush. For each growth stage, ANOVA with *, ** and *** for $P < 0.05$, $P < 0.01$ and $P < 0.001$, respectively. Values in a row followed by the same letter are not significantly different (Tukey's HSD test, $P < 0.05$). Pp: *Pratylenchus penetrans*; Pc: *Piloderma croceum*

	Root Flush					Shoot Flush				
	Control	*P. penetrans*	*P. croceum*	Pp × Pc	ANOVA	Control	*P. penetrans*	*P. croceum*	Pp × Pc	ANOVA
^{13}C excess										
SFt	6.39 ± 9.09	2.36 ± 2.52	1.79 ± 2.10	3.10 ± 4.0		22.65 ± 13.12b	39.10 ± 15.30a	28.80 ± 10.61ab	39.90 ± 14.54a	Pp*
SFt-1	25.74 ± 13.23	30.76 ± 11.16	23.59 ± 9.86	23.76 ± 11.60		26.38 ± 7.59	29.11 ± 9.37	27.08 ± 13.01	27.09 ± 7.38	
SFt -2	16.81 ± 7.59	13.77 ± 8.71	10.65 ± 5.44	19.19 ± 16.82		12.54 ± 11.68	8.56 ± 8.85	6.02 ± 1.49	4.18 ± 1.86	
Stem	10.01 ± 4.91	11.64 ± 2.08	13.50 ± 5.75	10.22 ± 3.81		11.17 ± 3.24b	9.37 ± 5.06b	16.27 ± 3.20a	11.57 ± 2.99ab	Pc*
Lateral roots	14.44 ± 10.26	10.06 ± 6.02	9.96 ± 8.25	7.23 ± 3.62		10.65 ± 6.89a	3.84 ± 2.12b	6.39 ± 2.41ab	8.44 ± 3.79ab	Pp × Pc*
Principal roots	26.61 ± 13.27b	30.41 ± 5.63ab	40.51 ± 12.33a	36.48 ± 14.79ab	Pc**	16.6 ± 8.77	10.03 ± 7.38	15.45 ± 7.66	8.81 ± 65	
^{15}N excess										
SFt	5.25 ± 9.78	1.54 ± 2.47	3.28 ± 3.08	1.50 ± 2.65		16.40 ± 9.26b	30.55 ± 16.45	24.18 ± 12.61ab	44.12 ± 8.16a	Pp**
SFt - 1	11.16 ± 7.10	15.30 ± 5.88	10.19 ± 6.74	11.10 ± 5.59		24.40 ± 20.77	12.96 ± 4.99	13.37 ± 8.13	20.07 ± 6.34	
SFt - 2	10.81 ± 7.88b	13.32 ± 8.62ab	5.76 ± 3.42b	23.65 ± 15.20a	Pp***	6.53 ± 5.73	4.27 ± 4.63	1.92 ± 1.72	2.94 ± 1.91	
Stem	26.14 ± 11.72a	22.16 ± 5.60b	27.44 ± 5.73a	19.29 ± 7.03b	Pp*	17.80 ± 10.56ab	14.08 ± 5.55b	27.59 ± 10.02a	14.05 ± 2.80b	Pp*
Lateral roots	16.69 ± 11.89a	14.74 ± 6.33a	9.99 ± 4.93b	10.25 ± 4.37b	Pc*	16.55 ± 13.52	16.09 ± 10.54	13.23 ± 7.16	8.56 ± 1.43	
Principal roots	29.96 ± 10.97 b	32.93 ± 8.79b	43.34 ± 7.38a	34.20 ± 12.90ab	Pc*	18.32 ± 12.43	22.04 ± 15.22	19.71 ± 6.16	10.26 ± 2.38	

Table A5 Effects of the nematode *Pratylenchus penetrans* and the Collembola *Protaphorura armata* on the amounts of individual phospholipid fatty acids (in nmol g^{-1} DW soil ± s.d.) in the rhizosphere of *Quercus robur* microcuttings. Presented are data of first (2 DPL) sampling time of oak microcuttings. ANOVA with *, ** and *** for $P < 0.05$, $P < 0.01$ and $P < 0.001$ or n.s $P > 0.05$, respectively. Values in a row followed by the same letter are not significantly different (Tukey's HSD test, $P < 0.05$). n.s: not statistically significant

		2 DPL				
		Control	Collembola	Nematodes	Combined	ANOVA
Fatty acid	Organism					
i15:0	Gram-positive bacteria	4.46 ± 1.41	5.31 ± 1.17	5.05 ± 1.42	5.30 ± 1.13	n.s
a15:0		2.95 ± 1.31	3.23 ± 0.76	2.91 ± 1.01	3.83 ± 1.21	n.s
i16:0		6.43 ± 2.15	7.38 ± 1.71	6.45 ± 2.21	7.23 ± 1.30	n.s
i 17:0		1.36 ± 0.47	1.52 ± 0.36	1.44 ± 0.53	1.55 ± 0.30	n.s
a17:0		1.48 ± 0.69	1.20 ± 0.61	1.11 ± 0.83	1.86 ± 0.63	n.s
cy 17:0	Gram-negative bacteria	5.39 ± 4.12	5.46 ± 2.82	6.34 ± 3.58	4.56 ± 2.63	n.s
cy 19:0		4.71 ± 2.82	4.84 ± 1.15	4.67 ± 2.08	5.17 ± 1.88	n.s
16:1ω7	Bacteria in general	3.22 ± 1.50	3.58 ± 0.93	4.31 ± 1.81	4.10 ±0.76	n.s
18:1ωc		7.33 ± 4.92	5.76 ± 1.98	6.62 ± 3.97	8.15 ± 2.97	n.s
18:1ωc	Fungi	2.29 ± 1.28	2.48 ± 0.92	2.58 ± 1.62	3.25 ± 0.75	n.s
18:2ω6		1.58 ± 1.11	1.84 ± 1.58	1.55 ± 1.58	2.60 ± 0.75	n.s
14:0	Miscellaneous origin	1.04 ± 0.56	1.13 ± 0.57	1.15 ± 0.65	1.33 ± 0.26	n.s
15:0		0.75 ± 0.54	1.24 ± 1.09	0.85 ± 0.62	0.88 ± 0.43	n.s
16:0		13.07 ± 6.64	14.19 ± 4.24	13.83 ± 5.59	13.56 ± 2.50	n.s
18:0		1.78 ± 0.81	1.55 ± 0.81	1.59 ± 0.92	1.91 ± 0.44	n.s

Table A6 Effects of the nematode *Pratylenchus penetrans* and the Collembola *Protaphorura armata* on the amounts of individual phospholipid fatty acids (in nmol g^{-1} DW soil ± s.d.) in the rhizosphere of *Quercus robur* microcuttings. Presented are data of second (5 DPL) sampling time of oak microcuttings. ANOVA with * for P < 0.05. Values in a row followed by the same letter are not significantly different (Tukey's HSD test, $P < 0.05$). n.s: not statistically significant

		5 DPL				
		Control	Collembola	Nematodes	Combined	ANOVA
Fatty acid	Organism					
i15:0	Gram-positive bacteria	4.62 ± 1.44	3.89 ± 1.51	4.11 ± 1.20	4.70 ± 0.86	n.s
a15:0		2.63 ± 0.99	2.55 ± 1.22	2.44 ± 0.83	2.69 ± 0.58	n.s
i16:0		6.13 ± 1.57	6.65 ± 1.43	5.01 ± 1.19	6.63 ± 1.30	C*
i 17:0		1.46 ± 0.58	1.39 ± 0.30	1.16 ± 0.23	1.42 ± 0.30	n.s
a17:0		1.34 ± 0.72	1.50 ± 0.44	1.03 ± 0.49	1.32 ± 0.31	n.s
cy 17:0	Gram-negative bacteria	6.66 ± 4.69	3.31 ± 1.54	4.69 ± 1.44	4.28 ± 1.31	n.s
cy 19:0		5.28 ± 2.97	4.14 ± 0.79	3.53 ± 0.57	4.58 ± 1.05	n.s
16:1ω7	Bacteria in general	3.62 ± 1.61	2.84 ± 0.96	3.57 ± 0.95	3.60 ± 0.78	n.s
18:1ω7c		7.38 ± 4.50	5.65 ± 1.88	5.47 ± 1.92	5.15 ± 1.98	n.s
18:1ω9c	Fungi	2.16 ± 0.73	2.46 ± 0.81	2.21 ± 0.76	2.31 ± 0.51	n.s
18:2ω6		1.64 ± 1.33	2.70 ± 1.77	2.09 ± 1.06	1.67 ± 1.59	n.s
14:0	Miscellaneous origin	1.19 ± 0.37	0.74 ± 0.65	1.01 ± 0.48	1.20 ± 0.24	n.s
15:0		1.03 ± 0.35	0.79 ± 0.37	0.76 ± 0.18	0.93 ± 0.20	n.s
16:0		14.00 ± 5.28	11.26 ± 2.30	11.16 ± 1.84	12.34 ± 2.47	n.s
18:0		1.69 ± 0.51	1.70 ± 0.29	1.32 ± 0.27	1.67 ± 0.22	n.s

Table A7 Effects of increasing relative abundance of nematode trophic groups in soil on the amounts of individual PLFAs, (nmol g^{-1} ± s.d.). Presented is data at first (4 weeks) sampling after application of amendments i.e. C: control; BF: *Acrobeloides buetschlii*; FF: A*phelenchoides saprophilus*: and PF: *Pratylenchus penetrans*: PF. Values in a row with the same letters are not significantly different (Tukey's HSD test, $P < 0.05$)

	C	BF	FF	PF	BF+FF	BF+PF	FF+PF	BF+FF+PF
i15:0 (G+)	3.19 ± 0.05c	3.30 ± 0.08abc	3.19 ± 0.01c	3.29 ± 0.05bc	3.39 ± 0.12ab	2.51 ± 0.10d	3.49 ± 0.19a	3.32 ± 0.04abc
a15:0 (G+)	2.00 ± 0.02b	2.04 ± 0.03ab	1.99 ± 0.04b	2.12 ± 0.07ab	2.15 ± 0.12a	1.54 ± 0.03c	2.17 ± 0.12a	2.06 ± 0.03ab
i16:0 (G+)	1.48 ± 0.04bc	1.52 ± 0.04abc	1.52 ± 0.20abc	1.43 ± 0.09c	1.63 ± 0.10ab	1.37 ± 0.02c	1.64 ± 0.09ab	1.66 ± 0.05a
i17:0 (G+)	0.99 ± 0.03ab	0.98 ± 0.06ab	0.93 ± 0.07ab	0.98 ± 0.07ab	1.00 ± 0.07ab	0.91 ± 0.08b	1.01 ± 0.03a	1.03 ± 0.03a
a17:0 (G+)	0.93 ± 0.20ab	0.82 ± 0.05ab	0.84 ± 0.16ab	0.85 ± 0.03ab	0.91 ± 0.06ab	0.75 ± 0.10b	0.97 ± 0.06a	0.95 ± 0.03ab
cy17:0 (G-)	1.46 ± 0.03c	1.40 ± 0.02cd	1.42 ± 0.03cd	1.45 ± 0.10c	1.64 ± 0.06b	1.35 ± 0.02d	1.84 ± 0.03a	1.67 ± 0.05b
cy19:0 (G-)	1.95 ± 0.11bcd	1.94 ± 0.07bcd	1.85 ± 0.07d	2.02 ± 0.05abc	2.05 ± 0.05ab	1.91 ± 0.03cd	2.11 ± 0.11a	2.14 ± 0.07a
16:1ω (B)	2.40 ± 0.17a	2.37 ± 0.09ab	2.13 ± 0.05bc	2.13 ± 0.32bc	2.31 ± 0.04ab	2.01 ± 0.04c	2.52 ± 0.02a	2.38 ± 0.04ab
16:1ω (B)	1.13 ± 0.02ab	1.21 ± 0.10a	1.02 ± 0.04bc	1.03 ± 0.17bc	1.11 ± 0.03ab	0.95 ± 0.07c	1.17 ± 0.06a	1.14 ± 0.03ab
18:1ω9t (B)	3.25 ± 0.46	3.15 ± 0.26	3.13 ± 0.06	3.33 ± 0.06	3.30 ± 0.05	3.09 ± 0.25	3.38 ± 0.08	3.43 ± 0.02
16:0 10-meth (A)	2.67 ± 0.08	2.68 ± 0.13abc	2.56 ± 0.09bc	2.62 ± 0.28abc	2.82 ± 0.06ab	2.45 ± 0.30c	2.89 ± 0.08a	2.86 ± 0.06ab
18:0 10-meth (A)	1.75 ± 0.25ab	1.65 ± 0.08b	1.69 ± 0.08ab	1.78 ± 0.15ab	1.88 ± 0.08ab	1.74 ± 0.14ab	1.90 ± 0.14ab	1.99 ± 0.03a
18:2ω6 (F)	0.90 ± 0.05	0.82 ± 0.05	0.85 ± 0.13	0.83 ± 0.06	0.93 ± 0.12	0.89 ± 0.26	0.85 ± 0.06	1.04 ± 0.06
18:1ω9c (F)	3.01 ± 0.55	2.86 ± 0.43	2.84 ± 0.37	3.08 ± 0.56	3.12 ± 0.12	3.02 ± 0.29	3.35 ± 0.07	3.29 ± 0.03
14:0	0.45 ± 0.02	0.48 ± 0.11	0.48 ± 0.05	0.47 ± 0.10	0.48 ± 0.11	0.37 ± 0.04	0.51 ± 0.05	0.46 ± 0.12
15:0	0.35 ± 0.04	0.46 ± 0.03	0.33 ± 0.01	0.35 ± 0.04	0.36 ± 0.05	0.29 ± 0.05	0.36 ± 0.03	0.33 ± 0.08
16:0	6.96 ± 0.41b	6.85 ± 0.10bc	6.96 ± 0.15b	7.42 ± 0.26ab	7.34 ± 0.51ab	6.30 ± 0.42c	7.49 ± 0.16ab	7.69 ± 0.30a
18:0	1.21 ± 0.15b	1.22 ± 0.12ab	1.17 ± 0.06b	1.30 ± 0.03ab	1.28 ± 0.11ab	1.26 ± 0.03ab	1.37 ± 0.10ab	1.43 ± 0.21a

Table A8 Effects of increasing relative abundance of nematode trophic groups in soil on the amounts of individual PLFAs, (nmol g^{-1} ± s.d.). Presented is data at second (8 weeks) sampling after application of amendments i.e. C: control; BF: *Acrobeloides buetschlii*; FF: *Aphelenchoides saprophilus*: and PF: *Pratylenchus penetrans*: PF. Values in a row with the same letters are not significantly different (Tukey's HSD test, $P < 0.05$)

	C	BF	FF	PF	BF+FF	BF+PF	FF+PF	BB+FF+PF
i15:0 (G+)	2.88 ± 0.05d	2.71± 0.12e	2.55 ± 0.07f	2.97 ± 0.04cd	3.02 ± 0.08bc	3.26 ± 0.05a	3.02 ± 0.01bc	3.09 ± 0.01b
a15:0 (G+)	1.86 ± 0.04c	1.68 ± 0.05d	1.68 ± 0.03d	1.98 ± 0.05b	1.89 ± 0.04c	2.11 ± 0.02a	1.89 ± 0.05c	1.99 ± 0.04b
i16:0 (G+)	1.45 ± 0.04c	1.48 ± 0.07bc	1.33 ± 0.06d	1.48 ± 0.06bc	1.55 ± 0.09abc	1.61 ± 0.05a	1.53 ± 0.03abc	1.58 ± 0.01ab
i17:0 (G+)	0.92 ± 0.05d	0.96 ± 0.08e	0.87 ± 0.03e	0.93 ± 0.03cd	0.98 ± 0.04b	1.02 ± 0.09bcd	0.99 ± 0.05bc	1.04 ± 0.01a
a17:0 (G+)	0.80 ± 0.02	0.73 ± 0.02	0.72 ± 0.03	0.82 ± 0.03	0.90 ± 0.06	0.85 ± 0.03	0.86 ± 0.02	1.02 ± 0.02
cy17:0 (G-)	1.30 ± 0.04d	1.30 ± 0.01d	1.20 ± 0.08e	1.56 ± 0.04b	1.59 ± 0.04b	1.60 ± 0.06b	1.49 ± 0.03c	1.80 ± 0.02a
cy19:0 (G-)	1.99 ± 0.5cd	2.04 ± 0.02c	1.88 ± 0.09e	1.95 ± 0.02de	2.12 ± 0.06b	2.12 ± 0.05b	2.07 ± 0.02bc	2.22 ± 0.04 a
16:1ω7 (B)	1.90 ± 0.02d	1.53 ± 0.04f	1.57 ± 0.06f	1.79 ± 0.04e	2.16 ± 0.04b	1.90 ± 0.06d	1.99 ± 0.02c	2.32 ± 0.05a
16:1ω5 (B)	0.93 ± 0.05cd	0.91 ± 0.03cd	0.86 ± 0.04d	0.95 ± 0.04bc	1.02 ± 0.04ab	1.02 ± 0.07ab	1.06 ± 0.02a	1.09 ± 0.04a
18:1ω9t (B)	3.06 ± 0.03c	3.10 ± 0.07c	2.70 ± 0.07e	2.88 ± 0.03d	3.10 ± 0.06c	3.08 ± 0.05c	3.29 ± 0.03b	3.53 ± 0.02a
16:0 10-meth (A)	2.47 ± 0.05d	2.55 ± 0.04cd	2.24 ± 0.04e	2.55 ± 0.02cd	2.64 ± 0.04b	2.65 ± 0.04b	2.61 ± 0.05bc	2.89 ± 0.05a
18:0 10-meth (A)	1.71 ± 0.02c	1.74 ± 0.02c	1.56 ± 0.07d	1.71 ± 0.06c	1.86 ± 0.07ab	1.81 ± 0.05bc	1.77 ± 0.05bc	1.93 ± 0.07a
18:2ω6 (F)	0.83 ± 0.08e	1.01 ± 0.02e	0.78 ± 0.05e	0.89 ± 0.06de	0.99 ± 0.04cd	1.23 ± 0.06b	1.73 ± 0.03a	0.99 ± 0.08cd
18:1ω9c (F)	2.72 ± 0.08e	2.79 ± 0.06de	2.36 ± 0.06f	2.91 ± 0.05c	3.03 ± 0.05b	2.90 ± 0.07cd	3.30 ± 0.07a	3.19 ± 0.02a
14:0	0.43 ± 0.04ab	0.38 ± 0.06b	0.40 ± 0.07ab	0.46 ± 0.08ab	0.51 ± 0.05a	0.47 ± 0.03ab	0.43 ± 0.05ab	0.44 ± 0.08ab
15:0	0.32 ± 0.03	0.29 ± 0.05	0.28 ± 0.06	0.34 ± 0.03	0.35 ± 0.03	0.34 ± 0.03	0.29 ± 0.04	0.33 ± 0.02
16:0	6.60 ± 0.57bc	7.09 ± 0.38abc	6.49 ± 0.26c	6.61 ± 0.22bc	6.47 ± 0.36c	7.11 ± 0.34abc	7.29 ± 0.36ab	7.35 ± 0.39a
18:0	1.20 ± 0.06b	1.42 ± 0.08a	1.12 ± 0.02b	1.22 ± 0.03b	1.24 ± 0.14b	1.22 ± 0.16b	1.24 ± 0.03b	1.24 ± 0.09b

Publications

Maboreke H.R., Feldhahn L., Bonn M., Tarkka M.T., Buscot F., Herrmann S., Menzel R., Ruess, L. (2016). Transcriptome analysis in oak uncovers a strong impact of endogenous rhythmic growth on interaction with plant-parasitic nematodes. BMC Genomics 17, 627 doi: 10.1186/s12864-016-2992-8

Caravaca F., **Maboreke H.**, Kurth F, Hermann S., Tarkka TM, Ruess L. (2015). Synergists and antagonists in the rhizosphere modulate microbial communities and growth of Quercurs robur L. Soil Biology and Biochemistry 82,65-73.

Maboreke H.R., Graf M., Grams T.E.E., Herrmann S., Scheu S., Ruess L. Multitrophic interactions in the rhizosphere of a temperate forest tree affect plant carbon flow into the belowground food web. (Submitted to Soil Biology and Biochemistry).

Tarkka M.T., Herrmann S., Wubet T., Feldhahn L., Recht S., Kurth F., Mailander S., Bonn M., Neef M., Angay O., Bacht, M., Graf, M., Maboreke, H., Fleischmann F., Grams T.E.E., Ruess L., Schadler M., Brandl R., Scheu, S., Schrey, S.D., Grosse, I., Buscot, F. (2014). OakContigDF159.1, a reference library for studying differential gene expression in Quercus robur L. during controlled biotic interactions: use for quantitative transcriptomic profiling of oak roots in ectomycorrhizal symbiosis. New Phytologist 199, 529-540

Herrmann S., Grams T.E.E., Tarkka M.T., Angay O., Bacht M., Bonn, M., Feldhahn, L., Graf M., Kurth F., Maboreke H., Mailander S., Recht S., Fleischman F., Ruess L., Schadler M., Scheu S., Schrey, S.D., Buscot F. (2016). Endogenous rhythmic growth, a trait suitable for the study of interplays between multitrophic interactions and tree development. Perspectives in Plant Ecology, Evolution and Systematics 19, 40-48

Declaration of the author's own contribution to manuscripts with multiple authors used in this thesis

Maboreke et al., 2016 was published based on part of the data (Transcriptomic responses of oak) presented in Chapter **3.1**. I performed this experiment, collected and analysed the data as well as write the manuscript. The bioinformatics analysis was performed in collaboration with Feldhahn L, Bönn M and Tarkka M. Herrmann S, Buscot F, Menzel R and Ruess L helped improve the manuscript.
Figure 17 and Tables 2, 3, 4 and 5 were modified from Maboreke et al., 2016.

Caravaca et al., 2015 was published using data presented in Chapter **3.2.** Caravaca F and I performed the experiment together. In addition, I cultured the nematodes, quantified the nematode sampled following the harvests performed part of the data analyses as well as assisted with the manuscript preparation. Kurth F provided and quantified the *Streptomyces* AcH 505. Ruess L, Herrmann S and Tarkka MT designed the research experiment.
Tables 12 and 13 have been adapted and modified from Caravaca et al., 2015

Maboreke et al., (submitted) was based on data presented in Chapter **3.3**. This experiment was performed in collaboration with Graf M. Herrmann S provided the microcuttings and Gramms T performed the stable isotopes labelling. I analysed the soil and animal fatty acids and ^{13}C incorporation, and nematode data as well as well as prepared the manuscript. Graf M analysed the ^{13}C bulk signature of the soil, plants and Collembola. Ruess L and Scheu S our supervisors helped improve the manuscript.

ACKNOWLEDGEMENTS

It gives me immense gratification to finally complete a colossal task of submitting my PhD thesis. My PhD journey had a rough start and I continued to face many challenges along the way but I would not have made it through without the encouragement and support from so many people. It has been a great privilege to spend these years in the department of Ecology at Humboldt Universität, and all members past and present will remain dear to me

Firstly, I would like to extend my heartfelt gratitude to my supervisor, Prof. Liliane Rueß. Thank you for your unwavering support, encouragement and all the constructive discussions we had as well as always being available to help and guide me with many aspects of my research work to produce quality work. Over the years you have taught me to always have a positive attitude and work through the challenges, a lesson I shall carry with me wherever I go.

Secondly, I would like to extend my sincere gratitude to German Science Foundation (DFG) for funding the research project (grant RU 780/5-1) which enabled me to realize my dream. I am also thankful for the KfF grant (2014) I received from the Institute of Biology for the Humboldt-Universität zu Berlin for the financial support.

My next debt of gratitude goes to the members of the TrophinOak research consortium, everyone was always willing to assist and answer my many never-ending questions. This work benefited greatly from a lot of collaborations and valuable contributions from many people in the project. I want to thank Fuen, it was a delight working with her and she has continued motivating me over the last years. A special thank you goes to Sylvie, Thorsten, Mika, Stefan and Francois for their invaluable contributions towards my research work. I would also want to acknowledge the contributions of all the technical staff I worked with namely, I. Krieg, B. Krause and Christof. I am forever indebted to the fellow PhD students who were always willing to assist with information and technical help. A massive thank you goes to the technical team from the Ecology work group, Petra Heese and Rainer Nehring.

I would also like to thank lot of people who helped during the PhD; my best and worst moments of this journey were shared with my colleagues. To me you were all more than just colleagues but rather my surrogate family who made me feel I was never alone. I thank you for your patience, generosity and assistance with everything; I would not have made it through these last years without your kindness. You all gave me something to look forward to each day even on “bad days” - you were my therapy. Michael, Anika, René, Olena, Andreas,

Jakob, Thomas, Ralph, Paul, Veronika and Heidi - from the depth of my heart I say “maita” which means thank you very much in Shona.

A special heartfelt thank you goes to my parents and family whose unwavering love, support and encouragement allowed me to go through all ups and downs especially in the past few years. I truly appreciate all the sacrifices and hope one day I can be able to pay forward this gift of love. I would also like to thank my friends who were a pleasant distraction. Everyone always wondered if I ever felt lonely but the truth is I rarely did because I was constantly showered with love and attention from family and friends, near and far. Guys, you have been the best cheerleaders throughout this journey, I could not have asked for more. Lastly, and most importantly, thanks to my rock, Ed – need I say more?

THESIS DECLARATION

I, Hazel R. Maboreke, hereby declare that I have completed the thesis independently using only the aids and tools specified. All aids used in this thesis as well as scientific ideas from or based on other sources were cited at the respective point. I have not applied for a doctor's degree in the doctoral subject elsewhere and do not hold a corresponding doctor's degree.

I, have taken due note of the Faculty of Mathematics and Natural Sciences PhD Regulations, published in the Official Gazette of Humboldt-Universität zu Berlin no. 21/2009 on 06/07/2009.